



UNIVERSITAT DE
BARCELONA

Thermally stable ion-exchange resins as catalysts for the liquid-phase dehydration of 1-pentanol to di-n-pentyl ether

Roger Bringué Tomás

ADVERTIMENT. La consulta d'aquesta tesi queda condicionada a l'acceptació de les següents condicions d'ús: La difusió d'aquesta tesi per mitjà del servei TDX (www.tdx.cat) i a través del Dipòsit Digital de la UB (diposit.ub.edu) ha estat autoritzada pels titulars dels drets de propietat intel·lectual únicament per a usos privats emmarcats en activitats d'investigació i docència. No s'autoritza la seva reproducció amb finalitats de lucre ni la seva difusió i posada a disposició des d'un lloc aliè al servei TDX ni al Dipòsit Digital de la UB. No s'autoritza la presentació del seu contingut en una finestra o marc aliè a TDX o al Dipòsit Digital de la UB (framing). Aquesta reserva de drets afecta tant al resum de presentació de la tesi com als seus continguts. En la utilització o cita de parts de la tesi és obligat indicar el nom de la persona autora.

ADVERTENCIA. La consulta de esta tesis queda condicionada a la aceptación de las siguientes condiciones de uso: La difusión de esta tesis por medio del servicio TDR (www.tdx.cat) y a través del Repositorio Digital de la UB (diposit.ub.edu) ha sido autorizada por los titulares de los derechos de propiedad intelectual únicamente para usos privados enmarcados en actividades de investigación y docencia. No se autoriza su reproducción con finalidades de lucro ni su difusión y puesta a disposición desde un sitio ajeno al servicio TDR o al Repositorio Digital de la UB. No se autoriza la presentación de su contenido en una ventana o marco ajeno a TDR o al Repositorio Digital de la UB (framing). Esta reserva de derechos afecta tanto al resumen de presentación de la tesis como a sus contenidos. En la utilización o cita de partes de la tesis es obligado indicar el nombre de la persona autora.

WARNING. On having consulted this thesis you're accepting the following use conditions: Spreading this thesis by the TDX (www.tdx.cat) service and by the UB Digital Repository (diposit.ub.edu) has been authorized by the titular of the intellectual property rights only for private uses placed in investigation and teaching activities. Reproduction with lucrative aims is not authorized nor its spreading and availability from a site foreign to the TDX service or to the UB Digital Repository. Introducing its content in a window or frame foreign to the TDX service or to the UB Digital Repository is not authorized (framing). Those rights affect to the presentation summary of the thesis as well as to its contents. In the using or citation of parts of the thesis it's obliged to indicate the name of the author.



UNIVERSITAT DE BARCELONA



Universitat de Barcelona
Facultat de Química
Departament d'Enginyeria Química

**THERMALLY STABLE ION-EXCHANGE RESINS AS CATALYSTS FOR THE
LIQUID-PHASE DEHYDRATION OF 1-PENTANOL TO DI-*n*-PENTYL ETHER**

Roger Bringué Tomàs

Barcelona, Abril del 2007

Programa de Doctorat d'Enginyeria del Medi Ambient i del Producte
Bienni 2002-2003

Memòria per a aspirar al grau de doctor per la Universitat de Barcelona presentada per en Roger Bringué Tomàs, Enginyer Químic.

Roger Bringué Tomàs

La present Tesi Doctoral ha estat realitzada en el Departament d'Enginyeria Química sota la direcció dels Doctors Javier Tejero Salvador i Montserrat Iborra Urios, qui n'autoritzen la presentació.

Dr. Javier Tejero Salvador

Dra. Montserrat Iborra Urios

Barcelona, Abril del 2007

Kinetics is nature's way
of preventing everything
from happening all at once
S.E. LeBlanc

Agraïments

Primer de tot voldria agrair a en Xavier i la Montse per haver dipositat la seva confiança en mi, i haver-me dirigit i aconsellat, sobretot en aquells moments d'espessor i bloqueig mental que de quan en quan afecten a un. Faig extensiu el meu sincer agraïment als membres de la línia de Catàlisi i Cinètica Aplicada pel seu suport i ajut en tot moment.

Als companys de laboratori i de departament, moltes gràcies pels bons moments que m'heu fet passar, ja sigui a la mateixa Facultat o fora d'ella, i sobretot pels cafès i dinars que heu compartit amb mi durant tots aquests anys.

No puc deixar de fer referència al Grup!, amics i amigues, moltes gràcies pel temps que ens hem dedicat i que espero que continuem dedicant-nos. En especial a tu, Nardi, per a què la nostra amistat no decaigui.

A la meva família, als que hi són i als que ja no, per haver-me fet veure que la vida no són només números ni fórmules, i per haver-me ensenyat la lliçó més important: saber estimar.

Finalment a tu, Sandra, per tots els projectes en comú que tenim oberts, per a què els concloquem i sempre tinguem ganes d'obrir-ne de nous.

A tots, moltes gràcies!

List of publications

- I. Bringué, R.; Iborra, M.; Tejero, J.; Izquierdo, J.F.; Cruz, V.J.; Cunill, F.; Fité, C
Thermally stable ion-exchange resins as catalysts for the liquid-phase dehydration of 1-pentanol to di-n-pentyl ether (DNPE), **Journal of Catalysis**, 244 (2006) 33-42
- II. R. Bringué, J. Tejero, M. Iborra, J. F. Izquierdo, C. Fité, F. Cunill
Water effect on the kinetics of 1-pentanol dehydration to di-n-pentyl ether (DNPE) on Amberlyst 70, **Topics in Catalysis**, (2007) in press
- III. R. Bringué, J. Tejero, M. Iborra, J. F. Izquierdo, C. Fité, F. Cunill
Experimental Study of the Chemical Equilibria in the Liquid-Phase Dehydration of 1-Pentanol to Di-N-Pentyl Ether, **Industrial and Engineering Chemical Research**, submitted

Participation in congresses

- ✓ **SECAT'03** *Obtención de di-n-pentil éter por deshidratación de 1-pentanol catalizada por resinas perfluorosulfonadas*. Ordeig, O., Bringué, R., Tejero, J., Iborra, M., Cunill, F., Izquierdo, J. F. y Fité, C. Reunión de la sociedad española de catálisis, (Málaga, 2003). Oral communication.
- ✓ **13th International Congress on Catalysis (ICC)** *Thermally stable ion-exchange resins as catalysts for the liquid-phase dehydration of 1-pentanol to di-n-pentyl ether*. R. Bringué, M. Iborra, J. Tejero, J F. Izquierdo, F. Cunill, y C. Fité. The International Association of Catalysis Societies (IACS) and the Catalysis Division of Société Française de Chimie (Paris 2004). Poster.
- ✓ **SECAT'05** *Deshidratación de 1-pentanol a di-n-pentil éter en fase líquida en presencia de resinas termoestables*. R. Bringué, M. Iborra, J. Tejero, J F. Izquierdo, F. Cunill, y C. Fité, Reunión de la sociedad española de catálisis (Madrid, 2005). Poster.
- ✓ **10th Mediterranean Congress of Chemical Engineering** *Comparison of catalysts in the Dehydration of 1-pentanol to di-n-pentyl ether*, R. Bringué, M. Iborra, J. Tejero, J F. Izquierdo, F. Cunill, y C. Fité, SEQUI i Fira de Barcelona (Barcelona 2005). Poster.

- ✓ **12th Nordic Symposium on Catalysis.** *Water Effect On The Kinetics Of The Dehydration Of 1-Pentanol To Di-N-Pentyl Ether (DNPE).* R. Bringué, J. Tejero, M. Iborra, J.F. Izquierdo, C. Fité, F. Cunill; (Trondheim 2006). Poster.

1. INTRODUCTION	
1.1 DIESEL FUEL AS A PETROLEUM PRODUCT	7
1.2. PHYSICAL PROPERTIES OF DIESEL FUEL	8
1.2.1 <i>Density</i>	8
1.2.2 <i>Distillation curve</i>	8
1.2.3 <i>Viscosity</i>	9
1.2.4 <i>Low temperature properties</i>	9
1.2.5 <i>Cetane number</i>	11
1.3 DIESEL FUEL ADDITIVES.....	11
1.3.1 <i>Engine performance additives</i>	11
1.3.2 <i>Fuel handling additives</i>	13
1.3.3 <i>Fuel stability additives</i>	14
1.3.4 <i>Contaminant control</i>	15
1.4 CONSUMPTION OF DIESEL FUEL	16
1.5 REFORMULATION OF DIESEL FUELS.....	17
1.6 DI-N-PENTYL ETHER	20
1.6.1 <i>Properties of DNPE</i>	20
1.6.2 <i>DNPE synthesis route</i>	21
1.6.3 <i>Dehydration of 1-pentanol to DNPE</i>	22
1.7 CATALYST DESCRIPTION	25
1.7.1 <i>Zeolites</i>	25
1.7.2 <i>Ion-exchange resins</i>	27
1.7.2.1 <i>Styrene divinylbenzene resins</i>	28
1.7.2.2 <i>Perfluoroalkane sulfonic resins</i>	30
1.7.2.3 <i>Properties of ion-exchange resins</i>	31
1.8 KINETIC ANALYSIS	34
1.8.1 <i>Steps of a catalytic process</i>	35
1.8.1.1 <i>External Mass transfer</i>	36
1.8.1.2 <i>Internal mass transfer</i>	37
1.8.1.3 <i>Surface reaction</i>	37
1.8.2 <i>Corrections of classical kinetic models</i>	41
2. OBJECTIVES	45
3. EXPERIMENTAL	49
3.1 MATERIALS.....	51

3.1.1	<i>Chemicals</i>	51
3.1.2	<i>Auxiliary gases</i>	51
3.1.3	<i>Catalysts</i>	51
3.1.3.1	Perfluoroalkanesulfonic resins.....	52
3.1.3.2	Styrene/Divinylbenzene resins	54
3.1.3.3	Zeolite	61
3.1.3.4	Carriers for nafion impregnation	62
3.2	EXPERIMENTAL SETUP	64
3.2.1	<i>DNPE reaction study</i>	64
3.2.1.1	Reactor	65
3.2.1.2	Temperature control	65
3.2.1.3	Outlet and analysis system.....	65
3.2.2	<i>Catalyst synthesis</i>	68
3.2.3	<i>Auxiliary devices</i>	69
3.2.3.1	Titration devices.....	69
3.2.3.2	Distillation column.....	69
3.2.3.3	GC/MS system.....	70
3.3	EXPERIMENTAL PROCEDURES	70
3.3.1	<i>Reactor start-up and operation</i>	70
3.3.1.1	Catalyst pretreatment	70
3.3.1.2	Experiment.....	71
3.3.2	<i>Catalyst synthesis</i>	72
3.3.3	<i>Titration</i>	74
4.	RESULTS AND DISCUSSION	77
4.1	GENERAL WORKING SCHEME	79
4.1.1	<i>System variables analysis</i>	79
4.1.2	<i>Experimental design</i>	80
4.1.3	<i>1-pentanol conversion, selectivity and yield to DNPE</i>	81
4.1.4	<i>Reaction rate and turnover number</i>	83
4.1.5	<i>Mass balance</i>	84
4.2	PRELIMINARY EXPERIMENTS.....	84
4.2.1	<i>Influence of catalyst loading</i>	84
4.2.2	<i>Influence of stirring speed</i>	87
4.2.3	<i>Influence of catalyst particle size</i>	90

4.3	CATALYSTS TESTS.....	93
4.3.1	1-pentanol Conversion	94
4.3.2	Selectivity.....	96
4.3.3	DNPE yield	99
4.3.4	Reaction rate and turnover number.....	100
4.3.5	Catalyst selection.....	103
4.4.	INFLUENCE OF 2-METHYL-1-BUTANOL	104
4.5	THERMODYNAMIC EQUILIBRIUM	106
4.5.1	Determination of the equilibrium constant.....	107
4.5.2	Experimental equilibrium constant.....	110
4.5.3	Pressure correction factor	113
4.5.4	Temperature dependence of the equilibrium constant.....	114
4.5.5	Comparison of experimental and theoretical values of equilibrium constants	120
4.5.5.1	DNPE synthesis.....	120
4.5.5.2	1-pentene formation	122
4.5.5.3	2-pentene formation	123
4.6	KINETIC ANALYSIS	124
4.6.1	LHHW kinetic models	124
4.6.2	Methodology of kinetic fitting.....	127
4.6.3	Selection of the LHHW kinetic model.....	129
4.6.4	Effect of water and dnpe on the reaction rate	136
4.6.5	Modified kinetic models	140
4.6.5.1	Solubility parameter	141
4.6.5.2	Inhibition factor	144
4.6.5.3	Freundlich-type factor.....	147
4.6.5.4	Langmuir-type factor.....	150
4.6.5.5	Selection of the modified kinetic model.....	152
4.6.6	Kinetic model with Freundlich-type correction factor applied to other catalysts..	155
4.6.7	Kinetic model with Freundlich-type correction factor applied to 1-pentene and 2-pentene synthesis reactions	156
4.7	CATALYST SYNTHESIS	159
4.7.1	Carriers characterization	159
4.7.2	Experimental design.....	166
4.7.3	Search for the method of impregnation	168

4.7.3.1 Method 1 (M-1)	168
4.7.3.2 Method 2 (M-2)	169
4.7.3.3 Method 3 (M-3)	171
4.7.4 <i>Effect of the initial %Nafion and Bet AREA</i>	176
4.7.4.1 Si-A	176
4.7.4.2 Si-C	177
4.7.4.3 Comparison of Si-a and Si-C derived catalysts	178
4.7.5 <i>Impregnated catalysts characterization</i>	181
4.7.6 <i>Impregnation method reproducibility and deactivation test</i>	184
5. Conclusions	189
6. RECOMMENDATIONS	197
7. NOTATION	201
8. INDEX OF EQUATIONS, TABLES AND FIGURES	207
9. REFERENCES	217
10. APPENDICES	223
Appendix I Specifications of diesel fuel (class A)	225
Appendix II Modified Unifac-Dortmund method	227
Appendix III Methods used for estimating physical properties	231
Appendix IV Thermochemical data	235
Appendix V General kinetic equation	239
Appendix VI Kinetic models fitting	241
Appendix VII Error analysis	251
Appendix VIII Modified kinetic models	253
Appendix IX Material Safety Data Sheets	259
11. Abstract in Spanish	281



Chapter 1. Introduction

1.1 DIESEL FUEL AS A PETROLEUM PRODUCT

Nowadays, *Petroleum* or *Crude oil* is the most important primary energy source, and is also the raw material for many chemicals products. It consists of complex mixtures of hydrocarbon molecules, but its composition varies widely from one crude to another.

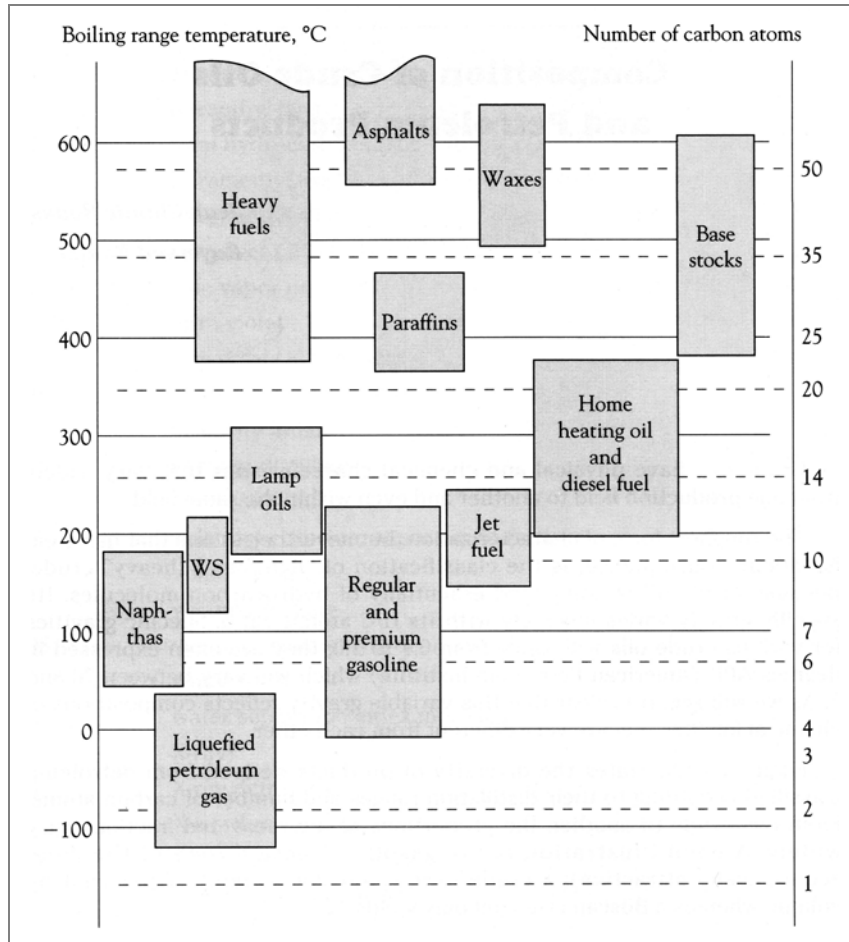


Figure 1. Principal petroleum products, their boiling range temperatures and their number of carbon atoms [1]

Figure 1 illustrates the diversity of products derived from petroleum classified according to their distillation ranges and number of carbon atoms. The proportions of the recovered fractions vary depending on the origin of the crude oil.

As it can be seen in the picture, *diesel fuels* are obtained in the fractional distillation of crude oil between 200 and 375°C at atmospheric pressure, and it is formed by hydrocarbons with

chains among 12-14 to 20-22 carbon atoms. Besides, diesel fuel can be formulated with products from other processes in the refinery. *Table 1* gives some physical-chemical characteristics of selected main refinery streams capable of being added to the diesel fuel pool. The result is a liquid fuel formed by complex mixtures of saturated and aromatic hydrocarbons. However, its composition is regulated within some limits, and its characteristics are defined in Spain by the R.D. 61/2006, January 31st, shown in *Appendix I*, which classifies diesel fuels into three classes:

- ✓ Class A: fuel used for the diesel engines in passenger cars and in utility vehicles.
- ✓ Class B: fuel for agricultural and maritime use.
- ✓ Class C: fuel for heating purposes.

1.2. PHYSICAL PROPERTIES OF DIESEL FUEL

The essential characteristics of diesel fuel necessary for satisfactory operation of the engine are the density, distillation curve, viscosity, behavior at low temperature, and diesel cetane number [1].

1.2.1 DENSITY

Imposing a minimum density is justified by the need to obtain sufficient maximum power for the engine, by means of an injection pump whose flow is controlled by regulating the volume. On the other hand, a limit to maximum density is set in order to avoid smoke formation at full load. Current limits are 820 to 845 kg/m³ at 15 °C.

1.2.2 DISTILLATION CURVE

The necessity of carrying out injection at high pressure and the atomization into fine droplets using an injector imposes very precise volatility characteristics for the diesel fuel. The distilled fraction in volume recovered should be:

- ✓ T₆₅: 65% at 250°C
- ✓ T₈₅: 85% at 350°C
- ✓ T₉₅: 95% at 360°C

1.2.3 VISCOSITY

A too-viscous fuel increases pressure drop in the pump and injectors which then tends to diminish the injection pressure and the degree of atomization as well as affecting the process of combustion. Inversely, insufficient viscosity can cause seizing of the injection pump.

The actual limits are from 2 to 4.5 mm²/s at 40°C, which is the temperature of the injection pump.

1.2.4 LOW TEMPERATURE PROPERTIES

Low temperature properties of diesel fuels are very important since they affect both refinery flow schemes and, mainly, the fuel feed system. The diesel fuel must pass through a very fine filter before entering the injection pump. It can happen that some paraffinic hydrocarbons crystallize at low temperature, plug the filter and immobilize the vehicle. The main low temperature characteristics are the *cloud point* (CP), the *pour point*, and the *cold filter plugging point* (CFPP).

The cloud point, usually between 0 and -10°C, is the temperature at which paraffin crystals begin to appear and affect the product clarity.

The pour point, between -15 and -30°C, is the temperature at which crystals increase in size and form networks that trap the liquid and hinder its ability to flow.

The cold filter plugging point, maximum -10°C in winter (maximum 0°C in summer), is the minimum temperature at which a given volume of diesel fuel passes through a filter in a limited time interval.

Feedstock	Paraffinic crude			Naphthenic crude		Vacuum distillate		Vacuum residue		Deasphalted atmospheric residue
Process	Atmospheric distillation			Atmospheric distillation		FCC	Hydrocracking	Visbreaking	Coking	Hydrocracking
Yield, w/w % ^a	30.3	32.8	36.7	29.2	47.2	10-15	30.40	5-15	35	20
Density at 15°C, kg/L	0.835	0.825	0.843	0.827	0.856	0.930	0.814	0.845	0.900	0.807
Distillation, °C										
IP	170	180	170	180	170	170	220	170	170	260
EP	370	375	400	350	370	370	370	370	370	380
Cloud point, °C	5	-2	1	-10	-20	-5	-17	-4	-8	-13
Pour point, °C	-12	-9	-6	-18	-33	-14	-20	-18	-20	-18
Cetane number	50	51	54	54	43	24	64	40	28	70
Sulfur content, w/w %	0.12	0.04	0.83	0.80	0.09	2.8	0.001	2.33	2.10	0.0005

^a Quantity of product obtained from the feedstock

Table 1. Examples of stocks used in formulating diesel fuels [1]

1.2.5 CETANE NUMBER

The cetane number (CN) is used to measure the quality of auto-ignition of diesel fuels and gives an idea of the ignition delay period. The behavior of the diesel fuel is compared to that of two pure hydrocarbons selected as a reference: n-cetane (hexadecane, $C_{16}H_{34}$) which is given the number 100, and α -methyl-naphthalene ($C_{11}H_{10}$) which is given the number 0. In practice, as reference base heptamethylnonane (HMN, $C_{16}H_{34}$) is used, with a cetane number of 15. Mixtures of n-cetane and HMN will have the following cetane number:

$$CN = \% \text{ n-cetane} + 0.15 \cdot \% \text{ HMN} \quad \text{Equation 1}$$

The cetane number of a diesel fuel will be that of the mixture of n-cetane and HMN that has the same auto-ignition behavior. In general, the higher the cetane number, the better and cleaner the combustion is.

There also exist several methods to estimate the cetane number of diesel fuels from their physical characteristics or their chemical structure. The most common formula was developed by the Ethyl Corporation (ASTM D 976):

$$CCI = 454.74 - 1641.416 \rho + 774.74 \rho^2 - 0.554 (T_{50}) + 97.083 (\log T_{50})^2 \quad \text{Equation 2}$$

where

CCI = calculated cetane index

ρ = density at 15°C in kg/L

T_{50} = temperature, °C, corresponding to the ASTM D 86 50% distilled point

1.3 DIESEL FUEL ADDITIVES

Due to legislation or to commercial purposes (e.g. improved premium diesel), some additives are added to diesel fuels in order to improve their performance in diesel engines. Diesel fuel additives are used for a wide variety of purposes; however they can be grouped into four major categories: engine performance, fuel handling, fuel stability and contaminant control.

1.3.1 ENGINE PERFORMANCE ADDITIVES

This class of additives can improve engine performance immediately, as cetane number improvers, or over long term operation, as detergent and lubricity additives.

Cetane number improver

Also called Diesel ignition improvers, these additives can reduce combustion noise and smoke.

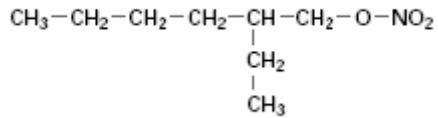


Figure 2. Cetane number improver: 2-ethylhexyl nitrate

2-ethylhexyl nitrate (EHN), also known as octyl nitrate, is the most widely used cetane number improver. EHN is thermally unstable and decomposes rapidly at the high temperatures in the combustion chamber. The products of decomposition (radicals) help initiating fuel combustion and, thus, shorten the ignition delay period from that of the fuel without the additive.

The increase in cetane number from a given concentration of EHN varies from one fuel to another. It is greater for a fuel whose natural cetane number is already relatively high. The incremental increase gets smaller as more EHN is added, so there is little benefit to exceeding a certain concentration. EHN is typically used in the concentration range of 0.05% mass to 0.4% mass and may yield a 3 to 8 cetane number benefit.

A disadvantage of EHN is that it decreases the thermal stability of some fuels.

Injector Cleanliness Additives

Fuel injector spray patterns are the key to an efficient combustion process in diesel engines. Deposition of carbonaceous, combustion waste products on the injector can have a detrimental effect on the spray pattern which may result in increased emissions and decreased fuel economy.

Ashless polymeric detergent additives can clean up fuel injector deposits and/or keep injectors clean. These additives are composed of a polar group that bonds to deposits and deposits precursors, and a non-polar group that dissolves in the fuel. Usually, they are oil-soluble polymers having amine or polyamine groups at one of their chain ends (see *Figure 3*), and help maintaining an optimum fuel spray pattern resulting in a reduced combustion noise, emissions and black smoke, and extending vehicle life. Detergent additives are typically used in the concentration range of 50ppm to 300ppm.

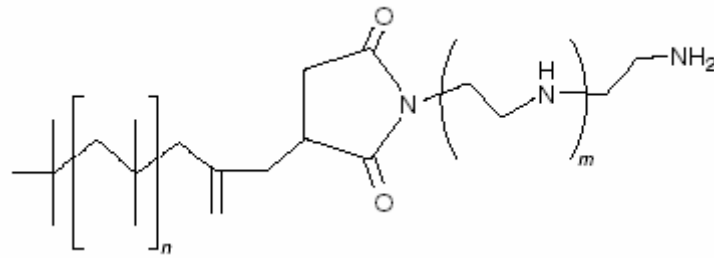


Figure 3. Chemical structure of a detergent additive of the poly(isobutenyl succinimide) type (PIBSI type) [2]

Lubricity Additives

Lubricity additives are used to compensate for the poor lubricity of severely hydrotreated diesel fuels. They contain a polar group that is attracted to metal surfaces, causing the additive to form a thin surface film. The film acts as a boundary lubricant when two metal surfaces come in contact. Two additive chemistries, fatty acids and esters, are commonly used. The fatty acid type is typically used in the concentration range of 10ppm to 50ppm. Since esters are less polar, they require a higher concentration range of 50ppm to 250ppm.

Smoke suppressants

Some organometallic compounds act as combustion catalysts. Adding these compounds to fuel can reduce the black smoke emissions that result from incomplete combustion. These additives are often used in vehicles equipped with particulate traps to lower particulate emissions.

1.3.2 FUEL HANDLING ADDITIVES

Antifoam additives

Some diesel fuels tend to foam as they are pumped into vehicle tanks. The foaming can interfere with filling the tank completely, or result in a spill. Most antifoam additives are organosilicone compounds and are typically used at concentrations of 10 ppm or lower.

De-icing additives

Free water in diesel fuel freezes at low temperatures. The resulting ice crystals can plug fuel lines or filters, blocking fuel flow. Low molecular weight alcohols or glycols can be added to diesel fuel to prevent ice formation. The alcohols/glycols preferentially dissolve in the free water, giving the resulting mixture a lower freezing point than that of pure water.

Low temperature operability additives

There are additives that can lower a diesel fuel's pour point or cloud point, or improve its cold flow properties (see *Table 2*). Most of these additives are polymers, such as ethylene-vinyl acetate copolymers (EVA) or polyacrylates with long linear alkyl chains, which interact with wax crystals that are formed in diesel fuel when it is cooled below the cloud point. The polymers mitigate the effect of wax crystals on fuel flow by modifying their size, shape and/or degree of agglomeration. Polymer/wax interactions are fairly specific, so a particular additive generally will not perform equally well in all fuels. The best additive and treat rate for a particular fuel can not be predicted, but it must be determined experimentally.

Additive type	Typical treat rate [ppm]	Typical benefit* [°C]
Cloud point	200-2000	3-4
CFPP	100-2000	15-20
Pour point	100-300	30-40

* Reduction from value for unadditized fuel

Table 2. Low temperature operability additive benefits [3]

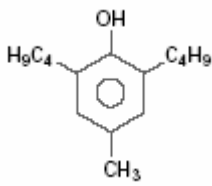
Drag reducing additives

Pipeline companies sometimes use drag reducing additives to increase the volume product they can deliver. These high molecular weight polymers reduce turbulence in fluids flowing in a pipeline, which can increase the maximum flow rate by 20% to 40%. Drag reducing additives are typically used in concentrations below 15ppm. When the additized product passes through a pump, the additive is broken down (sheared) into smaller molecules that have no effect on product performance in engines.

1.3.3 FUEL STABILITY ADDITIVES

Fuel instability results in the formation of gums that can lead to injector deposits or particulates that can plug fuel filters or the injection system. The need for a stability additive varies widely from one crude to another, since it depends on the crude oil source and the refinery processing and blending. Stability additives typically work by blocking one step in a multi-step reaction pathway.

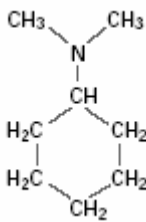
Antioxidants



2,6-di-t-butyl-4-methyl-phenol

One mode of fuel instability is oxidation, in which oxygen of dissolved air attacks reactive compounds in the fuel. This initial attack sets off complex chain reactions. Antioxidants work by interrupting the chains. Hindered phenols and certain amines, such as phenylenediamine, are the most commonly used antioxidants. They are typically used in the concentration range of 10 ppm to 80 ppm.

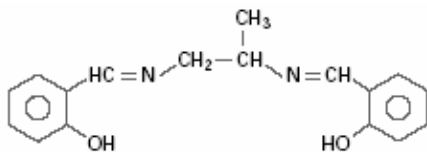
Stabilizers



N,N-dimethylcyclohexyl amine

Acid-base reactions are another mode of fuel instability. Stabilizers used to prevent these reactions typically are strongly basic amines and are used in the concentration range of 50 ppm to 150 ppm. They react with weakly acidic compounds to form products that remain dissolved in the fuel, but do not react further.

Metal deactivator



N,N-disalicyclidene-1,2-propanediamine (DMD)

When trace amounts of certain metals, especially copper and iron, are dissolved in diesel fuel, they catalyze the reactions involved in fuel instability. Metal deactivators chelate these metals, neutralizing their catalytic effect. These additives are typically used in the concentration range of 1 ppm to 15 ppm.

Dispersants

Multi-component fuel stabilizer packages may contain a dispersant. Dispersants do not prevent fuel instability reactions, but they disperse the particulates being formed, preventing them from clustering into aggregates large enough to plug fuel filters or injectors. They are typically used in the concentration range of 15 ppm to 100 ppm.

1.3.4 CONTAMINANT CONTROL

This class of additives is mainly used to deal with storage problems.

Biocides

The high temperatures involved in refinery processing effectively sterilize diesel fuel. But it quickly becomes contaminated with microorganisms present in air or water. Although growth of microorganisms can occur in working fuel tanks, static tanks used for storage purposes are a much better growth environment when water is present. Biocides are typically used in the concentration range of 200 ppm to 600 ppm.

Demulsifiers

Normally, hydrocarbons and water separate rapidly and cleanly. But if the fuel contains polar compounds that behave like surfactants and if free water is present, the fuel and water can form an emulsion. Any operation which subjects the mixture to high shear forces, like pumping the fuel, can stabilize the emulsion. Demulsifiers are surfactants that break up emulsions and allow fuel and water phases to separate. They are typically used in the concentration range of 5 ppm to 30 ppm.

Corrosion inhibitors

Since most of petroleum pipes and tanks are made of steel, the most common corrosion is the formation of rust in the presence of water. Over time, severe rusting can eat holes in steel walls, creating leaks. More immediately, the fuel is contaminated by rust particles, which can plug fuel filters or increase fuel pump and injector wear.

Among all diesel fuel additives explained above, the most important ones are those which improve low temperature flow properties, injector cleanliness additives and cetane number boosters. However, these additives are expensive and are always used in very small amounts.

1.4 CONSUMPTION OF DIESEL FUEL

In contrast to the U.S. market, which is clearly gasoline dominated, the European consumption of diesel fuel is much higher than of gasoline, and it is increasing year by year, as it is shown in Figure 4.

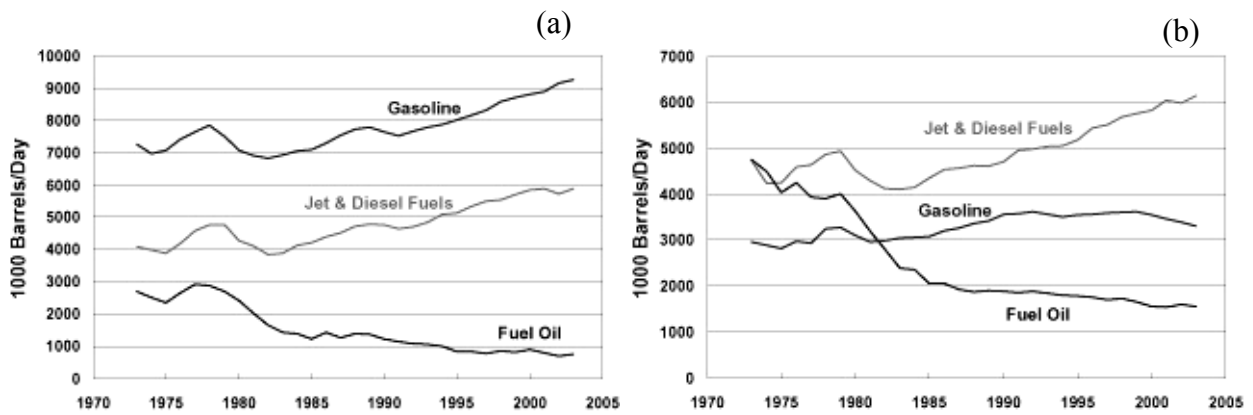


Figure 4. U.S. (a) and European (b) fuel consumption trends [4]

As for the Spanish market (see *Figure 5*), a similar trend is observed: an increase of the consumption of diesel fuels (an average annual ratio of 8.0 since 1997) and a decrease of gasoline's (an average annual ratio of -2.3% since 1997).

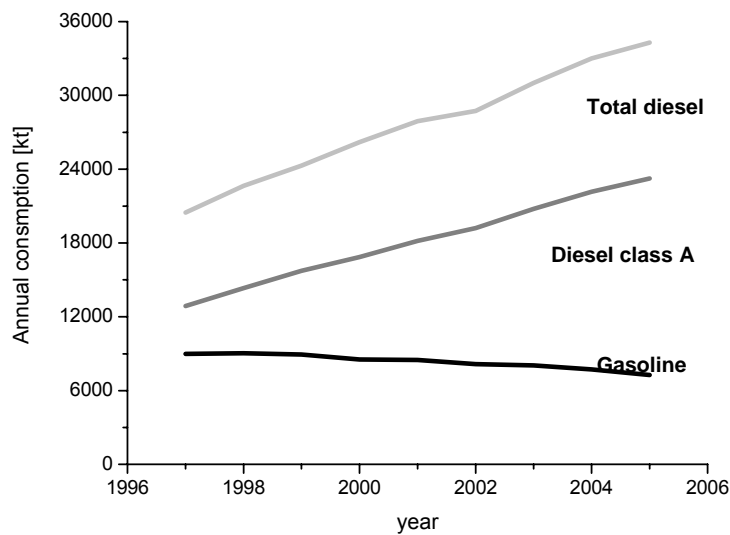


Figure 5. Spanish fuel consumption trends [5]

1.5 REFORMULATION OF DIESEL FUELS

As a consequence of the growing awareness of mankind to the potential damage to the earth's ecosystem, a fuel revolution is taking place: *reformulated fuels* are defined on a chemical composition base with additional performance standards rather than on a behavior base [6].

Diesel fuel specifications are becoming increasingly stringent as legislation is adopted to improve air quality by reducing emissions. As it can be seen in *Table 3*, the main attention has been focused on the sulfur content, lowering its standard from 500 to 50 mg/kg in six years, and with the objective of 30 mg/kg or even less in the horizon; since the contribution of sulfur content of diesel fuel to exhaust particulates has been well established [7].

	units	Before 2000	2000	2006
Sulfur	mg/kg	500	350	50
Density	kg/m ³ , max	860	845	845
Cetane number	min	49	51	51
T ₉₅	°C, max	370	360	360
PAH ^a	wt.%, max	n. r. ^b	11	11

^a Polyaromatic hydrocarbons

^b Not restricted

Table 3. Evolution of standards fixed by the European Union over the last years [8]

In addition to sulfur content, other contaminants have been studied, such as CO₂, CO, NO_x, olefins and aromatics. In *Table 4* the main exhaust contaminant gases and their major effects are shown.

Forthcoming diesel fuels will be likely characterized by a higher cetane number, lower density, and lower aromatics, polyaromatics and sulfur contents with respect to the current ones. A feasible option to comply with these regulations might be the use of reformulated diesel fuels containing appropriate high quality components [9], e.g. oxygenates, since classical diesel additives are too expensive to be used in great quantities.

Specie	Toxic	Non-toxic	Short range	Long range	Effect
CO ₂		X		X	Greenhouse
CO	X		X		Lethal effects
NO _x	X		X	X	O ₃ depletion contribution
Olefins		X		X	O ₃ depletion
SO _x	X		X		Acid rains
Benzene	X		X		Carcinogenic

Table 4. Main exhaust gases and their effects [6]

The ideal characteristics of an oxygenate compound to blend with diesel fuel are [10]:

- ✓ High cetane number
- ✓ High boiling point to satisfy the flash point specifications
- ✓ Good low temperature behavior, i.e. low CP and CFPP
- ✓ Miscibility with various types of diesel fuels
- ✓ Suitable density
- ✓ Feasible feedstock

During the 90's, researchers sought for ways to oxygenate diesel. However, most conventional fuel oxygenates, such as MTBE, TAME, MEK, etc., were not suitable for diesel fuel use. Ethanol as a diesel oxygenate, while compatible, does not blend effectively with diesel, since ethanol-diesel blends phase separate when exposed to small amounts of water and/or low temperatures, and other compounds must be added to assure a good blending [11]. Other alcohols were rejected due to their low cetane number [12].

In a comprehensive study on the blending properties of oxygenates in diesel fuels [12], eighty-four compounds were tested, including monoethers, polyethers and esters. It was observed that symmetrical and asymmetrical linear monoethers with ≥ 9 carbon atoms showed the best balance among blending cetane number and cold flow properties. In *Table 5* characteristics of some linear ethers as fuel component are shown.

	Diesel	DNPE	DNHE	MOE	DNPM
Density at 15-20°C (kg/m ³)	850	787	793	790	840
Boiling point (°C)	170-380	187	229	N/A	218
Viscosity (cSt)	3-4	1.6	N/A	0.9	N/A
Cetane number	48-51	109	118	89	97
CP (°C)*	-2 a +5	-20	-5	-17	0
CFPP (°C)*	-4 a +3	-22	-7	N/A	-7
Flash Point (°C)*	67	57	78	N/A	N/A

*blending properties; N/A not available

Table 5. Properties of some linear ethers [13]

In another study [14], two compounds, di-n-pentyl ether (DNPE) and di-n-pentoxymethane (DNPM), chosen because of their blending cetane number and large availability of the raw materials to produce them, were tested in an experimental engine. It was found that adding up

to 33% v/v of any of these compounds, an increase of 15 points in the blending cetane number was achieved. Furthermore, aromatics and sulfur contents decreased 12 and 0.35 points, respectively, due to dilution.

Marchionna et al. [15] studied the synthesis process of methyl-n-octyl ether (MOE) and compared its properties to DNPE and other diesel fuels. Their conclusions indicated that both linear ethers have similar properties as fuel additives, such as cetane number and low temperature behavior, but DNPE is preferred due to its more feasible feedstock.

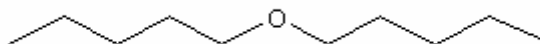
Van Heerder et al. [16] studied the effect of DNPE and di-n-hexyl ether (DNHE) on diesel engines. DNHE has a higher cetane number than DNPE, and both improve reformulated diesel properties such as viscosity and aromatics and sulfur contents. Notwithstanding, DNHE has both CP and CFPP considerably higher than DNPE, which is an important drawback.

Thus, it can be concluded that, from a technical point of view, DNPE is a suitable oxygenate to blend with diesel fuel, since it improves all diesel properties, and there is an attractive availability of potential feedstocks. Moreover, DNPE has shown to be very effective in reducing diesel exhaust emissions such as CO, NO_x, unburned hydrocarbons, particulates and smokes.

1.6 DI-N-PENTYL ETHER

1.6.1 PROPERTIES OF DNPE

DNPE (1,1'-oxybis pentane, amyl ether or 1-(pentoxy)pentane) is a symmetrical linear ether of 10 carbon atoms, C₁₀H₂₂O, with the following structure:



It is a colorless liquid, stable, volatile and its solubility in water is very low (< 0.3% wt., 12 times lower than MTBE). Although not being completely biodegradable, is nearly 15 times more biodegradable than MTBE. Information about the toxicological properties are scarce, but they do not seem to cause any particular concern.

DNPE has been chosen due to its blending properties with diesel fuel. When it is added to diesel, all properties are sensibly improved, as it can be seen in *Table 6*.

	Diesel	Diesel + DNPE (20%)	DNPE
Density, kg/m ³	848	835	787
Cetane number	51	62	109*
Pour point, °C	-9	-12	-25*
Cloud point, °C	-2	-6	-20*
CFPP, °C	-15	-17	-22*
Viscosity, cSt	3.6	3.3	1.6
Sulfur, mg/kg	350	280	-
Aromatics, %	37	29	-

*blending properties

Table 6. DNPE improvement in Diesel properties [10]

Another aspect that makes DNPE an interesting compound is the increase on the operating life of diesel engines in relation to the one predicted from its cetane number, due to the presence of the oxygen atom, since it causes a decrease on particulate [17] and NO_x. This is very important because NO_x and particulate represent the major pollutants from diesel engines and generally most measures to reduce NO_x emissions, especially in engine technology, cause an increase in particulate, and viceversa [10].

1.6.2 DNPE SYNTHESIS ROUTE

1-butene is an appropriate feedstock for obtaining DNPE in refinery. It could be obtained from dehydrogenation of n-butane, or as a by-product of some processes in plant, i.e. steam cracking. The synthesis route would consist of selective hydroformylation and hydrogenation of 1-butene to 1-pentanol, followed by the bimolecular dehydration reaction of the alcohol to di-alkyl ether.

In *Figure 6* a possible process flowsheet is shown: n-butane is dehydrogenated to 1-butene and butadienes. The latter are transformed into 1-butenes with a Selective Hydrogenation Unit (SHP). With a hydroformylation step, 1-butenes are converted into 1-pentanal, which is hydrogenated to 1-pentanol. Finally, DNPE is obtained by dehydration of the alcohol. The hydroformylation and subsequent hydrogenation of 1-butene also produces 2-metil-1-butanol, inevitably. The selectivity of this step is quite important, as it will be shown later in *section 4*.

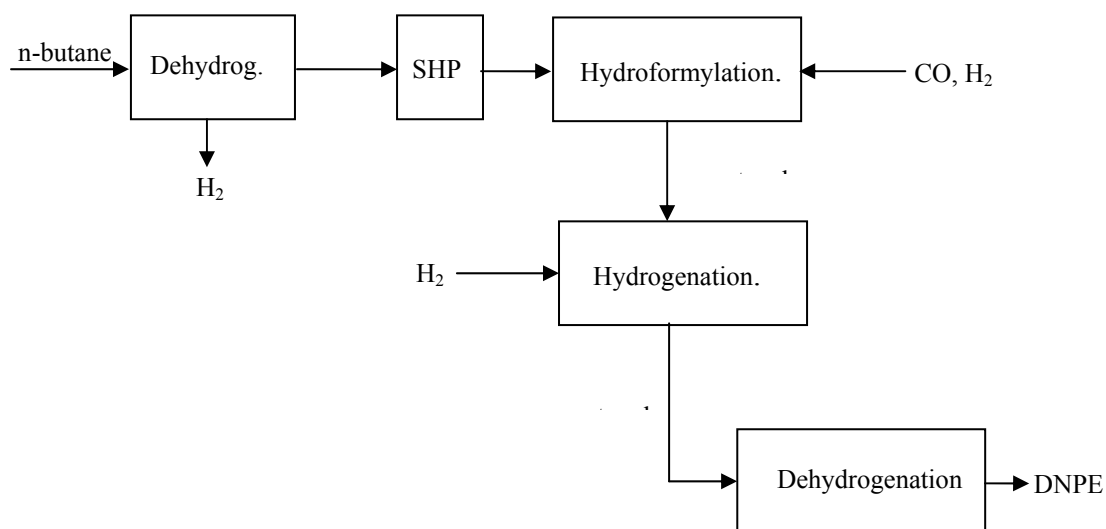
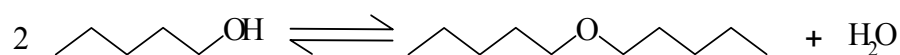


Figure 6. DNPE synthesis route

1.6.3 DEHYDRATION OF 1-PENTANOL TO DNPE

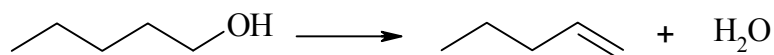
This work is focused on the intermolecular dehydration of 1-pentanol to DNPE. It is necessary the presence of an acid catalyst in order that the reaction takes place. Unfortunately, side reactions are inevitable. The reaction scheme is presented subsequently [18]:

Main reaction

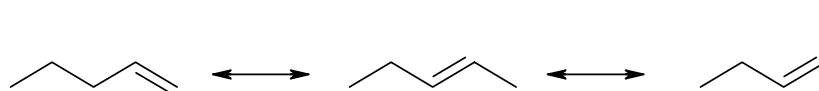


Olefins formation

Intramolecular dehydration of 1-pentanol to 1-pentene.

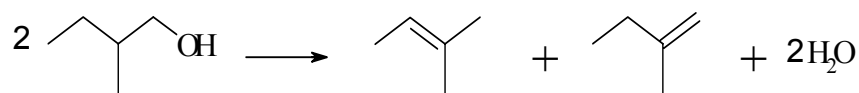


In acid catalysis, 1-pentene isomerization to 2-pentene (cis and trans) might occur

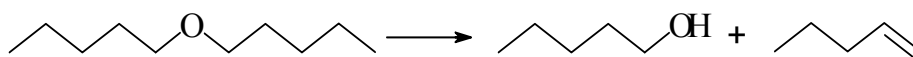


2-methyl-1-butanol, an impurity of 1-pentanol, can also dehydrate to form 2-methyl-1-butene

and 2-methyl-2-butene.

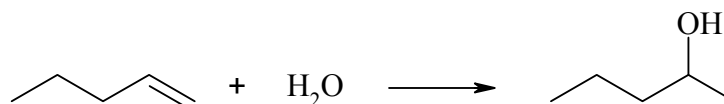


DNPE can decompose to 1-pentanol and 1-pentene.

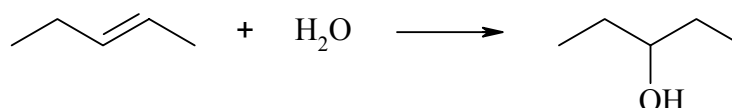
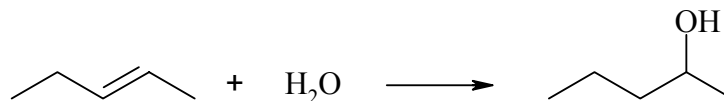


Olefin hydration

Olefins formed can react with water to form the corresponding alcohols. Thus, 1-pentene reacts with water to give 2-pentanol.



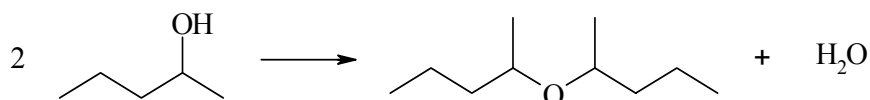
2-pentene can react with water to form 2-pentanol or, in less extent, 3-pentanol.



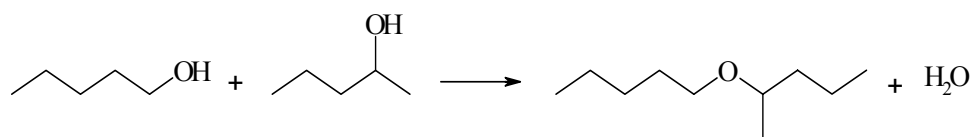
Branched ethers formation

Besides 1-pentanol, other alcohols of the reacting mixture can also dehydrate to form ethers.

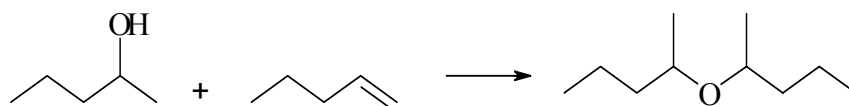
2,2-oxybis pentane can be formed by dehydration of 2-pentanol.



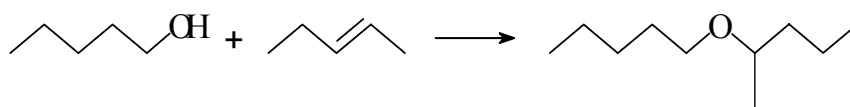
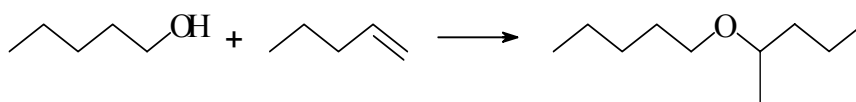
1,2-oxybis pentane can be obtained by 1 and 2-pentanol intermolecular dehydration.



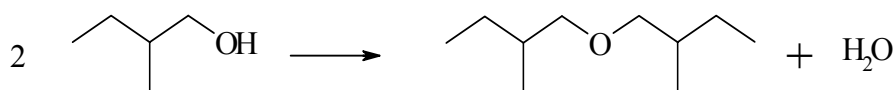
These ethers can also be formed by alcohol-olefin reaction. Thus, 2,2-oxybis pentane by 2-pentanol and 1 or 2-pentene reaction.



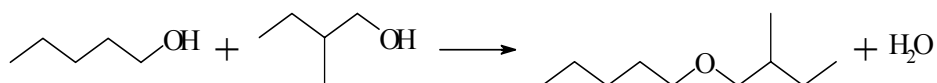
1,2-oxybis pentane by 1-pentanol and 1- or 2-pentene reaction.



By means of 2-methyl-1-butanol dehydration, 2-methyl-1-butyl ether is formed.



2-methyl-1-butyl 1-pentyl ether from 1-pentanol and 2-methyl-1-butanol.



2-methyl-1-butyl 2-pentyl ether by 2-pentanol and 2-methyl-1-butanol dehydration.

1.7 CATALYST DESCRIPTION

In order the reaction to occur, the presence of protons in the reacting medium is required. These will be provided by an acidic catalyst.

Catalysts are first classified into homogeneous and heterogeneous. Heterogeneous catalysts offer distinct advantages over homogeneous, both from technical and environmental standpoints. The advantages of a solid include reduced equipment corrosion, ease of product separation, less potential contamination in waste streams and recycle of the catalyst [19]. Furthermore, using a solid it may also increase the number of processing options such as a glass flow reactor and a fixed bed [20]. So, a solid acidic catalyst is thought to be the best option for the reaction studied.

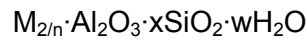
Among solid acidic catalysts a great variety can be found in literature [21]:

- ✓ Oxides such as γ -Al₂O₃, SiO₂, TeO₂
- ✓ Mixed oxides Al₂O₃/SiO₂, MgO/SiO₂, ZrO₂/SiO₂, heteropolyacids
- ✓ Mineral acid supported on porous solids
- ✓ Ion-exchange resins
- ✓ Salts which contain mineral acids
- ✓ Halurs of trivalent metals supported on porous material
- ✓ Zeolites
- ✓ Sulfated superacid solids such as ZrO₂ or TiO₂

The temperature range of the liquid phase dehydration of 1-pentanol is 120-190 °C, since under 120°C the reaction rate is very slow, and 190°C is near the critical temperature of 1-pentene. For this temperature range, the most feasible catalyst groups are zeolites and, above all, some thermostable ion-exchange resins [18,20,22].

1.7.1 ZEOLITES

Zeolites are crystalline aluminosilicates of metals of groups I and II of the periodic table of elements. They can be represented by the following general formula:



where n is the valence of the cation M and y may vary from 2 to infinite. Structurally, zeolites are crystalline polymers based on a three-dimensional arrangement of TO_4 tetrahedra (SiO_4 or AlO_4^-) connected through their oxygen atom to form subunits (unit cells). In *Figure 7* the structure of zeolite Faujasite Y is shown.

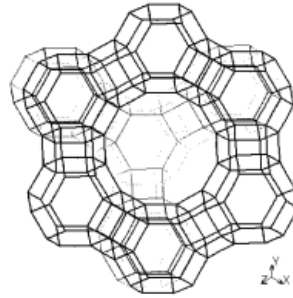
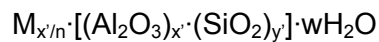


Figure 7. Structure of Faujasite Y

The structural formula of zeolites (i.e. the chemical composition of the unit cells) is the following:



where n is the valence of cation M , $x+y$ the total number of tetrahedra per unit cell, and y/x the atomic SiO_2/Al_2O_3 ratio varying from a minimal value of 1 (Lowenstein rule) to infinite. Metallic cations have some mobility, so they can be exchanged depending on the necessity.

In the ideal crystalline structure appears a uniform distribution of apertures. Diameters of these apertures range from 0.3 to 0.8 nm. Most of the zeolites can be classified into three categories:

- ✓ Small pore zeolites with free diameters of 0.3-0.45 nm
- ✓ Medium pore zeolites, 0.45-0.6 nm
- ✓ Large pore zeolites, 0.6-0.8 nm

However, the pore-openings of zeolite are temperature-dependant and after-synthesis treatments have also much influence on them [23].

In the last years, more attention has been paid to acid catalysts properties of zeolites, due to its great activity and selectivity, since they are stable up to very high temperatures and against oxidation-reduction reactions.

Catalyst properties of zeolites can be modified by means of different treatments, not only its acid or basic character, but also its selectivity (by changing its structure and pore diameter). Furthermore, they can be used as carriers for metallic catalysts or as a part of a bifunctional catalyst.

1.7.2 ION-EXCHANGE RESINS

Ion-exchange resins are organic solids formed by a polymeric matrix and an ensemble of functional groups which are bonded to the matrix. The polymeric matrix is made of hydrocarbon chains bonded together forming a three-dimensional hydrophobic structure, while functional groups are of hydrophilic nature. This structure makes ion-exchange resins insoluble in solvents that do not break carbon-carbon bonds of the matrix.

Although in a solid of this nature it is not appropriate to talk about pores, the space limited by the polymeric chains is called resin pore volume [24]. By adsorption of chemicals in the inner pores, the matrix can swell [25], the capacity to which depends on the nature of the resin and on the polarity of the medium. If the reaction medium contains different species, the more solvating one will be preferably adsorbed [19].

The chemical, thermal and mechanical stability depend on (1) the structure and cross-linking degree of the matrix, and (2) on the nature of the functional groups. The stiffness and mechanical stability of resins increase on increasing the crosslinking degree, but the thermal stability decreases.

Ion-exchange resins are used to exchange the ions of the functional group bonded to the polymeric matrix with the medium. Thus, its chemical behavior stem from the nature, number and distribution of the functional groups and of the matrix.

They can be classified on the basis of different criteria. If the **functional or active group** is taken into consideration, ion-exchange resins can be:

- ✓ Cationic: The active group is an acid on the protonic form. Among cationic

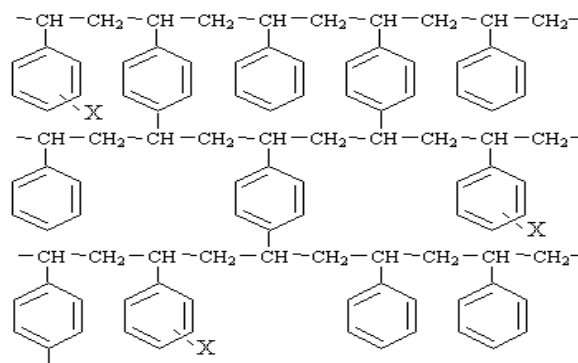
resins, strong (with sulfonic groups) or weak (with carboxylic groups) acid resins can be found.

- ✓ Anionic: The active group is a base or an organic salt. Among anionic resins, strong (quaternized ammonium group) or weak (tertiary amine groups) basic resins can be found.
- ✓ Mixed: Groups with simultaneously acid and basic character are bonded to the matrix. Among this class, aminophosphoric and aminocarboxylic resins can be found.

Ion-exchange resins can be also classified on the basis of its **polymeric matrix**. The most common are styrene divinylbenzene copolymers and perfluoroalkane sulfonic resins, though other types (e.g. polyacrylic) with their own characteristics exist.

1.7.2.1 STYRENE DIVINYLBENZENE RESINS

The polymerization of styrene yields linear polystyrene. When some divinylbenzene is added together with styrene, a tridimensional insoluble matrix of styrene-divinylbenzene (S-DVB) is then formed (*Figure 8*). Based on their structure S-DVB resins can be divided into two main classes:



X = functional group

Figure 8. Styrene-divinylbenzene matrix

- ✓ Microporous or gel-type resins: generally low crosslinked (1-8% DVB), they are solids with low surface areas in dry state ($< 1 \text{ m}^2/\text{g}$), which do not have permanent porosity, but swell to some extent in polar solvents [19]. Their pores, referred to as micropores, are very small (0.7 to 2 nm) [26], and only appear in the swollen state. Just like the surface area, the porosity decreases on increasing

% DVB, so that in microporous resins with more than 8% DVB only the external surface is accessible.

- ✓ **Macroporous resins:** they are obtained when the polymerization of styrene is carried out with 5-60 %DVB and in the presence of diluents, such as heptane, otherwise referred to as porogens. During the polymerization, phase separation occurs and, after the extraction of the diluent and drying, permanent pores or holes of various sizes are created, see *Figure 9*. Macroporous resins consist of large agglomerates of gel micro-spheres, and each micro-sphere shows smaller nodules (10-30 nm) that are more or less fused together. In between the nodules there is a family of very small pores (micropores), which are mainly responsible for the high surface area of these materials. In between the micro-spheres a second family of intermediate pores with diameter 8-20 nm (mesopores) is observed, which may account for moderate surface areas (up to 100 m²/g). A third family of large pores with diameter 30-80 nm is located between the agglomerates (macropores) [19], which yield very low surface area but large pore volume (up to 3 mL/g). Macropores are permanent and can be detected by standard techniques of pore analysis, e.g. adsorption-desorption of N₂ at 77 K. Meso- and micropores, which appear in polar liquid media able to swell the polymer, are non-permanent and can be detected by characterization techniques in aqueous media, such as Inverse Steric Exclusion Chromatography (ISEC) [27]. When the amount of DVB is increased, the surface area increases, unlike with microporous resins.

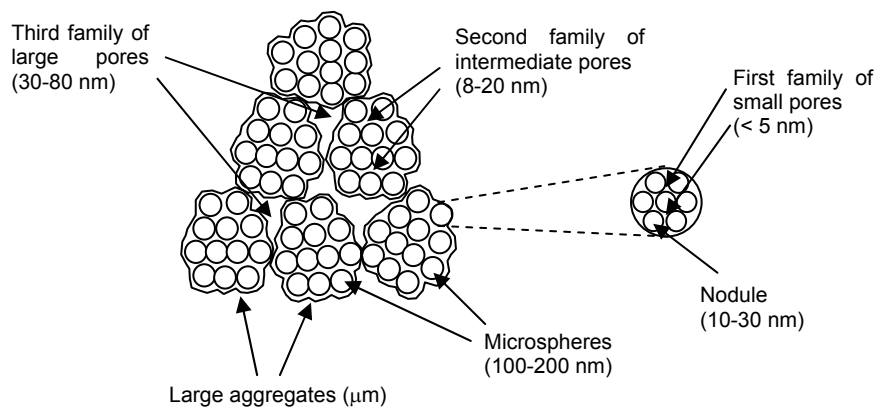


Figure 9. Schematic representation of the structure of a macroporous resin

1.7.2.2 PERFLUOROALKANE SULFONIC RESINS

These resins are known with the commercial name Nafion[®] (developed by Dr. Walter Grot, Du Pont de Nemours and Co., USA, end of 60's). Nafion is a copolymer of tetrafluoroethene (Teflon[®]) and perfluoro[2-(fluorosulfonylethoxy)]-propyl vinyl ether [28]. Its general structure is shown in *Figure 10*.

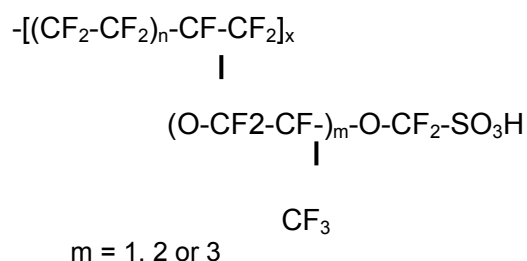


Figure 10. General structure of Nafion

A series of compositions may be produced in which n can be as low as 5 and as high as 13.5. Typically, n is about 6-7. The value of x is about 1000.

A stylized, semi-empirical view of a polar/nonpolar microphase separation in a hydrated ionomer can be seen below in *Figure 11*. This over-simplification shows a phase separated morphology of discrete hydrophobic and hydrophilic regions. The hydrophobic region is composed of the polymer fluorocarbon backbone. On the other hand, the hydrophilic region contains the ionic groups and their counter ions [29]. As a result of electrostatic interactions, these ionic groups tend to aggregate to form tightly packed regions referred to as clusters.

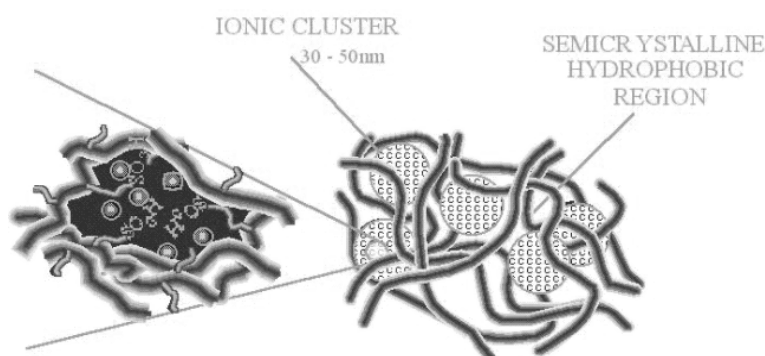


Figure 11. Stylized morphology of Nafion [29]

Perfluorinated resins are quite promising catalysts since they are stable up to 210°C.

Furthermore, due to the presence of F atoms, these catalysts are considered as superacidic, with Hammett acidity functions¹ similar to 100% acid sulfuric and 4 times higher than the one of DVB resins. Nafion resin is available commercially in the form of millimeter sized beads known as Nafion NR50 resin. The main drawbacks of this catalyst are its very low porosity and BET surface area (typically, 0.02 m²/g), which means that most of the active sites are buried within the polymer beads [30]. Moreover, the acid capacity is also very low (about 0.8 eq H⁺/kg). These three characteristics affect the catalytic activity of the catalyst directly and negatively, either in non-swelling solvents or in the gas phase [20].

In order to increase the acid site accessibility of Nafion resin-based catalysts, new classes of solid acid catalysts based on Nafion resin have been developed [20,30,31]:

- ✓ Nafion/Silica nanocomposite: known by the commercial name SAC, it consists on nanometric particles (10-20 nm) of Nafion resin entrapped in a porous silica framework. Thus, the surface area of the dispersed Nafion in the composite is much larger than that of the original Nafion material, resulting in a much improved accessibility of the acid sites on the catalyst. Furthermore, this composite can be used in reaction media which do not cause swelling of the Nafion resin, i.e. nonpolar solvents. The composites can be obtained by sol-gel coprecipitation of nano-sized Nafion particles and a silica source [32].
- ✓ Supported Nafion catalysts: They are Nafion particles supported on porous carriers which give much more surface area (up to 500 m²/g) and they can be prepared by simple techniques, such as impregnation.

1.7.2.3 PROPERTIES OF ION-EXCHANGE RESINS

The catalytic behavior of ion-exchange resins depends on their structure and on the number of accessible active sites. The higher the ion mobility within the resin, the less the differentiation in the adsorption process is. That is to say, the resin is more active but less selective. Therefore, the pore structure and the ability to swell of the catalyst have a great importance because they affect directly the diffusion of reactants and products, and, consequently, they affect the activity and the selectivity of the resin. On the other hand, the catalytic behavior is also influenced by the acidic (or basic) strength of the resin.

¹ See section 1.6.2.3

Subsequently, the most important properties of ion-exchange resins will be explained:

Crosslinking degree (S-DVB resins), porosity, surface area and swelling properties

The crosslinking degree, normally expressed as %DVB because it is the most common crosslinker, shows the weight percentage of crosslinker with respect to the total amount of monomers. However, the effective crosslinking degree is always less than the computed from initial monomer composition since the copolymerization is not uniform. The stiffness and mechanical stability of resins is enhanced on increasing the crosslinking degree, but the thermal stability decreases.

The porosity of ion-exchange resins is associated to the holes between the chains that form the tridimensional matrix. It is highly dependant on the crosslinking degree: on decreasing the %DVB, the porosity increases while the density decreases. In dry state gel-type resins do not present porosity, but it appears in swollen state. On the contrary, macroporous resins have permanent porosity.

The exchange capacity, water content, and swelling properties of resins increase on decreasing %DVB. Ion-exchangers with high %DVB present internal mass transfer limitations due to the high density of the matrix. In fact, from 10-12% DVB the number of accessible active sites decreases dramatically.

Another characteristic that is bonded to the crosslinking degree is the surface area. On macroporous resins, on increasing the %DVB, the surface area increases. On the other hand, the opposite behavior is observed on gel-type resins: the surface area increases on decreasing %DVB, but it only appears in the swollen state.

The swelling properties of gel-type resins are also dependent on the crosslinking degree. The swelling ratio increases as the amount of DVB decreases. When the crosslinking density is not locally homogeneous, the swelling ratio will also be non-uniform. The situation is more complex for the macroporous resins, which involve a polymer phase and the free space of the pores. In the presence of a polar medium, the pores are filled by the liquid and the polymer phase may be swollen to a varying extent. The swelling behavior of the polymer phase is the same as that of gel-type resins, except that the crosslinking degree is higher and probably more homogeneous [19].

Exchange capacity

The exchange capacity shows the number of functional groups that are accessible in given conditions. It is usually expressed as equivalents per mass or volume of resin and it is commonly determined by titration against standard base.

Again, the number of accessible functional groups depends on the resin structure and on the solvent properties of the medium.

Stability

The stability of resins is a key-factor since they are thought to be operative during long time. Catalysts should have high chemical, thermal and mechanical stability.

- ✓ Chemical stability: Under very oxidant conditions, namely in the presence of Chlor or Chromic acid, oxidizing agents may react with the polymer matrix causing a loss of exchange capacity and partial dissolution of the resin. As regards S-DVB resins, these substances destroy the crosslinking degree, as it is shown in *Figure 12*.

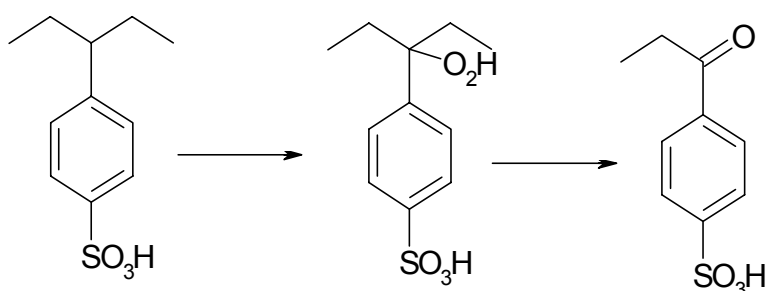


Figure 12. Degradation of a S-DVB resin

- ✓ Thermal stability: the thermal stability of ion-exchange resins depends on the structure of the polymeric structure and on the functional groups. The stability of Sulfonic S-DVB resin matrix depends on the crosslinking degree. Macroporous resins are less stable than microporous. On the other hand, oversulfonated resins are more stable than conventionally sulfonated. In liquid phase, thermal deactivation can occur either by means of sulfonic group hydrolysis or due to the formation of sulfone-bridge bonds.
- ✓ Mechanical stability: the mechanical or physical stability of a catalyst is defined in

the basis of its resistance to attrition and to osmotic shock. In general, macroporous resins are more stable than gel-type.

Density

The density is the weight of dry resin per volume unit. It depends on the matrix structure, on the crosslinking degree and on the nature and quantity of the functional groups. Usually the apparent density of sulfonic S-DVB resins falls in the range 1.14 - 1.45 g/cm³.

Water content

The water content of a ion-exchange resin is defined as the weight of water per total weight of the wet resin. Due to the hygroscopic characteristics of the active sites, ion-exchange resins have bounded water to the solid. They can also have not-bounded water on their surface. The amount of water retained by the resin depends on the number and nature of functional groups, as well as on the density of the polymer matrix. On increasing the crosslinking degree the water content diminishes.

Acidic strength

The acidic strength of a solid is defined as the ability of the surface to convert an adsorbed neutral base into its conjugate acid. If the reaction proceeds by means of proton transfer from the surface to the adsorbate, the acid strength is expressed by the Hammett acidity function H_0 ,

$$H_0 = pK_a + \log \frac{[B]}{[BH^+]} \quad \text{Equation 3}$$

where [B] and [BH⁺] are, respectively, the concentrations of the neutral base and its conjugate acid, and pK_a is pK_{BH^+} [33]. The more negative H_0 is, the more ability of the solid to exchange a proton with the medium.

The acid strength should not be confused with the exchange capacity (acid capacity when the catalyst is acidic).

1.8 KINETIC ANALYSIS

The dehydration of 1-pentanol to DNPE is catalyzed by a solid. In order for the reaction to occur, the reactants must reach the active sites of the catalyst and products should be removed from there to the bulk phase. The diffusion path may be divided into two parts: bulk fluid to the

outer surface of the pellet, and particle surface to active internal surface of the porous solid² [34, chapter 2].

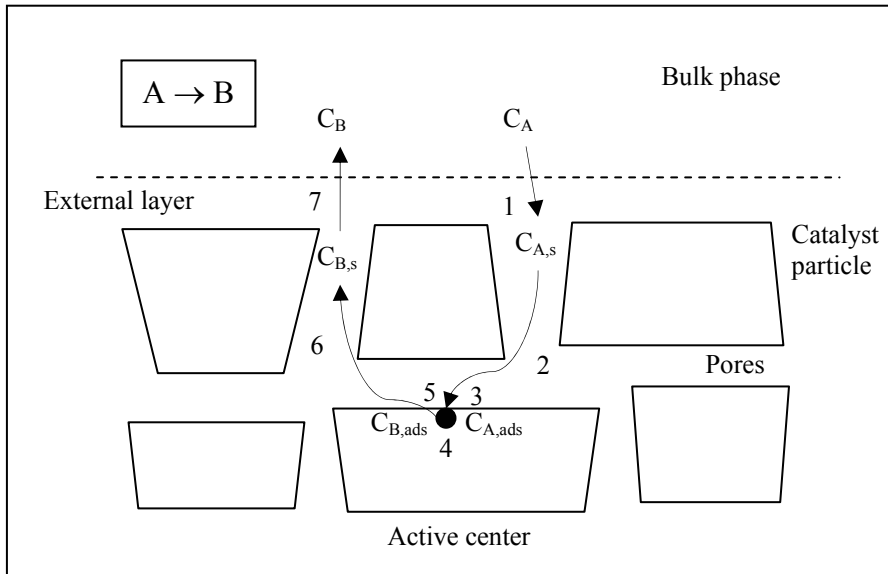


Figure 13. Steps of the catalytic process

1.8.1 STEPS OF A CATALYTIC PROCESS

So, the following steps are assumed in a catalytic process when the catalyst is porous (Figure 13):

1. Mass transfer of reactants from the bulk fluid to the external surface of the catalyst, named external mass transfer (EMT).
2. Diffusion of reactants through the catalyst pores to the active centers, internal mass transfer (IMT).
3. Adsorption of reactants on the active centers.
4. Chemical reaction.
5. Desorption of products.
6. Diffusion of products from the active centers to the external surface of the catalyst, IMT.
7. Mass transfer of products from the external surface of the catalyst to the bulk fluid, EMT.

² For non-porous catalysts, this latter step does not occur.

Steps 1, 2, 6 and 7, concerning EMT and IMT, are of physical nature, while steps 3, 4 and 5 are of chemical nature. The latter are grouped together under the term surface reaction.

1.8.1.1 EXTERNAL MASS TRANSFER

When a fluid passes over the surface of a particle, a laminar layer is developed in which the velocity parallel to the surface varies rapidly over a very short distance normal to the flow. The fluid velocity is zero at the solid surface but approaches the bulk-stream velocity at a plane not far from the surface. Thus, a stagnant boundary layer is formed, where the velocity of the fluid is low and there is little mixing [34].

The transfer of reactant from the bulk phase to the outer surface of the catalyst particle requires a driving force, the concentration difference. Whether this difference in concentration in the layer is significant or negligible depends on the velocity pattern in the fluid near the surface, on the physical properties of the fluid, and on the intrinsic rate of the chemical reaction at the catalyst; that is, depends on the mass transfer coefficient between fluid and surface and the rate constant for the catalytic reaction. The same reasoning suggests that there will be a temperature difference in the layer. Its magnitude will depend on the heat transfer coefficient between the fluid and catalyst surface, the reaction rate constant, and the heat of reaction.

In any case, i.e. concentration and/or temperature profile in the layer, the observed (global) rate is different than the intrinsic one evaluated at the concentration of reactant (or temperature) in the bulk fluid [35].

How these external physical processes affect the global rate can be studied quantitatively [34,35,36], but the ability to success on it depends on the availability of data or suitable correlations for the mass transfer and heat transfer coefficients.

On the other hand, it is possible to check the limitations of mass (and temperature) transfer by means of simple experiments: by evaluating the obtained global reaction rate at different velocity patterns in the fluid near the surface. That is to say, in the case of a stirred tank, by changing the stirring speed. If doing so, it is expected that the global reaction rate varies on increasing the stirring speed until a plateau is reached. Assuming that there are not internal mass transfer limitations, in the plateau the concentration profile is negligible, so the reaction rate is the intrinsic one.

1.8.1.2 INTERNAL MASS TRANSFER

Essentially all the active surface of porous catalyst particles is internal. The reaction that occurs within the pellet consumes reactant and evolves (or absorbs) the heat of reaction. This, in turn, induces internal concentration and temperature gradients which can be large enough to cause a significant variation in rate of reaction with position inside the catalyst particle [35]. The apparent activation energy, the selectivity, and other important observed characteristics of a reaction are also dependent upon the magnitude of these concentration gradients [34].

Because there is a continuous variation in concentration and temperature with the radius of the pellet, differential conservation equations are required to describe the concentration and temperature profiles. These profiles are used with the intrinsic rate equation to integrate through the pellet and thus obtain the average rate for the pellet. The differential equations involve the effective diffusivity and thermal conductivity of the porous pellet. This data is not always available, and it is difficult to predict them accurately [35].

Again, by means of simple experimentation it is possible to discern whether intraparticle mass and heat transfer is important or negligible. It is well accepted that all intrapellet transport effects will become less important as the pellet size decreases. Thus, analyzing the reaction rate of experiments with the same catalyst mass but different particle size, it is possible to determine from which d_p intraparticle mass and heat transfer limitations become important.

1.8.1.3 SURFACE REACTION

As commented before, the term surface reaction includes three steps: adsorption of reactants on the active centers, chemical reaction and desorption of products. Two types of adsorption are possible: physical and chemical adsorption, or chemisorption.

Physical adsorption is nonspecific and somewhat similar to the process of condensation. The forces attracting the fluid molecules to the solid surface are relatively weak, of the magnitude of van der Waals forces, and activation energies of this type of adsorption are low. It cannot explain the catalytic activity of solids for reactions between relatively stable molecules, because there is no possibility of large reductions in activation energy. Moreover, the amount of physical adsorption decreases rapidly as the temperature is raised, and the temperature at which most catalytic reactions occur is high enough to limit it [35]. However, physical-adsorption studies are valuable in determining total particle area, and it also provides the basis for estimating pore volume and size and distribution of pore radii [37].

Chemisorption is specific and involves forces much stronger than physical adsorption. Adsorbed molecules are held to the surface by valence forces of the same type as those occurring between atoms in molecules, being the activation energy of chemisorption of the same magnitude as for chemical reactions. An important feature of chemisorption is that its magnitude will not exceed the one corresponding to a monomolecular layer, the opposite to physical adsorption where multilayer adsorption occurs. This limitation is due to the fact that the valence forces holding the molecules on the surface diminish rapidly with distance, being too small to form the adsorbed compound when the distance from the surface is much greater than usual bond distances.

Two kinds of chemisorption are encountered: activated and, less frequently, non-activated. The first means that the rate varies with temperature according to a finite activation energy in terms of the Arrhenius equation. However, in some systems chemisorption occurs very rapidly, suggesting activation energy near zero, named non-activated chemisorption. It is often found that for a given gas and solid the initial chemisorption is nonactivated, while later stages of the process are slow and temperature dependent (activated adsorption) [35]. Chemisorption is very important since it constitutes the key step in the catalytic sequence [37].

In order to develop rate equations for catalytic reactions quantitative expressions for adsorption are necessary. At a constant temperature, these expressions are called adsorption isotherms. Three classical adsorption isotherms can be found in the literature: Langmuir, Freundlich and Temkin isotherms.

Langmuir isotherm

Irving Langmuir considered that the surface of catalysts was ideal and, hence some assumptions could be made:

1. The solid surface upon which adsorption occurs is homogeneous; i.e., it is energetically uniform, so that the free-energy change is the same for all molecules adsorbed.
2. There is no interaction between adsorbed molecules.
3. All the adsorption occurs by the same mechanism and the heat of adsorption is independent on the surface coverage.
4. The extent of adsorption is less than one complete monomolecular layer on the surface.

Adsorption rate is assumed to be proportional to the fraction of the surface which is unoccupied, $1-\theta$, and the partial pressure of the adsorbing gas, p :

$$r_{ads} = k_{ads} p (1 - \theta) \quad \text{Equation 4}$$

Desorption rate is assumed to be proportional to the concentration of the adsorbed gas (or fraction of the surface occupied, θ):

$$r_{des} = k_{des} \theta \quad \text{Equation 5}$$

At equilibrium, $r_{ads} = r_{des}$. From equations 3 and 4 the Langmuir isotherm can be deduced as follows:

$$\theta = \frac{\frac{k_{ads}}{k_{des}} \cdot p}{1 + \frac{k_{ads}}{k_{des}} \cdot p} = \frac{K_a p}{1 + K_a p} \quad \text{Equation 6}$$

The adsorption equilibrium constant, K_a , is assumed to be independent on the surface coverage and, therefore, adsorption enthalpy and entropy are constant during the adsorption process.

The Langmuir isotherm was proposed for adsorption of gases on solid surfaces, but is also applicable to liquids [35]. The ideality of the solid surface postulated by Langmuir could be summarized in the constancy of the heat of adsorption. Two other classical isotherms concerning real surfaces, i.e. with a dependency of the heat of adsorption on the coverage of the surface, are also found in the literature: Freundlich and Temkin isotherm.

Freundlich isotherm

This isotherm can be derived from the Langmuir isotherm by assuming a logarithmic decrease in the heat of adsorption with θ ,

$$\Delta H_a = -\Delta H_0 \ln \theta \quad \text{Equation 7}$$

The isotherm itself can be written as follows [38]:

$$\theta = c \cdot p^{1/n} \quad \text{Equation 8}$$

Here $n > 1$, and parameters n and c usually both decrease when increasing temperature [38]. Often this equation fits data over a wide range of values of θ and for systems that do not follow the Langmuir isotherm. But even for these systems, the Langmuir isotherm represents data well over a moderate range of coverage [36].

Temkin isotherm

By considering a linear decrease of the heat of adsorption with increasing θ , the Temkin isotherm can be derived from the Langmuir one, resulting in the following expression:

$$\theta = \frac{RT}{q_0\alpha} \ln A_0 p \tag{Equation 9}$$

where q_0 is the differential heat of adsorption at zero surface coverage, $A_0 = a_0 e^{-q_0/RT}$, and a_0 an α are constants.

Other isotherms, as the one proposed by Brunauer, Love and Keenan [39], also consider real surfaces, but they result in complex expressions of difficult application. In fact, the equivalence of the Langmuir, Freundlich, Temkin and Brunauer-Love-Keenan isotherms (see Figure 14) is demonstrated elsewhere [37,40].

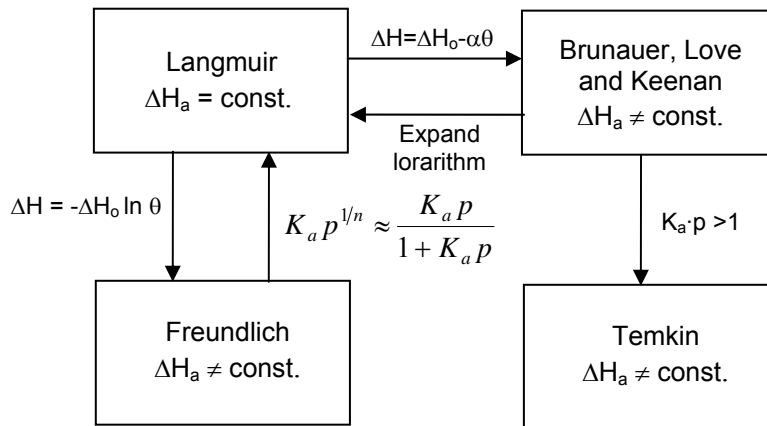


Figure 14. Equivalence of diverse adsorption equilibria

When multicomponent systems with adsorption of many species are encountered, only the Langmuir and Freundlich isotherms can describe them, and the equivalence of the latter two has already been explained. Thus, the ideal approach postulated by Langmuir will be used in this work to deduce the kinetics models.

1.8.2 CORRECTIONS OF CLASSICAL KINETIC MODELS

Although being postulated many years ago, kinetic models derived from Langmuir isotherm are widely used by researchers to describe kinetic mechanisms of liquid phase reactions of alcohol dehydration to ether [41,42,43].

However, in the case of sulfonic styrene-DVB resins sometimes these models do not explain accurately the behavior of the reacting media. A key step of the heterogeneous catalysis process is the adsorption of chemicals on the catalyst, so the interaction among the different species of the medium and the backbone and the active groups of the catalyst is crucial. It is well known that some species are preferably adsorbed on the catalyst, e.g. polar species on sulfonic S/DVB resins. Acidity and availability of sulfonic groups to catalyze the reaction change over the reaction because of swelling of the polymer backbone by the preferential adsorption of polar species (water, alcohol, etc.). To model the effect of such interaction, empirical or pseudo-empirical correction factors for the rate constant are found in the open literature.

Fite et al. included a solubility parameter to emphasize the role of the polarity of the reaction medium on the catalyst activity in the study of the liquid-phase synthesis of MTBE. First they included the Hilderbrandt solubility parameter of reaction media as an empirical correction factor of the kinetic rate constant, $1/\delta_M$, defined as follows:

$$\delta_M = \sum_i \Phi_i \delta_i = \sum_i \Phi_i \frac{\sqrt{\Delta H_{v,i} - RT}}{V_i^L} \quad \text{Equation 10}$$

where $\Delta H_{v,i}$ is the molar enthalpy of vaporization, V_i^L the liquid molar volume and Φ_i is the volume fraction for the pure component i [44]. Other authors also used this empirical correction factor for modeling other reactions [45,46].

Afterwards, Fite et al. developed further the application of the solubility parameters into the kinetic rate equations of the synthesis of MTBE [47]. They introduced a parameter with physicochemical meaning accounting for the interaction between the medium and the resin. The parameter is related to the swelling of resin backbone and to the accessibility to the active centers of a macroporous sulfonic resin. The interaction between the reacting medium and the resin was considered as a solution process. By analogy with the activity of a non-electrolyte in a solvent, the reaction medium-resin affinity can be quantified by means of the following parameter [48]:

$$\Psi = \exp \left[\frac{\bar{V}_M \phi_p^2}{RT} (\delta_M - \delta_p)^2 \right] \quad \text{Equation 11}$$

where \bar{V}_M is the molar volume of the reaction medium, ϕ_p is the volume fraction of the resin, δ_M is the solubility parameter of the reacting medium and δ_p is the solubility parameter of the resin. The parameter δ_p could be estimated by means of a contribution group method or it could be adjusted.

Special attention has to be paid to water. As a highly polar species, it is preferably adsorbed on sulfonic ion-exchange resins and an inhibition effect is attributed to it. Water is supposed to have such a great affinity for sulfonic groups that it excludes the reactants and suppresses the catalytic reaction almost completely [49]. Water effect on the reaction rate has been modeled by correction factors analogous to those mostly used to describe catalyst deactivation by poisoning. The approach is to share the rate constant into the product of the true rate constant and an inhibition factor, which should take values between 0 and 1 and depends on temperature and water concentration in the liquid-phase.

Yang et al. studied the kinetics of the liquid-phase synthesis of tert-amyl methyl ether from tert-amyl alcohol and methanol using Amberlyst 15 as catalyst [50]. The inhibition of water was included in the rate constants as follows:

$$k_i = \frac{k_{i0}}{1 + K_{H_2O} C_{H_2O}} \quad \text{Equation 12}$$

where k_{i0} was the reaction rate constant without the effect of water, and K_{H_2O} was the inhibition coefficient of water, only a function of the temperature.

Limbeck et al. studied the effect of water on the liquid-phase cyclization etherification of 1,4-butanediol to give tetrahydrofuran and water [51]. They proposed the following empirical approach:

$$r = \eta(a_{H_2O}) \cdot k \frac{K_{BD} a_{BD}}{1 + K_{BD} a_{BD}} \quad \text{Equation 13}$$

where

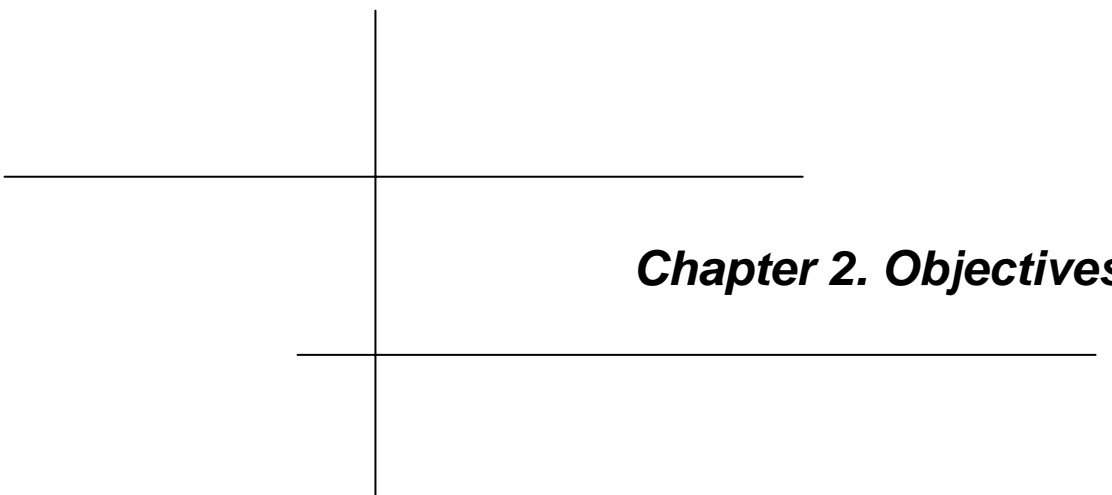
$$\eta(a_{H_2O}) = \frac{1}{1 + K_{H_2O} \sqrt{a_{H_2O}}} \quad \text{Equation 14}$$

The inhibition factor should take a value between 0 and 1 and it depends on the temperature and the activity of water.

Finally, Du Toit et al. studied the inhibiting effect of water on the synthesis of mesityl oxide from acetone. They modeled this effect as if water adsorbed on the catalytic sites, using the Freundlich adsorption isotherm combined with a power law rate expression [52], as follows:

$$r = k_1 \left(c_{Ac}^2 - \frac{1}{K_{eq}} c_{MSO} \cdot c_{H_2O} \right) \left(1 - K_F \cdot (c_{H_2O})^{1/\alpha} \right) \quad \text{Equation 15}$$

where subscripts *Ac* and *MSO* correspond to acetone and mesityl oxide, K_F and α are constants.



Chapter 2. Objectives

2. Objectives

The aim of this work was to study **the liquid-phase dehydration of 1-pentanol to DNPE and water** over acidic catalysts. To achieve this, the following objectives were raised:

1. To make the **start-up** of the experimental setup and **test the influence** of the variables of operation: **catalyst loading, stirring speed** and **catalyst particle size**.
2. To **test different commercial catalysts** in order to select one to perform the kinetic analysis and equilibrium experiments.
3. To study the **thermodynamic equilibrium** of the dehydration of 1-pentanol to DNPE and water.
4. To perform a **kinetic analysis** of the reaction by taking into account the classical **Langmir-Hinshelwood-Hougen-Watson models**-
5. To consider the influence of the products, especially water, on the kinetic equation with the aim to propose **corrected kinetic equations**.
6. To prepare some **Nafion/silica supported catalysts** for the studied reaction in order to increase the surface area of Nafion NR50.



Chapter 3. Experimental

3.1 MATERIALS

In *Appendix IX*, safety cards of the main chemicals used in this work are shown.

3.1.1 CHEMICALS

1-Pentanol (99% pure, <1% 2-methyl-1-butanol and pentanal), 1-pentene (>98,5% pure) and 2-pentene (cis+trans, >98,5%) were supplied by Fluka. Di-n-pentyl ether ($\geq 99\%$) was obtained and purified in the laboratory. Bidistillate water was used. 1,4-Dioxane (99,5%) was supplied by Panreac. 2-methyl-1-butanol ($\geq 98\%$) was used for analysis purposes.

Hydrochloric acid 1M, sodium chloride chemically pure, sodium hydroxide 0.1 M and potassium biphtalate purum (Panreac) were used for titration. Methanol and hexene (Panreac) were used for cleaning purposes, and 2-propanol (Romil) for the impregnation process.

3.1.2 AUXILIARY GASES

Nitrogen (> 99.995 % pure) and Helium (> 99.998 % pure) were used as auxiliary gases. The first was used to pressurize the equipment, and the latter as carrier gas of the chromatograph.

3.1.3 CATALYSTS

In this work several catalysts were tested: (i) the thermal stable resins Amberlyst 70, Amberlyst DL-H/03 and Amberlyst DL-I/03 (the last two were experimental samples) supplied by Rohm and Haas; (ii) conventional S/DVB resins CT-224 (Purolite), four batches of Dowex 50Wx4 (Aldrich) and Amberlyst 36wet (Rohm and Haas); (iii) the perfluoroalkanesulfonic resins Nafion NR50 and Nafion 117 (Aldrich); (iv) a nanocomposite SAC 13 (Aldrich); (v) H-Beta zeolite (Südchemie). Moreover, some catalysts were prepared by impregnation in the laboratory. For this purpose, Nafion perfluorinated ion-exchange resin, 5% wt. (Aldrich), three silicas of nominal surface areas of 200, 300 and 500 m²/g (Davison), three aluminas (α -aluminum oxide 10 m²/g nominal area; weakly acidic Typ 506-C-I Brockman I 155 m²/g nominal area; acidic Typ 504C Brockman I 155 m²/g nominal area; supplied by Aldrich) and a silica-alumina of 600 m²/g nominal area (silica alumina catalyst support, grade 135; supplied by Aldrich) were used.

3.1.3.1 PERFLUOROALKANESULFONIC RESINS

In Table 7 the main characteristics of Nafion-derived catalysts are shown. The three catalysts are stable up to more than 200°C, but their main drawback is their low acidity.

Catalyst	State	% Nafion (w/w)	Shape	Size	Acidity (eqH ⁺ /kg)
NR-50	Solid	100	Sphere	d _p = 2350 μm	0.89
N-117	Solid	100	Membrane	Área: 8 x 10in thickness: 0.007in	0.91
SAC-13	Solid	13	Extrudates	Length= 1 - 4.5mm	0.15
Nafion (5% w/w)	Liquid	5	--	--	--

Catalyst	T _{max} (°C)	ρ _s ^a (g/cm ³)	Water content (%)	S _g ^b (m ² /g)	V _g ^c (cm ³ /g)	d _{pore} (nm)
NR-50	220	2.04	2-3	0.35 ± 0.01	---	---
N-117	200	2	4-5	0.005	---	---
SAC-13	200	2.09	2-3	177 ± 1	0.6	13.6

^a Skeletal density, measured by Helium displacement; ^b Surface Area, BET method (N₂ for S_g ≥ 1 m²/g; Kr for S_g < 1 m²/g); ^c Pore volume, determined by adsorption of N₂ at 77 K and P/P₀ = 0.99

Table 7. Properties and structural parameters of perfluoroalkanesulfonic resins

Nafion NR50

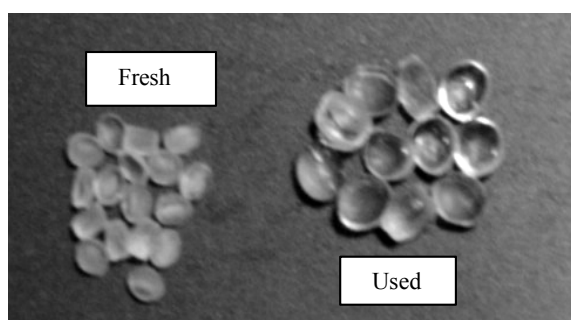


Figure 15. Swelling of Nafion NR50

Nafion NR50 is a gel-type resin as it does not present pores in dry state. It has a very low surface area, but it swells during the experiment, as it can be seen in Figure 15. It consists on big dense spherical particles with only 0.81 eq H⁺/kg, but with a great acidic strength. The lack of porosity can also be observed in Figure 16, where a SEM (Scanning electronic microscopy) image is shown.

In the foreground of the picture cut up Teflon fibers can be observed, while in the background the compact structure of Nafion NR50 can be stated.

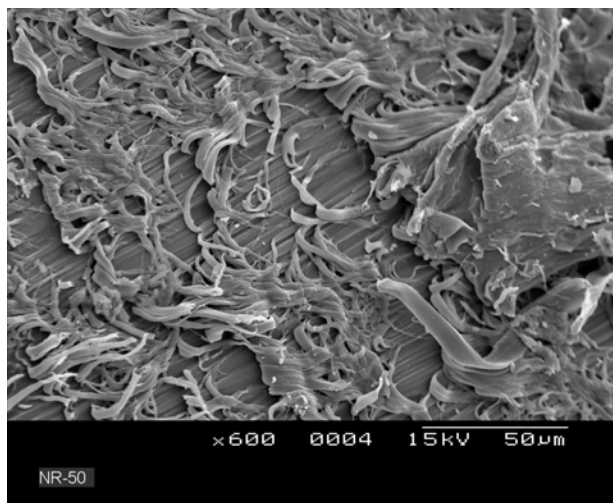


Figure 16. SEM image of Nafion NR50

Nafion N117

This catalyst is a different formulation of Nafion NR50, being thin membranes instead of pseudo spherical particles. Although not viable for industrial use, with this catalyst internal mass transfer limitations can be checked since all active centers are assumed to be accessible on the external surface. Moreover, since it has practically the same acid capacity as NR50, results can be compared directly.

SAC 13

SAC 13 is a nanocomposite that is obtained when dispersing nanoparticles of NR50 in a silica matrix via sol-gel reaction. The result is a porous catalyst in which the polymer surface area is much greater than that of the original perfluorinated catalyst, with the corresponding increase in the number of accessible acid sites [53].

In *Figure 17* the SEM image shows the different texture of the nanocomposite compared to *Figure 16*. Its name, SAC 13, indicates that the catalyst has a 13% wt. of Nafion NR50 entrapped within the silica matrix. The surface area and pore diameter of the composites are tailored by controlling the pH during preparation [54].

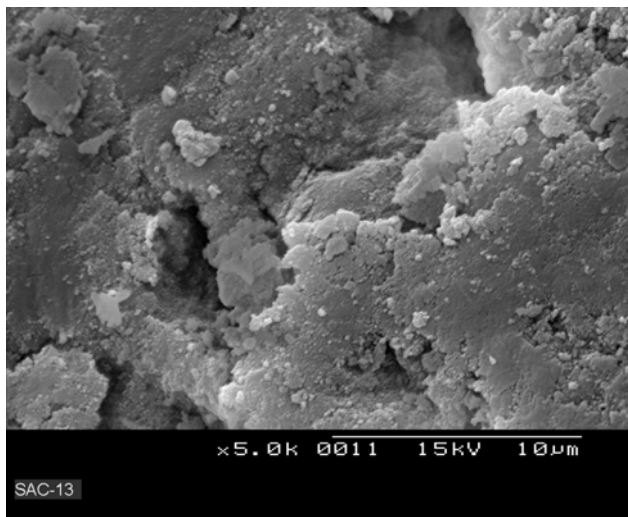


Figure 17. SEM image of SAC 13

The main drawback of this catalyst is that the acidity is still lower than that of Nafion NR50, but, on the contrary, all active centers are accessible even in non-polar conditions.

In Table 8 the composition of the solution of Nafion 5 wt.% in mixture of lower aliphatic alcohols and water is shown.

5.33 wt.% Nafion
27 wt.% 2-propanol
1.7 wt.% methanol
18.3 wt.% 1-propanol
0.4 wt.% other alcohols
46.6 wt.% water

Table 8. Composition of Nafion 5 wt.% solution

3.1.3.2 STYRENE/DIVINYLBENZENE RESINS

Three thermally stable and three conventional resins were tested. In *Table 9* their main characteristics are shown.

Particle diameter was determined with a Beckman Coulter LS Particle Size Analyzer, and data shown in *Table 9* were measured in dry state. For catalysts A70, A36, DL-H/03 and DL-I/03, the particle size was also measured in water and in 1-pentanol media in order to quantify

the swelling of the resins. Finally, for Dowex 50 and A70 the particle size was measured in DNPE, as well.

	Short name	Structure ^a	%DVB	d_p [μm]	% water	Acidity ^c [eq H^+ /kg]	T_{max} [$^{\circ}\text{C}$]
Amberlyst 36wet	A36	M	15	634	46-48	4.87	150
Amberlyst DL-I/03	DL-I/03	M	Medium ^b	644	51-55	5.46	170
Amberlyst DL-H/03	DL-H/03	M	Low ^b	698	50-52	3.39	170
Amberlyst 70	A70	M	Low ^b	551	53-55	3.01	200
CT-224	CT224	G	4	466	55-60	5.14	150
Dowex 50Wx4-50	Dow50	G	4	599	63-64	4.95	150
Dowex 50Wx4-100	Dow100	G	4	211	61-62	4.95	150
Dowex 50Wx4-200	Dow200	G	4	105	63-64	4.83	150
Dowex 50Wx4-400	Dow400	G	4	52	64-66	4.80	150

^a M = macroporous; G = gel-type or microporous; ^b value not available; ^c measured by titration

Table 9. Properties of S/DVB resins

Amberlyst 70

In *Figure 18* the distribution of particle diameters in different media is shown. In 1-pentanol (the initial state of most experiments) this resin does not swell, but it does when water is present in the reaction medium. Since water is preferentially adsorbed on the resin (see *section 1.6.2*), as the experiment runs the particle swells. It is to be noted that a fraction of this catalyst collapses into smaller particles of about 200-300 μm when water is present in the medium.

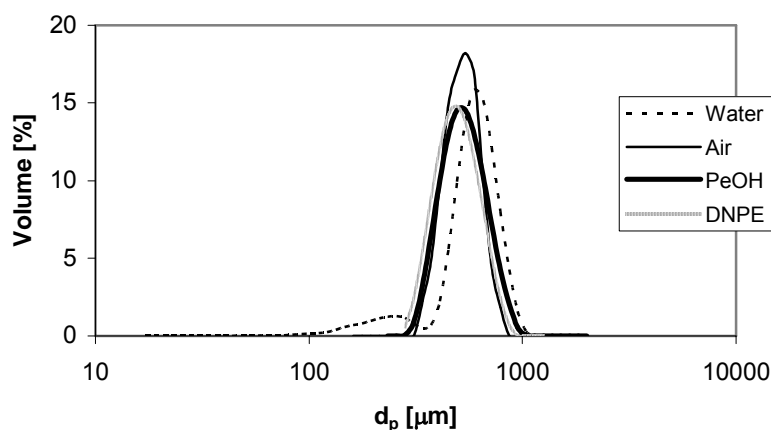


Figure 18. Swelling of Amberlyst 70 in polar solvents

On the other hand, A70 particles did not swell in a DNPE medium, that is to say it does not swell in non-polar conditions.

Amberlyst 36wet

In *Figure 19* the distribution of particle diameters in different media is shown. Here both 1-pentanol and water are able to swell the resin. Again, when water is added some small particles appear.

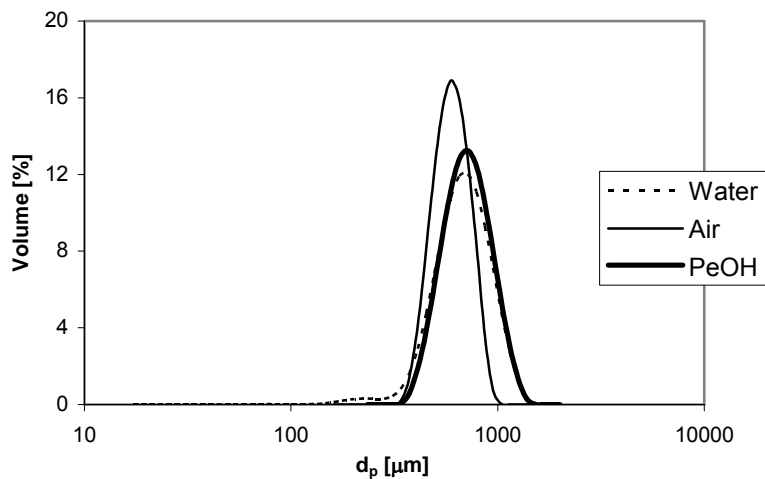


Figure 19. Swelling of Amberlyst 36wet in polar solvents

Amberlyst DL-H/03

In *Figure 20* the distribution of particle diameters in different media is shown. Just like A70, catalyst particles only swell when water is present in the media, and a small fraction of lower d_p appears in this medium.

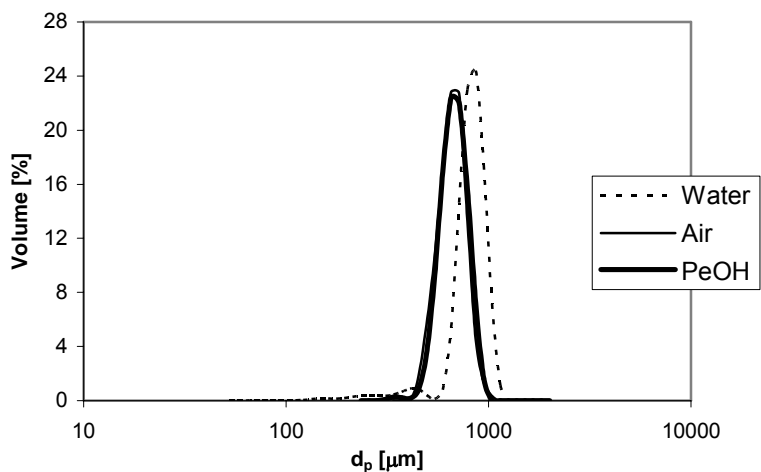


Figure 20. Swelling of Amberlyst DL-H/03 in polar solvents

Amberlyst DL-I/03

In *Figure 21* the distribution of particle diameters in different media is shown.

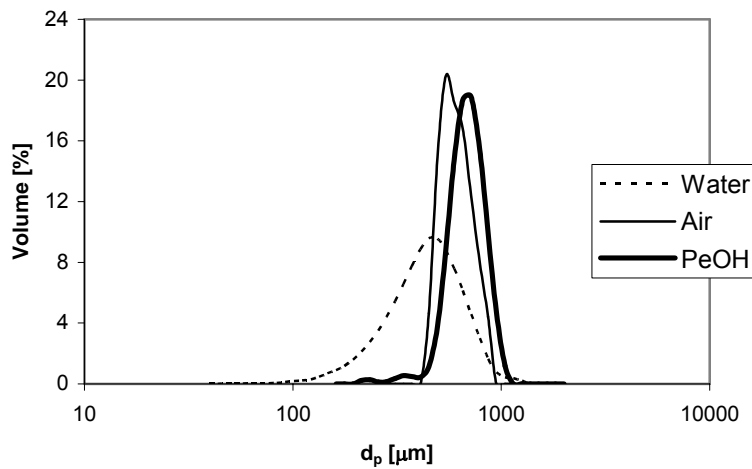


Figure 21. Swelling of Amberlyst DL-I/03 in polar solvents

When this catalyst is in contact with 1-pentanol, it swells considerably. But when water is present in the medium, a great fraction of this catalyst collapses into smaller particles. In this case this phenomenon was observed visually after the experiments.

As seen so far, water was able to swell the four macroporous resins A70, A36, DL-H/03 and DL-I/03. However, a different behavior was observed with 1-pentanol. Macroporous resins with a low DVB content, A-70 and DL-H/03, did not swell in the alcohol medium. On the other hand, A-36 and DL-I/03, with a medium DVB content, did swell considerably.

CT-224

In *Figure 22* the distribution of particle diameters in different media is shown.

This microporous resin swells in presence of 1-pentanol, as well. When put into contact with water, a fraction of the distribution of particle sizes (probably the biggest one) collapses into smaller particles of about 161 μ m, while the other particles swell considerably.

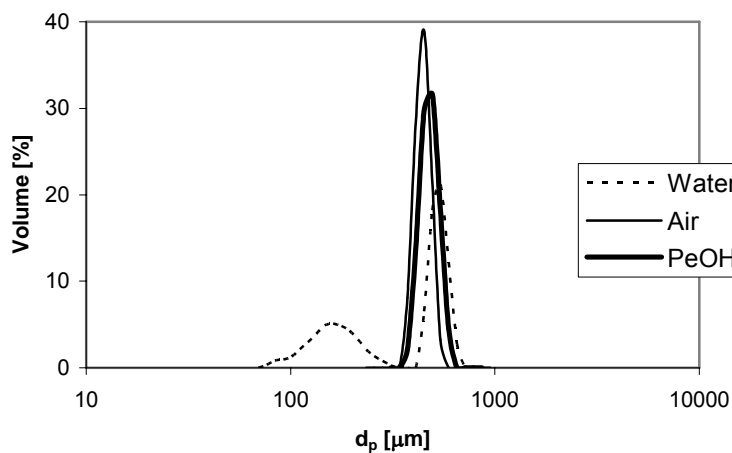


Figure 22. Swelling of CT224 in polar solvents

Dowex 50WX4

In Figure 23 the distribution of particle diameters in different media is shown. Practically the same distributions were obtained when analysis were performed with air and DNPE. On the other hand, 1-pentanol and, especially water, swelled catalyst particles in great extent. Furthermore, a small fraction of fines appeared in water.

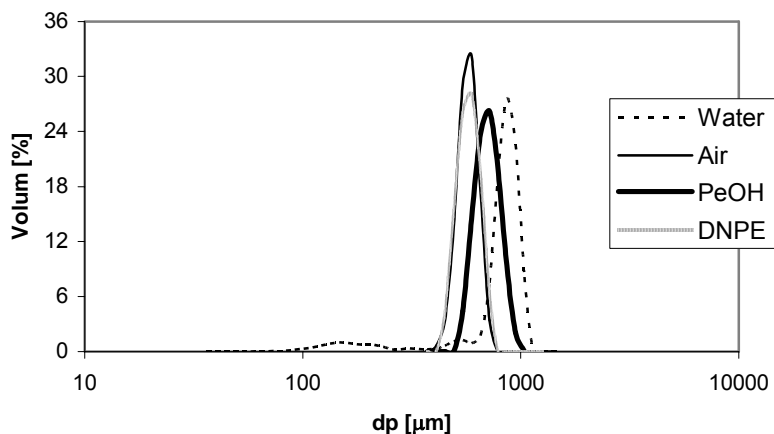


Figure 23. Swelling of Dowex 50WX4 in polar solvents

In Table 10, the mean particle diameters of all catalysts in different media and the increase of particle volume are shown.

	mean d_p [μm]				% volume increase		
	Air	1-pentanol	Water	DNPE	1-pentanol	Water	DNPE
A70	551.0	564.9	609.4	528	8	35	-12
A36	634.0	765.4	729.1		76	52	
DL-H/03	697.9	711.1	848.2		6	80	
DL-I/03	643.8	723.1	480.4		42	-58	
CT-224	465.8	502.8	407.4		26	-33	
Dowex 50	599.3	742.7	830.1	607	90	166	4

Table 10. Mean d_p in different media and volume increase with respect to air

As it can be stated, resin particles swell so significantly when brought into contact with polar solvents that, as an extreme case, some of them (macroporous resins with higher DVB content) collapse into smaller particles.

In *Table 11* structural parameters of resins in dry state and swollen in water are presented. The porosity is the fraction of pore volume per total volume of the resin and is calculated by means of Equations 16 and 17, for dry state and swollen in water respectively.

$$\theta = \frac{V_g}{V_g + \frac{1}{\rho_s}} \cdot 100 \quad \text{Equation 16}$$

$$\theta = \frac{V_g + V_{sp} - \frac{1}{\rho_s}}{V_g + V_{sp}} \cdot 100 \quad \text{Equation 17}$$

where V_{sp} is the specific volume of swollen polymer and V_g is the pore volume.

As it can be seen in *Table 11*, A36 and DL-I/03 (medium crosslinking degree) have permanent macropores in dry state, whereas in A70 and DL-H/03 (low crosslinking degree) macropores appear on swelling in polar medium. By comparing surface areas, pore volume and mean pore diameters between dry and swollen state it is clear that new intermediate pores (mesopores) are accessible in the presence of polar solvents in the four macroporous Amberlyst resins. On the other hand, on gel-type resins CT224 and Dowex 50Wx4 no macropores are originated when swelling on polar media.

	Dry state					Swollen in water (ISEC method)				
	ρ_s^a [g/cm ³]	S_g^b [m ² /g]	V_g^c [cm ³ /g]	d_{pore}^d [nm]	θ^e [%]	S_g [m ² /g]	V_g [cm ³ /g]	d_{pore}^d [nm]	V_{sp} [cm ³ /g]	θ [%]
A36	1.4494	28.6	0.21	34.3	23.2	147	0.333	9.1	0.999	48.2
DL-I/03	1.6191	19.8	0.17	34.4	21.6	153	0.459	12.0	0.744	48.7
DL-H/03	1.4611	0.087				283	0.577	8.2	0.873	52.8
A70	1.5197	0.0181				176	0.355	8.1	1.19	57.4
CT224	1.4236	0.0188							1.81	61.2
Dow50	1.4259	0.0109							1.92	63.5
Dow100	1.4302	0.0296							1.84	62.0
Dow200	1.4344	0.0413							1.94	64.1
Dow400	1.4436	0.0772							1.9	63.5

^a Skeletal density measured by Helium displacement; ^b Surface Area, BET method (N₂ for $S_g \geq 1$ m²/g; Kr for $S_g < 1$ m²/g); ^c Pore volume, determined by adsorption of N₂ at 77 K and $P/P_0 = 0.99$; ^d Assuming pore cylindrical model; ^e porosity

Table 11. Structural parameters of resins in dry state and swollen in water

ISEC also provides information on the volume distribution of the differently dense gel fractions in the swollen polymer mass. A good view of the three-dimensional polymer network of swollen polymer is given by the Ogston geometrical model [55], in which micropores are described by spaces between randomly oriented rigid rods. The specific volume of swollen polymer (volume of the free space plus that occupied by the skeleton), V_{sp} , is the characteristic parameter of this model. The Ogston model allows distinguishing zones of swollen gel phase of different density or polymer chain concentration (total rod length per unit of volume of swollen polymer, nm⁻²), and the pore size is described as the total rod length per unit of volume.

Figure 24 shows the pore distribution of the swollen gel phase, probably quite representative of the swollen resins morphology in aqueous solution of alcohol. As it can be seen, Amberlyst 36 and DL-I/03 show polymer concentrations ≥ 1.5 nm/nm³, typical of a very dense polymer mass, poorly accessible, whereas Amberlyst 70, Amberlyst DL-H/03, CT-224, and Dowex resins show a significant fraction of polymer concentration of 0.4-0.8 nm/nm³ corresponding to a moderately expanded gel. Porosity in swollen state quantifies both V_g (mesopores) and V_{sp} (micropores) jointly. Macroporous resins, with low V_{sp} , show lower porosity than the gel-type ones.

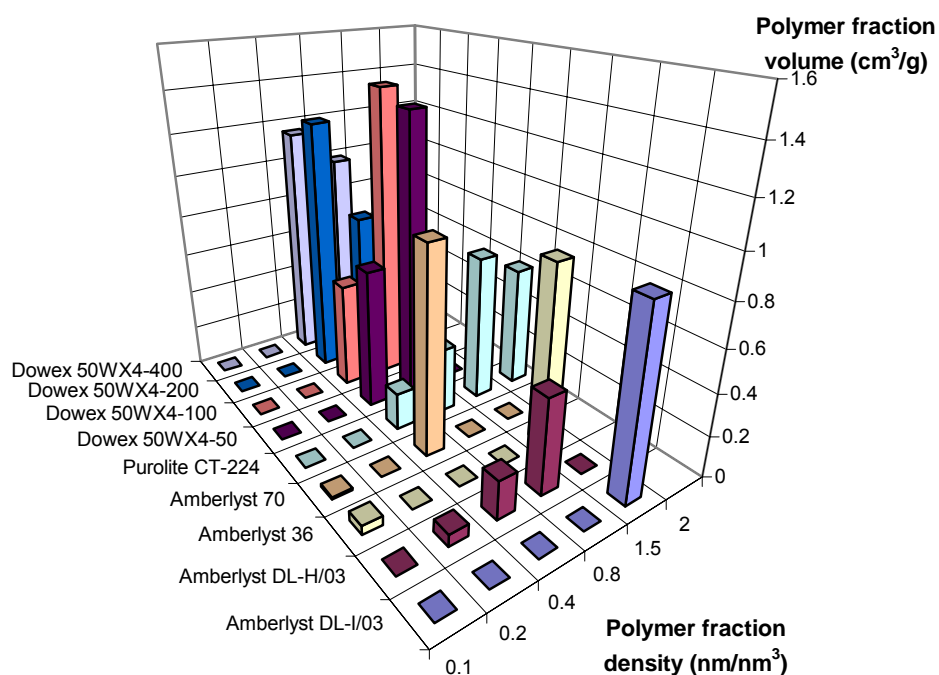


Figure 24. ISEC pattern displayed by resins in water

3.1.3.3 ZEOLITE

The zeolite H-Beta (H-BEA25) was selected because it works very well in etherification reactions of isobutene with alcohol both in liquid and in gas phase [56,57,58,59,60]. Table 12 shows the physical and structural properties of this zeolite. It consists of a collection of aggregates of small crystallites ranging from 0.7 to 40 μm ; the mean size being about 8 μm . Distribution of aggregates size was determined in water and 1-pentanol by a laser technique with a Microtrack SRA analyzer. TEM (Hitachi H600-AB) and SEM (Hitachi S-2300) electron micrographs showed that zeolite powders were composed of small crystallites typically in the range 0.1-0.3 μm .

$\text{SiO}_2/\text{Al}_2\text{O}_3$ molar ratio was measured by X-ray fluorescence (PW1400, Philips; detector: LiF crystal; excitation source: Rh). Acid site density was estimated by assuming one Brönsted acid site per lattice Al free of residual cations such as Na^+ [61].

Textural properties were obtained from N_2 adsorption-desorption isotherms recorded at 77 K with an Accusorb ASAP 2020 sorptometer, after out-gassing the zeolite at 500°C for 4h. BET surface area was measured by using recorded data at $0.05 \leq P/P_0 \leq 0.25$. Pore volume, V_g , was estimated from the volume of N_2 adsorbed at relative pressure of 0.99. External surface area, S_{ext} , and micropore volume, V_{μ} , were computed by the t-method of Lippens-de Boer [62]. Pore

size distribution in the meso and macropore range ($2 \leq d_{\text{pore}} \leq 50$ nm) was calculated by the Barret-Joyner-Halenda method based on Kelvin equation [63,64]. As *Table 12* shows, the estimates of S_{ext} and S_{meso} agree quite well. The distribution curve can be seen elsewhere showing that H-BEA-25 has pores in the range 2-50 nm [59].

	H-BEA-25
SiO ₂ /Al ₂ O ₃	25.1
Brønsted acid site concentration (mmol g ⁻¹)	1.2
Mean particle size (μm)	8.1
Mean crystal size ^a (μm)	0.2-0.3
Mean crystal size ^b (μm)	0.1-0.3
Skeletal density, ρ _s (g cm ⁻³)	2.237
BET surface area, S _g (m ² g ⁻¹)	594
Pore volume, V _g (cm ³ g ⁻¹)	0.724
External surface area, S _{ext} ^c (m ² g ⁻¹)	246
Micropore volume, V _μ ^c (cm ³ g ⁻¹)	0.150
Mesopore surface, S _{meso} ^d (m ² g ⁻¹)	232
Mesopore volume, V _{meso} ^d (cm ³ g ⁻¹)	0.626
Mean mesopore diameter, \bar{d}_{pore} (nm)	10.8
Micropore diameter ^e (nm)	0.65 x 0.56; 0.75 x 0.57

^aFrom TEM micrographs; ^bFrom SEM micrographs; ^cCalculated by the t-method of Lippens-de Boer [62]; ^dCalculated according to Ref. [63]; ^eValues obtained from molecular models [64]

Table 12. Physical and structural properties of the zeolite H-Beta

3.1.3.4 CARRIERS FOR NAFION IMPREGNATION

As commented before, seven catalysts were prepared by impregnating Nafion NR50 on seven different carriers, in order to increase the surface area of Nafion NR50.

In *Table 13* some physical and structural properties of the carriers are shown. Some discrepancies were observed among BET surface areas, nominal areas, and surface areas determined from N₂ desorption isotherm. This will be discussed in *section 4.7.3*.

3. Experimental

Carrier	Short name	ρ_s [g/cm ³]	S_g^a [m ² /g]	V_g^b [cm ³ /g]	S_{pore}^b [m ² /g]	d_{pore}^c [nm]	d_p [μ m]	Acidity [eq H ⁺ /kg]
Weakly acidic γ -Al ₂ O ₃	Al-1	3.1869	176.5	0.2110	188.6	4.5	115.8	-
Acidic γ -Al ₂ O ₃	Al-2	3.2202	157.2	0.2330	182.7	5.1	104.7	-
α -Al ₂ O ₃	Al-3	3.9834	0.6647	0.0020	0.586	14.0	7.74	-
Silica A	Si-A	2.1942	221.4	1.426	233.6	24.4	39.68	-
Silica B	Si-B	2.1513	306.4	1.728	314.1	22.0	79.12	-
Silica C	Si-C	2.1054	486.7	1.765	514.8	13.7	67.11	-
Silica-alumina	Si-Al	2.0538	470.6	0.6449	532.4	4.8	63.56	2.7

^aBET surface; ^bDetermined from adsorption isotherm of N₂ at 77K; ^cAssuming pore cylindrical model

Table 13. Physical and structural properties of carriers

Furthermore, the carriers were characterized by X-ray Fluorescence in order to check for impurities (Table 14).

Carrier	Si	Zr	Ti	Al	Na	Ca	Fe	S	P	Cl	Ga
Al-1	x	-	-	xxx	xx	-	x	-	-	xx	x
Al-2	-	-	-	xxx	xx	-	x	-	-	xx	x
Al-3	x	-	-	xxx	xx	x	x	-	-	-	x
Si-B	xxx	x	X	x	x	x	x	-	-	-	-
Si-C	xxx	x	X	x	x	x	x	x	-	-	-
Si-A	xxx	xx	-	-	x	x	x	-	-	-	-
Si-Al	xxx	xx	-	xxx	-	x	x	xx	x	-	-

x = trace element; xx = minor element; xxx = major element; - = element not present

Table 14. X-ray fluorescence analysis of the different carriers

Finally the water content and organic compound content (2h at 600°C) was also checked. The amount of organic compounds was not high, so carriers were used without previous calcinations

Carrier	%Organics	%Water content
Al ₂ O ₃ -1	4.86	0.00
Al ₂ O ₃ -2	4.41	0.09
Al ₂ O ₃ -3	0.23	0.00
SiO ₂ -A	4.04	3.36
SiO ₂ -B	2.71	3.84
SiO ₂ -C	1.58	3.64
SiO ₂ -Al ₂ O ₃	5.90	11.52

Table 15. Organics and water content of carriers

3.2 EXPERIMENTAL SETUP

3.2.1 DNPE REACTION STUDY

In Figure 25 the scheme of the set up where all experiments concerning the dehydration of 1-pentanol to DNPE were executed, is shown. In subsequent sections, the main parts of experimental devices will be explained in detail.

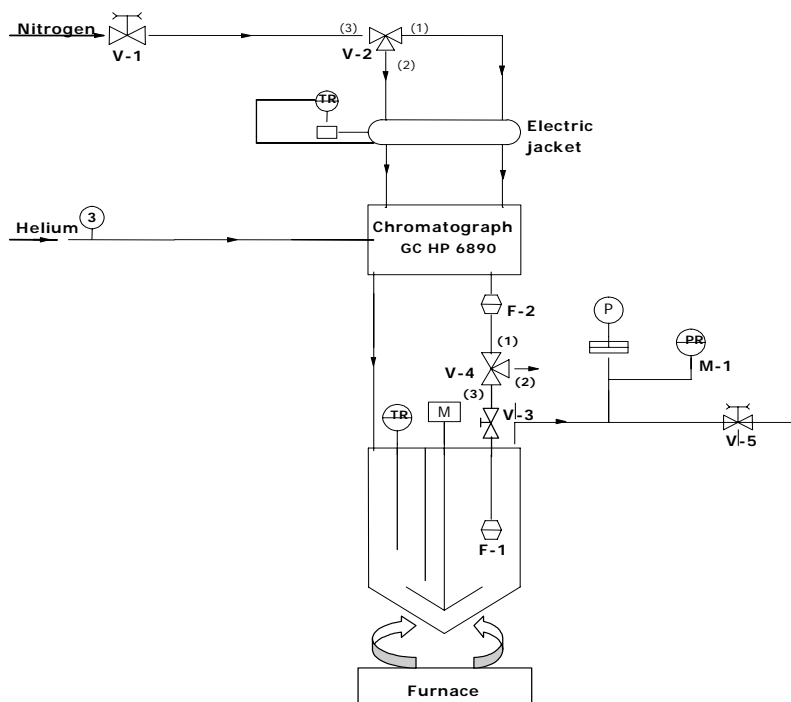
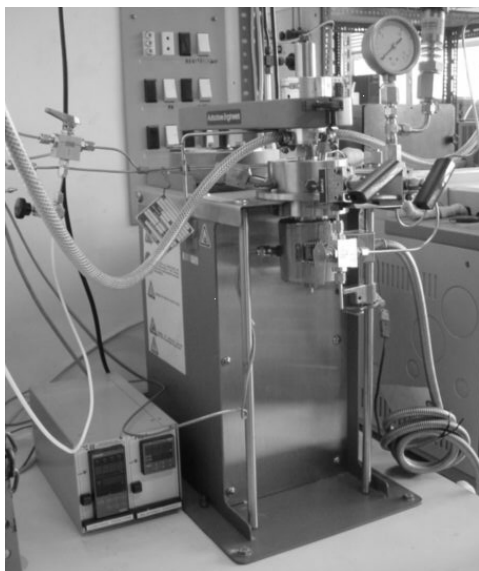


Figure 25. Scheme of the DNPE synthesis experimental setup

3.2.1.1 REACTOR

A stainless steel (316 SS) reactor Autoclave Engineers operated in batch mode (although it could also operate in continuous wise) with a nominal volume of 100 mL (*Figure 26*) was used. The maximum operating pressure was 76 bar at 454°C, and the minimum operating temperature was -29°C.



The stirrer (M) was a six-blade Dispersimax turbine model Magnedrive II Series 0, 7501 and the stirring speed was controlled by a frequency variator T-verter N2 Series. A baffle was placed inside the reactor to improve agitation. The Nitrogen inflow, which was the only inlet in batch mode, was used to pressurize the reactor at a constant pressure. The outlet, through a 2µm filter (F-1), permitted to take out liquid samples to the chromatograph, so the reactor composition could be monitored online. Both inlet and outlet were heated by an electric jacket.

Figure 26. Picture of the experimental setup In this setup also safeties were built-in, like a safety valve (V-5) and a rupture disc, which breaks when pressure increases over 50 bar.

3.2.1.2 TEMPERATURE CONTROL

A temperature control unit controlled the temperature of the reactor. This system consisted of an electric furnace A TC 22 Pro 9 equipped with two temperature control units connected to two thermocouples: TOHO TTM-125 controlled the temperature of the reactor, while TOHO TTM-104 dealt with the temperature of reactor wall. The temperature control unit was able to keep the temperature within ± 0.1 °C from the set point.

3.2.1.3 OUTLET AND ANALYSIS SYSTEM

Liquid samples could be withdrawn when valve V-3 was opened and the three-way valve V-4 was on the correct position. Two filters (F-1 and F-2) prevented that catalyst particles could damage the chromatograph valves.

3. Experimental

The composition of liquid mixtures was analyzed by using a split mode operation in a HP6890A GLC apparatus equipped with a TCD detector (to determine water). A 50 m × 0.2 mm × 0.5 μm methyl silicone HP 90915-001 capillary column was used. The column was temperature programmed with a 6 min initial hold at 45°C followed by a 30 °C min⁻¹ ramp up to 180°C and held for 5 min. Helium was used as carrier gas at a total flow rate of 30 mL·(min)⁻¹. In *Figure 27* the main parameters of the chromatograph control unit concerning the oven and the column are shown.

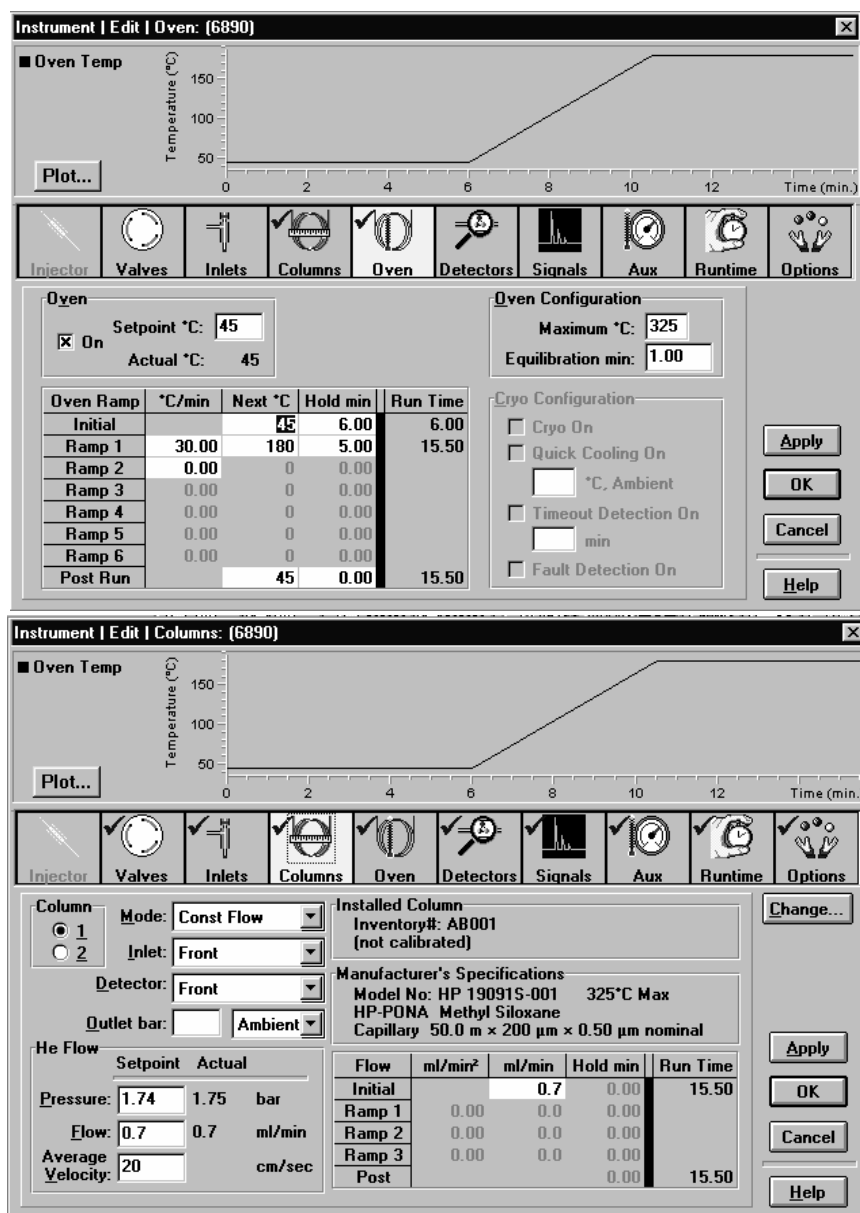


Figure 27. Control parameters of the oven and the column of HP 6890 GC

3. Experimental

The following species were analyzed: 1-pentanol, DNPE and water; C₅ alkenes (1-pentene, cis-2-pentene and trans-2-pentene); branched ethers (2,2-oxybis pentane, 2-methyl-1-butyl 2-pentyl ether, 2-methyl-1-butyl 1-pentyl ether, 1,2-oxybis pentane and 2-methyl-1-butyl ether); and 1-pentanol impurities (2-methyl-1-butanol and pentanal). Retention times are shown in *Table 16*.

Nitrogen	4.02
Water	4.27
1-pentene	5.75
trans-2-pentene	6.07
cis-2-pentene	6.21
Pentanal	10.03
2-methyl-1-butanol	10.09
1-pentanol	10.63
2-methyl-1-butyl ether	13.48
2,2-oxybis pentane	13.53
2-methyl-1-butyl 2-pentyl ether	13.65
2-methyl-1-butyl 1-pentyl ether	13.68
1,2-oxybis pentane	13.97
1,1-oxybis pentane (DNPE)	14.08

Table 16. Retention time [min] of all species

The chromatograph was controlled by a computer with Chemstation software. *Figure 28* shows a typical report.

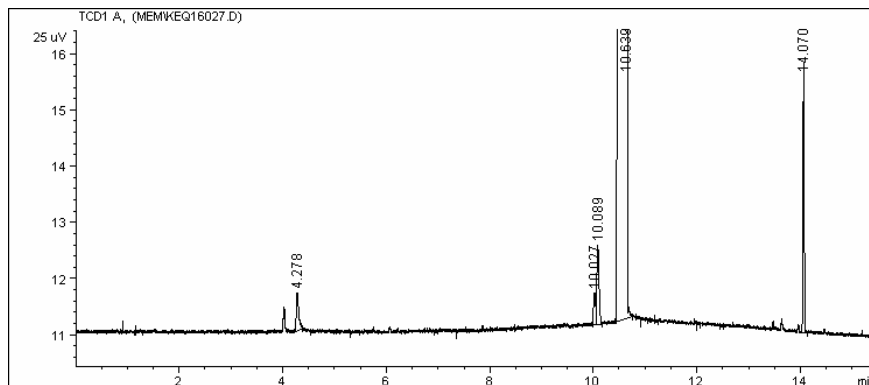
As well as the chromatograph, reactor temperatures and pressure were monitored online on the computer with Labview software. Temperature setpoints were set with the computer, and some safety alarms were programmed in order to prevent sudden increases of temperature and pressure.

3. Experimental

Data File C:\HPCHEM\1\DATA\MEM\KEQ16027.D
HP-6890-GC 2/07/02 11:59:59 ROGER

Injection Date : 2/07/03 11:44:19
Sample Name : Vial : 2
Acq. Operator : ROGER Inj : 1 Inj Volume : External
Method : C:\HPCHEM\1\METHODS\DNPE.M
Last changed : 15/06/01 19:01:11
Methode de dnpe

Area Percent Report



Sorted By : Signal
Multiplier : 1.0000
Dilution : 1.0000

Signal 1: TCD1 A,
Results obtained with standard integrator!

Peak #	RetTime [min]	Type	Width [min]	Area [25 uV*s]	Height [25 uV]	Area %
1	4.278	BB	0.0488	2.19992	6.67274e-1	0.23782
2	10.027	BV	0.0384	1.37974	5.68460e-1	0.14916
3	10.089	VB	0.0431	4.15971	1.39651	0.44968
4	10.639	BB	0.0851	909.89667	137.94804	98.36403
5	14.070	BB	0.0245	7.39387	4.77111	0.79931
Totals :				925.02990	145.35140	

*** End of Report ***

Figure 28. Chromatographic report example

3.2.2 CATALYST SYNTHESIS

Catalysts were prepared by impregnation of a solution of Nafion perfluorinated ion-exchange resin 5% wt, over some carriers.



Figure 29. Impregnation setup

The impregnation setup was very simple as it can be seen in *Figure 29*. It consisted of a 500 mL balloon with magnetic agitation where the carriers and the active solution were mixed.

After the impregnation process, the same balloon was connected to a Büchi R-200 rotavapor. It was equipped with a V-500 vacuum pump and a V-800 vacuum controller and a B-490 water bath.

Finally, a Büchner-Kitasato-water-vacuum-pump set was used to filter the catalyst.

3.2.3 AUXILIARY DEVICES

In this section, secondary devices used both in DNPE and catalyst synthesis are presented.

3.2.3.1 TITRATION DEVICES

A BRAND Digital Bürette, and a dispenser were used for titration purposes. Besides, some erlenmeyers with magnetic agitation were also employed. This device was used to compute the acidity both of the commercial catalysts tested and the catalysts prepared in the lab.

3.2.3.2 DISTILLATION COLUMN



Figure 30. Distillation column

A 1-meter distillation column (see *Figure 30*) packed with Pall rings was used to purify chemicals.

Atmospheric distillation was carried out to purify the commercial 1-pentanol to a purity higher than 99%. Moreover, 1-pentanol was recovered after experiments and re-used afterwards. C5 alkenes were obtained likewise.

Vacuum distillation was performed to obtain DNPE, which was used for analysis purposes.

3.2.3.3 GC/MS SYSTEM

A HP 6890 Gas chromatograph coupled to a Selective Mass Detector 5973N was used to identify the species formed during the experiments.

3.3 EXPERIMENTAL PROCEDURES

The experimental section can be divided into six parts: preliminary experiments, catalyst tests, influence of 2-methyl-1-butanol, thermodynamic equilibrium, catalyst impregnation and impregnated catalyst tests. Except for catalyst impregnation, all of them follow practically the same procedure, which is explained in the subsequent section.

3.3.1 REACTOR START-UP AND OPERATION

The same working procedure was followed to carry out all the experiments under equal conditions, in order to develop a good kinetic description of the reaction and be able to compare all catalysts directly.

The working procedure could be divided into two parts: catalyst pretreatment and the experiment.

3.3.1.1 CATALYST PRETREATMENT

As it can be seen in *Table 7* and *Table 9*, all catalysts were saturated with water. A pretreatment is necessary in order to know exactly the amount of catalyst introduced in the reactor and, especially, to activate their active centers.

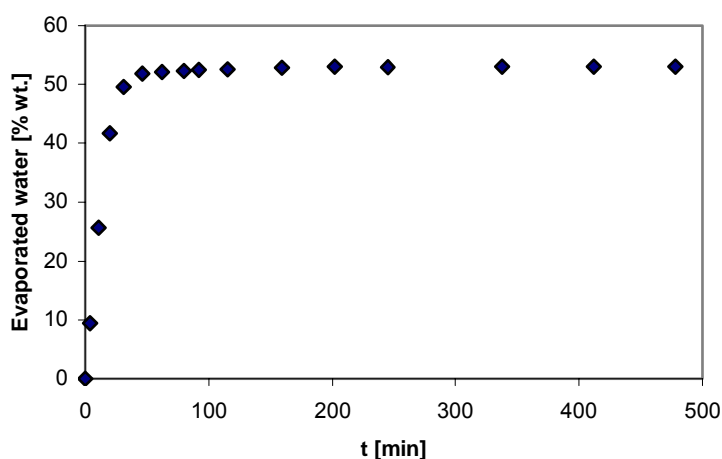


Figure 31. Evaporated water vs time. 100°C atmospheric oven, 3.945 g wet A70

As it can be seen in *Figure 31* most of the water content was taken out after one hour in the atmospheric oven. To ensure that the catalyst was dry, all catalysts were dried in a vacuum oven during two hours, except for zeolite H-BEA-25 that was dried at 300°C during 3 hours at atmospheric muffle.

3.3.1.2 EXPERIMENT

Once the catalyst was ready and the reactor clean, the following steps were followed:

Chromatograph

1. Switch on the chromatograph before the computer. Once both devices are switched on, load the Chemstation software Instrument 1 online, which controls the chromatograph. Wait until the base line is stable (about 1 hour)
2. Load analysis method *DNPE2.m*, if manual injection is required. Inject 0.1 μL of the sample to be analyzed.
3. Load analysis method *DNPE.m*, which corresponds to valve injection.

Start-up

1. Weigh and load the chemicals (about 70 mL) and catalyst.
2. Close the reactor with the dynamometric key in two times: 10 and 30 N·m.
3. Check for leakages pressurizing with nitrogen.
4. Set the pressure at 10 bar.
5. Switch on the electric furnace and jacket.
6. Load Labview software *Microreactor catalytic* on the computer.
7. Switch on the stirrer (500rpm during preheating) and set reactor temperature. Reactor wall temperature should be set 40°C above reactor setpoint.
8. Set the electric jacket temperature at 100°C.
9. Wait until the desired temperature is reached.
10. Pressurize the reactor at the desired pressure (16 bar).
11. Change the stirrer speed to the desired.

This moment was set as initial time ($t = 0$)

Sample analysis

This procedure was repeated as many times as desired.

1. Valve V-4 should be on the correct position.
2. Open valve V-3.

3. Wait 6 min to let the sample flow towards the chromatograph.
4. Push *START* button on the chromatograph panel.
5. Wait until chromatograph valves return to original position (30 s) and change valve V-2 to reuse the sample.
6. Depressurize 3-4 bar in order to help the sample to return to the reactor.
7. Close valve V-3.
8. Purge the sample line by changing valve V-4 and V-2 positions.

End of the experiment

When the experiment finished, the following steps were followed:

1. Close valve V-1 (nitrogen), press *Finalizar experiment* in Labview software *Microreactor catalytic*, switch off the electric furnace and jacket and stop the stirrer.
2. Close Chemstation software *Instrument 1 online*.
3. Switch off the TCD detector and the filament, connect the Gas saver and fix the Oven setpoint at 100°C:
 - Push *Front det* button of the chromatograph panel
 - Push *off* button on *Temp* and *Filament*
 - Push *Front inlet* button of the chromatograph panel
 - Push *on* button on *Gas Saver*
 - Push *Oven* button of the chromatograph panel
 - Fix the setpoint at 100°C

3.3.2 CATALYST SYNTHESIS

Catalysts were prepared by impregnation of carriers with a solution of Nafion. One of the aims of this work was to develop an impregnation method recipe. The final method, named Method 3, is described subsequently, and in *section 4.7.1* the steps followed to achieve it are explained. In *Table 17* a scheme of the method of impregnation is shown.

Pre-impregnation procedure

1. Wash the carrier with 50 mL of methanol in a Büchner funnel connected to a Kitasato. Repeat this once more.
2. Dry the carrier 3 hours in an atmospheric oven at 100°C and then in vacuum conditions and 110°C during one night.
3. Weigh the appropriate quantities of carrier and Nafion solution and the balloon where the impregnation will be performed.

4. Prepare 150mL of solvent (37% 2-propanol and 63% water)

Impregnation process

- Mix in a dried balloon (one night in an atmospheric oven) the carrier, the Nafion solution and the solvent during 6 hours at room temperature and ambient pressure.

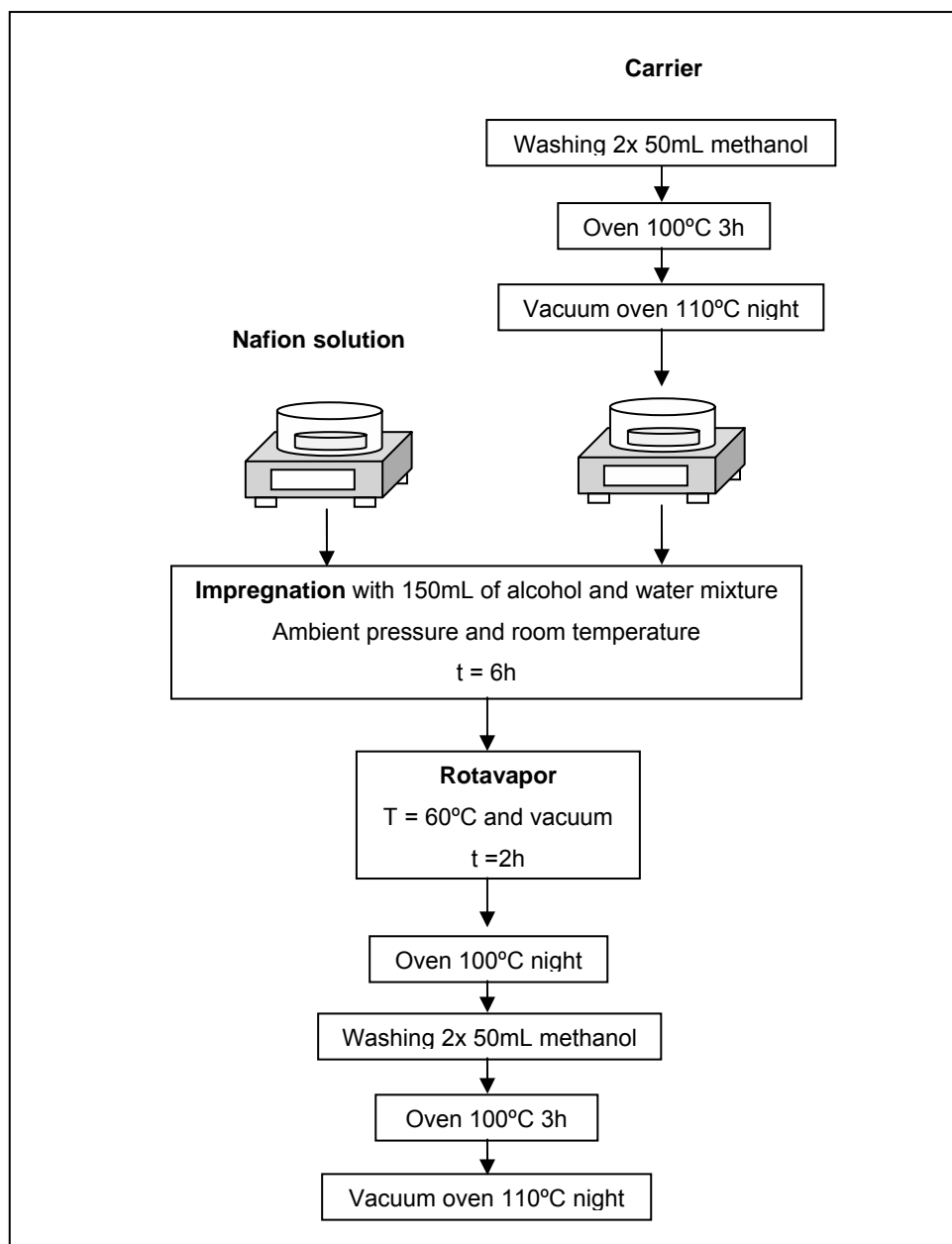


Table 17. Scheme of the method of impregnation

Post-impregnation procedure

1. Evaporate the solvent in a rotavapor during 2 hours (or until the solvent is completely evaporated) at the conditions shown in *Table 18*.

Bath temperature	60°C (balloon 50% immersed)
Cooling temperature	20°C
Cooling flow	40-50 L/h
Rotation speed	2 nd position (of 9)
Condensation	Between 2/3 and 3/4 of the coil
Vacuum conditions	30 min at 300 mbar ($\Delta P^* = 10$ mbar) 15 min at 250 mbar ($\Delta P = 10$ mbar) 15 min at 200 mbar ($\Delta P = 10$ mbar) 15 min at 150 mbar ($\Delta P = 10$ mbar) 15 min at 125 mbar ($\Delta P = 5$ mbar) 30 min at 100 mbar ($\Delta P = 5$ mbar)

* ΔP is the value from which the pump starts to run

Table 18. Operation conditions of the rotavapor

2. Put the balloon with the impregnated catalyst in an atmospheric oven at 100°C overnight.
3. Weigh the balloon with the catalyst.
4. Wash the impregnated catalyst with 50 mL of methanol in a büchner funnel connected to a Kitasato. Repeat this once more.
5. Dry the catalyst 3 hours at 100°C in an atmospheric oven and then one night at 110°C in vacuum conditions.

3.3.3 TITRATION

Two methods were used to determine the acidity of the catalyst. For most ion-exchange resins, a modified Fisher-Kunin method [65] was followed. On the other hand, carriers and supported catalysts prepared in the lab were titrated by direct exchange due to its low acidity and by the fact that some silicas solubilized in basic medium.

Modified Fisher-Kunin method

1. Dried catalyst (*section 3.3.1.1*) is weighed and introduced into an 250-mL Erlenmeyer.
2. 150 mL of standardized (with Potassium biphtalat) NaOH 0.1N and 50 mL of NaCl

3. Experimental

2.5% wt. are added to the Erlenmeyer.

3. The Erlenmeyer is covered and the matter is mixed during at least 8 hours.
4. 25 mL of the solution are titrated with standardized HCl 0.1N (with NaOH), using methyl orange as indicator.
5. Step 4 is repeated at least twice.

The main drawback of this method is the difficulty to appreciate the color change, since methyl orange changes from yellow (basic) to red (acidic).

Direct exchange method

1. Dried catalyst (*section 3.3.1.1*) is weighed and introduced into an 250-mL Erlenmeyer together with 200 mL of NaCl 0.04N
2. The Erlenmeyer is covered and the matter is mixed during at least 8 hours.
3. 50 mL of solution are titrated with standardized NaOH 0.1N, using phenolphthalein as indicator.
4. Step 3 is repeated at least twice.



Chapter 4. Results and discussion

4.1 GENERAL WORKING SCHEME

In the following figure a general scheme of the experimental procedure is shown.

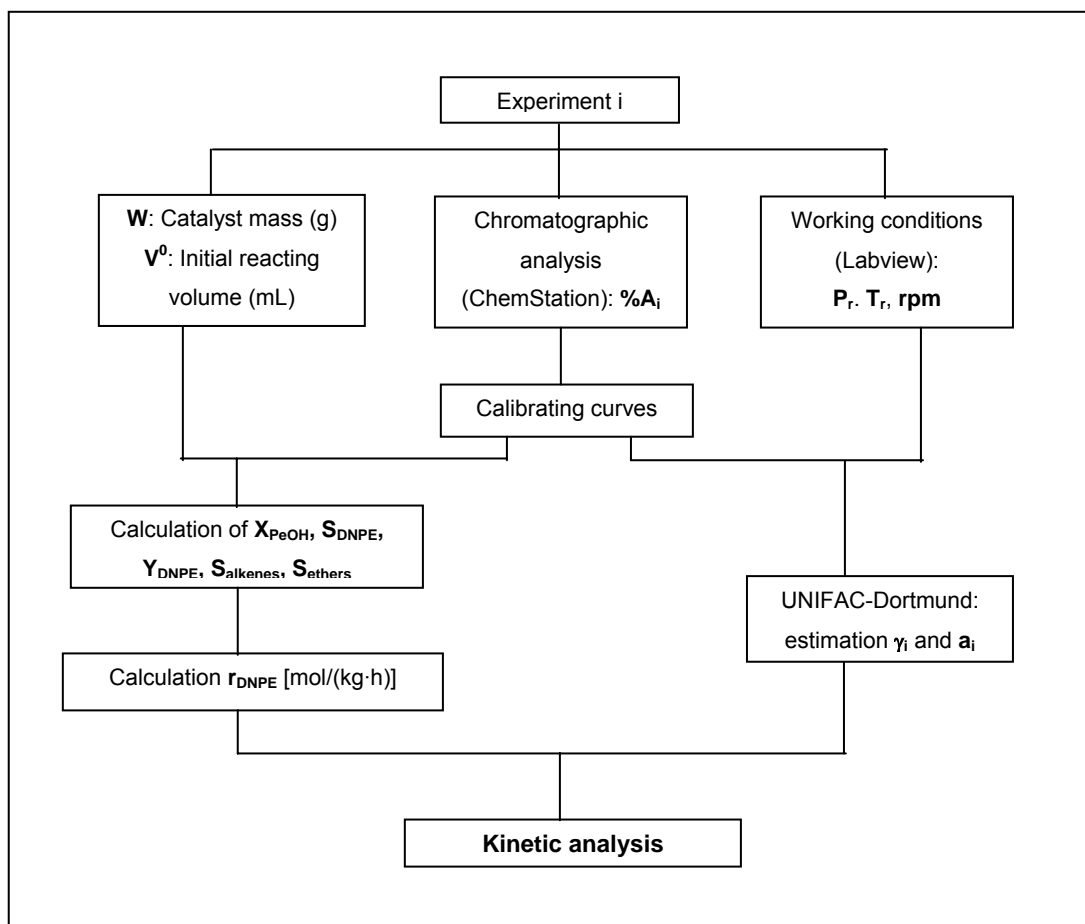


Figure 32. General scheme of the experimental procedure

In subsequent sections the scheme here presented is explained in detail.

4.1.1 SYSTEM VARIABLES ANALYSIS

An analysis of the system variables was done, in order to check which of them affected the reacting environment, and how their influence was.

The reacting system studied presented four degrees of freedom: V^0 (initial reacting volume), **catalyst**, d_p (catalyst particle size) and W_{cat} (catalyst mass). The experimental setup added five more: **P** (pressure), **T** (temperature), **N** (stirring speed), **t** (length of experiment) and **operation**

mode (continuous or discontinuous wise).

The initial reacting volume has no influence on the kinetics of the reaction, and it was just a functional variable of the system. It was decided to start with **70 mL** of solution, since it was enough to wet the thermocouples and the filter and to leave a gas chamber to prevent from liquid expansion when heated.

As the study was in the liquid-phase, it was necessary to work at moderate pressures. Among the chemicals involved in the reaction, olefins are the ones with higher vapor pressure, P_v (see Table 19). Nevertheless, since selectivity to DNPE was quite high for all catalysts tested and therefore the production of alkenes was not important, water became the main problem.

Compound	$P_{v180^\circ\text{C}}$ [bar]
1-pentanol	3.3
1-pentene	27.6
water	10.2

If an ideal system is assumed (Raoult's law), and taking into account the maximum conversion achieved, the vapor pressure for the mixture was estimated to be 7 bar. Working pressure was fixed at 16 bar to avoid the vaporization of the chemicals during the experiment.

Table 19. Vapor pressures at 180°C

The length of the experiment does not influence the kinetics of the reaction, but it affects magnitudes such as 1-pentanol conversion or DNPE yield. Except for equilibrium experiments, the length of the tests was set at 6 hours, since it was found to be enough to obtain data with small associated standard error.

The operation mode should not affect the kinetics. So, it was decided to work in discontinuous mode because of its simplicity.

The influence of the other variables was studied experimentally and results are presented henceforward.

4.1.2 EXPERIMENTAL DESIGN

The study of the dehydration of 1-pentanol to DNPE presented in this memory was divided into six blocs, as follows:

- 1) *Previous experiments*: the influence of W_{cat} , N and d_p , all of them related to mass transfer phenomena, was checked.

- 2) *Catalyst selection*: eight catalysts of different nature were tested with the aim of finding one active, selective and resistant enough to be able to carry out a deep kinetic analysis and use it industrially. The influence of the temperature was also studied.
- 3) *Influence of 2-methyl-1-butanol*: the behavior of the main impurity of 1-pentanol was studied at the same reacting conditions than DNPE synthesis experiments.
- 4) *Thermodynamic equilibrium*: the equilibrium constant of the dehydration of 1-pentanol was determined at different temperatures in order to compute the standard enthalpy and entropy changes of reaction, and to have confident values of K, for upgrading the kinetic studies.
- 5) *Kinetic analysis*: a deep kinetic study was undertaken to find a model that fitted the experimental data and to compute the activation energy of the reaction.
- 6) *Catalyst synthesis*: some Nafion/silica supported catalysts were prepared in the laboratory with the objectives of (1) finding a suitable method of impregnation, and (2) increasing the surface area of the original Nafion resin.

4.1.3 1-PENTANOL CONVERSION, SELECTIVITY AND YIELD TO DNPE

As it is represented in *Figure 32*, experimental data consisted mainly on reports from the gas chromatograph in which the percentage of area of every chemical, $\%A_i$, was given. The apparatus had been calibrated with standard mixtures prepared from pure compounds in the laboratory, giving as a result the calibrating equations shown in *Table 20* and *Table 21* that relate $\%A_i$ to mass fractions ($\%w_i$). In some cases, multivariable fits were used.

Compound	Calibrating curve
Water	$\%w_{\text{water}} = 0.60648 \cdot \%A_{\text{water}} + 3.658 \cdot 10^{-3} \cdot \%A_{\text{PeOH}} \cdot \%A_{\text{water}}$
1-pentene	$\%w_{1\text{-pentene}} = 0.89499 \cdot \%A_{1\text{-pentene}}$
2-pentene	$\%w_{2\text{-pentene}} = 0.81603 \cdot \%A_{2\text{-pentene}} + 1.4287 \cdot 10^{-2} \cdot \%A_{2\text{-pentene}} \cdot \%A_{\text{water}}$ $- 1.7258 \cdot 10^{-2} \cdot \%A_{1\text{-pentene}} \cdot \%A_{2\text{-pentene}}$
1-pentanol	$\%w_{\text{PeOH}} = 1.0946 \cdot \%A_{\text{PeOH}} - 9.4929 \cdot 10^{-4} \cdot (\%A_{\text{PeOH}})^2$ $- 1.6637 \cdot 10^{-3} \cdot \%A_{\text{PeOH}} \cdot \%A_{\text{DNPE}}$
DNPE	$\%w_{\text{DNPE}} = 1.0206 \cdot \%A_{\text{DNPE}} + 8.1029 \cdot 10^{-3} \cdot \%A_{\text{PeOH}} \cdot \%A_{1\text{-pentene}}$ $+ 6.0354 \cdot 10^{-3} \cdot \%A_{\text{water}} \cdot \%A_{\text{DNPE}}$
2-methyl-1-butyl ether	$\%w_{2\text{m1bether}} = -0.0191 + 1.0747 \cdot \%A_{2\text{m1bether}}$

Table 20 Calibrating curves for the PeOH system

4. Results and discussion

For equilibrium experiments, since 1,4-dioxan was used as solvent, new calibrating equations were obtained, which are shown in *Table 21*.

In the particular case of branched ethers, %w_i was assumed to be %A_i. This assumption does not lead to an important error because these products were detected in very small quantities.

Compound	Calibrating curve
Water	$\%w_{\text{water}} = 0.76468 \cdot \%A_{\text{water}} - 0.015941 \cdot \%A_{1\text{-pentene}} \cdot \%A_{\text{DNPE}}$
1-pentene	$\%w_{1\text{-pentene}} = -0.05655 + 0.8533 \cdot \%A_{1\text{-pentene}}$
2-pentene	$\%w_{2\text{-pentene}} = 0.79392 \cdot \%A_{2\text{-pentene}} - 6.1223 \cdot 10^{-3} \cdot \%A_{2\text{-pentene}} \cdot \%A_{\text{DNPE}}$
1-pentanol	$\%w_{\text{PeOH}} = 0.94966 \cdot \%A_{\text{PeOH}} - 5.5547 \cdot 10^{-3} \cdot \%A_{\text{PeOH}} \cdot \%A_{\text{DNPE}} + 7.0747 \cdot 10^{-6} \cdot (\%A_{\text{DNPE}})^3$
DNPE	$\%w_{\text{DNPE}} = 0.91144 \cdot \%A_{\text{DNPE}} + 0.1335 \cdot \%A_{\text{DNPE}} \cdot \%A_{1\text{-pentene}}$
1,4-Dioxan	$\%w_{\text{dioxan}} = -4.9402 + 1.0981 \cdot \%A_{\text{dioxan}}$

Table 21 Calibrating curves for the 1,4-dioxan system

From mass fractions the other magnitudes followed in every experiment can be calculated:

Mass:
$$m_i = w_i \times m_{\text{reactor}}^0 \quad \text{Equation 18}$$

Mole:
$$n_i = \frac{m_i}{M_i} \quad \text{Equation 19}$$

Mole fraction:
$$x_i = \frac{n_i}{\sum_k n_k} \quad \text{Equation 20}$$

Activity:
$$a_i = x_i \times \gamma_i \quad \text{Equation 21}$$

where m_{reactor}^0 is the initial mass of chemicals charged into the reactor, M_i and γ_i are the molecular mass and the activity coefficient of i , respectively.

It was necessary to work with activities instead of concentrations because of the non-ideality of the system. Activity coefficients were estimated by means of UNIFAC-DORTMUND predictive method, shown in *Appendix II* [66].

When the composition of the reactor was known, the following magnitudes were computed:

$$\text{1-pentanol conversion} \quad X_p = \frac{n_{PeOH}^0 - n_{PeOH}(t)}{n_{PeOH}^0} \times 100 \left[\frac{\% \text{ mol}}{\text{mol}} \right] \quad \text{Equation 22}$$

$$\text{Selectivity to DNPE} \quad S_{DNPE} = \frac{2 \cdot n_{DNPE}(t)}{n_{PeOH}^0 - n_{PeOH}(t)} \times 100 \left[\frac{\% \text{ mol}}{\text{mol}} \right] \quad \text{Equation 23}$$

Selectivity to DNPE was defined as the % of the mol of 1-pentanol reacted to DNPE with respect to the total mol of 1-pentanol reacted. Selectivity to alkenes, $S_{alkenes}$ (1-pentene and 2-pentene), and branched ethers, S_{ethers} , were defined in a similar way.

$$\text{Yield to DNPE} \quad Y_{DNPE} = \frac{2n_{DNPE}(t)}{n_{PeOH}^0} \times 100 = X_p \cdot S_{DNPE} \left[\frac{\text{molDNPE}}{\text{molPeOH}} \right] \quad \text{Equation 24}$$

In Equations 22, 23 and 24 magnitudes computed from different analysis are compared, which could lead to the propagation of the intrinsic error of each of them. To avoid this, and considering all the chemical reactions involved, they could be written as follows:

$$X_p(t) = \frac{2 \cdot n_{DNPE}(t) + n_{alkenes}(t) + 2 \cdot n_{ethers}(t)}{n_{PeOH}(t) + 2 \cdot n_{DNPE}(t) + n_{alkenes}(t) + 2 \cdot n_{ethers}(t)} \times 100 \quad \text{Equation 25}$$

$$S_{DNPE}(t) = \frac{2 \cdot n_{DNPE}(t)}{2 \cdot n_{DNPE}(t) + n_{olefins}(t) + 2 \cdot n_{ethers}(t)} \times 100 \quad \text{Equation 26}$$

$$S_{alkenes}(t) = \frac{n_{alkenes}(t)}{2 \cdot n_{DNPE}(t) + n_{alkenes}(t) + 2 \cdot n_{ethers}(t)} \times 100 \quad \text{Equation 27}$$

$$S_{ethers}(t) = \frac{2 \cdot n_{ethers}(t)}{2 \cdot n_{DNPE}(t) + n_{alkenes}(t) + 2 \cdot n_{ethers}(t)} \times 100 \quad \text{Equation 28}$$

4.1.4 REACTION RATE AND TURNOVER NUMBER

Considering the performance equation of a discontinuous stirred tank reactor, the reaction rate was computed as follows:

$$r = r_{DNPE} = \frac{1}{W_{cat}} \cdot \frac{dn_{DNPE}}{dt} \left[\frac{\text{mol DNPE}}{\text{kg} \cdot \text{h}} \right] \quad \text{Equation 29}$$

First, an empirical function was fitted to the experimental data (n_{DNPE} vs. t), which was derived subsequently.

The initial turnover number, which gives an idea of the efficiency of the active centers, was defined as the initial reaction rate per equivalent of $-\text{SO}_3\text{H}$ group:

$$r_{eq}^0 = \frac{r^0}{\text{acid capacity}} \left[\frac{\text{mol DNPE}}{\text{h} \cdot \text{eq H}^+} \right] \quad \text{Equation 30}$$

4.1.5 MASS BALANCE

As the reactor works batch-wise, the system is closed, without inlets or outlets, so the mass balance is reduced to the following expression:

$$\text{Mass}_{t=0} = \text{Mass}_{t=6h} \quad \text{Equation 31}$$

The mass balance was checked in all experiments by weighing the reactor before and after the run. In all cases the mass lost was less than 5%, an acceptable value for experiments performed with this technique.

4.2 PRELIMINARY EXPERIMENTS

Preliminary experiments were carried out in order to check whether the measured reaction rates were free of mass transfer effects. The influence of the **mass of catalyst**, **stirring speed** and **catalyst particle size** was studied.

4.2.1 INFLUENCE OF CATALYST LOADING

Experiments with different catalyst loadings were performed with the aim of finding the optimal catalyst mass for the experimental setup. The effect of the amount of catalyst on the reaction was studied at 423 K with Purolite CT-224 (CT224), since in a previous work it was found to be a suitable catalyst for the reaction [18]. Working conditions of these experiments are shown in *Table 22*.

Catalyst	T [°C]	N [rpm]	W _{cat} [g]	d _p [μm]
CT-224	150	500	0.5 to 5	466

Table 22. Working conditions: catalyst loading

Results of catalyst loading experiments are shown in Table 23. Initial reaction rate, r_{DNPE}^0 , 1-pentanol conversion at t=6 h, X_p , and selectivity to DNPE, alkenes and branched ethers at t=6 h are presented.

As expected, the catalyst loading had a great influence on the reaction. At t = 6 h, 1-pentanol conversion increased on increasing catalyst mass, while selectivity to DNPE decreased.

W _{cat} [g]	r_{DNPE}^0 [mol/(h·kg)]	X_p [%]	S _{DNPE} [%]	S _{alkenes} [%]	S _{ethers} [%]
0.5	13.9 ± 1.9	13.6 ± 0.2	95.6 ± 0.9	2.7 ± 0.3	1.49 ± 0.01
1.0	14.3 ± 1.1	20.5 ± 0.3	94.85 ± 0.05	3.11 ± 0.05	2.05 ± 0.02
1.5	12.9 ± 0.9	26.5 ± 0.5	94.70 ± 0.01	3.07 ± 0.05	2.25 ± 0.01
2	14.6 ± 0.4	32.6	94.34	3.1	2.58
3	10.9 ± 0.2	41.3 ± 0.5	93.60 ± 0.05	3.45 ± 0.05	3.00 ± 0.02
4	11.5 ± 0.6	47.9	93.25	3.5	3.29
5	10.0 ± 0.5	49.5	92.85	3.6	3.56

Table 23. Results of catalyst loading experiments

The influence of catalyst loading on the initial reaction rate and on 1-pentanol conversion is illustrated in *Figure 33* and *Figure 34*.

It can be seen that for catalyst mass ≤ 2 g (catalyst loadings below 3.5% w/w) measured initial reaction rates were independent on the catalyst mass within the limits of the experimental error. But, for catalyst mass > 2 g, the initial reaction rate decreased on increasing the catalyst mass, which could indicate that an excess of catalyst could introduce a source of inaccuracy in the estimation of reaction rate because of some saturation effect of the reaction system by the solid.

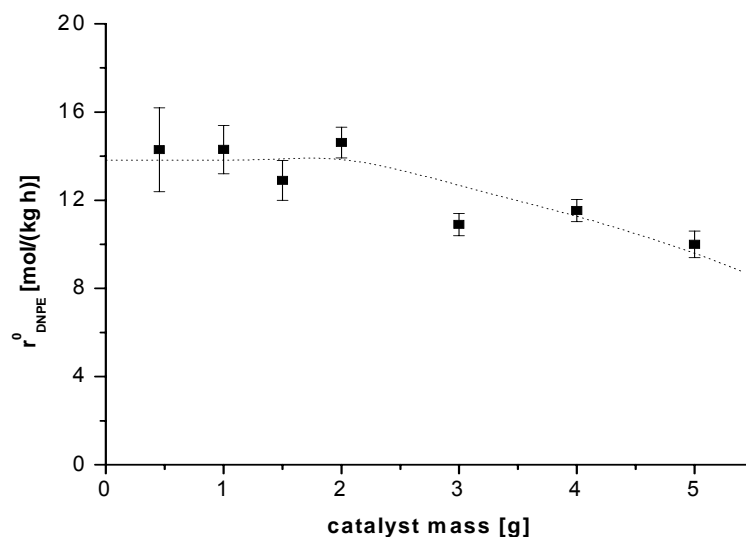


Figure 33. Effect of catalyst mass on reaction rate

As expected, 1-pentanol conversion increases on increasing the catalyst loading. The slope of *Figure 34* decreases on increasing the catalyst mass, which confirms the saturation effect of the system for $W > 2$ g, since, though this behavior is expected when chemical equilibrium is reached, the system is still far from it, as will be seen in *section 4.5*.

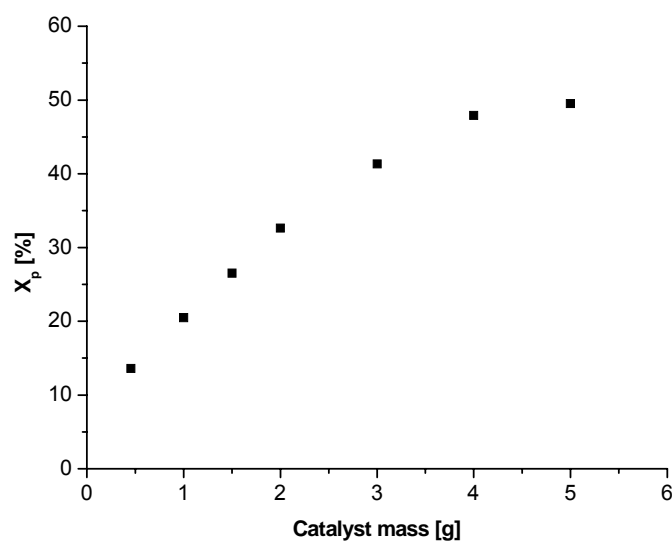


Figure 34. Effect of catalyst mass on X_p at $t=6h$

Finally, as it can be seen in *Table 23*, selectivity to DNPE decreases on increasing the catalyst mass. This could be explained by the fact that on increasing conversion, olefin

formation reactions that only need one molecule of 1-pentanol to occur, become increasingly competitive with DNPE formation.

The same behavior is expected for other catalysts, so, in order to measure reliable reaction rates, the catalyst mass used in subsequent experiments was 1g (catalyst loading of about 2% w/w) for all the catalysts.

4.2.2 INFLUENCE OF STIRRING SPEED

The influence of the external mass transfer was evaluated by performing experiments at different stirring speeds. Working conditions of these experiments are shown in *Table 24*.

Catalyst	T [°C]	N [rpm]	W _{cat} [g]	d _p [μm]
CT224	150	50 to 700	1	466
Dow 50	150	50 to 700	1	599
Dow 100	150	50 to 700	1	211
Dow 200	150	50 to 700	1	105
Dow 400	150	50 to 700	1	52
A70	190	50 to 700	1	571
NR50	180	50 to 700	1	2353

Table 24. Working conditions: stirring speed

As it can be observed, four batches of the same catalyst (Dowex 50WX4) were tested at the same temperature, and they were compared with another DVB resin of similar particle size (CT224). Furthermore, the perfluoroalkane resin Nafion NR50 (NR50), with a much higher d_p, was also checked at 180°C. Finally, A70 was tested at 190°C. Initial reaction rates at all stirring speeds for every catalyst are shown in *Table 25*.

Figure 35 illustrates the influence of stirring speed on the measured initial reaction rate for Dowex 50WX4 batches 50, 100, 200 and 400 mesh. Batches 400 and 200, of smaller d_p, showed the same behavior, i.e. the reaction rate increased on increasing stirring speed reaching a plateau at 300 rpm. On the other hand, batches 100, 50 and also CT-224, of similar particle size as Dow50, had the opposite behavior: the reaction rate decreased on increasing N until a plateau was reached at 300 rpm, as well.

N [rpm]	Dow 50	Dow 100	Dow 200	Dow 400	NR50 ^a	A70 ^b	CT-224
50	17.6	15.5	11.9	9.6		91.6	18.9
100	15.4	15.6	12.1	10.8	35.9		16.6
200	14.1			12.1		107.9	
300	13.2	14.3	13.4	12.5	36.1		16.0
400				12.4		116.2	
500	13.2 ± 2.1	13.3 ± 1.4	14.2 ± 1.6	12.3 ± 0.7	33.4 ± 2.8	111.9 ± 8.9	14.3 ± 0.7
700	13.1	14.3	13.6	12.5	39.6	106.8	14.1

^a T=180°C; ^b T=190°C

Table 25. Initial reaction rates [mol/(kg-h)] vs. N for all catalyst (T=150°C)

So, for stirring speeds higher than 300 rpm the activity of the catalyst was not masked by external mass transfer within the limits of the experimental error, while for lower stirring speeds measured initial reaction rate differed probably due to the appearance of a significant concentration profile in the liquid bulk phase near the catalyst particles, which could have a temperature profile associated. This point, which is sometimes found in the literature [67], deserves more work for a complete explanation.

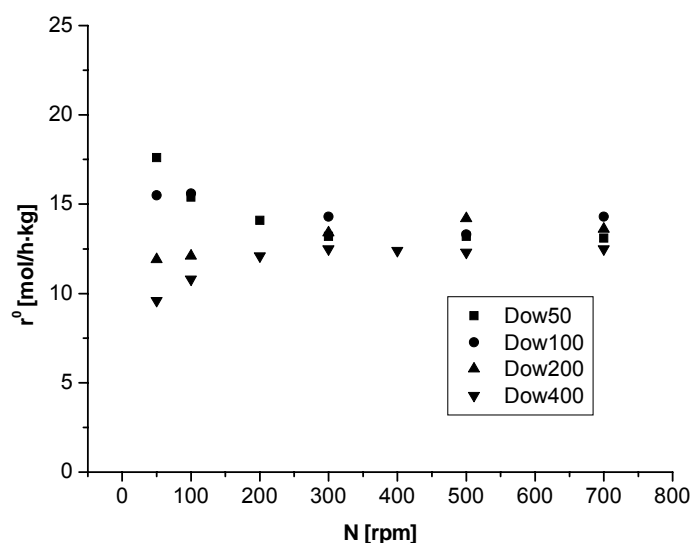
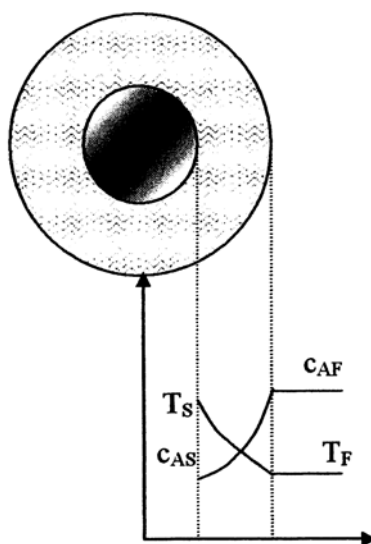


Figure 35. Initial reaction rate vs. N; T=150°C, 1 g catalyst

The expected trend was the observed for smaller particles, i.e. an increase of the initial reaction rate on increasing the stirring speed. The external mass transfer (and heat transfer) depends on the velocity of the fluid and also on the particle size. The bigger the particle is, the bigger the layer around it. So, in those catalysts of bigger size, the limitations of mass transfer

will be more important (see Section 1.8.1.1).

As it is represented in Figure 36, the effect of external mass transfer limitations would lead to the formation of concentration and temperature profiles in the external layer round the catalyst particle, i.e., the concentration on the surface of the catalyst would be lower than that of the bulk phase; on the other hand, as the dehydration of 1-pentanol to DNPE is exothermic (see section 4.5), the temperature on the catalyst surface would be higher than on the bulk phase. While a decrease of the concentration on the catalyst surface would lead to a diminution of the reaction rate, a temperature rise would have the opposite effect. The average temperature of larger catalyst particles (nearly 10 times the smaller ones) would be higher than the measured one, leading to an increase of the reaction rate. Initial reaction rates for catalyst CT224 were higher than those of Dow50 because of its higher exchange capacity, since the initial reaction rate is clearly influenced by this property, as will be explained in more detail in section 4.3.4.



s catalyst surface; F bulk phase

Figure 36. Concentration and temperature profile in the external layer. Exothermic reaction

Finally, in Table 25 the effect of the stirring speed on the initial reaction rate for catalyst NR50 at 180°C and A70 at 190°C (the highest tested temperature) are also shown. As for A70, the initial reaction rate is not affected by the stirring speed for $N > 200$ rpm within the limits of experimental error. With regard to NR50, differences in initial reaction rates were not

appreciated on the whole stirring speed range explored.

Despite being of the same size as Dow 50, initial reaction rate data of A70 showed that the stirring speed had almost no effect on the initial reaction rate. This catalyst was tested at 190°C where limitations of mass transfer should be more noticeable than at 150°C due to the faster reaction rate at higher temperatures. However, on increasing the temperature mass and temperature transfer coefficients also increase. Both effects seem to compensate for each other, as experimental results showed. The same could happen to catalyst NR50, though its particle diameter is much larger than that of DVB resins.

It was assumed that other catalysts had the same behavior, so in subsequent experiments stirring speed was fixed at 500 rpm to avoid mass transfer limitations.

4.2.3 INFLUENCE OF CATALYST PARTICLE SIZE

The diffusion of chemicals through the catalyst depends on the particle size in great manner. In fact, the influence of internal mass transfer can be evaluated by testing catalyst batches of different d_p . In order to obtain intrinsic reaction rates experimentally, and so to obtain a more accurate kinetic model, working in d_p range where such influence is negligible is preferred.

Catalyst	T [°C]	N [rpm]	W_{cat} [g]	d_p [μm]
Dow 50	120 to 150	500	1	599
Dow 100	120 to 150	500	1	211
Dow 200	120 to 150	500	1	105
Dow 400	120 to 150	500	1	52
N117	140 to 180	500	1	-
A70*	190	500	1	571
			1	250 – 400
			1	400 – 600
			1	600 – 800
			1	> 800
CT224*	150	500	1	466
			1	100 – 160

*The commercial bead was sieved

Table 26. Working conditions: catalyst particle size

Although internal mass transfer limitations seemed not to be important in the last section, some experiments were carried out to assure it. Tests were performed with four commercial batches of catalyst Dowex 50WX4 (Dow 50, Dow 100, Dow 200 and Dow 400), with N117, a membrane formulation of Nafion NR50, with four sieved fractions of Amberlyst 70 (A70), and with a sieved fraction of CT224. Dowex and CT224 catalysts were chosen as representative of microporous DVB resins, and A70 as thermoestable macroporous resin. Working conditions of these experiments are shown in *Table 26*.

In *Figure 37* the initial reaction rate versus the inverse of the particle diameter of Dowex catalysts is plotted. As it can be observed, the initial reaction rate is independent on the particle diameter within the limits of the experimental error. Particles seem to swell enough in contact with the polar medium to permit the diffusion of chemicals through the pores, allowing a good accessibility to the inner active centers. Thus, it can be concluded that the influence of the internal mass transfer is negligible for this catalyst and working conditions.

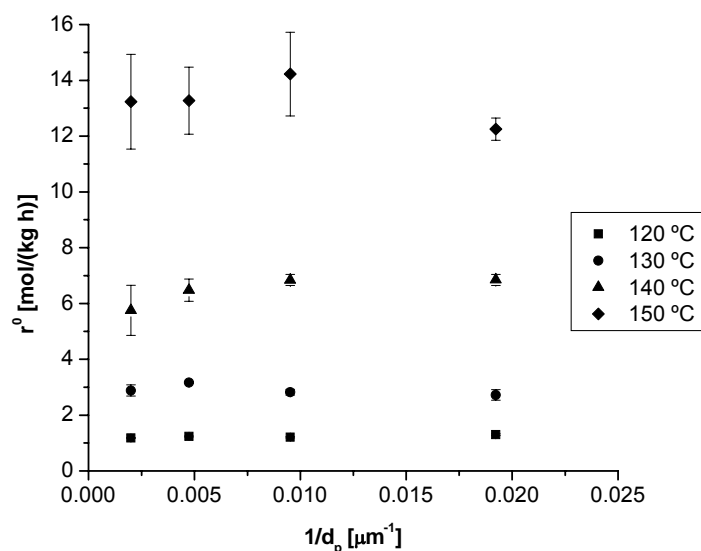


Figure 37. r^0 vs. $1/d_p$ and T ; $N=500\text{rpm}$, 1 g Dowex

In *Figure 38* the initial reaction rate at 190°C versus the inverse of the mean particle diameter of A70 sieved fractions is plotted. Filled circles correspond to the mean diameter of sieved fractions, while the open circle corresponds to the mean diameter of the commercial bead. As it can be stated in the figure, within the limits of the experimental error the influence of the internal mass transfer was negligible for catalyst A70 at 190°C and, consequently, at lower temperatures as well.

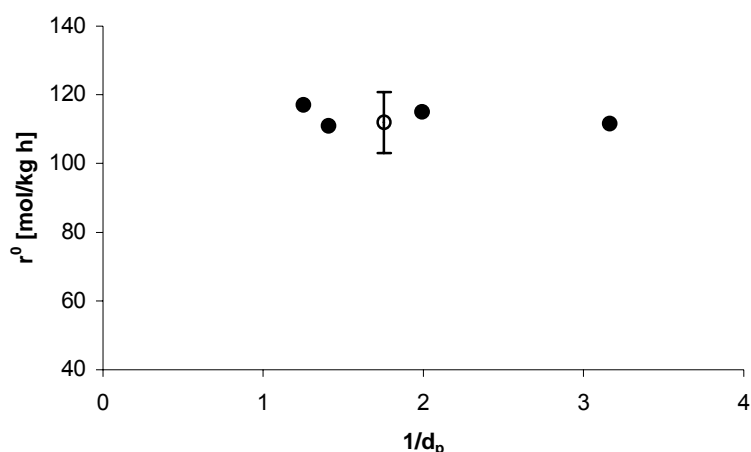


Figure 38. r^0 vs. $1/d_p$; $T=190^\circ\text{C}$; $N=500\text{rpm}$, 1 g A70

Finally, a CT-224 sieved fraction of $126\mu\text{m}$ of mean diameter was compared to the commercial bead at 150°C . Both presented the same initial reaction rate: 15.3 ± 0.4 the sieved fraction and 15.6 ± 0.2 the commercial bead.

Two microporous DVB resins at 150°C and a thermostable macroporous resin at 190°C showed that the influence of the internal mass transfer was negligible. Although it was not proved with all DVB resins, it was assumed that the other DVB resins had the same behavior. In fact, if A70, which is a macroporous resin with a more rigid structure than microporous ones, did not show diffusion limitations at 190°C , this assumption seems clear to be correct for other DVB catalysts and lower temperatures.

As for NR50, experiments with a membrane formulation of Nafion (Nafion 117), i.e. with all active centers on the external surface, showed that diffusion limitations were not important with this catalyst (see *Figure 39*).

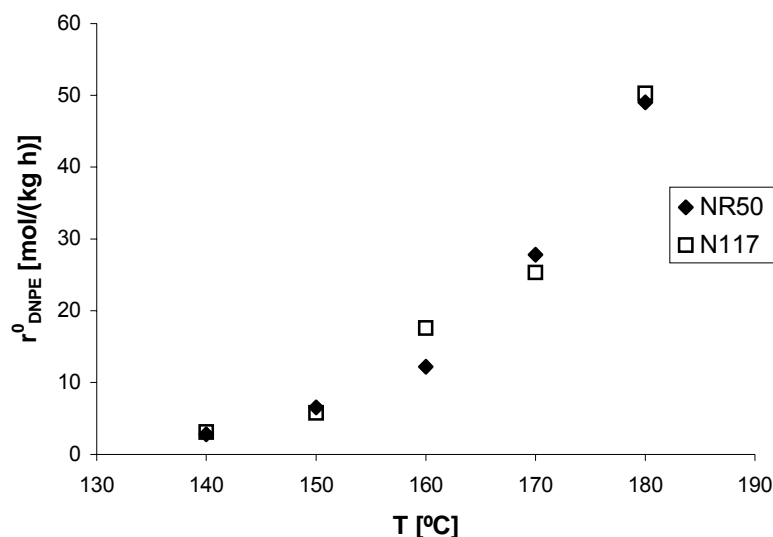


Figure 39. Nafion NR50 vs. N117. T=180°C, N=500rpm, 1 g catalyst

As for Beta zeolite, the influence of diffusion is reduced to negligible proportions with crystals of less than 100 μm [59].

4.3 CATALYSTS TESTS

Eight catalysts were tested in order to find the appropriate one to, on one hand, carry out an exhaustive kinetic study and, on the other hand, be able to use it in industry. It should show enough activity and selectivity, as well as good mechanical and thermal stability, in the temperature range explored. Finally, it should be feasible from an economical standpoint.

As commented in *section 3.1.3*, three families of catalysts of different nature were studied: a perfluoroalkanesulfonic catalyst, **Nafion NR50**; a zeolite, **H-BEA-25**; and six S/DVB resins, four of them macroporous, **Amberlyst 36, 70, DL-H/03** and **DL-I/03**, and two of them microporous, **CT-224** and **Dowex 50WX4** (four batches of different d_p). Catalysts DL-H/03 and DL-I/03 were experimental samples provided by Rohm and Haas, while the other catalysts were commercial. Batch-wise experiments were performed with the same amount of catalyst and stirring speed, lasting all of them 6 hours. 1-pentanol conversion, the selectivity of the reaction, yield to DNPE and the reaction rate were followed along the time.

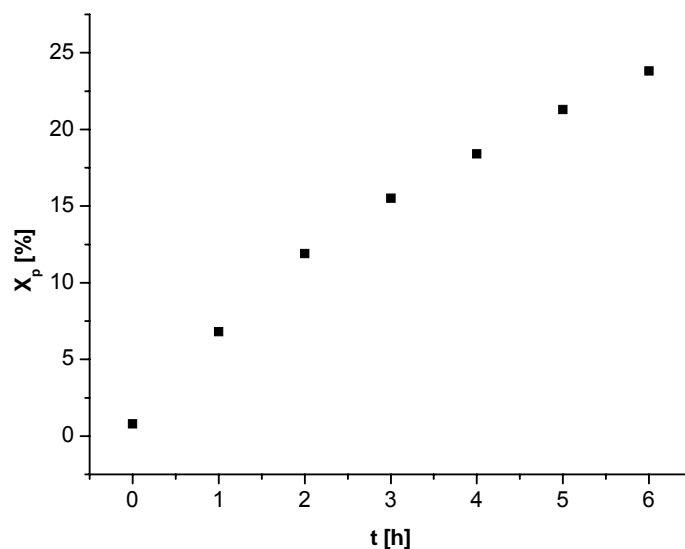
In *Table 27*, the working conditions of these tests are shown.

Catalyst	T [°C]	N [rpm]	W _{cat} [g]
A36	120 to 150	500	1
A70	140 to 190	500	1
DLH/03	130 to 170	500	1
DLI/03	130 to 170	500	1
CT224	120 to 150	500	1
Dowex 50WX4-50	120 to 150	500	1
Dowex 50WX4-100	120 to 150	500	1
Dowex 50WX4-200	120 to 150	500	1
Dowex 50WX4-400	120 to 150	500	1
NR50	140 to 190	500	1
BEA25	140 to 190	500	1

Table 27. Working conditions: catalyst selection

4.3.1 1-PENTANOL CONVERSION

Typically, 1-pentanol conversion increased along time, as it is shown in *Figure 40*, where an experiment at 150°C with catalyst A-36 is presented. It can be seen that for short reaction times the increase is sharper than at long times, when the inverse reaction becomes more important. Nevertheless, the system is still far from equilibrium at $t = 6\text{h}$ and 150°C.

Figure 40. X_p vs. time. A-36 as catalyst, 150°C

4. Results and discussion

In *Table 28* values of 1-pentanol conversion at 6 hours of reaction for all catalysts and temperatures tested are summarised. As it can be observed, 1-pentanol conversion increased on increasing temperature, reaching the highest value (67.7%) at 190°C with the thermostable catalyst A-70. It is followed by catalysts NR50 and the zeolite, two thermostable catalysts, as well. The high dependence of conversion on reaction temperature makes the maximum working temperature of catalysts an important parameter when choosing one for this reaction.

In general, at a given temperature, e.g. 150°C, where all catalyst can be compared, the higher the acid capacity, the higher the conversion was. Thus, the highest conversion at this temperature was achieved by catalyst DL-I/03, followed by A-36, while with catalyst A-70 low values were obtained. NR50 and BEA-25, with the lowest acid capacity, were the least active catalysts at 150°C. The same behavior was found at each temperature: X_p lessens in the order: S/DVB resins, NR50 and H-BEA-25. The higher acid strength of NR50 would be the cause of the higher activity of the Nafion catalyst over H-BEA-25 (see *Table 32* in *section 4.3.4*).

T (°C)	A36	A70	DLH/03	DLI/03	CT224	Dow50	Dow100	Dow200	Dow400	NR50	BEA25
120	3.6				1.9	2.1	2.2	2.1	2.3		
130	8.0		4.1	8.1	4.7	5.1	5.7	5.4	4.9		
140	13.9	7.0	8.1	13.5	11.5	10.6	10.5	10.3	10.5	4.4	2.2
150	23.8 ±0.02	13.7	15.6	25.9	20.9 ±0.7	19.4 ±0.7	20.1	20.3 ±0.6	19.5 ±0.2	9.7	4.3
160		25.1	27.5	33.8						17.5	8.9
170		41.8	43.5 ±0.4	44.7 ±0.5						33.5	16.8
180		54.1								49.4	32.0 ±0.6
190		67.7 ±0.3								59.4 ±0.9	50.3

Table 28. 1-pentanol conversion [%] vs. T at t = 6 h for all catalysts tested

Reproducibility of experiments was found to be very good. In *Table 28* the associated standard error of those experiments replicated is shown. The relative error with regard to 1-pentanol conversion was less than 4%. As for the four batches of catalyst Dowex 50WX4, the same conversion levels within the limits of experimental error were achieved at all temperatures. This was expected, as no influence of internal mass transfer was detected due to the particle swelling in the polar medium (see *section 4.2.3*).

4.3.2 SELECTIVITY

In Table 29 selectivity to DNPE at $t = 6$ h of all the catalysts and at all temperatures tested is shown.

In general, selectivity to DNPE decreases with temperature due to the formation of alkenes and, consequently, branched ethers. When increasing the temperature, the kinetic constants of all the reactions (main and side-reactions) are enhanced. As it will be seen later, activation energies of some side-reactions (mainly those leading to 1-pentene and 2-pentene formation) are higher than the one of DNPE formation. That is to say that the dependence of the kinetic constants on the temperature also is more important. So an increase of the temperature will lead to an increase on the selectivity to by-products. This can be observed in Figure 41.

T (°C)	A36	A70	DLH/03	DLI/03	CT224	Dow50	Dow100	Dow200	Dow400	NR50	BEA25
120	91.2				96.4	100.0	99.7	99.7	100.0		
130	89.7		95.7	87.9	96.8	99.5	99.3	99.6	100.0		
140	88.4	98.1	96.2	86.6	97.6	98.8	98.8	98.9	99.0	99.0	89.0
150	85.2	97.8	95.5	83.6	97.3	97.3	98.2	98.1	98.5	99.0	89.6
160		96.8	94.9	79.9						98.9	91.8
170		95.5	92.5	75.6						98.3	92.2
180		93.0								97.8	92.2
190		90.8								96.2	94.8

Table 29. Selectivity to DNPE [%] vs. T at $t = 6$ h for all catalysts tested

The amount of alkenes and branched ethers were generally quite similar, whereas 2-pentanol and other alcohols were not detected. This suggests that branched ethers could be formed by reaction between an alkene and the appropriate alcohol.

Dow50 at lower temperatures (120-140°C) and NR50 at higher temperatures (150-190°C) were the most selective catalysts to DNPE.

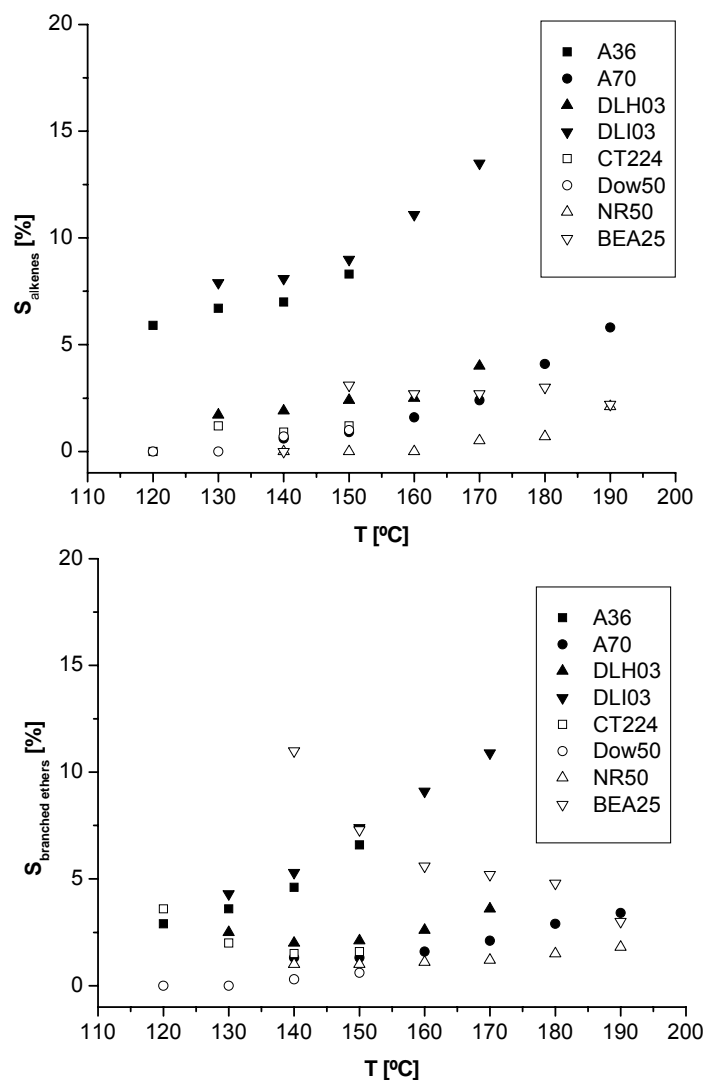


Figure 41. S_{alkenes} and S_{ethers} vs. T at $t = 6\text{h}$ for all catalysts tested

Zeolite H-BEA-25 showed a different behavior than the other catalysts: selectivity to DNPE increased with temperature. Accordingly, a decrease of selectivity to branched ethers and a slightly increase of selectivity to alkenes is also observed. These facts suggest that at higher temperatures this catalyst could be a good option to catalyze the dehydration of 1-pentanol to DNPE.

At 150°C, considering S/DVB resins, S_{DNPE} increased with V_{sp} (specific volume of the swollen polymer phase, see Table 11 in section 3.1.3.2) reaching an almost constant value of 98%, which corresponds to gel-type resins with high V_{sp} , as it is shown in Figure 42.

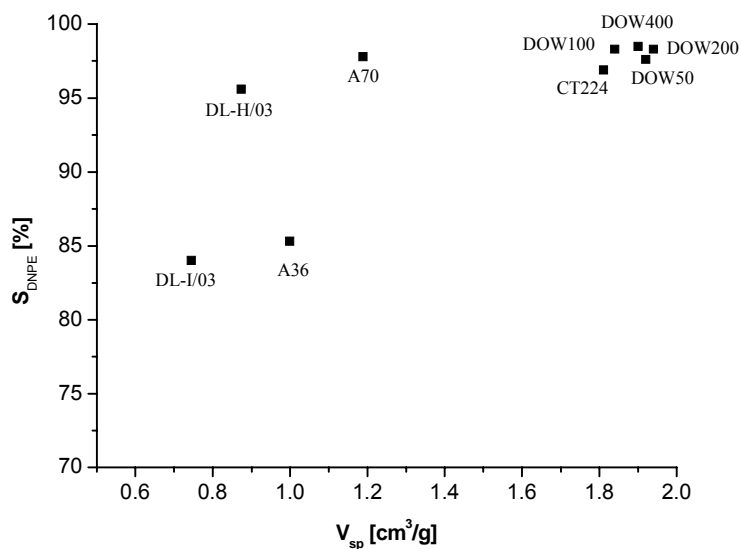


Figure 42. S_{DNPE} vs. V_{sp} , $T = 150^\circ C$, $t = 6h$

Catalysts with low V_{sp} (macroporous A-36 and DL-I/03 both with a high crosslinking degree) were not much selective to DNPE. When plotting S_{DNPE} vs. V_{sp} , such resins seemed to follow a different trend than gel-type resins and macroporous resins with a moderately expanded gel phase as Amberlyst 70 and DL-H03. However a global trend seemed to appear when plotting S_{DNPE} against porosity of swollen S/DVB polymer, as it is shown in Figure 43.

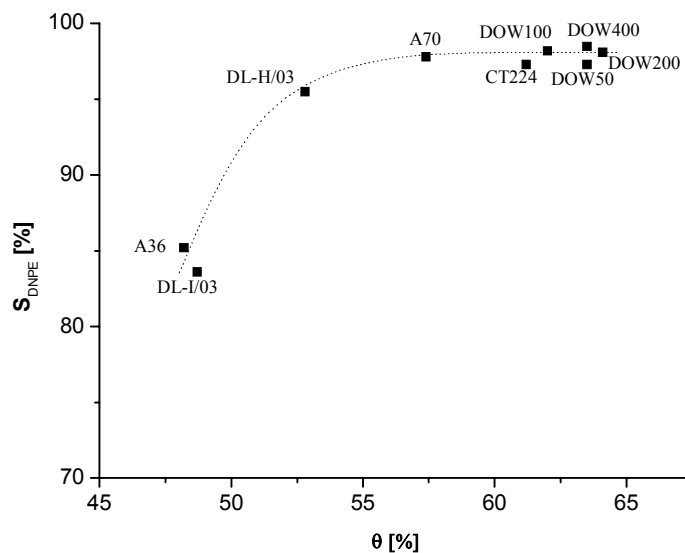


Figure 43. S_{DNPE} vs. θ , $T = 150^\circ C$, $t = 6h$

An estimation of porosity in swollen state can be made by taking into account the ISEC values of V_{sp} and V_g , and the skeletal density of the catalyst as defined in *Equation 17* in *section 3.1.3.2*.

A-36 has higher V_{sp} than DL-H/03, but the last one has a greater mesoporous phase, resulting in a higher porosity. Selectivity is influenced by acid strength of S/DVB sulfonated copolymers. Resins with higher acid strength catalyze more easily the dehydration to olefin so that S_{DNPE} decreases, as figures of Amberlyst 36 and Amberlyst DL/I-03 show.

As it can be seen in *Figure 24* (*section 3.1.3.2*), gel phase of Amberlyst 36 and DL-I/03 are quite stiff since they have a polymer density of $1.5\text{--}2\text{ nm}\cdot\text{nm}^{-3}$ in swollen state. On the contrary, Amberlyst 70, DL/H-03 and Dow 50 have polymer densities of $0.4\text{ to }1.5\text{ nm}\cdot\text{nm}^{-3}$. As a consequence they have a much more flexible polymer network. Polymer density of CT-224 ranges from $0.4\text{ to }2\text{ nm}\cdot\text{nm}^{-3}$, although the concentration fraction between $0.4\text{ and }1.5\text{ nm}\cdot\text{nm}^{-3}$ is significant enough. So, assuming that reaction takes place mainly in the gel-phase, less rigid polymers can accommodate better the reaction intermediate and so are more selective.

The mechanism of the alcohol dehydration varies depending on the water content of the reaction medium [68]. In a large excess of water, the reaction mechanism involves the in-situ formation of an oxonium ion (specific acid catalysis), which is a good leaving group by protonation. The ether is then formed by the nucleophilic attack of alcohol on the oxonium ion in a bimolecular reaction (S_N2 type) [69]. The dehydration to pentenes occurs through a monomolecular reaction of elimination (E_1 type). However, when there is no water in the system or, alternatively, alcohol is in excess, it is possible that the mechanism involves initial reaction of 1-pentanol at $-\text{SO}_3\text{H}$ site to form 1-pentylsulfate (general acid catalysis), which is a much better leaving group than oxonium ion [70]. The ether would be formed by the nucleophilic attack of second alcohol on the sulfate in a S_N2 bimolecular reaction. Whichever the reaction mechanism is, the S_N2 reaction is limited to a great extent by steric hindrance on little swollen polymers, and the occurrence of E_1 increases, leading to an increase of the selectivity to alkenes and branched ethers.

4.3.3 DNPE YIELD

As it has been defined in *section 4.1.3*, DNPE yield takes into account 1-pentanol conversion and selectivity to DNPE, so it is a good indicator of the goodness of a catalyst for the reaction studied. DNPE yield at $t = 6\text{ h}$ increased with temperature, as it can be seen in *Table 30*.

The highest yield was achieved at 190°C with catalyst A-70, followed by NR50 at the same temperature. It is to be noted that DNPE yield for DL-I/03 was lower than the one that could be assumed from its high activity at all temperatures. This fact is because of the low selectivity to DNPE shown in all the experiments.

DNPE yield had a similar behavior as 1-pentanol conversion: thermostable resins reached much higher values at elevated temperatures but conventional S/DVB catalysts were better at lower ones. On the other hand, zeolite H-BEA-25 showed promising results at 190°C indicating that it could be a good catalyst at higher temperatures.

T (°C)	A36	A70	DLH/03	DLI/03	CT224	Dow50	Dow100	Dow200	Dow400	NR50	BEA25
120	3.3				1.8	2.1	2.2	2.1	2.3		
130	7.2		3.9	7.1	4.6	5.1	5.7	5.4	4.9		
140	12.3	6.9	7.7	11.7	11.2	10.5	10.3	10.2	10.4	4.4	2.0
150	20.2	13.4	14.9	21.7	20.3	18.8	19.7	20.5	19.2	9.6	3.8
160		24.3	26.1	27.0						17.3	8.1
170		39.9	40.2	33.8						32.9	15.5
180		50.3								48.3	29.5
190		61.4								57.1	47.7

Table 30. DNPE yield [%] vs. T at t = 6h for all catalysts tested

4.3.4 REACTION RATE AND TURNOVER NUMBER

The reaction rate, which is a good indicator of the activity of a catalyst, was computed along the time as explained in *section 4.1.4*. In *Table 31* the initial reaction rates at all temperatures are shown.

As expected, r_{DNPE}^0 strongly increases with temperature and, again, the highest value is achieved at 190°C with catalyst A-70, followed by NR50. If catalysts are compared at the same temperature, e.g. 150°C, it can be seen that there is a correlation between the initial reaction rate and the acid capacity among S/DVB resins: the higher the acid capacity, the higher the reaction rate. Thus, macroporous resins Amberlyst 36 and DL-I/03, and microporous CT224,

with the higher acid capacity, give the highest values of r_{DNPE}^0 at 150°C. However, this cannot explain values of r_{DNPE}^0 achieved with NR50, much higher than expected by considering only its acid capacity. The activity of NR50 is due to the high acid strength of $-\text{SO}_3\text{H}$ groups in Nafion resins [18].

T (°C)	A36	A70	DLH/03	DLI/03	CT224	Dow50	Dow100	Dow200	Dow400	NR50	BEA25
120	1.8				1.0	1.2	1.2	1.2	1.3		
130	4.5		2.2	5.2	2.5	2.9	3.2	2.8	2.7		
140	9.1	3.9	5.6	9.3	7.3	5.8	6.5	6.8	6.8	2.5	0.8
150	18.9	8.1	11.0	18.4	15.7	13.2	13.3	14.2	12.3	5.8	1.8
160		15.6	21.4	36.1						10.9	4.3
170		33.6	41.9	60.2						24.8	8.8
180		48.7								43.6	18.2
190		111.9								67.3	32.7

Table 31. Initial reaction rate [mol/(kg-h)] vs. temperature

In Table 32, values of the Hammett acidity function, ($-\text{H}_0$) are shown [71]. Compared to S/DVB resins, the higher acid strength of NR50 is due to the electronegativity of F atoms in the skeleton of the catalyst [72]. It should be noted that the Hammett acidity function depends on the solvent where the catalyst is placed. Thus, acid strength of Amberlyst 35 decreases considerably when put in contact with water. The effect of water on DVB resins will be discussed further in section 4.6.4.

To stress the influence of the acid strength of catalysts on DNPE synthesis, initial reaction rates per equivalent of $-\text{SO}_3\text{H}$ group (H^+ for H-BEA-25) or turnover numbers, r_{eq}^0 , were computed (Table 33).

As it can be seen in Figure 44, at 150°C, r_{eq}^0 of NR50 is twice that of S/DVB resins, which confirms the high acid strength of NR50 and explains the unexpected activity shown despite its low acid capacity.

Catalyst	Aqueous conditions	Non-aqueous conditions
H ₂ SO ₄ (100%)	12	12
H ₂ SO ₄ (86%) ^(b)	8.5	8.5
H ₂ SO ₄ (70%)	5.9	5.9
H ₂ SO ₄ (63%)	4.9	4.9
H ₂ SO ₄ (48%)	2.66	2.66
H ₂ SO ₄ (35%)	2.16	2.16
Nafion NR50 ^(b)	8.4	
Amberlyst 35 ^(a)	2.65	5.6
Amberlyst 15 ^(a)	2.2	
Zeolite HZSM-5		5.7
Zeolite HY		4.4
Zeolite H-Beta ^(c)		4.4 < - H ₀ < 5.7

^aAmberlyst 15 is assumed to be representative of conventionally sulfonated resins (a SO₃-H group per benzene ring), whereas Amberlyst 35 of oversulfonated ones [73]; ^bFarcasiu et al [74]; ^cBeck and Haw [75]

Table 32. Hammet acidity [71]

On the other hand, it is worth noting that oversulfonated S/DVB resins show r_{eq}^0 a bit higher than conventional resins, which indicates that their acid strength is higher in the reacting medium. Other S/DVB resins show similar r_{eq}^0 , so their acid strength could be comparable.

T (°C)	A36	A70	DLH/03	DLI/03	CT224	Dow50	Dow100	Dow200	Dow400	NR50	BEA25
120	0.4				0.2	0.2	0.2	0.2	0.3		
130	0.9		0.6	1.0	0.5	0.6	0.6	0.6	0.6		
140	1.9	1.3	1.7	1.7	1.4	1.2	1.3	1.4	1.4	2.8	0.7
150	3.9	2.7	3.2	3.4	3.1	2.7	2.7	2.9	2.6	6.5	1.5
160		5.2	6.3	6.6						12.2	3.6
170		11.2	12.4	11.0						27.8	7.3
180		16.2								49.0	15.2
190		37.3								75.6	27.3

Table 33. Turnover numbers [mol/(eq H⁺·h)] vs. temperature

As for zeolite H-BEA-25, it shows the lowest r^0 and r_{eq}^0 of all the catalysts tested. This fact could be explained because the reaction of DNPE synthesis proceeds primarily on the external surface [57,58,59], and in this zeolite, the external surface accounts for about a 40% of total surface. Moreover, total amount of active centers is a fourth of those conventional resins.

As a result, density of acid sites at the surface is quite low, especially when compared with that of ion-exchangers. In this way, the formation of the reaction intermediate could be hindered by the low surface concentration of H^+ , which is illustrated by the very low turnover number of the zeolite, despite acid strength of H^+ in zeolites is similar to that of ion-exchangers.

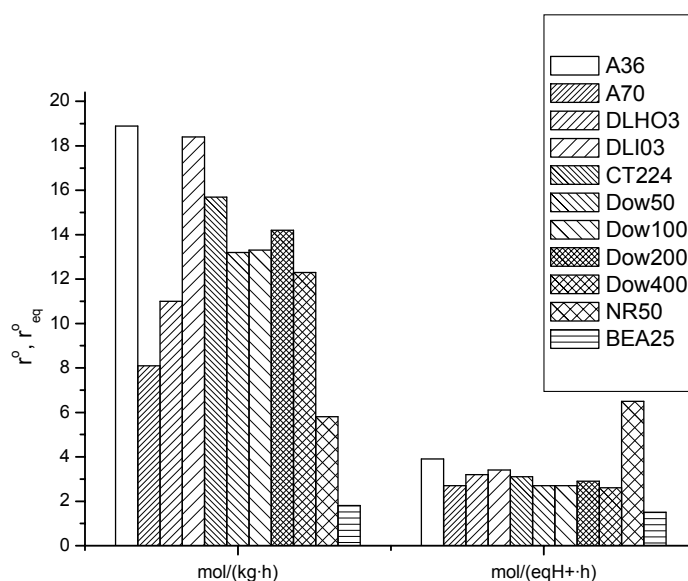


Figure 44. Initial reaction rate and turnover number at 150°C

4.3.5 CATALYST SELECTION

One of the aims of this work was to select a catalyst which could be used in industry for the dehydration of 1-pentanol to DNPE. Furthermore, a catalyst was also needed to perform a deep kinetic analysis and for equilibrium experiments. The following conclusions with respect to catalyst tests could be drawn from the previous sections:

- ✓ At lower temperatures, up to 150°C, S/DVB resins were the most active and selective catalysts. But their low maximum working temperature was an important drawback for the production of DNPE.

- ✓ Among thermally stable resins, Amberlyst 70 appeared as the best choice for the dehydration of 1-pentanol to DNPE, since it was more selective to the ether. Compared to the other S/DVB resins, its thermal stability led to higher conversion and yield, with reasonable selectivity, even at 190°C.
- ✓ Nafion NR50 was the most selective catalyst and it was quite active at higher temperatures because of its high acid strength. But its activity at lower temperatures was not high due to the low concentration of sulfonic groups into the polymer matrix. Furthermore, it is too expensive for industrial use.
- ✓ H-BEA-25 zeolite was the least active among the catalysts tested, although high conversion was achieved at 190°C, which could indicate that it could be a promising catalyst at higher temperatures.

For industrial use, an active, cheap and, especially, selective catalyst is needed. Selectivity to DNPE is important to minimize purifying costs, so the operating temperature would not be very high. Therefore, one of DVB resins, probably **Dowex 50WX4**, would be the catalyst chosen due to its high selectivity to DNPE and activity at 150°C. It should be pointed out that the DNPE production would not be performed in a batch reactor as the one used in this work, but with simultaneous water withdrawing in order to swift the equilibrium to full consumption of 1-pentanol, such as in a catalytic membrane reactor or in a catalytic distillation system.

On the other hand, for kinetic and equilibrium experiments an active and selective catalyst is also needed, but with a higher temperature operating range to shorten the experiments. The best option seems to be the thermostable ion-exchange resin **Amberlyst 70**, due to its wide temperature range, high activity and acceptable selectivity.

4.4. INFLUENCE OF 2-METHYL-1-BUTANOL

As explained in *section 1.5.2*, a process scheme to obtain DNPE could be the hydroformylation of n-butenes to n-pentanal, followed by hydrogenation of the aldehyde intermediate product. With this hydrogenation step not only 1-pentanol would be obtained but 2-methyl-1-butanol as well.

Catalyst	Ratio 2m1BuOH/1-PeOH	T [°C]	N [rpm]	W _{cat} [g]
DL-H/03	100/0%	170	500	1
	50/50%			
	15/85%			
	5/95			

Table 34. Working conditions: 2-methyl-1-butanol influence

The influence of 2-methyl-1-butanol in the dehydration of 1-pentanol to DNPE was studied. Experiments were carried out with different mixtures of 2-methyl-1-butanol/1-pentanol (*Table 34*) at 170°C with Amberlyst DL-H/03 as catalyst. The experimental procedure was the same as for catalyst selection (500 rpm, 1 g catalyst, 6 h), so results were compared to the experiments performed at 170°C with the same catalyst and “pure” 1-pentanol, which had a 0.5% of 2-methyl-1-butanol as impurity.

In *Figure 45* the amount (in % of chromatographic Area) of the following ethers formed is shown: DNPE (symmetrical linear ether formed from 2 molecules of 1-pentanol), 2-methyl-1-butyl ether (symmetrical branched ether formed from 2 molecules of 2-methyl-1-pentanol), and other ethers (asymmetrical ethers).

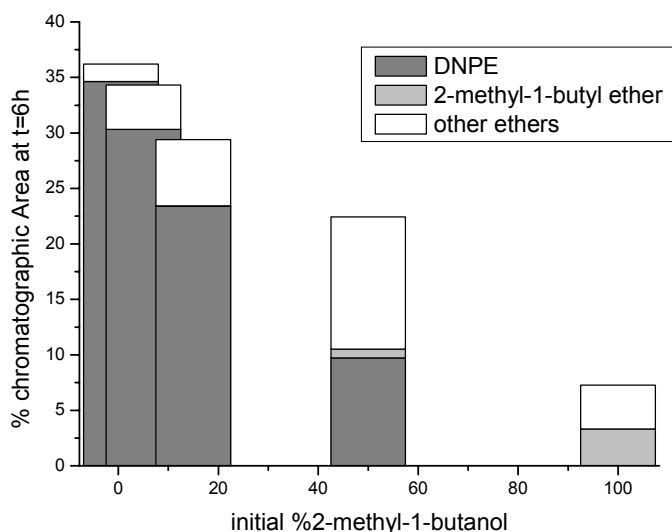


Figure 45. Amount of ethers formed at t=6h and 170°C with different initial 2-methyl-1-butanol concentrations

It can be observed that the total amount of ethers decreased on increasing the initial

concentration of the branched alcohol. In particular, the selectivity to DNPE, which was the desired product (symmetrical and linear ethers have higher cetane number than asymmetrical and branched ones), fell dramatically, while 2-methyl-1-butyl ether was scarcely produced.

In *Figure 46* the amount of olefins formed is shown, divided into 1-pentanol derived (1-pentene and cis/trans-2-pentene) and 2-methyl-1-butanol derived (2-methyl-1-butene, etc.). The olefin formation increased considerably on increasing the concentration of 2-methyl-1-butanol. In fact, almost all the olefins formed corresponded to 2-methyl-1-butanol derived. However, the global reactivity decreased considerably on increasing the initial amount of branched alcohol, due to steric hindrance, probably.

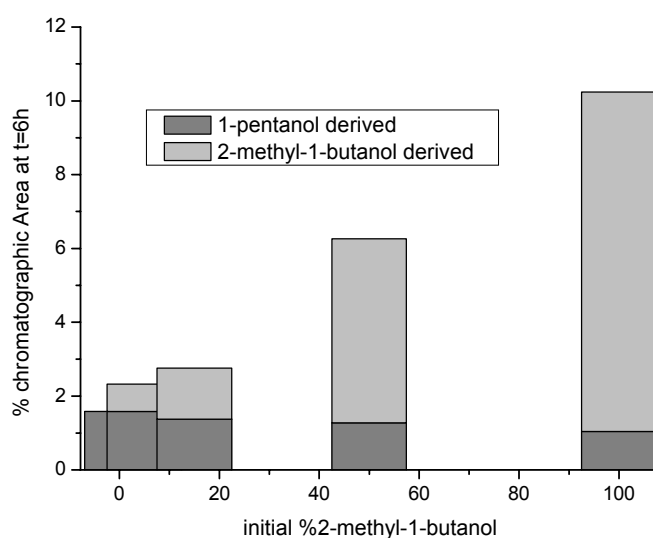


Figure 46. Amount of olefins formed at t=6h and 170°C with different initial 2-methyl-1-butanol concentrations

Thus, at 170°C and Amberlyst DL-H/03 as catalyst, on increasing the initial 2-methyl-1-butanol concentration the olefin formation was enhanced, since a great part of the branched alcohol that reacted did it to form olefins. A similar behavior is expected with other catalysts.

As a conclusion, it is necessary that hydroformylation of n-butene fraction should be very selective to 1-pentanal, in order to switch the reaction to the production of ethers, DNPE mainly.

4.5 THERMODYNAMIC EQUILIBRIUM

No information was found in the literature concerning thermodynamic quantities of the

reaction of dehydration of 1-pentanol to DNPE, such as the enthalpy change of reaction in liquid phase, $\Delta_r H_m$, the entropy change of reaction, $\Delta_r S_m$, or the free energy change, $\Delta_r G_m$, and, as a consequence, of the equilibrium constant.

Therefore, a series of experiments was undertaken to determine values of the equilibrium constant by direct measurement of the mixture composition at equilibrium at several temperatures. Then the enthalpy change of DNPE synthesis could be calculated and compared with quantities estimated theoretically.

4.5.1 DETERMINATION OF THE EQUILIBRIUM CONSTANT

Besides the etherification reaction products, 1-pentene and specially 2-pentene (*cis* and *trans*) were detected in some extent in preliminary experiments at high temperatures and long reaction time.

1-Pentene could be produced by means of the monomolecular dehydration of 1-pentanol to 1-pentene and water, and/or by decomposition of DNPE to 1-pentanol and 1-pentene. Since 1-pentanol concentration was very low throughout the experiments, the most likely reaction for 1-pentene production was DNPE decomposition. 2-Pentene was produced through isomerization of 1-pentene.

Some branched ethers, e.g. 1,2-oxybis pentane, 2,2-oxybis pentane, 2-methyl-1-butyl 2-pentyl ether and 2-methyl-1-butyl 1-pentyl ether, were detected in very small amounts. Since 2-pentanol was not detected, these ethers were formed by direct reaction of 1-pentanol and 2-methyl-1-butanol with olefins.

The formation of branched ethers shifted the main reaction to the decomposition of the ether, so the system reached a quasi-equilibrium state wherein the molar fractions of DNPE and 1-pentanol had a very slight trend to decrease, as it can be observed in *Figure 47*, whereas those of water rose very slowly. This fact was observed at higher temperatures, when to attain a constant composition was rather difficult. In this case, the assessment of the equilibrium state was done by checking the constancy of the calculated equilibrium constant, within the limits of the experimental error, instead of checking the composition constancy.

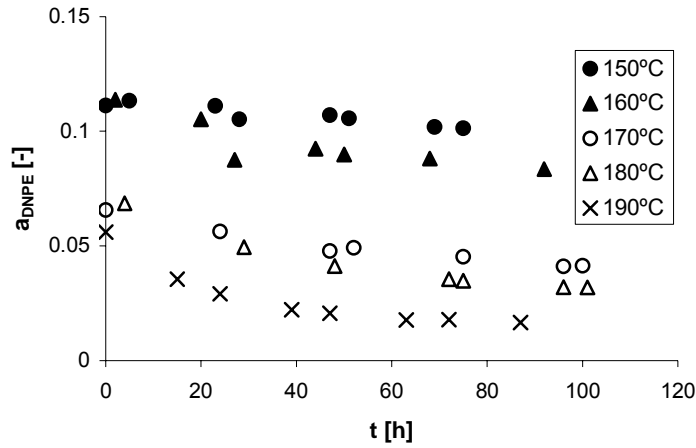


Figure 47. Equilibrium activities of DNPE at 150-190°C

Therefore, three reactions were studied at equilibrium conditions: 1-pentanol dehydration to DNPE and water (denoted by DNPE in subsequent equations); DNPE decomposition reaction to 1-pentanol and 1-pentene (denoted by 1-pentene), and isomerization of 1-pentene to 2-pentene (denoted by 2-pentene). In the last reaction, cis-2-pentene and trans-2-pentene were joined together and considered as 2-pentene.

In order to take into account the non-ideality of the mixture, activity coefficients of compounds, γ_i , were estimated by the UNIFAC-DORTMUND predictive method [66], including all compounds detected during the experiments. The thermodynamic equilibrium constant for a liquid phase reaction of a non-ideal system is given by

$$K_a = \prod_{i=1}^S (a'_i)_e^{v_i} = \prod_{i=1}^S (\gamma_i)_e^{v_i} (x_i)_e^{v_i} = \prod_{i=1}^S (\gamma_i)_e^{v_i} \prod_{i=1}^S (x_i)_e^{v_i} = K_\gamma \cdot K_x \quad \text{Equation 32}$$

where K_γ of the three reactions were calculated by

$$K_\gamma^{\text{DNPE}} = \frac{\gamma_{\text{DNPE}} \cdot \gamma_{\text{water}}}{\gamma_{1\text{-pentanol}}^2} \quad \text{Equation 33}$$

$$K_\gamma^{1\text{-pentene}} = \frac{\gamma_{1\text{-pentene}} \cdot \gamma_{1\text{-pentanol}}}{\gamma_{\text{DNPE}}} \quad \text{Equation 34}$$

$$K_\gamma^{2\text{-pentene}} = \frac{\gamma_{2\text{-pentene}}}{\gamma_{1\text{-pentene}}} \quad \text{Equation 35}$$

4. Results and discussion

where superscripts DNPE, 1-pentene and 2-pentene refer to 1-pentanol dehydration to DNPE and water, DNPE decomposition reaction to 1-pentanol and 1-pentene, and 1-pentene isomerization to 2-pentene, respectively. K_x were calculated in a similar way by changing activity coefficients by molar fractions:

$$K_x^{\text{DNPE}} = \frac{x_{\text{DNPE}} \cdot x_{\text{water}}}{x_{1\text{-pentanol}}^2} \quad \text{Equation 36}$$

$$K_x^{1\text{-pentene}} = \frac{x_{1\text{-pentene}} \cdot x_{1\text{-pentanol}}}{x_{\text{DNPE}}} \quad \text{Equation 37}$$

$$K_x^{2\text{-pentene}} = \frac{x_{2\text{-pentene}}}{x_{1\text{-pentene}}} \quad \text{Equation 38}$$

Figure 48 shows the evolution of activities of 1,4-dioxan, DNPE, 1-pentanol, water, 1-pentene and 2-pentene of a model experiment at 180°C. Activities increased or decreased to reach equilibrium or quasi-equilibrium conditions in circa 48 hours.

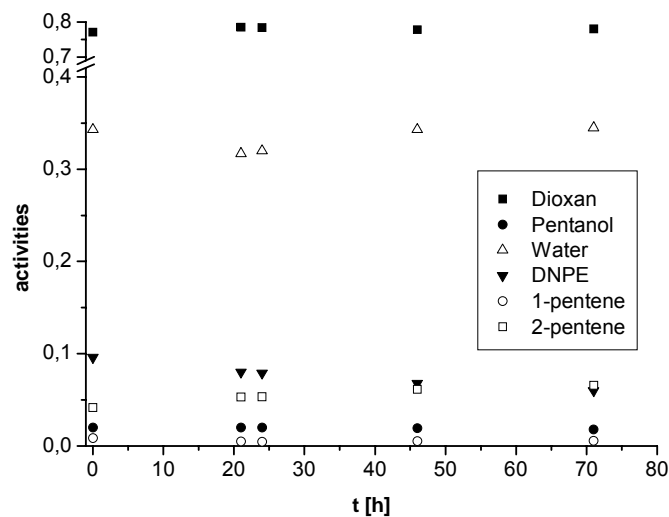


Figure 48. Evolution of activities during an experiment at 180°C over time

As the system was diluted with 1,4-dioxan, its activity was clearly higher than the others (it should be noted that the y axis is broken from 0.4 to 0.7). Water activities were also quite high compared to the others, mainly because of its high activity coefficient (higher than 2). On the other hand, 1-pentene activities were always very small (around 0.004) due to its low molar fraction. This fact supposed a drawback for the equilibrium characterization, since 1-pentene

concentrations were near the detector threshold of the chromatograph, especially at lower temperatures.

In *Figure 49* the evolution of calculated K_a 's over time is shown for the same model experiment plotted in *Figure 48*, which states that pseudo-equilibrium conditions were achieved.

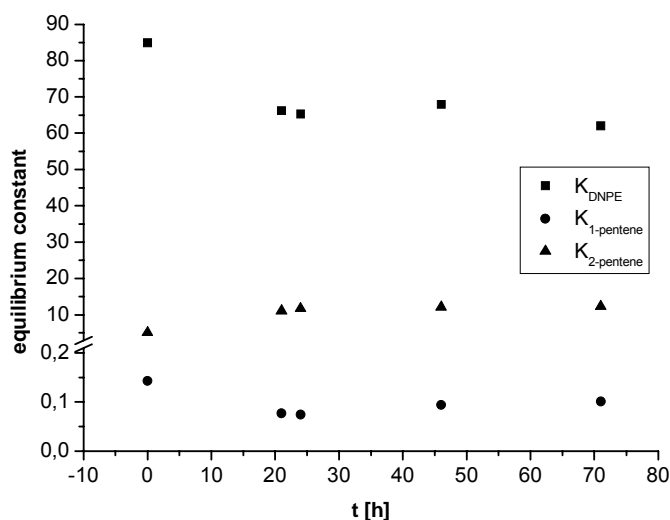


Figure 49. Evolution of the calculated equilibrium constants of an experiment at 180°C over time

4.5.2 EXPERIMENTAL EQUILIBRIUM CONSTANT

Experiments were carried out at the same set up as the used in the catalysts tests. A mixture near equilibrium conditions was charged into the reactor to shorten the experiments. In *Table 35* the working conditions of this kind of experiments are shown.

Catalyst	Solvent	T [°C]	N [rpm]	W_{cat} [g]
A70	1,4-dioxan	150 to 190	350	1 to 5

Table 35. Working conditions: equilibrium experiments

In order to ensure that only a single phase existed during the whole experiment, the use of a solvent was necessary. Preliminary equilibrium experiments showed that two phases (organic and water) were formed during long-time runs when 1-pentanol conversions were high and the amount of water was important. Some solvents were tested, such as acetone, sulfolan,

dimethylsulfoxide and 1,4-dioxan. The latter was chosen since it was the only one that ensured a single phase in tests at 20°C. Blank experiments performed with the same amount of catalyst used in subsequent experiments showed that 1,4-dioxan did not react under the experimental conditions. Moreover, the peak of 1,4-dioxan did not overlap the peaks of reactants, products or by-products in chromatographic analysis.

Amberlyst 70 was used as catalyst since it proved to have a good activity, selectivity and it was thermally stable up to 190°C. The stirring speed was lowered to 350rpm (still higher than 300rpm, where mass transfer limitations began) to prevent solid particles attrition. Catalyst mass was not fixed in order to check whether it had any effect on the equilibrium constant. Finally, temperature ranged from 150 to 190°C.

Reaction time to achieve equilibrium conditions varied depending on the temperature and catalyst mass. Typically, the reacting system lasted 48-72 hours to reach equilibrium conditions. Table 36 shows the experimental conditions of the experiments and the equilibrium constants calculated for the dehydration of 1-pentanol to DNPE and water. K_y^{DNPE} were calculated by means of Equation 33, and K_x^{DNPE} by means of Equation 36. K_a^{DNPE} were computed from Equation 32. Values of this equilibrium constants are the average of that of the calculated at quasi-equilibrium during the experiments.

T [°C]	W [g]	K_x^{DNPE}	K_y^{DNPE}	K_a^{DNPE}	K_{DNPE}
150	4.265	22.7	2.440	55.5	55.5 ± 0.5
160	3.226	23.3	2.371	55.2	54.6 ± 0.9
160	3.63	23.0	2.342	53.9	
170	1.666	23.7	2.200	52.0	52.1 ± 0.1
170	4.215	24.8	2.104	52.2	
180	1.014	23.7	2.150	50.8	49.5 ± 1.9
180	1.700	23.1	2.088	48.2	
190	2.100	24.4	1.954	47.7	47.7 ± 1.2

Table 36. Experimental conditions and obtained equilibrium constants of the dehydration of 1-pentanol to DNPE and water

Duplicate runs were made at some temperatures, and the reproducibility of experiments was found to be quite good. K_{DNPE} is the average value of K_a^{DNPE} when duplicate experiments were made. As it can be seen, the catalyst mass used had no effect on the measured equilibrium

constant, as expected, and values of K_y proved the non-ideality of the mixture. K^{DNPE} values were high enough to state that the main reaction is clearly shifted to the products at equilibrium, what assures good conversion levels of 1-pentanol to ether in industrial etherification processes. Moreover, it hardly changed with temperature, which points out that conversion is quite promising to produce the ether in all the experimental temperature range. The equilibrium constant of the dehydration of 1-pentanol to DNPE and water decreased with temperature, so it is an exothermic reaction. However, the variation with the temperature was not very high, which implies that the enthalpy change of reaction is small.

In Table 37 and Table 38 the equilibrium constants of DNPE decomposition reaction to 1-pentene and 1-pentanol, and the isomerization of 1-pentene to 2-pentene are shown. The equilibrium constant of DNPE decomposition reaction increased with temperature, so it is an endothermic reaction. As a consequence, this reaction could be a drawback in an industrial reactor operated at conversions of 1-pentanol close to equilibrium, especially at high temperatures. Fortunately, the equilibrium constant of this side reaction was very low in the temperature range explored. This was mainly caused by the low activities of 1-pentene obtained in all equilibrium experiments, especially at lower temperatures, i.e. 1-pentene was produced in low extent (or when it was produced it quickly isomerized to 2-pentene which is more stable). This fact was a drawback for the chromatographic analysis since some analysis of this compound could have an important inaccuracy associated. On the other hand, the equilibrium constant of the isomerization of 1-pentene to 2-pentene (cis and trans) decreased with temperature, so it is an exothermic reaction.

T [°C]	W [g]	$K_x^{1\text{-pentene}} \cdot 10^4$	$K_y^{1\text{-pentene}}$	$K_a^{1\text{-pentene}} \cdot 10^4$	$K_{1\text{-pentene}} \cdot 10^4$
150	4.265	2.7	1.616	4.3	4.3 ± 0.3
160	3.226	4.2	1.637	6.8	6.8 ± 0.1
160	3.63	4.1	1.644	6.7	
170	1.666	7.4	1.601	11.8	10.9 ± 1.3
170	4.215	5.6	1.757	9.9	
180	1.014	9.2	1.633	14.9	15.9 ± 1.4
180	1.700	10.2	1.671	17.0	
190	2.1	13.1	1.864	24.4	24.4 ± 2.5

Table 37. Experimental conditions and obtained equilibrium constants of DNPE decomposition reaction to 1-Pentanol and 1-Pentene

$K_{\gamma}^{1\text{-pentene}}$ values proved again the non-ideality of the mixture, which was expected a priori due to the difference in the polarity among 1-pentanol, water and 1-pentene. On the other hand, $K_{\gamma}^{2\text{-pentene}}$ values were very close to 1, since both alkenes have similar polarities.

$K_a^{2\text{-pentene}}$ values were much higher than 1, so the isomerization reaction was clearly shifted to 2-pentene (cis and trans). This agrees with the general rule of alkene stability, which states that the more substituted alkene should predominate in the thermodynamic equilibrium state.

T [°C]	W [g]	$K_x^{2\text{-pentene}}$	$K_{\gamma}^{2\text{-pentene}}$	$K_a^{2\text{-pentene}}$	$K_{2\text{-pentene}}$
150	4.265	18.3	1.053	19.3	19.3 ± 0.6
160	3.226	15.1	1.053	15.9	16.8 ± 0.6
160	3.63	16.8	1.050	17.6	
170	1.666	13.6	1.039	14.1	14.0 ± 0.2
170	4.215	13.5	1.029	13.9	
180	1.014	12.0	1.035	12.5	12.3 ± 0.3
180	1.700	11.8	1.026	12.1	
190	2.100	11.7	1.01	11.8	11.8 ± 0.1

Table 38. Experimental conditions and obtained equilibrium constants of the isomerization of 1-pentene to 2-pentene

4.5.3 PRESSURE CORRECTION FACTOR

Deviation in K_a values due to the difference between the working pressure and the pressure at the standard state was evaluated by means of the Poynting correction factor K_{Γ} . It can be estimated by [76]

$$K_{\Gamma} = \exp\left[\frac{P-1}{RT} \sum_{i=1}^s v_i V_i\right] \quad \text{Equation 39}$$

where V_i is the molar volume of compound i .

In *Table 39* the molar volumes estimated at working temperatures with the HBT method [77] and the correction factors for the three reactions are shown. It can be seen that neglecting K_{Γ} introduced an error in the calculation of K_a that is lower than the experimental one. Therefore, it can be assumed that the equilibrium constant is only a function of temperature.

T [°C]	V _{PeOH} ^a [Lmol ⁻¹]	V _{DNPE} ^a [Lmol ⁻¹]	V _{water} ^a [Lmol ⁻¹]	V _{1-pentene} ^a [Lmol ⁻¹]	V _{2-pentene} ^a [Lmol ⁻¹]	K _T ^{DNPE}	K _T ^{1-pentene}	K _T ^{2-pentene}
150	0.125	0.205	0.019	0.170	0.144	0.989	1.039	0.989
160	0.127	0.208	0.019	0.180	0.153	0.989	1.042	0.989
170	0.129	0.212	0.020	0.193	0.164	0.989	1.046	0.988
180	0.132	0.215	0.020	0.207	0.178	0.989	1.051	0.988
190	0.134	0.219	0.020	0.225	0.195	0.989	1.056	0.988

^aCalculated with the HBT method [see *Appendix III*]

Table 39. Molar volumes of 1-pentanol, DNPE, water, 1-pentene and 2-pentene, and correction factors for the three reactions

4.5.4 TEMPERATURE DEPENDENCE OF THE EQUILIBRIUM CONSTANT

The thermodynamic equilibrium constant can be related to thermodynamic properties of the system by means of the well-known equation

$$K_a = \exp\left(\frac{-\Delta_r G_{(l)}^0}{RT}\right) \quad \text{Equation 40}$$

The standard free energy change for the liquid-phase reaction can be computed from the standard enthalpy and entropy change, as follows

$$\Delta_r G_{(l)}^0 = \Delta_r H_{(l)}^0 - T \cdot \Delta_r S_{(l)}^0 \quad \text{Equation 41}$$

The temperature dependence of the equilibrium constant can be expressed by using *Equations 40* and *41*:

$$\ln K_a = \frac{\Delta_r S_{(l)}^0}{R} - \frac{\Delta_r H_{(l)}^0}{RT} \quad \text{Equation 42}$$

If the enthalpy change of reaction is assumed to be **constant over the temperature range**, by fitting *Equation 42* to experimental values of equilibrium constant (see *Figure 50*), the standard molar enthalpy change of reaction, $\Delta_r H_{(l)}^0$, can be obtained from the slope and the standard molar entropy change of reaction, $\Delta_r S_{(l)}^0$, from the intercept. Then, the dependence of K_a on temperature could be written for each reaction as follows:

$$\ln K_a^{DNPE} = \frac{(783.4 \pm 75.5)}{T} + (2.18 \pm 0.17) \quad \text{Equation 43}$$

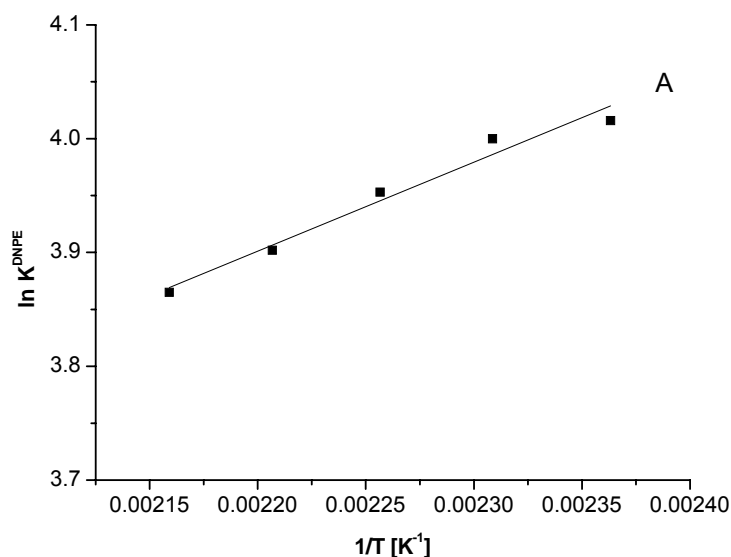
$$\ln K_a^{1\text{-pentene}} = \frac{(-8464.8 \pm 106.2)}{T} + (12.26 \pm 0.24) \quad \text{Equation 44}$$

$$\ln K_a^{2\text{-pentene}} = \frac{(2549.3 \pm 249.0)}{T} - (3.08 \pm 0.53) \quad \text{Equation 45}$$

where T is the temperature in *Kelvins*. This Equations show that on increasing the temperature, K_a^{DNPE} and $K_a^{2\text{-pentene}}$ decreased (exothermic reaction), while $K_a^{1\text{-pentene}}$ increased (endothermic reaction). In *Table 40* values of $\Delta_r H_{(l)}^0$ and $\Delta_r S_{(l)}^0$ computed from experimental data considering $\Delta_r H_{(l)}^0$ constant over the temperature range are shown. Values of $\Delta_r G_{(l)}^0$ calculated from *Equation 41* are also shown.

Reaction	$\Delta_r H_{(l)}^0$	$\Delta_r S_{(l)}^0$	$\Delta_r G_{(l)}^0$
DNPE	-6.5 ± 0.6	18 ± 1	-12 ± 1
1-pentene	70.4 ± 0.9	102 ± 2	40 ± 2
2-pentene	-21 ± 2	-26 ± 5	-14 ± 4

Table 40. Standard enthalpy, entropy and free energy changes, when considered constant over the T range



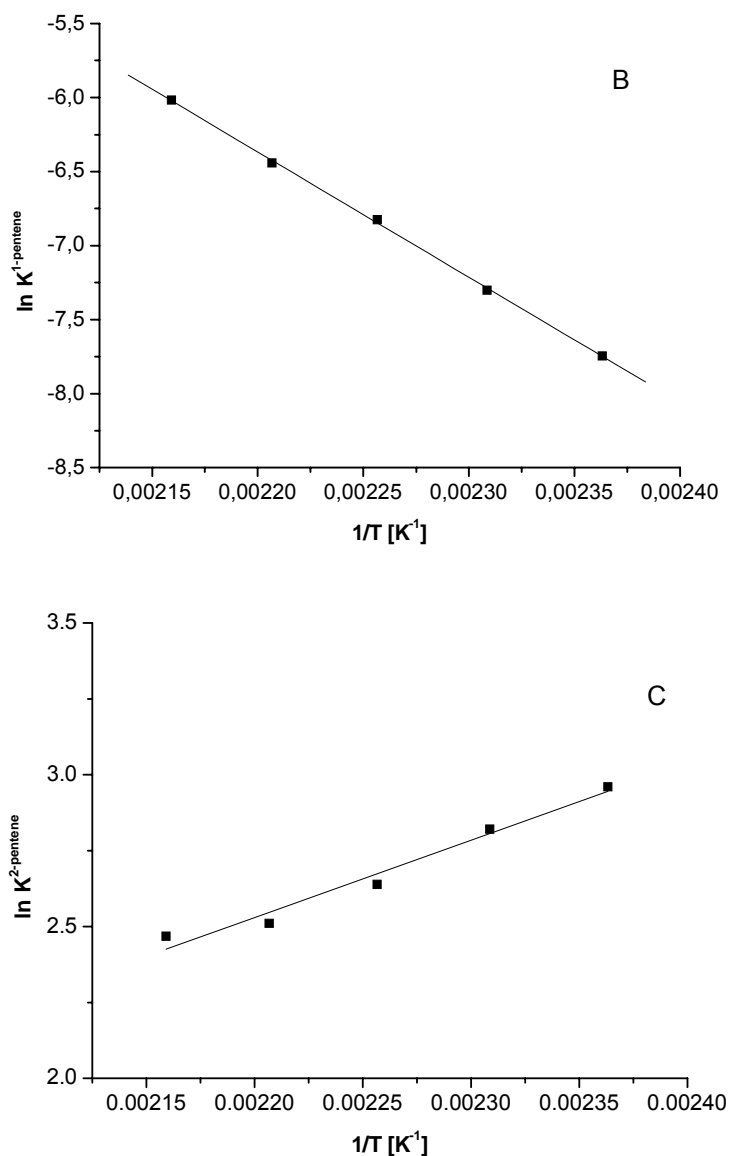


Figure 50. In K vs. 1/T. Comparison between values obtained experimentally (■) and those predicted (–) from Eq. 43 (A), 44 (B), 45 (C)

On the other hand, if the standard enthalpy of reaction is **not considered to be constant over the temperature range**, its dependence on the temperature can be computed from the Kirchoff equation:

$$\frac{d\Delta H_{(l)}^0}{dT} = \sum_{i=1}^S \nu_i \cdot C_{p(l)i} \quad \text{Equation 46}$$

4. Results and discussion

where $C_{p(i)}$ are the molar heat capacities in the liquid phase of compounds that take part in the reaction, which can be expressed in the polynomial form as follows

$$C_{p(l)i} = a_i + b_i T + c_i T^2 + d_i T^3 \quad \text{Equation 47}$$

By integrating *Equation 46*, and considering *Equation 47*, the following expression can be obtained:

$$\Delta_r H_{(l)}^0 = I_K + aT + (b/2)T^2 + (c/3)T^3 + (d/4)T^4 \quad \text{Equation 48}$$

$$\text{where } a = \sum_{i=1}^S \nu_i a_i; \quad b = \sum_{i=1}^S \nu_i b_i; \quad c = \sum_{i=1}^S \nu_i c_i; \quad d = \sum_{i=1}^S \nu_i d_i$$

The dependence of the equilibrium constant on temperature is deduced from the van't Hoff equation

$$\frac{d \ln K}{dT} = \frac{\Delta_r H_{(l)}^0}{RT^2} \quad \text{Equation 49}$$

Considering *Equation 49*, the integration of the van't Hoff equation leads to

$$\ln K = I_H - \frac{I_K}{RT} + \frac{a}{R} \ln T + \frac{b}{2R} T + \frac{c}{6R} T^2 + \frac{d}{12R} T^3 \quad \text{Equation 50}$$

	units	1-pentanol	DNPE	water	1-pentene	2-pentene
$C_p = a + bT + cT^2 + dT^3$	J/(mol K)					
a		177.73 ^a	-126.85 ^b	106.61 ^c	46.12 ^d	56.75 ^d
b		0.1872	2.3799	-0.2062	0.8055	0.7201
c		$-3.456 \cdot 10^{-4}$	$-3.240 \cdot 10^{-3}$	$3.777 \cdot 10^{-4}$	$-2.694 \cdot 10^{-3}$	$-2.563 \cdot 10^{-3}$
d		$7.892 \cdot 10^{-7}$	$1.550 \cdot 10^{-6}$	$-1.226 \cdot 10^{-7}$	$4.236 \cdot 10^{-6}$	$4.096 \cdot 10^{-6}$
$\Delta_f H_m^0 (298.15K)$	kJ/mol	-351.62 ^e	-435.2 ^f	-285.830 ^c	-46.94 ^g	-58.24 ^g
$S_m^0 (298.15)$	J/(mol K)	258.9 ^h	394.44 ⁱ	69.95 ^c	262.6 ^j	256.8 ^k

^aEstimated by Rowlinson-Bondi method and fitted to a third order equation [77]. ^bObtained by calorimetry and fitted to a third order equation. ^cCalculated from Shomate equation and fitted to a third order equation [78].

^dEstimated by Lyman-Dannen method and fitted to a third order equation [77]. ^eMosselman et al. [79]. ^fMurrin et al. [80]. ^gWilberg et al. [81]. ^hCounsel et al. [82]. ⁱEstimated by a modified Benson method [83]. ^jMesserly et al. [84]. ^kChao et al. [85]

Table 41. Thermochemical data of 1-pentanol, DNPE, water, 1-pentene and 2-pentene

In *Table 41*, thermochemical data of the compounds involved in the three reactions is

presented (see Appendix IV). The integration constants I_K and I_H can be calculated from the temperature dependence relationship of the experimental equilibrium constant of each reaction. By fitting Equation 50 to the experimental values of equilibrium constant at different temperatures (see Figure 51), I_K can be obtained from the slope and I_H from the intercept. By means of Equations 41, 42, and 48 the molar changes of reaction $\Delta_r S_{(l)}^0$, $\Delta_r G_{(l)}^0$ as a function of temperature for each reaction can be obtained as follows:

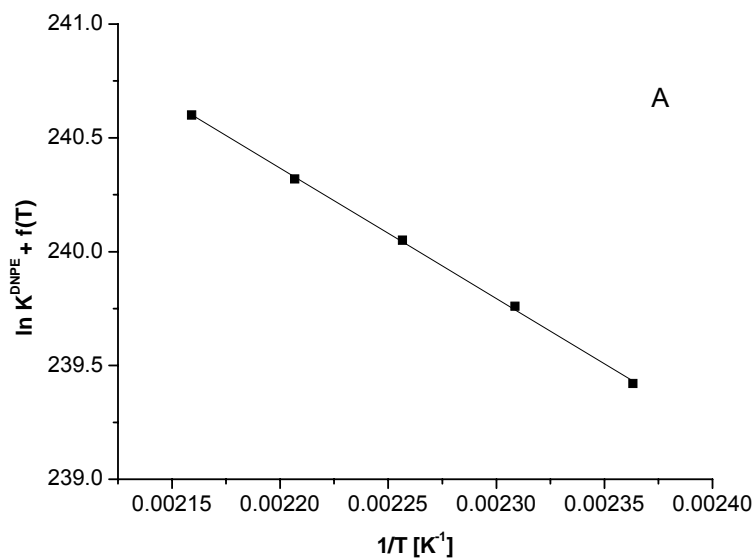
$$\Delta_r S_{(l)}^0 = R \cdot I_H + a + a \ln T + bT + \frac{c}{2}T^2 + \frac{d}{3}T^3 \quad \text{Equation 51}$$

$$\Delta_r G_{(l)}^0 = I_K - R \cdot I_H T - aT \ln T - \frac{b}{2}T^2 - \frac{c}{6}T^3 - \frac{d}{12}T^4 \quad \text{Equation 52}$$

In Table 42 values of I_K , I_H , and a , b , c and d for every reaction studied are presented.

	units	DNPE	1-pentene	2-pentene
I_K	J/mol	47749.1	11844.8	-19969.58
I_H	adim	253.004	-227.536	-8.65609
a	J·(mol·K) ⁻¹	-375.689	350.693	10.6329
b	J·(mol·K) ⁻²	1.79924	-1.38719	-8.5368E-02
c	J·(mol·K) ⁻³	-2.171E-03	2.007E-04	1.307E-04
d	J·(mol·K) ⁻⁴	-1.514E-07	3.476E-06	-1.401E-07

Table 42. Temperature dependence relationship parameters of K , $\Delta H_{(l)}^0$, $\Delta S_{(l)}^0$, $\Delta G_{(l)}^0$ for the three reactions



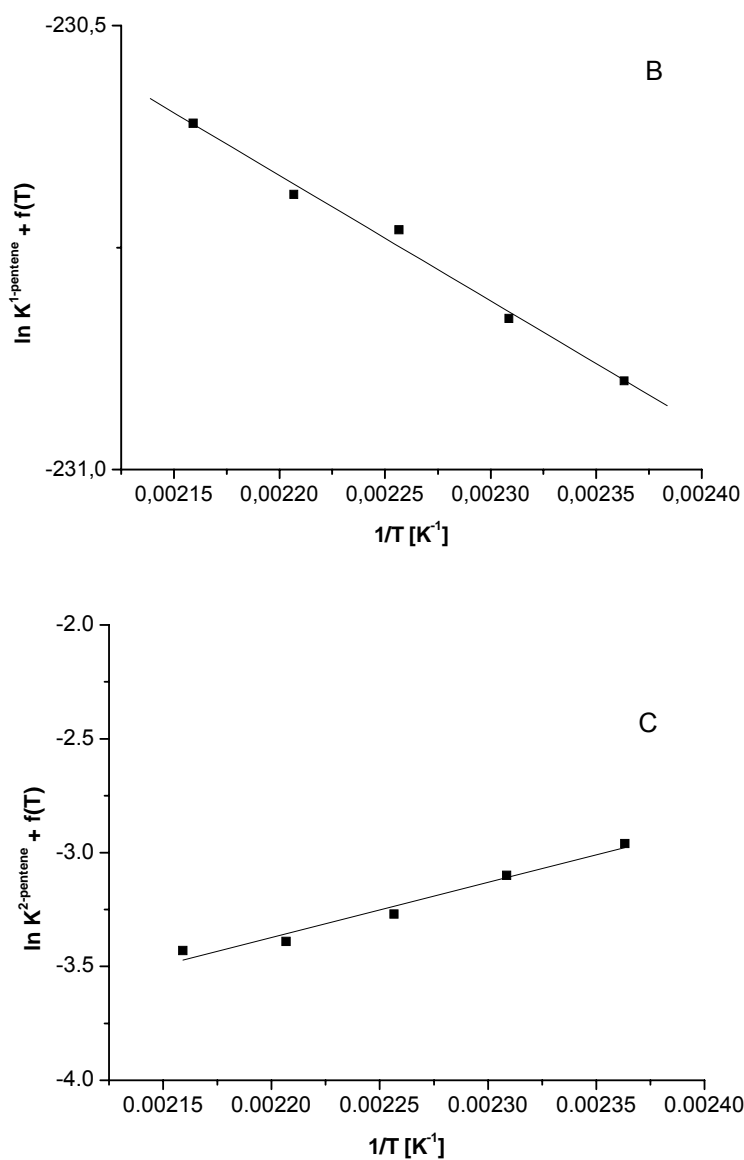


Figure 51. $\ln K + f(T)$ vs. $1/T$. Comparison between experimental values (■) and those predicted from Eq. 50 (–) for DNPE (A), 1-pentene (B) and 2-pentene (C) reactions

In Table 43 values of the standard molar enthalpy, entropy and free energy changes at 25°C of the three reactions are shown, considering that they change with temperature in the range explored.

Reaction	$\Delta_r H_{(l)}^0$	$\Delta_r S_{(l)}^0$	$\Delta_r G_{(l)}^0$
DNPE	-3.8 ± 0.6	26 ± 3	-11.5 ± 0.3
1-pentene	63.4 ± 0.9	83 ± 5	38.6 ± 0.5
2-pentene	-20 ± 2	-22 ± 11	-13 ± 1

Table 43. Standard enthalpy, entropy and free energy changes, when not considered constant over the T range

4.5.5 COMPARISON OF EXPERIMENTAL AND THEORETICAL VALUES OF EQUILIBRIUM CONSTANTS

In this section, experimental and theoretical values of the standard enthalpy, entropy and free energy changes of the three reactions studied are compared. Since data of these magnitudes had not been published before, theoretical values are those computed from thermochemical data of every chemical involved in the reaction scheme found in data banks, which are mainly experimental values.

4.5.5.1 DNPE SYNTHESIS

Values of the standard molar enthalpy, entropy and free energy changes of the dehydration of 1-pentanol to DNPE at 25°C determined for $\Delta_r H_{(l)}^0$ assumed to be constant and for $\Delta_r H_{(l)}^0$ variable with temperature are gathered in *Table 44*. Besides, theoretical values computed from $\Delta_f H_m^0$, and S_m^0 of *Table 41* are also shown.

DNPE	$\Delta_r H_{(l)}^0$ (kJ·mol ⁻¹)	$\Delta_r S_{(l)}^0$ (J·mol ⁻¹ K ⁻¹)	$\Delta_r G_{(l)}^0$ (kJ·mol ⁻¹)
$\Delta_r H_{(l)}^0$ constant	-6.5 ± 0.6	18.1 ± 1.4	-11.9 ± 1.1
$\Delta_r H_{(l)}^0$ as f(T)	-3.8 ± 0.6	25.7 ± 3.1	-11.5 ± 0.3
theory ^a	-17.8	-48.4	-3.4

^aComputed from data of *Table 41*

Table 44. Energy, entropy and enthalpy changes for DNPE synthesis

$\Delta_r H_{(l)}^0$ for the ether production reaction is not very high, neither if $\Delta_r H_{(l)}^0$ is considered to be constant nor variable with temperature, which was in agreement with the low sensitivity to temperature of K_a^{DNPE} . Both values are lower than that obtained from the molar formation

enthalpies of 1-pentanol, DNPE and water shown in *Table 41*. However, they are in the trend shown by values of other di-*n*-alkyl ethers compiled in *Table 45*, which were computed from experimental formation enthalpies and entropies found in data banks (see *appendix IV*).

Ether	$\Delta_f H_{(l)}^0$ [kJ/mol]	$\Delta_r S_{(l)}^0$ [J/(K·mol)]
DME	-10.2 ± 0.9 [86,87,88]	-37.86 [89,90]
DEE	-11.1 ± 2.6 [80,91]	3.73 [92,93]
DNPrE	-9.4 ± 1.4 [79,94]	8.25 [82,95]
DNBE	-9.8 ± 1.5 [79,94]	N/A
DNPE	-17.8 ± 4.1 ^a -6.51 ± 0.63 ^b -3.77 ± 0.58 ^c	-48.41 ^a 18.10 ^b 25.86 ^c

^aTable 41; ^bThis work with $\Delta_f H_{(l)}^0$ constant; ^cThis work $\Delta_f H_{(l)}^0$ variable with temperature; N/A The molar entropy of DNBE is not yet reported in data banks.

Table 45. $\Delta_f H_{(l)}^0$ and $\Delta_r S_{(l)}^0$ for some alkyl ethers computed from molar formation enthalpies and entropies

$\Delta_f H_{(l)}^0$ for 1-pentanol (Mosselman et al.) is a reliable value as a similar one was found in another experimental work [96]. On the other hand, to the best of our knowledge only Murrin et al. found a value for DNPE computed from combustion enthalpies. From $\Delta_f H_{(l)}^0$ of *Table 44* and $\Delta_f H_{(l)}^0$ of 1-pentanol and water of *Table 41*, a $\Delta_f H_{(l)}^0$ of **-(423.9 ± 1.2)** kJ/mol can be obtained for DNPE if $\Delta_f H_{(l)}^0$ is considered to be constant or **-(421.1 ± 1.2)** kJ/mol if variable with temperature. These values are lower by 3% than that of Murrin et al. and by 1.5% than that estimated by an improved Benson group-additive method (-430.1) kJ/mol [83].

In *Table 45* the standard entropy of reaction of some alkyl ethers are also shown. By comparing $\Delta_r S_{(l)}^0$ for these reactions, it seems that the entropy change increases as the number of carbon atoms of the molecule does. The value found in this work agrees with this trend, but the expected from formation entropies does not. The molar entropy of DNPE is still not reported in data banks, and the modified Benson method seems to underestimate it. A $S_{(l)}^0$ of **465.95** J/(K·mol) (**473.71** if $\Delta_f H_{(l)}^0$ is considered variable with temperature) for DNPE can be computed from $\Delta_r S_{(l)}^0$ and data from *Table 41*, which is near 20% higher than the estimated by the modified Benson method (394.4 J (K·mol)⁻¹). Deviations of the improved Benson method in the estimation of the standard entropy, although not so important, were also observed for di-*n*-propyl ether, DNPrE, the symmetrical ether derived from propanol. The experimental value [94],

$323.9 \text{ J (K}\cdot\text{mol)}^{-1}$, is 5% higher than the one estimated by the modified Benson method ($308.6 \text{ J/(K}\cdot\text{mol)}$). To the best of our knowledge, no experimental value of $S_{(l)}^0$ for di-*n*-butyl ether, DNBE, has been published yet. As a general conclusion, it seems that deviations on the estimation of $S_{(l)}^0$ of lineal symmetrical ethers increase with the number of carbons of the molecule.

4.5.5.2 1-PENTENE FORMATION

Values of the standard molar enthalpy, entropy and free energy changes of the decomposition reaction of DNPE to 1-pentanol and 1-pentene at 25°C, determined for $\Delta_r H_{(l)}^0$ assumed to be constant and for $\Delta_r H_{(l)}^0$ variable with temperature are gathered in *Table 46*. Besides, theoretical values computed from $\Delta_r H_m^0$, and S_m^0 of *Table 41* are also shown.

1-pentene	$\Delta_r H_{(l)}^0$ (kJmol ⁻¹)	$\Delta_r S_{(l)}^0$ (Jmol ⁻¹ K ⁻¹)	$\Delta_r G_{(l)}^0$ (kJmol ⁻¹)
$\Delta_r H_{(l)}^0$ constant	70.4 ± 0.9	101.9 ± 2.0	40.0 ± 2.0
$\Delta_r H_{(l)}^0$ as f(T)	63.4 ± 0.9	83.1 ± 4.8	38.6 ± 0.5
theory ^a	36.7	122.1	0.3

^aComputed from data of Table 41

Table 46. Energy, entropy and enthalpy changes for 1-pentene reaction

Experimental values differed considerably from the theoretical ones. As commented before, the activity of 1-pentene was very low in all experiments, especially at 150°C and 160°C. Thus, equilibrium constant values at these temperatures probably had an important error associated.

DNPE decomposition was considered to be the most likely reaction of 1-pentene synthesis, though it could also be formed via 1-pentanol monomolecular dehydration. The main argument for was the lower 1-pentanol activities compared to that of DNPE. However, the second reaction scheme was also checked in order to prove it.

So, the same reasoning and calculations were performed considering that 1-pentanol suffered a monomolecular dehydration to 1-pentene and water. In *Table 47*, the enthalpy change of reaction if considered constant and variable with temperature for this reaction are shown.

1-pentene	$\Delta_r H_{(l)}^0$ (kJmol ⁻¹)	$\Delta_r S_{(l)}^0$ (Jmol ⁻¹ K ⁻¹)	$\Delta_r G_{(l)}^0$ (kJmol ⁻¹)
$\Delta_r H_{(l)}^0$ constant	73.0 ± 3.4	141.2 ± 7.7	30.9 ± 5.7
$\Delta_r H_{(l)}^0$ as f(T)	68.7 ± 3.5	130.1 ± 18.4	29.9 ± 2.0
theory ^a	18.8	73.7	-3.1

^aComputed from data of Table 41

Table 47. Energy, entropy and enthalpy changes for 1-pentanol monomolecular dehydration reaction

As it can be stated, obtained values were much higher (fourfold) than the computed from thermochemical data. Besides, standard errors of the enthalpy change of reaction were higher in the case of the 1-pentanol dehydration, which can be explained by the worst fit of $\ln K$ versus $1/T$.

Thus, comparing both reaction schemes, DNPE decomposition reaction seemed to be the responsible for 1-pentene production.

4.5.5.3 2-PENTENE FORMATION

Values of the standard molar enthalpy, entropy and free energy changes of the isomerization of 1-pentene to 2-pentene at 25°C, determined for $\Delta_r H_{(l)}^0$ assumed to be constant and for $\Delta_r H_{(l)}^0$ variable with temperature are gathered in *Table 48*. Besides, theoretical values computed from $\Delta_f H_m^0$, and S_m^0 of *Table 41* are also shown.

2-pentene	$\Delta_r H_{(l)}^0$ (kJmol ⁻¹)	$\Delta_r S_{(l)}^0$ (Jmol ⁻¹ K ⁻¹)	$\Delta_r G_{(l)}^0$ (kJmol ⁻¹)
$\Delta_r H_{(l)}^0$ constant	-21.2 ± 2.1	-25.6 ± 4.7	-13.6 ± 3.5
$\Delta_r H_{(l)}^0$ as f(T)	-19.7 ± 2.1	-21.6 ± 11.0	-13.3 ± 1.2
theory ^a	-11.3	-6.0	-9.5

^aComputed from data of Table 41

Table 48. Energy, entropy and enthalpy changes for 2-pentene reaction

Experimental values differed from the computed from formation enthalpies. However, if only the temperature range 170-190°C was considered, a value of $-(13.0 \pm 4.2)$ kJ/mol (-14.7 ± 4.1)

kJ/mol if $\Delta_r H_{(l)}^0$ is considered constant over the temperature range) was computed from experimental data. This value agrees fairly well with the theoretical one. $\Delta_r S_{(l)}^0$ computed from experimental data at 170-190°C was **-6.9 J/(mol·K)** (**-11.4 kJ/mol** if $\Delta_r H_{(l)}^0$ is considered constant over the temperature range) and $\Delta_r G_{(l)}^0$ **-11.0 kJ/mol** (**-11.3 kJ/mol** if $\Delta_r H_{(l)}^0$ is considered constant over the temperature range).

4.6 KINETIC ANALYSIS

One of the aims of this work was to perform a kinetic analysis in order to find a mechanism that represents the dehydration of 1-pentanol to DNPE over solid catalysts. Furthermore, one unique model for all catalyst tested was sought.

4.6.1 LHHW KINETIC MODELS

It was assumed, since it was proved experimentally, that external and internal mass transfers were very rapid in comparison with the chemical processes occurring on and within the catalyst particle. That is to say, studied kinetic models only considered chemisorption, surface chemical reaction and desorption.

Catalytic reaction rate expressions can be derived for ideal surfaces in two ways:

1. By expressing the rate in terms of surface coverage, θ , and then employing the Langmuir isotherm to relate θ to fluid concentrations. This is the approach employed by Hinshelwood [97], commonly named as the *Langmuir-Hinshelwood formulation*.
2. By expressing the rate in terms of surface concentration of adsorbed species and free sites, and then using the Langmuir isotherm to relate these concentrations to that of the fluid. This approach was established by Hougen and Watson [98], and it is known as the *Hougen-Watson formulation*.

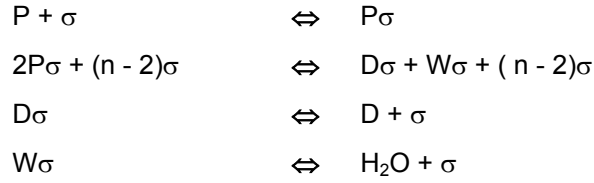
Since the Hougen-Watson formulation, is a modification of the Langmuir-Hinshelwood one, the resulting kinetic models are known, and will be referred to, as Langmuir-Hinshelwood-Hougen-Watson (LHHW) models.

It was assumed that the system studied presented four elementary steps:

1. 1-pentanol adsorption
2. Surface reaction

3. DNPE desorption
4. Water desorption

The LHHW mechanism proposed is the following:



where n is the number of active sites involved in the process.

A derivation of the LHHW mechanism, the Eley-Rideal (ER) model, assumes that one adsorbed molecule reacts with one molecule on the fluid phase. If so, a possible second step could be written as follows (considering that DNPE remains adsorbed):



For both mechanisms, one or more additional active sites, σ , could take part in the process. In order to take into account the non-ideality of the mixture, rate equations were expressed in terms of 1-pentanol, DNPE and water activities. Activity coefficients were estimated by the UNIFAC-DORTMUND predictive method. Rate equations of each step of the LHHW mechanism are:

$$\begin{aligned}
 r_1 &= k_{a,P} \cdot \left(a_P \cdot \hat{c}_\sigma - \frac{\hat{a}_P}{K_{a,P}} \right) \\
 r_2 &= \hat{k} \cdot \hat{a}_P^2 - \hat{k}' \cdot \hat{a}_D \cdot \hat{a}_w \\
 r_3 &= k_{a,D} \cdot \left(\frac{\hat{a}_D}{K_{a,D}} - a_D \cdot \hat{c}_\sigma \right) \\
 r_4 &= k_{a,w} \cdot \left(\frac{\hat{a}_w}{K_{a,w}} - a_w \cdot \hat{c}_\sigma \right)
 \end{aligned}$$

where $k_{a,i}$ is the adsorption rate coefficient of compound i
 a_i is the activity of compound i in the fluid phase

\hat{a}_i is the activity of compound i adsorbed on the active sites

\hat{c}_σ is the free-site concentration

$K_{a,i}$ is the adsorption equilibrium constant of compound i

\hat{k}, \hat{k}' are the direct and reverse rate constants, respectively

and for the ER mechanism:

$$r_2 = \hat{k} \cdot \hat{a}_P \cdot a_P - \hat{k}' \cdot \hat{a}_D \cdot \hat{a}_W$$

The surface reaction is assumed to be the rate-limiting step, which is well accepted for this type of catalysis. As 1-pentanol is the only reactant it does not have to compete with other species to adsorb on the active sites, and desorption of products is thought to be rapid at working temperatures. Thus, the LHHW formalism leads to the following basic kinetic model (see Appendix V):

$$r = \frac{\hat{k} \cdot K_P^2 \cdot \left(a_P^2 - \frac{a_D \cdot a_W}{K_{eq}} \right)}{\left(1 + K_P \cdot a_P + K_D \cdot a_D + K_W \cdot a_W \right)^n}$$

If the ER mechanism is considered, the model can be written as follows:

$$r = \frac{\hat{k} \cdot K_P \cdot \left(a_P^2 - \frac{a_D \cdot a_W}{K_{eq}} \right)}{\left(1 + K_P \cdot a_P + K_D \cdot a_D \right)}$$

where K_{eq} is the overall equilibrium constant and the exponent n of the denominator corresponds to the number of active sites involved in the surface reaction step. From the basic kinetic model, three parts can be distinguished:

1. Kinetic term: $\hat{k} \cdot K_{a,P}^2$
2. Driving force: $\left(a_P^2 - \frac{a_D \cdot a_W}{K_{eq}} \right)$
3. Adsorption term: $\left(1 + K_{a,P} \cdot a_P + K_{a,D} \cdot a_D + K_{a,W} \cdot a_W \right)^n$

All possible kinetic models derived from the basic kinetic model with $n = 1, 2$ and 3 were fitted systematically to find the model that better represents reaction rate data for each catalyst. Firstly, models were divided into two classes:

- ✓ Class I: the amount of free active sites is assumed to be negligible, so the 1 of the adsorption term of the basic kinetic equation can be neglected.
- ✓ Class II: the 1 of the adsorption term of the basic kinetic equation is not neglected.

Secondly, simplified models were obtained by assuming the adsorption of alcohol, ether and/or water negligible in front of that of the other. To sum up, 42 models were fitted to experimental data. These models can be found in *Table 49*.

The experimental thermodynamic equilibrium constant (see *section 4.5*) was introduced in the following form:

$$K_{eq} = \exp\left(\frac{778.69}{T} + 2.1886\right) \quad \text{Equation 53}$$

Kinetic and adsorption equilibrium constants were grouped for mathematical fitting purposes. The temperature dependence of A , B , C , k_1 , K_P , K_W and K_D is defined as follows:

$$A = \exp(b_i) \exp\left[-b_{i+1}\left(\frac{1}{T} - \frac{1}{\bar{T}}\right)\right] \quad \text{Equation 54}$$

Fitted parameters were b 's. The subtraction of the mean experimental temperature was included to minimize the mathematic correlation between fitted parameters.

4.6.2 METHODOLOGY OF KINETIC FITTING

The methodology followed in the kinetic fitting procedures is shown schematically in *Figure 52*. Experimental data consisted on activities (1-pentanol, water and DNPE) and reaction rates. For each catalyst all temperatures were fitted together. The Marquardt-Levenberg optimization model was used to find the minimum sum of squares of the lack of fit.

TYPE	CLASS I	n	Model	CLASS II	n	Model
1	$r = A \frac{\left(a_p^2 - \frac{a_D a_W}{K_{eq}} \right)}{a_p^n}$	1	113	$r = \frac{k_1 \left(a_p^2 - \frac{a_D a_W}{K_{eq}} \right)}{(1 + K_p a_p)^n}$	1	141
		2	114		2	142
		3	115		3	143
2	$r = A \frac{\left(a_p^2 - \frac{a_D a_W}{K_{eq}} \right)}{a_D^n}$	1	117	$r = \frac{k_1 \left(a_p^2 - \frac{a_D a_W}{K_{eq}} \right)}{(1 + K_D a_D)^n}$	1	145
		2	118		2	146
		3	119		3	147
3	$r = A \frac{\left(a_p^2 - \frac{a_D a_W}{K_{eq}} \right)}{a_W^n}$	1	121	$r = \frac{k_1 \left(a_p^2 - \frac{a_D a_W}{K_{eq}} \right)}{(1 + K_W a_W)^n}$	1	149
		2	122		2	150
		3	123		3	151
4	$r = \frac{A \left(a_p^2 - \frac{a_D a_W}{K_{eq}} \right)}{(a_p + B a_D)^n}$	1	125	$r = \frac{k_1 \left(a_p^2 - \frac{a_D a_W}{K_{eq}} \right)}{(1 + K_p a_p + K_D a_D)^n}$	1	153
		2	126		2	154
		3	127		3	155
5	$r = \frac{A \left(a_p^2 - \frac{a_D a_W}{K_{eq}} \right)}{(a_p + B a_W)^n}$	1	129	$r = \frac{k_1 \left(a_p^2 - \frac{a_D a_W}{K_{eq}} \right)}{(1 + K_p a_p + K_W a_W)^n}$	1	157
		2	130		2	158
		3	131		3	159
6	$r = \frac{A \left(a_p^2 - \frac{a_D a_W}{K_{eq}} \right)}{(a_D + B a_W)^n}$	1	133	$r = \frac{k_1 \left(a_p^2 - \frac{a_D a_W}{K_{eq}} \right)}{(1 + K_D a_D + K_W a_W)^n}$	1	161
		2	134		2	162
		3	135		3	163
7	$r = \frac{A \left(a_p^2 - \frac{a_D a_W}{K_{eq}} \right)}{(a_p + B a_D + C a_W)^n}$	1	137	$r = \frac{k_1 \left(a_p^2 - \frac{a_D a_W}{K_{eq}} \right)}{(1 + K_p a_p + K_D a_D + K_W a_W)^n}$	1	165
		2	138		2	166
		3	139		3	167

Table 49. Kinetic models

Once all models were fitted, the selection process was done on the basis of the following conditions:

1. Statistical standpoints
 - ✓ Minimum sum of squares
 - ✓ Random residuals
 - ✓ Low parameter correlation

2. Physicochemical meaning
 - ✓ Positive activation energy
 - ✓ Negative adsorption enthalpies
 - ✓ Negative adsorption entropies

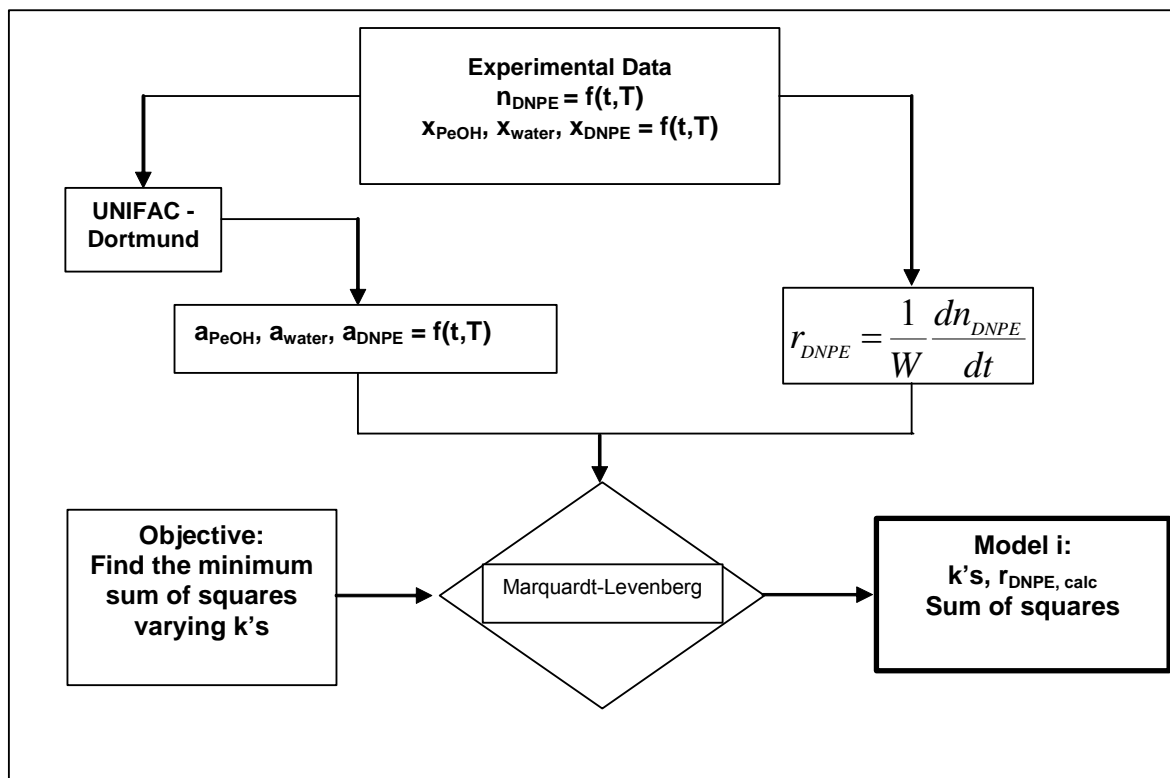


Figure 52. Kinetic analysis methodology

4.6.3 SELECTION OF THE LHHW KINETIC MODEL

In *Appendix VI* the results of the model fitting for all catalyst are shown. In *Table 50* a summary is presented. Only those models that fit experimental data satisfactorily are marked. There was only one group of models, Class I - type 4 (models 125, 126 and 127), that were able to fit data of all catalysts. A second group, Class I - type 5, fitted experimental data of all catalyst except for two, but the sum of squares of these models were higher than that of the first group of models, anyway.

4. Results and discussion

	Model	A36	A70	DLH/03	DLI03	CT224	Dow50	Dow100	Dow200	Dow400	NR50
I-1	n=1	113									
	n=2	114									
	n=3	115									
I-2	n=1	117									
	n=2	118									
	n=3	119									
I-3	n=1	121									
	n=2	122									
	n=3	123									
I-4	n=1	125	X	X	X	X	X	X	X	X	X
	n=2	126	X	X	X	X	X	X	X	X	X
	n=3	127	X	X	X	X	X	X	X	X	X
I-5	n=1	129		X	X	X	X	X	X	X	X
	n=2	130		X	X	X	X	X	X	X	X
	n=3	131		X	X	X	X	X	X	X	X
I-6	n=1	133									
	n=2	134									
	n=3	135									
I-7	n=1	137									
	n=2	138								X	
	n=3	139									
II-1	n=1	141				X					X
	n=2	142				X					X
	n=3	143				X					X
II-2	n=1	145	X	X	X	X		X			
	n=2	146	X	X	X	X		X			X
	n=3	147	X	X	X	X		X			X
II-3	n=1	149	X	X	X	X		X			
	n=2	150	X	X	X	X		X			X
	n=3	151	X	X	X	X		X			X
II-4	n=1	153									
	n=2	154	X	X	X			X			
	n=3	155	X	X	X			X			
II-5	n=1	157									
	n=2	158		X							
	n=3	159									
II-6	n=1	161			X						
	n=2	162		X	X						
	n=3	163		X	X						
II-7	n=1	165				X					
	n=2	166				X					
	n=3	167				X	X				X

X The model fitted experimental data satisfactorily

Table 50. Kinetic models that fit experimental data satisfactorily

Thus, the best model was:

$$r = \frac{A \left(a_p^2 - \frac{a_D a_W}{K_{eq}} \right)}{(a_p + B a_D)^n} \quad \text{Equation 55}$$

where $n = 1, 2$ and 3 , A included the rate constant (its meaning depends on the value of n , as it will be seen later) and B dealt with the equilibrium adsorption constants as follows, $B = K_{aD}/K_{aP}$.

In addition to the mechanistic aspects commented before, the proposed kinetic equation implies some other assumptions, namely:

1. The number of unoccupied active centers is negligible. This fact is quite feasible for liquid-phase reactions
2. Water does not appear in the adsorption term, although it adsorbs preferably on sulfonic groups, due to its high polarity and to the possibility of forming up to 4 hydrogen bonds with SO_3H groups. A plausible explanation is that water occupies probably a large amount of active sites, but almost constant, without a significant variation of its extent, so that water activity does not affect significantly the number of active sites on which water adsorbs.

It was difficult to discern how many active centers took place in the reaction mechanism, since the sum of square was very similar for $n = 1, 2$ and 3 . Furthermore, contradictory trends were observed: for some catalyst, the sum of squares increased on increasing n , but for others the contrary happened.

Instead of the sum of squares it is usually used the corrected sum of squares³ to compare the fittings, especially when magnitudes compared are different. Here, the corrected sum of squares was used to compare the fittings of all the catalysts (different reactions rates were obtained depending on the catalyst and on the temperature range). In *Figure 53* the corrected sum of squares of all catalysts for Class I – type 4 models are shown.

$$^3 \text{SSQ}_{corrected} = \sum \left| \frac{r_{exp} - r_{calc}}{r_{exp}} \right|$$

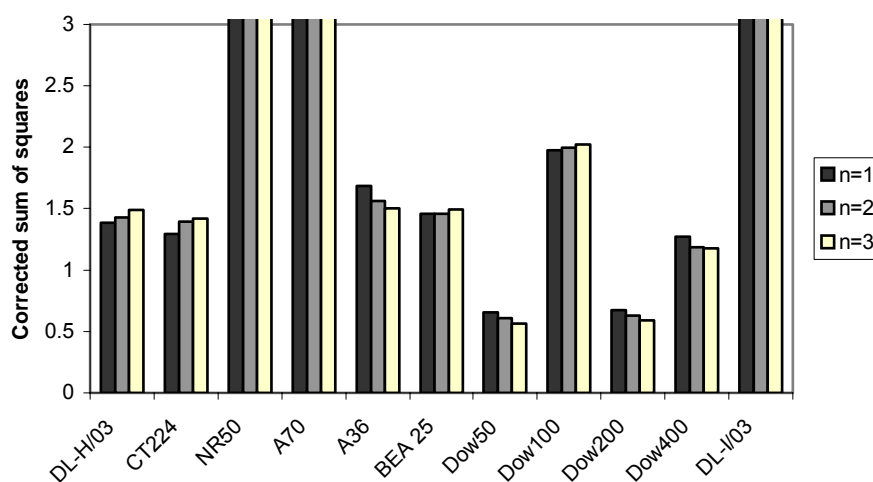


Figure 53. Corrected sum of squares of Class I – type 4 models

Except for catalysts NR50, A70 and DL-I/03, corrected sums of squares of the other catalysts were quite similar.

Figure 54 shows the calculated reaction rates by Model 125 plotted versus the experimental ones for Amberlyst DL-H/03 at all temperatures: the fitting was satisfactory at all temperatures. Similar plots were obtained with the other catalysts (and other n 's) except for NR50, A70 and DL-I/03. Residuals were also satisfactory and parameters were low correlated.

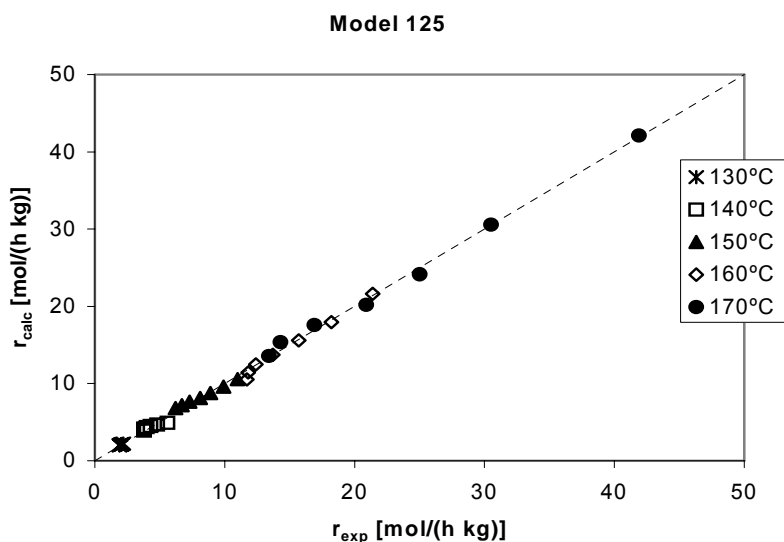


Figure 54. Model 125 estimated vs. experimental reaction rates at all temperatures for DL-H/03

Rate constants and adsorption equilibrium constants have an Arrhenius-type dependence with the temperature:

$$k = A_0 \exp\left(\frac{-E_a}{RT}\right) \quad \text{Equation 56}$$

where A_0 is the pre-exponential factor and E_a the activation energy. Concerning the adsorption equilibrium constant, instead of activation energy, the factor inside the exponential form is the enthalpy of adsorption.

Depending on the number of active centers involved in the reaction mechanism, n , the constant A of models 125, 126 and 127 corresponds to different associations of constants (see *Table 51*).

$n = 1$	$n = 2$	$n = 3$
$A = \hat{k} \cdot K_{a,p}$	$A = \hat{k}$	$A = \frac{\hat{k}}{K_{a,p}}$

Table 51. Constant associations of Class I – type 4 models

Thus, when $n = 1$ or 3 , the temperature dependence computed from *Equation 56* will correspond to an apparent activation energy with different meaning, while for $n = 2$, it will be the activation energy.

Almost all apparent activation energies (*Table 52*) were on the range 110-120 kJ/mol, so that the temperature dependences on each catalyst is of the same order. Errors shown in this table were estimated with the Jackknife method and correspond to the 99% confidence interval (see *Appendix VII*). Since calculated activation energies were quite similar for all catalysts, the assumption made in former sections proved to be acceptable: the influence of the internal mass and heat transfer is negligible for all catalysts tested under the working conditions described.

Catalyst	n = 1		n = 2		n = 3	
	E _a	A ₀	E _a	A ₀	E _a	A ₀
DL-H/03	110.5± 0.2	4.8E+14	111.1	5.6E+14	111.6	6.3E+14
DL-I/03	113.2± 0.8	2.1E+15	110.8	1.0E+15	111.1	1.1E+15
CT224	119.1± 0.5	8.2E+15	122.1	1.9E+16	122.8	2.3E+16
NR50	109.2± 0.6	1.7E+14	111.5	3.0E+14	112.6	4E+14
Dow50	114.7± 0.4	2.1E+15	115.2	2.4E+15	115.4	2.5E+15
Dow100	106.6± 0.4	2.1E+14	106.7	2.1E+14	106.6	2.1E+14
Dow200	114.8± 0.4	2.2E+15	115.4	2.6E+15	115.6	2.7E+15
Dow400	97.8± 0.4	1.5E+13	99.1	2.2E+13	99.8	2.6E+13
A70	114.6± 1.1	1.2E+15	114.7	1.2E+15	115.3	1.4E+15
A36	110.1± 0.4	8.9E+14	109.5	7.3E+14	109.2	6.7E+14
BEA25	121.2± 0.4	1.8E+15	121.1	1.7E+15	120.7	1.5E+15

Table 52. Apparent activation energies [kJ/mol] for models 125, 126 and 127

Only E_a values for CT-224 were found in the open literature (see Table 53). Values reported here are in the middle of the quoted range. It is to be noted that the value 146 ± 4 kJ/mol reported in [99] is probably influenced by the short range of alcohol and ether activities of the experimental range. Moreover, the lowest (99 ± 8 kJ/mol) can be explained by the fact that used catalyst mass was excessively high [18].

E _a (kJ/mol)	Ref.
146 ± 4	99
119.1-122.8	This work
115 ± 6	100
99 ± 8	18*

*From Arrhenius plot of initial reaction rates

Table 53. Activation energy found in literature for catalyst CT224

From the temperature dependence of B ($B=K_{aD}/K_{aP}$), $\Delta H_D - \Delta H_P$ and $\Delta S_D - \Delta S_P$ can be estimated, which are shown in Table 54.

Catalyst	n = 1		n = 2		n = 3	
	$\Delta H_{DNPE} - \Delta H_{PcOH}$	$\Delta S_{DNPE} - \Delta S_{PcOH}$	$\Delta H_{DNPE} - H_{PcOH}$	$\Delta S_{DNPE} - \Delta S_{PcOH}$	$\Delta H_{DNPE} - \Delta H_{PcOH}$	$\Delta S_{DNPE} - \Delta S_{PcOH}$
DL-H/03	7.7 ± 14	0.024 ± 0.038	13.3	0.035	15.9	0.041
DL-I/03	53 ± 22	0.139 ± 0.056	37.3	0.101	33.7	0.090
CT224	-140.7 ± 45	-0.34 ± 0.11	-31.1	-0.080	-11.0	-0.029
NR50	184 ± 44	0.40 ± 0.12	106.3	0.243	80.8	0.185
Dow50	272.5 ± 56	0.65 ± 0.14	146.7	0.363	105.5	0.261
Dow100	37.5 ± 45	0.095 ± 0.022	27.7	0.069	23.0	0.057
Dow200	256.6 ± 64	0.634 ± 0.015	142.3	0.351	102.5	0.252
Dow400	-143.9 ± 77	-0.362 ± 0.14	-48.3	-0.122	-21.1	-0.055
A70	63 ± 2814	0.146 ± 0.076	46.0	0.110	40.5	0.097
A36	9.1 ± 11	0.037 ± 0.029	4.8	0.021	4.6	0.019
BEA25	148.7 ± 100	0.32 ± 0.28	39.2	0.088	24.2	0.055

Table 54. $\Delta H_D - \Delta H_P$ and $\Delta S_D - \Delta S_P$ for models 125, 126 and 127

These values point out that, except for CT-224 and Dow400, DNPE adsorption is stronger than that of 1-pentanol. However, the high standard error associated to these estimates rather suggest that adsorption of ether is less significant than that of 1-pentanol, which could imply little sensitivity to such parameters in the fitting procedure.

Catalysts NR50, A70 and DL-I/03 showed corrected sums of squares much higher than other catalysts. The behavior of catalyst DL-I/03 could be explained by the fact that it had a low mechanical stability (see section 3.1.3.2) and it probably deactivated when water was produced. In fact, this catalyst was always recovered as very small particles after every experiment. On the other hand, catalysts NR50 and A70 did not suffer any change apparently (apart from swelling). The main difference among these catalysts and the others was that the temperature range of both was increased up to 190°C. At those temperatures, reactions rates were higher and thus the sum of squares, but when computing the corrected sum of squares this effect should be minimized.

As it can be stated in *Figure 55* deviations appear at higher temperatures (180 and 190°C). At these temperatures the kinetic model should be upgraded. It might be noted that at higher temperatures more water (and DNPE) was formed during the experiment. As commented in *section 1.7.2*, water has been reported to have an inhibiting effect on the active centers activity. This effect is not taken into account by Class I – type 4 models.

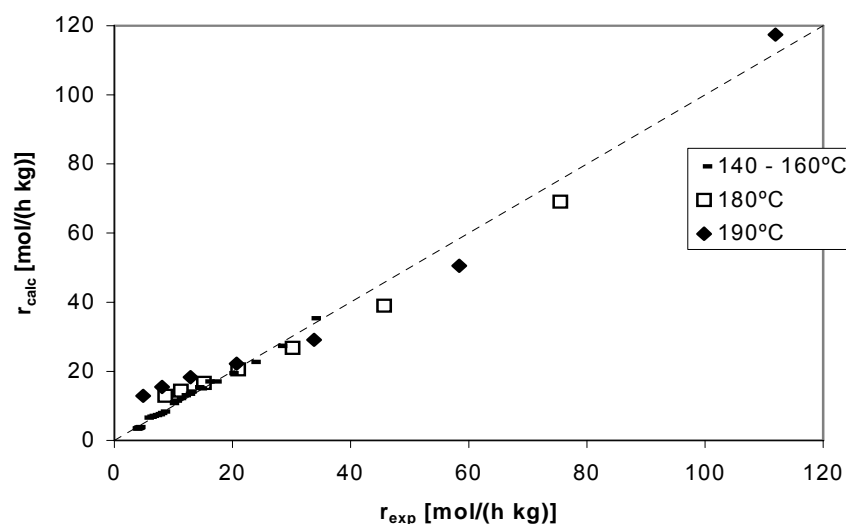


Figure 55. Model 125 estimated vs. experimental reaction rates at all temperatures for A70

4.6.4 EFFECT OF WATER AND DNPE ON THE REACTION RATE

In order to quantify the effect of water on the kinetics of the dehydration of 1-pentanol to DNPE, some additional experiments were carried out with different initial amounts of water. Furthermore, to stress this inhibiting effect, the same was performed with initial amounts of DNPE (see *Table 55*).

	Water	DNPE
160°C	1%	2%
	2%	8%
	4%	16%
	8%	32%
180°C	0.5%	2%
	1%	4%
	1.5%	
	2%	

Table 55. Initial % wt. of water and DNPE tested

These experiments were performed with catalyst A70 under the same conditions as the other tests, i.e. 1g of catalyst and 500 rpm, at 160 and 180 °C. These temperatures were chosen in order to break the typical trend obtained with “normal” experiments where only 1-

pentanol was added initially, i.e. activities of water and DNPE used for kinetic fitting purposes increased with temperature since at higher temperatures the reaction is faster. As it can be seen in *Figure 56* this trend is broken with this kind of experiments.

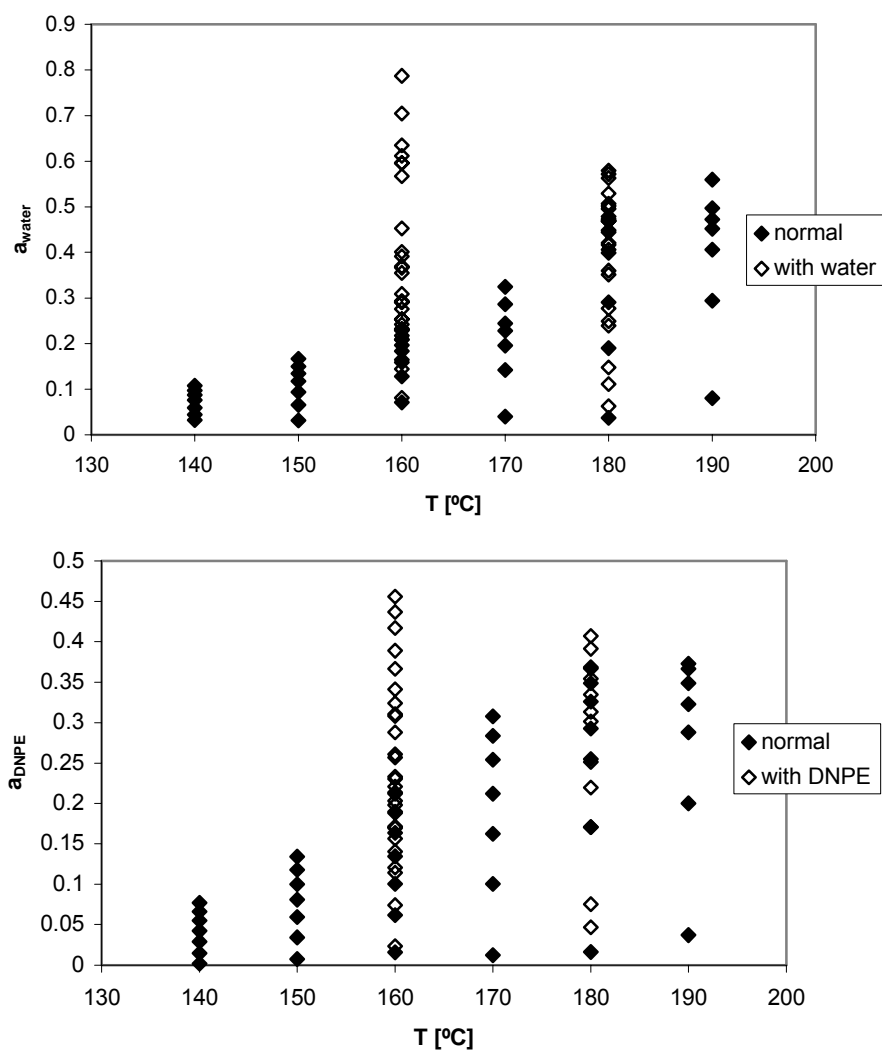


Figure 56. Water and DNPE activities of experiments with catalyst A70

In *Figure 57* initial reaction rates versus initial activities of water and DNPE of experiments performed at 160°C are shown. PeOH dot corresponds to the experiment with 1-pentanol. Water and DNPE curves correspond to experiments carried out with mixtures of 1-pentanol/water and 1-pentanol/DNPE, respectively.

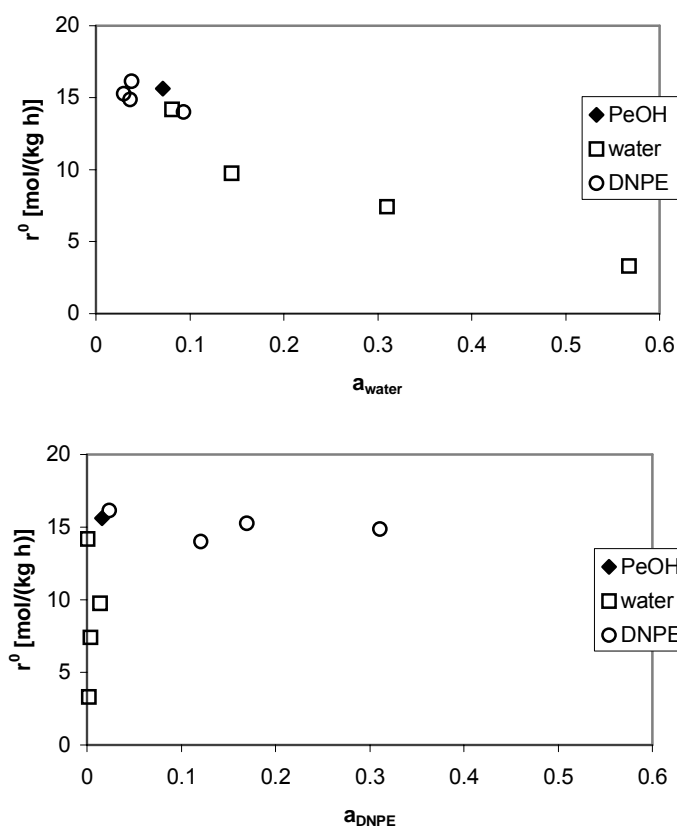


Figure 57. Initial reaction rate vs. water and DNPE activities at 160°C

The initial reaction rate seems to be very dependent on water activity, while practically independent on the DNPE activity in the range explored.

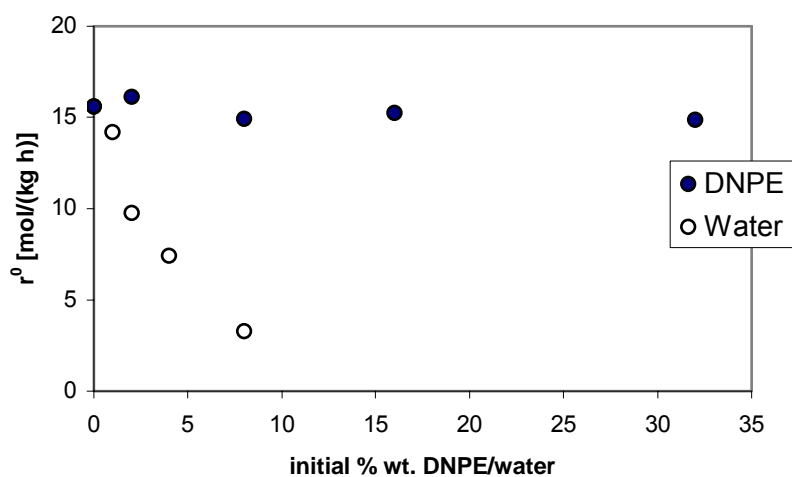


Figure 58. Initial reaction rate vs. initial %wt. of water and DNPE at 160°C

In *Figure 58* the initial reaction rates versus the initial weight percentage of water and DNPE of the experiments performed at 160°C with catalyst A70 are shown. As it can be stated, the initial reaction rate was practically constant when increasing the initial amount of DNPE from 0 to 32 % wt. The same behavior was observed on experiments carried out at 180°C. On the other hand, the initial reaction rate (and so 1-pentanol conversion) fell dramatically on increasing the amount of water fed to the reactor. In fact, the initial reaction rate when 8% wt. of water was added to the reactor was 79% lower, and the mol of DNPE obtained after 6 hours of experiment was 40% lower than when only 1-pentanol was fed to the reactor. This effect could not be caused by dilution since it would be much more important in the case of DNPE. So an inhibition of the active centers occurred when water was in some extent in the reaction medium.

% water	r^0 [mol/(h kg)]
0	75.5
0.5	74.1
1	64.5
1.5	49.5
2	43.4

As it can be seen in *Table 56*, the same occurred at 180°C. In fact, the inhibition seemed to be slightly enhanced by the temperature, since the reaction rate decreased a 42% when 2% wt. water was added and at 160°C it decreased a 38% with the same amount of initial water. This can be clearly stated in *Figure 59*, where the quotient of initial reaction rate by initial reaction rate free of inhibition effect at 160 and 180°C

Table 56. r^0 vs. %water at 180°C

is shown. Obviously this ratio should be one if the inhibition effect was negligible (experiments without initial water), and zero if the active centers were completely inhibited. The curve of experiments performed at 180°C is always below the one at 160°C.

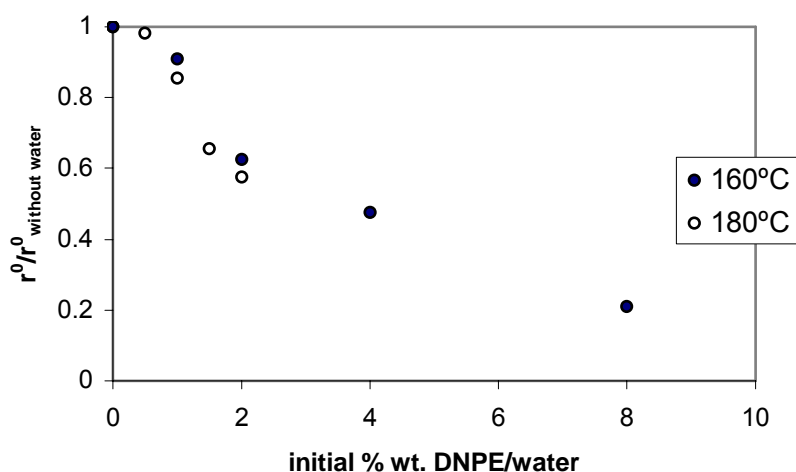


Figure 59. Inhibitor effect of water at different temperatures

Figure 60 plots the reaction rates predicted by model 125 versus the experimental ones, including the experiments with initial amounts of water and DNPE. When compared to Figure 55, where only runs with 1-pentanol were considered, a similar plot was obtained, i.e. a good fit was achieved when small amounts of water was present in the reaction medium (low temperatures and conversions) but deviations appeared at higher temperatures and when water was present in some extent.

The apparent activation energy computed from model 125 taking into account experiments with initial water and DNPE (129.7 ± 0.2) was a 13% higher with respect to the same model but without water and DNPE from the beginning.

So, the inhibiting effect of water was proved experimentally. The next step was to introduce this effect on the kinetic model.

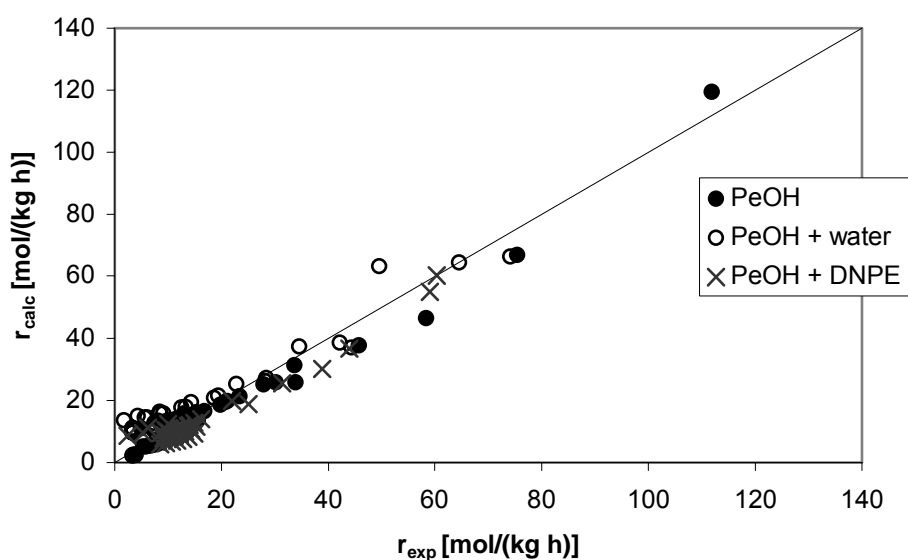


Figure 60. Model 125 estimated vs. experimental reaction rates of experiments with initial mixtures of 1-pentanol, 1-pentanol and water, and 1-pentanol and DNPE

4.6.5 MODIFIED KINETIC MODELS

Model 125 was the best model among all LHHW and ER models tested (least sum of squares of the lack of fit) for catalyst A70, but, curiously, water did not appear on the adsorption term, as if it did not adsorb on the polymeric matrix of the resin. However, it is widely accepted that water adsorbs on ion-exchange resins and that it has an inhibition effect on the catalyst activity. In fact, swelling of catalyst particles shown in plots of section 3.1.3.2 is a clear prove of

water sorption. So a modification of Model 125 with a factor that included water was thought to be necessary.

Water effect on the reaction rate has been modelled by correction factors analogous to those mostly used to describe catalyst deactivation by poisoning. The approach, as it can be seen in *Equation 57*, is to share the rate constant into a product of the true rate constant, k_0 , and an inhibition factor, which should take values between 0 and 1 and depends on temperature and water concentration in the liquid-phase. At first sight it can be seen as the fraction of active centres free of water, i.e.,

$$k = k_0 \cdot f(a_w, T) = k_0 (1 - \theta_w) \quad \text{Equation 57}$$

where \hat{k}_0 is the true rate constant, and $f(a_w, T)$ the inhibition factor.

Some kinetic models that included the effect of water were found in the open literature (see *section 1.7.2*) and most of them were tested for the 1-pentanol/water/DNPE system. They were adapted to the reaction in study and, in some cases, improved. For this purpose, only experimental data of catalyst A70 at all temperatures was used, including all experiments with initial amounts of water and DNPE. The correction factors were initially introduced in Class I-type 4 models (models 125, 126 and 127) which were the LHHW-type models that fit better experimental data for all catalysts. In *Appendix VIII* all the fitting results are shown.

4.6.5.1 SOLUBILITY PARAMETER

The solubility parameter, as it is defined in *section 1.7.2* was included on the kinetic model as follows:

$$r = \frac{A \cdot \Psi \left(a_p^2 - \frac{a_D a_w}{K_{eq}} \right)}{(a_p + B a_D)^n} \quad \text{Equation 58}$$

with $n = 1, 2$ and 3 . Ψ was computed as defined by *Equations 10 and 11*:

$$\delta_M = \sum_i \Phi_i \delta_i = \sum_i \Phi_i \frac{\sqrt{\Delta H_{v,i} - RT}}{V_i^L}$$

$$\Psi = \exp \left[\frac{\bar{V}_M \phi_p^2}{RT} (\delta_M - \delta_p)^2 \right]$$

where $\Delta H_{V,i}$ is the molar enthalpy of vaporization, V_i^L the liquid molar volume, Φ_i is the volume fraction for the pure component i , \bar{V}_M is the molar volume of the reaction medium, ϕ_p is the volume fraction of the resin, δ_M is the solubility parameter of the reacting medium and δ_p is the solubility parameter of the resin. As well as done before, A and B were defined as follows:

$$A = \exp(b_1) \exp\left[-b_2 \left(\frac{1}{T} - \frac{1}{\bar{T}}\right)\right]$$

$$B = \exp(b_3) \exp\left[-b_4 \left(\frac{1}{T} - \frac{1}{\bar{T}}\right)\right]$$

All the steps followed are shown in *Appendix VIII*. One new parameter, the resin solubility parameter, δ_p , which was assumed to be constant in the temperature range, was added to the fitting procedure (fitted parameters were δ_p , b_1 , b_2 , b_3 and b_4).

In *Table 57* the individual solubility parameters of 1-pentanol, DNPE, water, 1-pentene and 2-pentene at different temperatures are shown. As it can be seen, δ_i values decreased on increasing the temperature. Water had the higher solubility parameter, followed by 1-pentanol, the two most polar molecules. On the other hand, the olefins presented the lowest values, as they are the least polar compounds. DNPE falls between olefins and 1-pentanol.

T [°C]	$\delta_i \text{ (J/m}^3\text{)}^{1/2}$				
	PeOH	DNPE	Water	1-pentene	2-pentene
100	20290	15681	45683	11877	11361
120	19589	15201	44446	11066	10896
130	19225	14953	43802	10515	10466
140	18849	14699	43142	9873	9920
150	18461	14439	42465	9136	9267
160	18061	14173	41770	8285	8508
170	17646	13899	41053	7266	7630
180	17214	13617	40313	5901	6586
190	16763	13326	39546	2524	5204

Table 57. Individual solubility parameters

In *Table 58* fitted parameters as well as the computed activation energy, the sum of squares of the lack of fit (SSQ) and the variation of SSQ with respect to the initial Model 125 are shown.

The introduction of the solubility parameter (in the form Ψ) yield to an increase of the sum of squares, so to a worse fit. The estimated solubility parameter of the resin is similar to the one computed by Cruz et al. [46]: $25.3 \text{ (MJ/m}^3)^{1/2}$ for catalyst Amberlyst 35.

$\delta_p \text{ (J/m}^3)^{1/2}$	28923 ± 11
b_1	1.68 ± 0.002
b_2	14419 ± 22
b_3	-1.763 ± 0.021
b_4	13269 ± 140
$E_a \text{ [kJ/mol]}$	119.9 ± 0.2
SSQ	3477
% SSQ variation	34

Table 58. Fitted parameters of Model 125 with the solubility parameter

The addition of the solubility parameter to the kinetic model did not suppose any improvement on the fitting, as shown in *Figure 61*. As it can be seen in *Appendix VIII*, models 126 and 127 led to the same conclusion. In fact, the sum of squares of the lack of fit is clearly higher for Models 126 and 127 than for 125. So, it seems that the latter is the model that predicts better the reaction rates, at least for catalyst A-70.

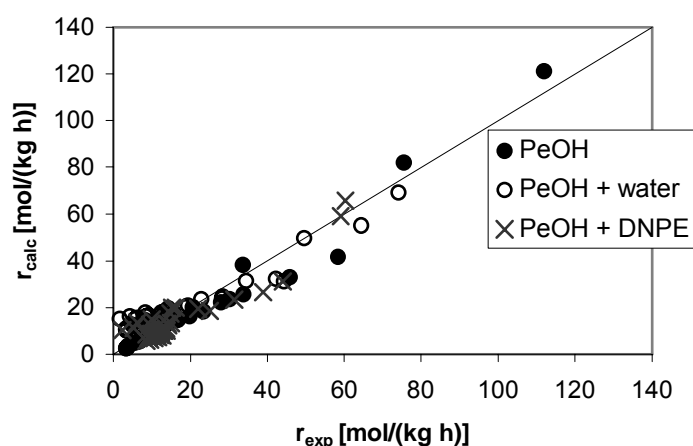


Figure 61. Reaction rate prediction of Model 125 modified with the solubility parameter vs. experimental reaction rates

The solubility parameter proved to be a very good tool for taking into account the varying

swelling degree of the resin during the runs due to the different polarity of chemicals involved in the reaction, e.g. the synthesis of MTBE with different isobutene/methanol ratios [47]. But when water is present in the reaction medium (and in the present study water was produced along the experiment) its behavior changes. Since water has a very high affinity with the sulfonic groups of the catalyst (it is able to form up to four hydrogen bonds with them), small amounts of water are enough to swell completely the polymeric matrix. Thus, once the catalyst is completely swollen, it does not change its structure along the experiment and the solubility parameter loses its interest.

Figure 62 plots the correction factor that includes the solubility parameter versus the activity of water at different temperatures. Two different areas can be observed: on the first part of the figure, the obtained correction factor decreased sharply for low activities of water reaching a value close to 1. Then, it did not change much with temperature and with the water activity when this compound was present in the reaction medium. This phenomenon agrees with the reasoning presented above, i.e. small quantities of water are enough to swell completely the polymeric matrix of the resin. Values of Ψ were very close to 1, which is only possible when solubility parameters of the medium and catalyst are very similar (see Equation 11).

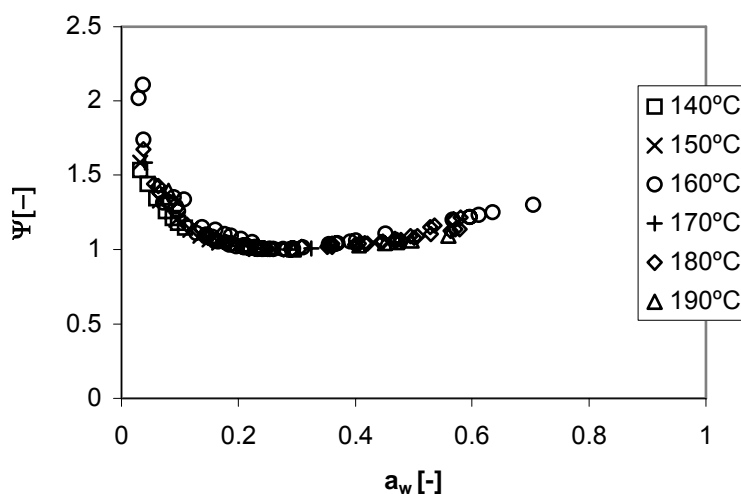


Figure 62. Computed Ψ vs. a_w at different temperatures

4.6.5.2 INHIBITION FACTOR

The inhibition factor, as it is defined in section 1.7.2, was included on the kinetic model as follows:

$$r = \eta(a_w) \frac{A \left(a_p^2 - \frac{a_w a_D}{K_{eq}} \right)}{(a_p + B \cdot a_D)^n} \quad \text{Equation 59}$$

with

$$\eta(a_w) = \frac{1}{1 + K_w \sqrt{a_w}} \quad \text{Equation 60}$$

$$K_w = \exp \left[K_{w1} - K_{w2} \left(\frac{1}{T} - \frac{1}{\bar{T}} \right) \right]$$

where $\eta(a_w)$ is the inhibition factor, and the proportionality factor K_w is not comparable to a sorption constant of water. It can only be looked as empirical since a Langmuir adsorption model assuming water adsorption on two sites with cleavage is unrealistic. Again, $n = 1, 2$ and 3 . With respect to LHHW models, two more parameters were included (K_{w1} and K_{w2}).

Table 59 shows fitted parameters as well as the computed activation energy, the sum of squares of the lack of fit and the variation of SSQ with respect to Model 125. Model 125 with the inhibition factor predicted the reaction rates better than Model 125 alone, leading to a decrease of the sum of squares of 33%.

K_{w1}	1.46 ± 0.01
K_{w2}	-6615 ± 77
b_1	2.81 ± 0.01
b_2	11595 ± 38
b_3	-1.82 ± 0.02
b_4	12906 ± 99
E_a [kJ/mol]	96.4 ± 0.3
SSQ	1748
% SSQ variation	-33

Table 59. Fitted parameters of model 125 with η

In Figure 63 reaction rates predicted by Model 125 with the inhibition factor versus the experimental ones are shown. In comparison to Figure 60 (Model 125), the prediction of reaction rates when water was present in the reaction medium was enhanced with the addition of the inhibition factor since all data points are closer to the diagonal of the picture (and so SSQ

was lower). Nevertheless, some deviations can be still observed when high amounts of water is present, which correspond to lower values of r of experiments at higher temperatures.

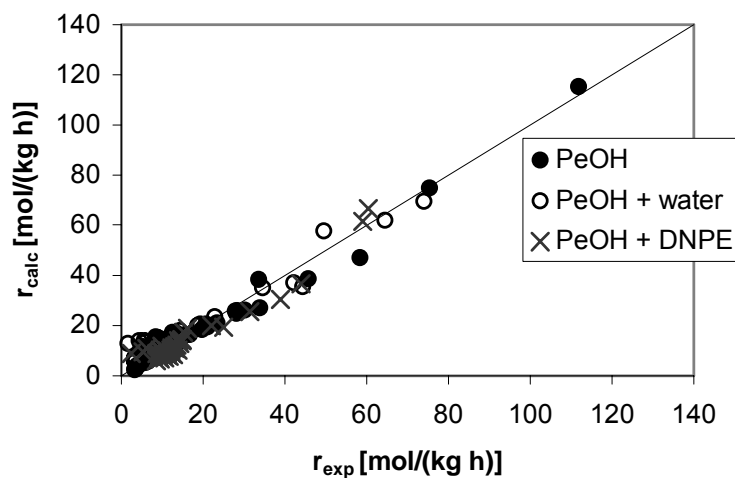


Figure 63. Reaction rate prediction of model 125 modified with the Inhibition factor vs. experimental reaction rates

Figure 64 plots the inhibition factor versus the activity of water at different temperatures.

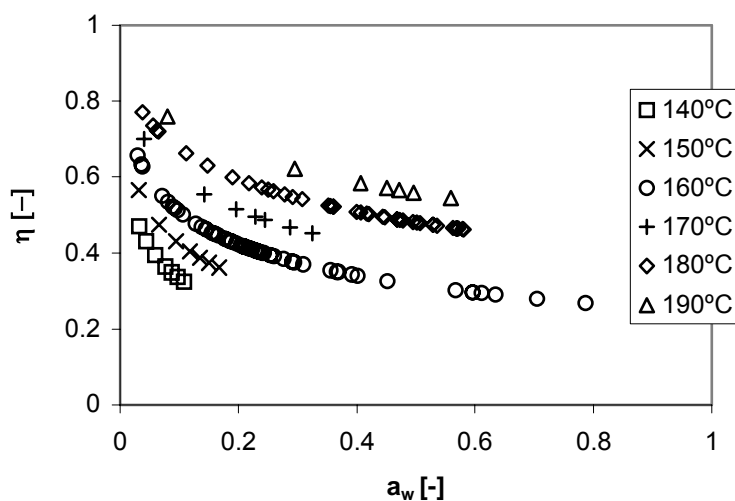


Figure 64. Computed η vs. a_w at different temperatures

The inhibition factor decreased first sharply, and then smoothly, on increasing the activity of water, reaching a plateau at higher activities. Besides, it increased on increasing the temperature, due to the temperature dependence of K_w .

4.6.5.3 FREUNDLICH-TYPE FACTOR

A factor including a Freundlich adsorption isotherm-like expression (from now on named Freundlich factor) was included as a correction or inhibition factor on Model 125 as follows:

$$r = \frac{A \left(a_p^2 - \frac{a_w a_D}{K_{eq}} \right)}{\left(a_p + B \cdot a_D \right)^n} \cdot \left(1 - K_F a_w^{1/\alpha} \right) \quad \text{Equation 61}$$

where

$$\alpha = \frac{K_\alpha}{T} \quad \text{Equation 62}$$

$$K_F = \exp \left[K_{F_1} - K_{F_2} \left(\frac{1}{T} - \frac{1}{\bar{T}} \right) \right]$$

K_F is the proportionality factor (du Toit et al. considered that this parameter was independent on the temperature, but it can be found elsewhere, see *section 1.7.1.3*, that it should decrease on increasing the temperature). α should decrease with temperature, as well.

With respect to Model 125, three new parameters were added to the fitting procedure. *Equation 61* was checked with $n = 1, 2$ and 3 . Results are shown in *Appendix VIII*.

K_α	358 ± 1
K_{F1}	495 ± 4
K_{F2}	2971 ± 49
b_1	2.122 ± 0.003
b_2	13716 ± 2
b_3	-17.4 ± 5
b_4	-33649 ± 37871
E_a [kJ/mol]	114.0 ± 0.1
SSQ	690
% SSQ variation	-73

Table 60. Fitted parameters of Model 125 + Freundlich

In *Table 60* fitted parameters of Model 125 corrected with the Freundlich-type expression are

shown, as well as the computed activation energy, the sum of squares of the lack of fit and the variation of SSQ with respect to Model 125.

A great reduction of the sum of squares was achieved with this model. Notwithstanding, values of parameters b_3 and b_4 , which corresponded to B of Equation 61 (the association parameter of adsorption equilibrium constants) indicated that this factor was not significant in the fitting procedure.

The temperature dependency of B was similar to K_F in Equation 62, so a value of (-17.4) in the first exponential term led to values of $B \approx 0$ in the whole temperature range. Furthermore, the great value of the 99% confidence interval of parameter b_4 confirmed this point.

Thus, the term $(B \cdot a_D)$ was taken out of the model and the resulting model (model 113 + Freundlich, as defined in Table 49) was fitted to experimental data:

$$r = \frac{A \left(a_p^2 - \frac{a_w a_D}{K} \right)}{a_p} \cdot \left(1 - K_F a_w^{1/\alpha} \right) \quad \text{Equation 63}$$

New fitted parameters are shown in Table 61. As the sum of squares was the same and fitted parameters were very similar to the shown in Table 60, it could be concluded that the term $(B \cdot a_D)$ was not significant on the kinetic model. In fact, only parameter b_2 slightly changed, remaining the rest of parameters constant. So Model 113 + Freundlich (Equation 63) was chosen as the Freundlich-type corrected kinetic model. The activation energy was very similar to the obtained with other models and catalysts.

K_α	358 ± 1
K_{F1}	495 ± 1
K_{F2}	2971 ± 13
b_1	2.122 ± 0.003
b_2	13710 ± 15
E_a [kJ/mol]	114.0 ± 0.1
SSQ	690
% SSQ variation	-73

Table 61. Fitted parameters of Model 113 + Freundlich

Figure 65 plots the predicted reaction rates versus the experimental ones. The fitting achieved with Model 113 + Freundlich was very satisfactory, as it can be observed in the figure, even when water was in great extent on the reaction medium.

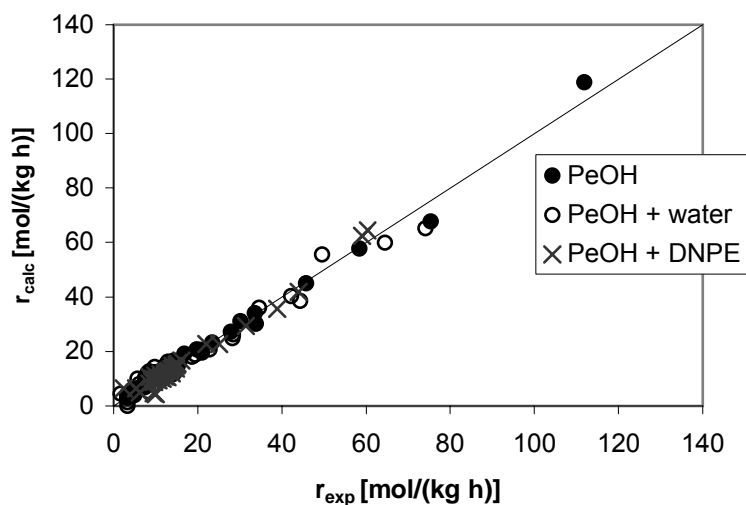


Figure 65. Reaction rate prediction of model 125 modified with the Freundlich factor vs. experimental reaction rates

Figure 66 shows the computed Freundlich-type correction factor at different temperatures. It decreased on increasing the activity of water and temperature. Unlike the other correction factors (solubility parameter and inhibition factor), the Freundlich-type one constantly decreased on increasing the activity of water, without reaching any plateau (at least in the range of activities and temperature explored).

On the other hand, K_F increased on increasing the temperature, while α decreased. This point agrees with experimental observations of liquid-phase adsorptions [101]. So, the Freundlich-type expression could not be seen as an adsorption equilibrium relation, but as a deactivation process in which water blocks the active centers, being K_F the deactivation constant.

From the variation of K_F on the temperature, a pseudo-activation energy for the deactivation process could be computed, giving a value of 24.7 ± 0.1 kJ/mol.

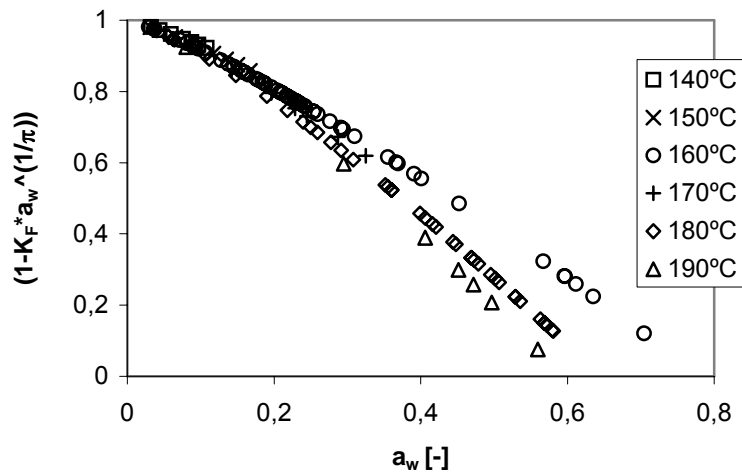


Figure 66. Computed Freundlich factor vs. a_w at different temperatures

4.6.5.4 LANGMUIR-TYPE FACTOR

Finally, in order to compare the different correction factors, a classical LHHW-type correction factor is presented:

$$r = \frac{A \left(a_p^2 - \frac{a_w a_D}{K} \right)}{\left(a_p + B \cdot a_D \right)^n} \cdot \frac{1}{1 + K_w a_w} \quad \text{Equation 64}$$

where

$$K_w = \exp \left[K_{w_1} - K_{w_2} \left(\frac{1}{T} - \frac{1}{\bar{T}} \right) \right] \quad \text{Equation 65}$$

K_w is the adsorption constant of water. Here two additional parameters with respect to the initial model were added to the fitting procedure. Equation 64 was checked for $n = 1, 2$ and 3 . Results of the fittings for the different n 's are presented in Appendix VIII.

Fitted parameters for Model 125 modified with the Langmuir-type factor are shown in Table 62, as well as the computed activation energy, the sum of squares of the lack of fit and the variation of SSQ with respect to Model 125. b 's parameters correspond to the association constants A and B , as in former sections.

b_1	2.410 ± 0.003
b_2	12700 ± 24
b_3	-2.27 ± 0.02
b_4	14023 ± 100
K_{w1}	1.461 ± 0.008
K_{w2}	-5317 ± 70
E_a [kJ/mol]	105.6 ± 0.2
SSQ	1465
% SSQ variation	-44

Table 62. Fitted parameters of Model 125 + Langmuir

Figure 67 plots the predicted reaction rates by this modified model versus the experimental ones. As it can be observed, the reaction rate prediction was better than the obtained with the initial Model 125, but some deviations were still visible for low values of reaction rate, which mainly corresponded to experiments with initial water and DNPE. The correction factor decreased on increasing water activity, as Figure 68 shows.

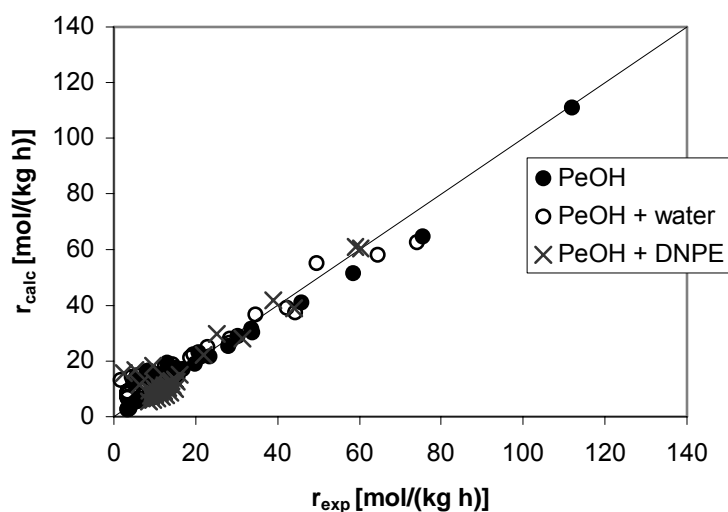
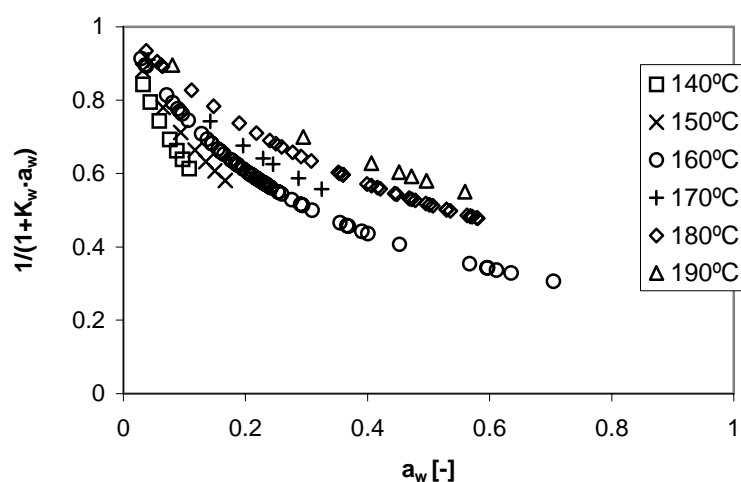


Figure 67. Reaction rate prediction of Model 125 modified with the Langmuir factor vs. experimental reaction rates

As commented before, K_w could be compared to the water adsorption equilibrium constant. It decreased on increasing the temperature, as it was expected. From K_{w2} the enthalpy of adsorption of water could be directly computed, giving a value of $-(44.2 \pm 0.9)$ kJ/mol.

Figure 68. Computed Langmuir factor vs. a_w at different temperatures

4.6.5.5 SELECTION OF THE MODIFIED KINETIC MODEL

For catalyst A70, the best fittings concerning the modified kinetic models were achieved when $n = 1$, i.e. when only one active center was involved in the surface reaction step, as it can be stated in *Appendix VIII*.

	Model 125	Solubility parameter	Inhibition factor	Langmuir-type factor	Freundlich-type factor
b_1	1.827 ± 0.002	1.684 ± 0.002	2.808 ± 0.006	2.410 ± 0.003	2.122 ± 0.003
b_2	15601 ± 19	14419 ± 22	11595 ± 38	12700 ± 24	13710 ± 15
b_3	-1.14 ± 0.02	-1.76 ± 0.02	-1.82 ± 0.02	-2.27 ± 0.02	
b_4	12941 ± 108	13269 ± 140	12906 ± 99	14023 ± 100	
δ_p		28923 ± 11			
K_{w1}			1.46 ± 0.01	1.461 ± 0.008	
K_{w2}			-6615 ± 77	-5317 ± 70	
K_{F1}					495 ± 1
K_{F2}					2971 ± 13
K_α					358 ± 1
E_a [kJ/mol]	129.7 ± 0.2	119.9 ± 0.3	96.4 ± 0.3	105.6 ± 0.2	114.0 ± 0.1
SSQ	2602	3477	1748	1465	690
SSQ variation	0	34	-33	-44	-73
$\Delta H_{ads,w}$ [kJ/mol]				-44.2 ± 0.6	

Table 63. Fitting results comparison of all modified kinetic models

In Table 63 fitted parameters of all modified kinetic models for $n = 1$ are gathered. Moreover, activation energies, SSQ and variation of SSQ with respect to the initial model are presented. Finally, equivalent $\Delta H_{ads,w}$ computed as if K_w were considered as adsorption equilibrium constant of water are also shown.

The solubility parameter did not suppose any enhancement on the fitting with respect to Model 125. On the other hand, the other correction factors led to a decrease of the SSQ. The improvement in the prediction of reaction rate when water was present backs up the assumption that it inhibits the reaction by irreversible adsorption on sulfonic groups, hindering 1-pentanol to adsorb on active sites and following the reaction. Furthermore, from the approach followed, \hat{k}_o , the rate constant free of water effect should be greater than \hat{k} . As seen in Table 64 this point is fulfilled.

T (°C)	Model 125	Inhibition factor	Freundlich-type factor	Langmuir-type factor
	\hat{k} , mol/(h·kg)	\hat{k}_o , mol/(h·kg)	\hat{k}_o , mol/(h·kg)	\hat{k}_o , mol/(h·kg)
140	0.72	3.35	1.26	1.93
150	1.76	6.49	2.75	3.98
160	4.12	12.2	5.82	7.97
170	9.29	22.3	11.9	15.4
180	20.2	39.8	23.5	29.1
190	42.4	69.0	45.1	53.1

Table 64. Rate constants for model 125 and modified kinetic models

The inhibition factor, η , enhanced the prediction of the initial LHHW Model 125. This inhibition factor can only be seen as empirical, since a Langmuir adsorption model assuming water adsorption on two sites with cleavage is unrealistic.

A better prediction was achieved with the Langmuir-type factor, to which the following physical meaning could be given: one molecule of water adsorbed on one active center. Then water blocked or inhibited it from 1-pentanol molecules. Thus, the parameter K_w could be assimilated to the adsorption equilibrium constant of water, with a $\Delta H_{ads,w}$ of $-(44.2 \pm 0.6)$ kJ/mol, which roughly agrees with the range $(-34$ to -38 kJ/mol) found in literature from adsorption experiments [102]. This model, though not being the best one, gives a physical meaning to the deactivating faculties of water on ion-exchange resins, so it should be

considered for other studies.

The **best** reaction rate prediction was achieved with the kinetic model including the **Freundlich-type correction factor**. At first sight, the fitting upgrade could be ascribed to the addition of one more adjustable parameter, or else that the Freundlich adsorption power-type expression for water is flexible enough to fit rate data properly. The final expression of the kinetic model proposed is:

$$r = \frac{\hat{k}_0 \cdot K_{a,p} \left(a_p^2 - \frac{a_w a_D}{K} \right)}{a_p} \cdot \left(1 - K_F a_w^{1/\alpha} \right)$$

$$\hat{k}_0 \cdot K_{a,p} = \exp \left[(2.122 \pm 0.003) + (13710 \pm 15) \cdot \left(\frac{1}{T} - \frac{1}{423} \right) \right]$$

$$K = \exp \left(\frac{778.69}{T} + 2.1886 \right)$$

$$K_F = \exp \left[(495 \pm 1) + (2971 \pm 13) \cdot \left(\frac{1}{T} - \frac{1}{423} \right) \right]$$

$$\alpha = \frac{(358 \pm 1)}{T}$$

The implications of this kinetic model are the following:

- ✓ The rate-limiting step is the surface reaction.
- ✓ One molecule of 1-pentanol of the bulk phase reacts with an adsorbed one.
- ✓ DNPE is formed and released to the bulk phase.
- ✓ Water formed blocks or inhibits the active sites, hindering 1-pentanol molecules to adsorb on them.

This empirical expression could be assimilated to a deactivation process, being K_F the deactivation rate constant. From the variation of K_F on temperature, a value of 24.7 ± 0.1 of pseudo-activation energy of the deactivation process could be computed. The apparent activation energy of the dehydration of 1-pentanol to DNPE estimated from the variation of reaction rate constant on the temperature was 114.0 ± 0.1 kJ/mol. This value is very similar to the obtained when experiments with initial water and DNPE were not included in the fitting procedure, i.e. when there was not much water on the reaction media (0 – 2% wt), and the reaction rate constant approached the true reaction rate constant.

	b_1	b_2	K_{F1}	K_{F2}	K_{α}
b_1	1				
b_2	0.0	1			
K_{F1}	0.0	-0.1	1		
K_{F2}	0.1	-0.1	0.3	1	
K_{α}	0.1	0.0	-0.2	0.1	1

Table 65. Correlation matrix of fitted parameters for catalyst A-70

From a statistical standpoint, fitting results were very good. In Table 65 the correlation matrix of fitted parameters is shown. All values, except the diagonal of the matrix, are far from 1 (which implies linear correlation between parameters).

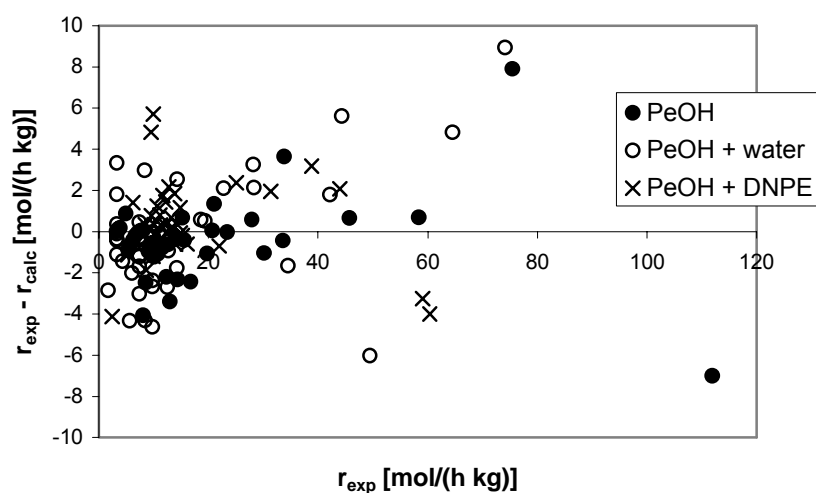


Figure 69. Residuals distribution for Amberlyst 70 fitting

In Figure 69 the residuals distribution is shown. As it can be stated, a random distribution of residuals was obtained.

4.6.6 KINETIC MODEL WITH FREUNDLICH-TYPE CORRECTION FACTOR APPLIED TO OTHER CATALYSTS

The kinetic model with the Freundlich factor was fitted to experimental data of all the catalysts tested, in order to check whether this model was just a good fit for catalyst A70 or it was a good general description of the dehydration of 1-pentanol to DNPE.

In Table 66 the results of the new fitting procedure for all catalysts are shown. Besides fitted parameters, the activation energy computed from b_2 and the SSQ of models 125 and the kinetic model with the Freundlich factor are also presented.

	A36	DLH/03	DLI03	CT224	Dow50	Dow100	Dow200	Dow400	NR50	BEA25
b_1	1,96	2,43	2,97	1,47	1,49	1,50	1,48	1,48	2,74	1,46
b_2	12783	12927	11411	14892	13172	12817	13367	12355	12319	14447
K_{F1}	290	404	199	120	119	119	124	447	114	65
K_{F2}	2332	807	4724	7998	15140	15141	1508	128	7443	116478
K_α	881	967	3666	607	-8978	-8962	-21616	-2187	-3606	-27989
E_a [kJ/mol]	106	107	95	124	110	107	111	103	102	120
SSQ ₁₂₅	4	6	234	1	2	3	2	1	434	6
SSQ _{Freundlich}	2	7	35	1	1	2	0.4	1	47	3

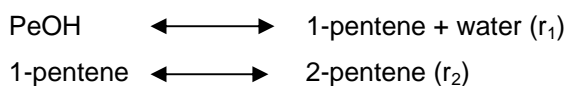
Table 66. Fitting results of Freundlich-type expression for all catalysts tested

As it can be stated in the table, in almost all catalysts the modified kinetic model with the Freundlich-type expression improved the fitting. The enhancement was very important in those catalysts that showed a worse fit with model 125: NR50 and DL-I/03. These two catalysts, together with A70, were the most active ones in the dehydration of 1-pentanol as for DVB resins and, as a consequence, produced more water.

So the introduction of a correction factor that deals with the inhibiting effect of water on ion-exchange resins could explain better the behavior of this kind of catalysts in such media.

4.6.7 KINETIC MODEL WITH FREUNDLICH-TYPE CORRECTION FACTOR APPLIED TO 1-PENTENE AND 2-PENTENE SYNTHESIS REACTIONS

The main reactions that involve 1-pentene and 2-pentene synthesis are the following:



Here the decomposition of DNPE to 1-pentanol and 1-pentene was not considered because the activities of DNPE were low during these experiments. The reaction rate for 1-pentene can be written as follows:

$$r_{1-pentene} = \frac{1}{W} \frac{dn_{1-pentene}}{dt} = r_1 - r_2 \quad \text{Equation 66}$$

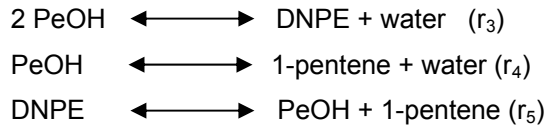
Following the same reasoning done in section 4.6.1, and considering that neither 1-pentene nor 2-pentene adsorbed on the active centers, Equation 66 becomes:

$$r_{1-pentene} = \frac{k_1 K_{PeOH} \left(a_{PeOH} - \frac{a_{1-pentene} a_w}{K^{1-pentene}} \right) - k_2 K_{1-pentene} \left(a_{1-pentene} - \frac{a_{2-pentene}}{K^{2-pentene}} \right)}{K_{PeOH} a_{PeOH}} \quad \text{Equation 67}$$

$$= k_1 \left(1 - \frac{a_{1-pentene} a_w}{a_{PeOH} K^{1-pentene}} \right) - \frac{k_2 K_{1-pentene}}{K_{PeOH}} \left(\frac{a_{1-pentene} - \frac{a_{2-pentene}}{K^{2-pentene}}}{a_{PeOH}} \right)$$

where K_i were the experimental thermodynamic equilibrium constants, K_i are the equilibrium adsorption constants and k_i are the apparent rate constants of the two reactions. With the Freundlich-type correction factor, the kinetic model becomes:

$$r_{1-pentene} = \left(k_1 \left(1 - \frac{a_{1-pentene} a_w}{a_{PeOH} K^{1-pentene}} \right) - \frac{k_2 K_{1-pentene}}{K_{PeOH}} \left(\frac{a_{1-pentene} - \frac{a_{2-pentene}}{K^{2-pentene}}}{a_{PeOH}} \right) \right) \left(1 - K_F a_w^{1/\alpha} \right) \quad \text{Equation 68}$$



In section 4.5, concerning equilibrium experiments, only reactions 3 and 5 were considered since pentanol activities were very small along the experiments. As kinetic experiments were performed using 1-pentanol as feed, the most likely reaction of 1-pentene synthesis was (r_4). Notwithstanding, the relationship among the thermodynamic equilibrium constants of the three reactions is as follows: $K_4 = K_3 \cdot K_5$

Equations 67 and 68 were fitted to experimental data, following the same methodology explained in section 4.6.2. The adjustable parameters were b_1 and b_2 for k_1 and b_3 and b_4 for $\frac{k_2 K_{1-pentene}}{K_{PeOH}}$. The Freundlich-type correction factor was not fitted, but it was used the one

obtained in section 4.6.5.3 for catalyst A70. In Table 67 fitted parameters of the Langmuir and the modified kinetic model, the activation energies and SSQ for both models are shown.

	Equation 67	Equation 68
b_1	0.283	0.397
b_2	15000	15000
b_3	5.15	5.23
b_4	12000	12000
K_{F1}		358
K_{F2}		495
K_{α}		-2971
E_a (kJ/mol)	125	125
SSQ	18.8	15.5

Table 67. Fitted parameters, E_a and SSQ for 1-pentene and 2-pentene synthesis

The modified kinetic model improves the fitting, but, as it can be seen in Figure 70, some deviations appear. The activation energy of the first reaction (1-pentene synthesis) was 125 kJ/mol. From b_4 the apparent activation energy of the second reaction (2-pentene synthesis) can be computed, giving a value of 100kJ/mol.

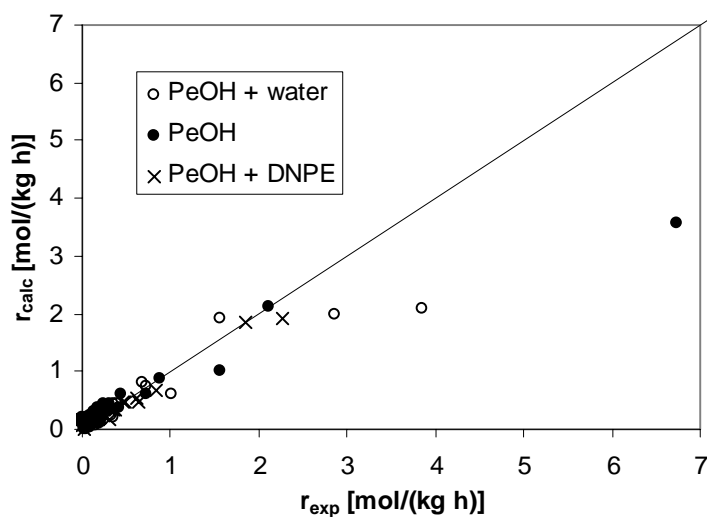


Figure 70. Reaction rate prediction of the modified model vs. experimental reaction rates for 1-pentene and 2-pentene synthesis

4.7 CATALYST SYNTHESIS

As pointed out in *section 4.3*, Nafion NR50 could be a promising catalyst for liquid-phase reactions at 170-210°C, despite its very low surface area and acid capacity. High 1-pentanol conversion and selectivity to DNPE at 190°C proved this point. Its high thermal stability and acid strength were responsible for the activity shown at all temperatures, higher than it could be expected from its acid capacity. The low surface area was overcome by the catalyst ability to swell in presence of polar compounds as 1-pentanol and water. However, the activity of this catalyst falls dramatically either in non-swelling solvents or in gas phase, due to the low accessibility to the acid sites [20]. As commented in *section 1.6.2.2*, new classes of solid acid catalysts based on Nafion resin have been developed, such as Nafion/silica nanocomposites or Nafion supported on carriers.

In this work Nafion was supported on seven carriers by impregnation and the resulting catalysts were characterized and tested on the dehydration of 1-pentanol to DNPE. Results were compared to the obtained with NR50 and the nanocomposite SAC 13. This technique of catalyst synthesis was chosen for its simplicity.

4.7.1 CARRIERS CHARACTERIZATION

Among the carriers tested, three silicas of nominal surface areas of 200 (abbreviated **Si-A**), 300 (**Si-B**) and 500 m²/g (**Si-C**), three aluminas (α -aluminum oxide 10 m²/g nominal area, **Al-3**; weakly acidic γ -aluminum oxide (pH \approx 6 in water) Typ 506-C-I Brockman I 155 m²/g nominal area, **Al-1**; acidic γ -aluminum oxide (pH \approx 4.5 in water) Typ 504C Brockman I 155 m²/g nominal area, **Al-2**) and a silica-alumina of 600 m²/g nominal area (**Si-Al**) were used.

The following analyses were carried out in order to characterize the carriers:

- ✓ Density
- ✓ XR fluorescence
- ✓ BET
- ✓ Particle size
- ✓ Organic and water content
- ✓ Acidic capacity

Furthermore, blank experiments were performed to check whether the carriers presented any activity on the dehydration of 1-pentanol.

Density

Measures of density were made with a Helium pycnometer AccuPyc 1330 at room temperature and 12.1964 cm³ of cell volume. In *Table 68* measured densities are presented.

Carrier	Density [g/cm ³]
Al-1	3.1869 ± 0.0081
Al-2	3.2202 ± 0.0073
Al-3	3.9834 ± 0.0018
Si-A	2.2942 ± 0.0073
Si-B	2.1513 ± 0.0019
Si-C	2.1054 ± 0.0141
Si-Al	2.0538 ± 0.0073

Table 68. Measured densities of carriers tested

Aluminas presented higher densities than silicas, while the lowest value was measured in the silica-alumina. However, differences on densities should not affect the impregnation process.

X-ray fluorescence

Qualitative analyses were performed with a XDL Fisherscope spectrophotometer in order to determine the composition of the carriers (see *Table 14*).

Aluminas presented less different impurities but with higher concentration, while silicas had more impurities but most of them were traces. This could affect the impregnation process since the active part could be neutralized by the impurities.

BET analysis

This analysis gives much information about the surface of the carriers. BET surface area (S_g), pore volume (V_g) and surface (S_{pore}) were measured with a Micromeritics ASAP 2000. The mean pore diameter (d_{pore}) was computed from the total pore volume and area ($4 \cdot V_g / S_{pore}$). In *Table 69* the results of BET analysis are shown.

Carrier	Si	Zr	Ti	Al	Na	Ca	Fe	S	P	Cl	Ga
Al-1	x	-	-	xxx	xx	-	x	-	-	xx	x
Al-2	-	-	-	xxx	xx	-	x	-	-	xx	x
Al-3	x	-	-	xxx	xx	x	x	-	-	-	x
Si-B	xxx	x	x	x	x	x	x	-	-	-	-
Si-C	xxx	x	x	x	x	x	x	x	-	-	-
Si-A	xxx	xx	-	-	x	x	x	-	-	-	-
Si-Al	xxx	xx	-	xxx	-	x	x	xx	x	-	-

x = trace element; xx = minor element; xxx = major element; - = element not present

Table 14. X-ray fluorescence

Some discrepancies appeared between nominal and measured BET surfaces. Al-3 and Si-Al presented the highest deviations. Among the Aluminas, Al-3 did not present either surface area or pore volume in great extent, so it was practically non-porous. The other two aluminas had similar characteristics.

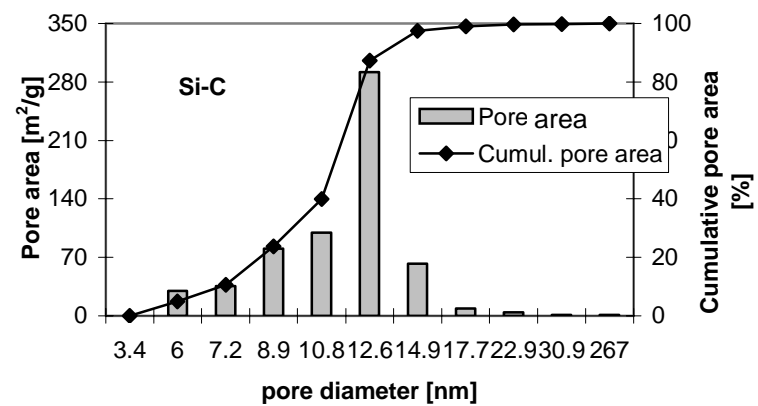
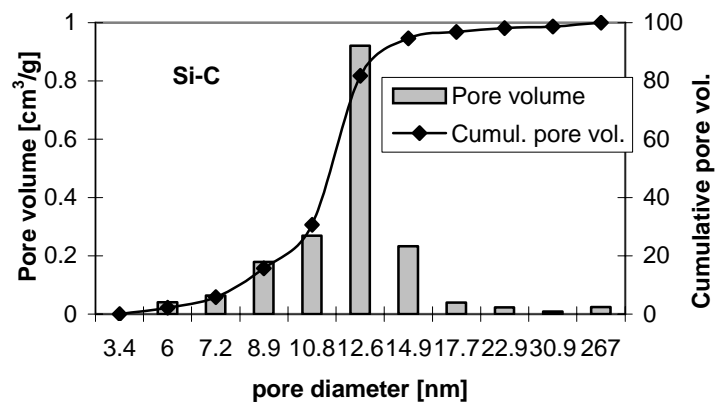
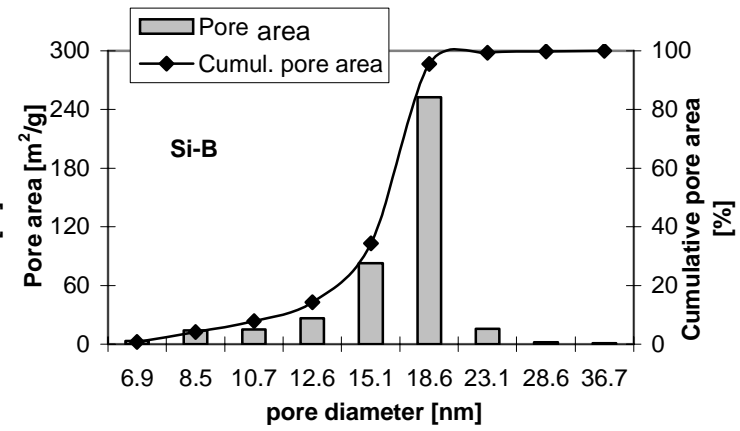
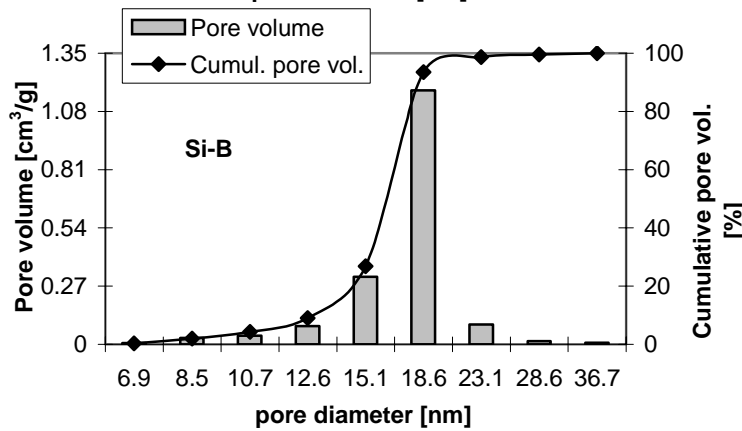
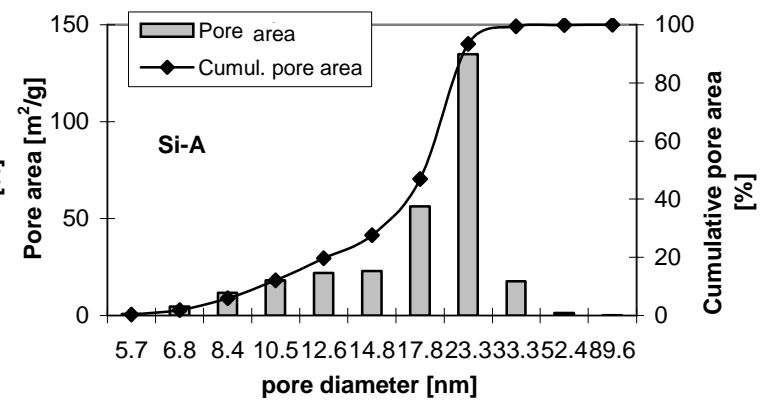
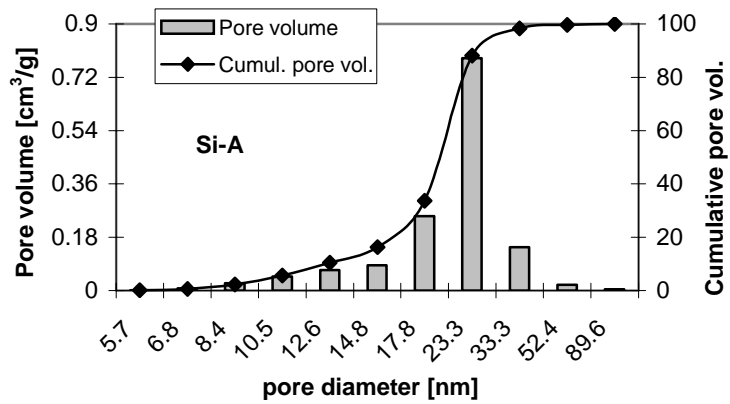
Carrier	BET nominal [m ² /g]	S _g [m ² /g]	V _g [cm ³ /g]	S _{pore} [m ² /g]	d _{pore} [*] [nm]
Al-1	155	176.5	0.2110	188.6	4.5
Al-2	155	157.2	0.2330	182.7	5.1
Al-3	10	0.6647	0.0020	0.586	14.0
Si-A	200	221.4	1.426	233.6	24.4
Si-B	300	306.4	1.728	314.1	22.0
Si-C	500	486.7	1.765	514.8	13.7
Si-Al	600	470.6	0.6449	532.4	4.8

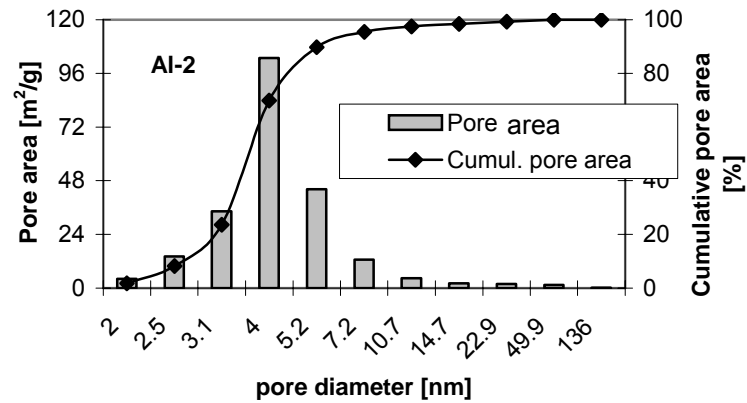
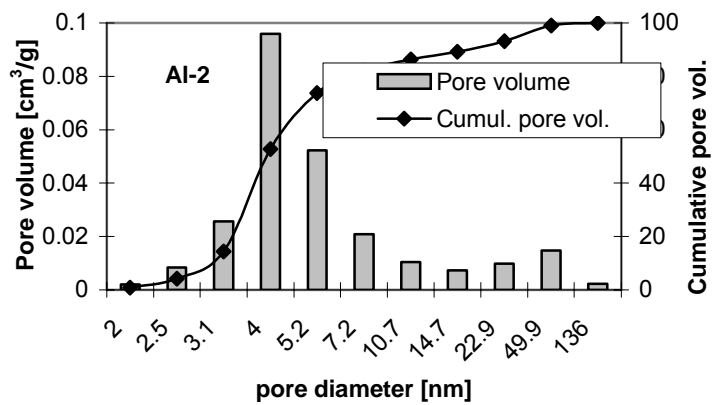
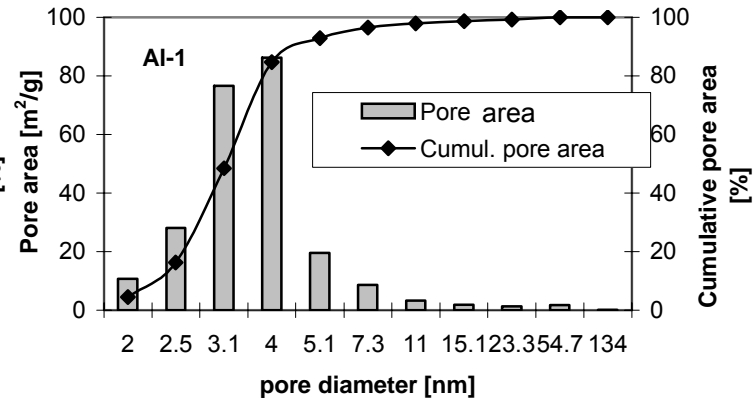
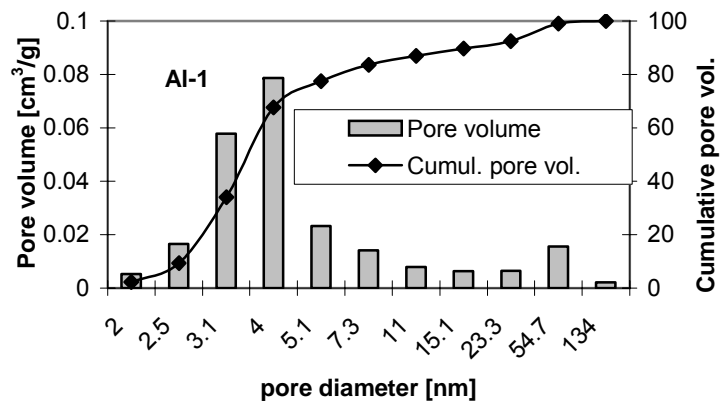
* computed from $4 \cdot V_g / S_{pore}$

Table 69. Results of BET analysis

As for the silicas, pore volume and surface increased on increasing the BET surface, as expected. On the other hand, measured pore surfaces were always higher than BET surfaces and presented important discrepancies for Al-3, Si-C and Si-Al.

In the following pictures the BJH desorption pore distribution of all carriers is presented. For each carrier the distribution of pore volume and area is shown, as well as their cumulative curves. In all figures the cumulative curves can be read on the right hand axis, while the distributions on the left hand one.





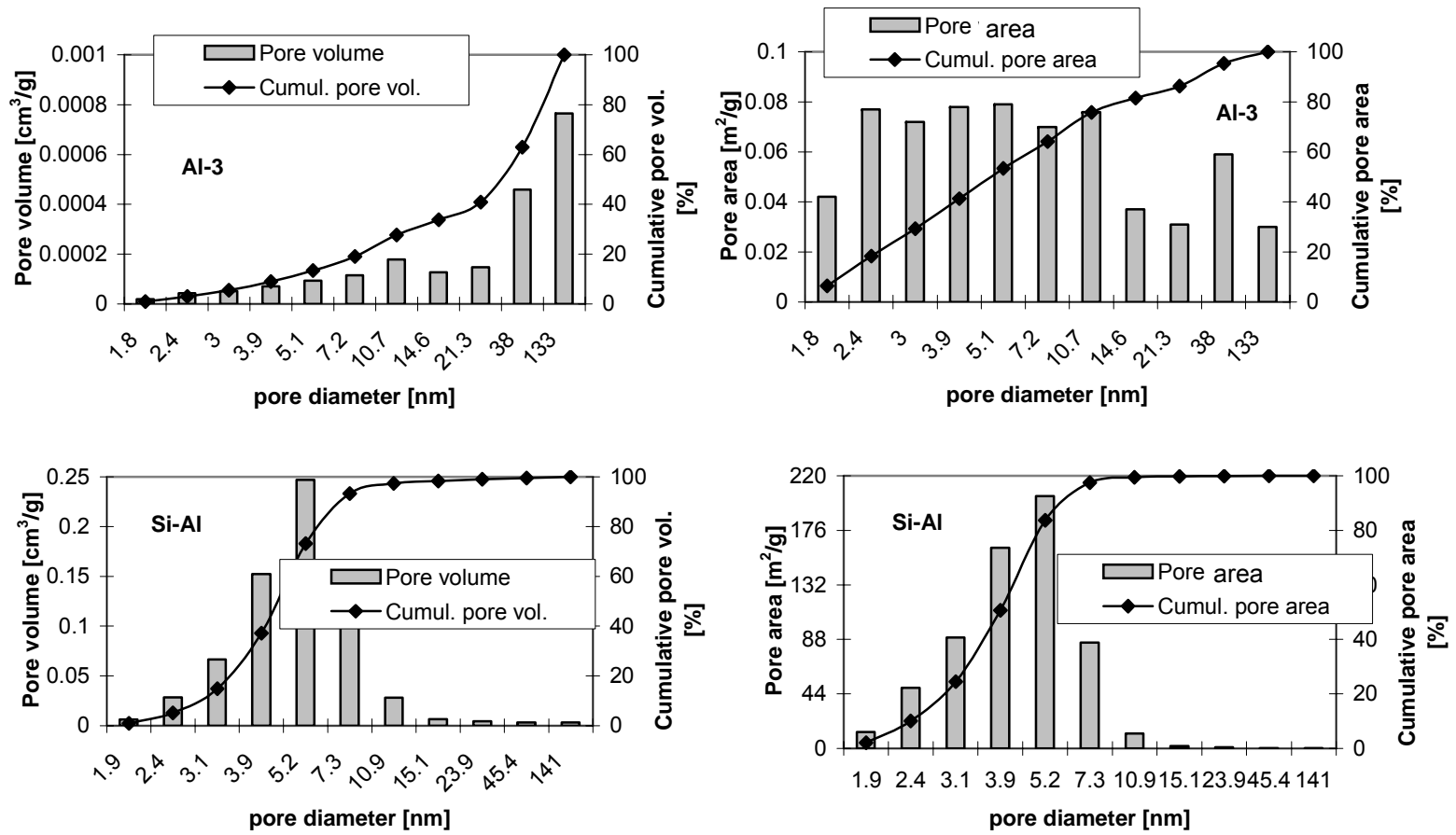


Figure 71. Desorption pore distribution of carriers

Particle size

The mean particle diameter was determined with a Beckman Coulter LS Particle Size Analyzer. In *Table 70* the particle diameters of all carriers are shown. Al-3 had such a small particle diameter that when it was tested in the setup it plugged the filter placed in the outlet of the reactor. So this carrier was rejected, and impregnation tests were performed with the other six.

Carrier	d_p [μm]
Al-1	115.8
Al-2	104.7
Al-3	7.7
Si-A	39.7
Si-B	79.1
Si-C	67.1
Si-Al	63.6

Table 70. Measured particle diameters

Organic and water content

Carriers were first dried in a vacuum oven and then placed in a muffle at 600°C for 2 hours. Finally they were weighed. In *Table 71* organic and water content of tested carriers are shown.

Most of the carriers presented an organic content below 5%, so they were not calcinated before use.

Carrier	Organics [%]	Water [%]
Al-1	4.9	0.0
Al-2	4.4	0.1
Al-3	0.2	0.0
Si-A	1.6	3.6
Si-B	4.0	3.4
Si-C	2.7	3.8
Si-Al	5.9	11.5

Table 71. Organic and water content

Acidic capacity

The acidic capacity of carriers was measured by direct exchange titration. The Fisher-Kunin

titration method could not be used since the alkali medium solubilized the Silica. In *Table 72* the acidity of the carriers tested is presented.

Carrier	meq H ⁺ /g
Al-1	0
Al-2	0
Al-3	0
Si-A	0.01
Si-B	0.01
Si-C	0.01
Si-Al	2.69

Table 72. Measured acidity of carriers

Only Si-Al presented some acidity by itself, so it could have some activity in the dehydration of 1-pentanol.

Activity on the dehydration of 1-pentanol

The activity of the carriers was checked in the dehydration of 1-pentanol to DNPE at 180°C. None of the carriers were active enough at working conditions, except for the silica-alumina, which presented some 1-pentanol conversion, as expected from acidic capacities.

4.7.2 EXPERIMENTAL DESIGN

The experimental of this part of the work was planned as follows:

1. Impregnations were first performed in order to find the appropriate method.
2. When the definitive method was clear, the study of the influence of the properties of carriers and the amount of active solution on the final catalysts were carried out. Catalysts synthesized were characterized and its activity tested on the dehydration of 1-pentanol to DNPE.
3. Finally, the reproducibility of the method of impregnation was checked.

17 impregnations were performed with different carriers and initial Nafion concentrations. In *Table 73*, the list of all the impregnations is shown. The resulting catalyst name was: carrier_method_theoretical %nafion. For example, Si-B_3_13 corresponds to the impregnated catalyst from Si-B following Method 3 and an initial Nafion % of 13.

Impregnation	Method	Carrier	BET* (m ² /g)	% Nafion	Catalyst name
I-1	M-1	Si-A	200	13	Si-A_1_13
I-2	M-2	Si-B	300	13	Si-B_2_13
I-3	M-2	Si-C	500	13	Si-C_2_13
I-4	M-2	Al-1	155	13	Al-1_2_13
I-5	M-2	Al-2	155	13	Al-2_2_13
I-6	M-2	Si-Al	600	13	Si-Al_2_13
I-7	M-2	Si-A	200	13	Si-A_2_13
I-8	M-3	Si-A	200	13	Si-A_3_13
I-9	M-3	Si-B	300	13	Si-B_3_13
I-10	M-3	Si-C	500	13	Si-C_3_13
I-11	M-3	Si-A	200	26	Si-A_3_26
I-12	M-3	Si-A	200	6.5	Si-A_3_6.5
I-13	M-3	Si-C	500	26	Si-C_3_26
I-14	M-3	Si-C	500	39	Si-C_3_39
I-15	M-3	Si-A	200	39	Si-A_3_39
I-16	M-3	Si-C	500	65	Si-C_3_65
I-17	M-3	Si-C	500	26	Si-C_3_26b

*Nominal BET surfaces of carriers

Table 73. List of impregnations

Impregnations 1 to 7 were used for the search of the impregnation method, I-8 to I-16 for the study of the effect of the properties of carriers on the impregnation of Nafion, and I-17 was a repetition of I-13 and was used for reproducibility purposes.

The activity of the synthesized catalysts was checked at the same experimental setup as the one described above for kinetic and equilibrium experiments. The reaction carried out was the dehydration of 1-pentanol to DNPE at 180°C, with 1g of impregnated catalyst and 500rpm.

The reason for the choice of this reacting system was the topic in which this work was framed. But it could be thought that another reacting system, e.g. a non polar medium, would have permitted to distinguish the effect of the surface area more clearly, since the ability to swell of Nafion particles in polar medium is well known.

As the activity of a catalyst is very influenced by its acidic capacity, experiments performed with impregnated catalysts always led to lower conversions and reaction rates than the obtained with Nafion NR50. This fact was due to their lower acidic capacity and the complete accessibility

of NR50 in PeOH media. Thus, synthesized catalysts would not be a good choice for the reaction studied. However, the turnover number, as defined in *equation 30* in *section 4.1.4*, was always better for impregnated catalysts than for Nafion NR50, which could give us the idea that these catalysts would work better in other reacting media.

4.7.3 SEARCH FOR THE METHOD OF IMPREGNATION

The use of Nafion supported catalysts is widely cited in the literature [31,103,104,105]. There, most of supported catalysts were prepared following an impregnation technique, but the method is never explained in detail. So it was necessary to develop a new method of impregnation which was improved as experience was acquired.

Basically, the impregnation technique consists of four steps:

1. Pre-treatment of the carrier and preparation of the impregnation medium
2. Impregnation process
3. Evaporation of the medium
4. Post-treatment of the catalyst

Three methods of impregnation were tested (M1, M2 and M3), being each one the evolution of the former. Subsequently these methods are explained, with a special focus on the improvements introduced in each step. In *section 3.3.2* Method 3 is explained in detail.

4.7.3.1 METHOD 1 (M-1)

Method 1 was the result of gathering all the information concerning impregnation found in literature and then developing our own receipt.

Step 1. Pre-treatment of the carrier and preparation of the impregnation medium

As explained in *section 3.1.3.4*, the amount of organic compounds in the carriers was not high, so they were used without previous calcination. Carriers were dried, weighed and introduced in a balloon with 150mL of a solution of alcohols and water that was used as solvent. The composition of the medium was very similar to the composition of the Nafion solution presented in *Table 8* in *section 3.1.3.1*.

Step 2. Impregnation process

The appropriate amount of Nafion solution was added to the balloon. Then the medium was stirred during 6h at ambient pressure and temperature.

Step 3. Evaporation of the medium

The same balloon was then connected to a rotavapor and the solvent evaporated during 2h at 60°C.

Step 4. Post-treatment of the catalyst

The impregnated catalyst was first dried at ambient conditions during 3 or 4h, and then during one night at 110°C in vacuum.

I-1 was the only impregnation performed following M-1, and results were not successful. It was observed that during the evaporation process there was a loss of catalyst due to sudden evaporation of the solvent.

4.7.3.2 METHOD 2 (M-2)

A new rotavapor was acquired which permitted to program a sequential increase of the vacuum in order to make the evaporation process less violent. Another modification of M1 was the decrease of the stirring speed (position 2 of 9, circa 70rpm). It was observed that with higher agitation the catalyst formed a compact and hard agglomeration after the evaporation of the solvent, which made its handling rather difficult and the subsequent drying process more complicated. Finally, a modification of the solvent composition was also introduced. Instead of the mixture of alcohols presented in *Table 8* of *section 3.1.3.1*, only 2-propanol (37% v/v) and water (63% v/v) were used.

I-2 to I-7 were impregnations performed following M-2 with the six carriers tested. The goal for all of them was to achieve a deposition of a 13% wt. of Nafion on the carrier. Since all impregnations were carried out under the same conditions, the behavior of the carriers could be compared, although M-2 was not the definitive method.

Results of impregnations via M-2 are shown in *Figure 72*. As it can be observed, only the three catalysts derived from the silica carriers and the one from the silica-alumina presented some conversion. However, values for *Si-Al_2_13* were far from the obtained with the silicas.

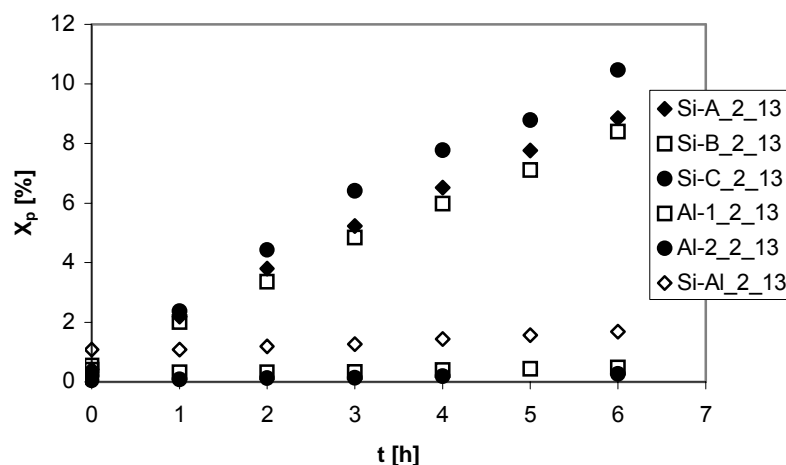


Figure 72. Activity of impregnated catalysts via M-2 at 180°C

In Table 74 BET surface areas, mean pore diameter of all carriers and 1-pentanol conversion at $t = 6$ h of the resulting catalyst are compared.

Carrier	S_g [m ² /g]	d_{pore} [nm]	X_p [%]
Al-1	176.5	4.5	0.5
Al-2	157.2	5.1	0.1
Si-B	221.4	24.4	8.8
Si-C	306.4	22.0	8.4
Si-A	486.7	13.7	10.5
Si-Al	470.6	4.8	1.1

Table 74. Carrier properties and 1-pentanol conversion after 6 h at 180°C of derived catalysts via M-2

The two alumina derived catalysts presented 1-pentanol conversions slightly higher than the obtained in blank experiments, but their activity was practically inappreciable. BET surface areas of aluminas were similar to the one of Si-A, but their pore diameters were clearly lower, of about 5 nm.

Si-Al had the highest BET surface of all the carriers tested, but also with a pore diameter around 5 nm. So BET and pore diameter values could not explain by their own the low success of the impregnation process on the aluminas. It seems, then, that the acidic character of the aluminas (and the silica-alumina) is an important drawback for the impregnation of Nafion on it, at least without any pre-treatment. In fact, a slightly higher 1-pentanol conversion was achieved

with the weakly acidic alumina derived catalyst (A1-1_2_13) than with the acidic one (A1-2_2_13).

At this point, it was decided to continue the work only with the three silicas, since they proved to be good carriers for the deposition of Nafion. The differences among the three silicas were the BET surface and pore distribution.

4.7.3.3 METHOD 3 (M-3)

The main improvement of this method was the introduction of a washing process of the carrier and the impregnated catalyst (Figure 73).

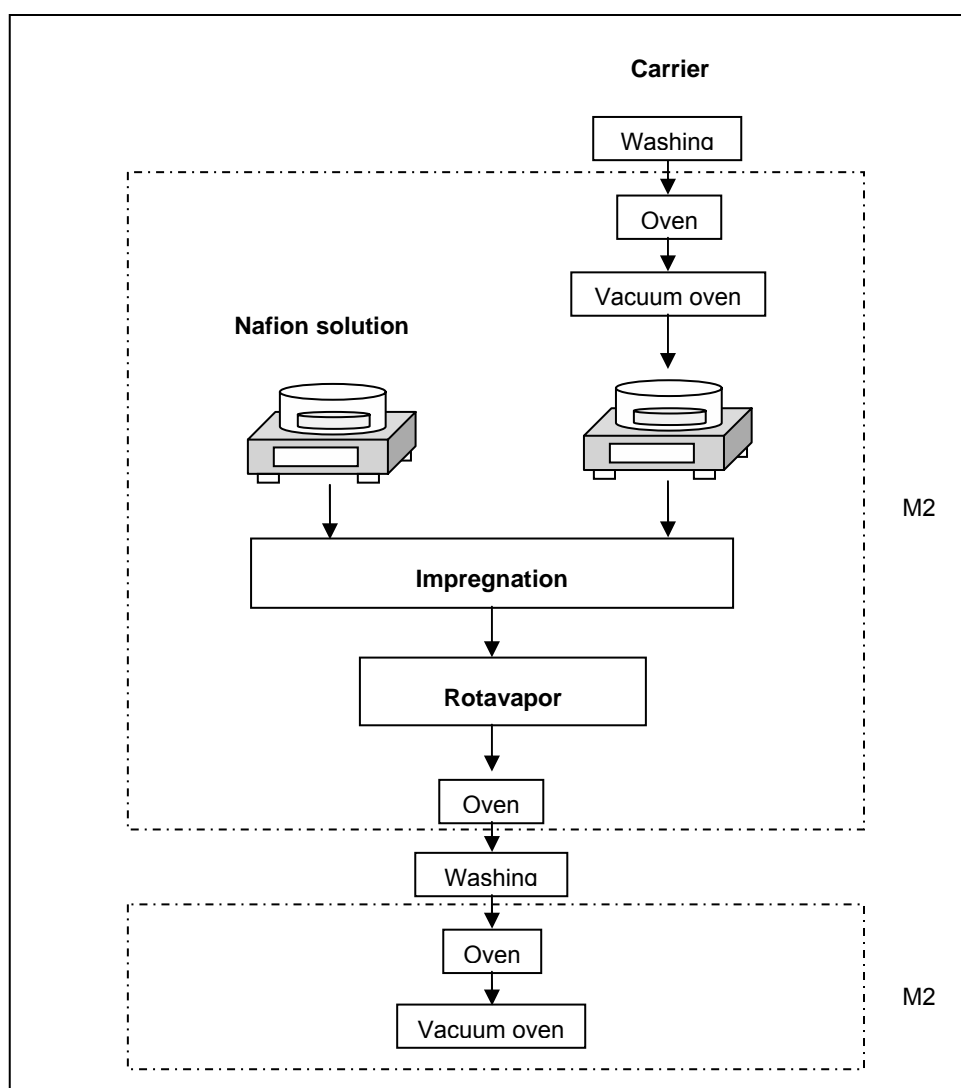


Figure 73. Improvement of method of impregnation 2 (M2)

The washing was performed in a Büchner funnel with 50 mL of methanol. This process was repeated once more, so a total of 100 mL of methanol were used.

This procedure was thought to be necessary in order to clean the carriers before the impregnation process, as well as to eliminate all Nafion which was not bonded to the carrier, but could be on the pores after the evaporation of the solvent in the rotavapor (Figure 74). Together with non-bonded Nafion rests of solvent could be also found if the evaporation was not complete. By washing with methanol this residual solvent and Nafion would be dragged.

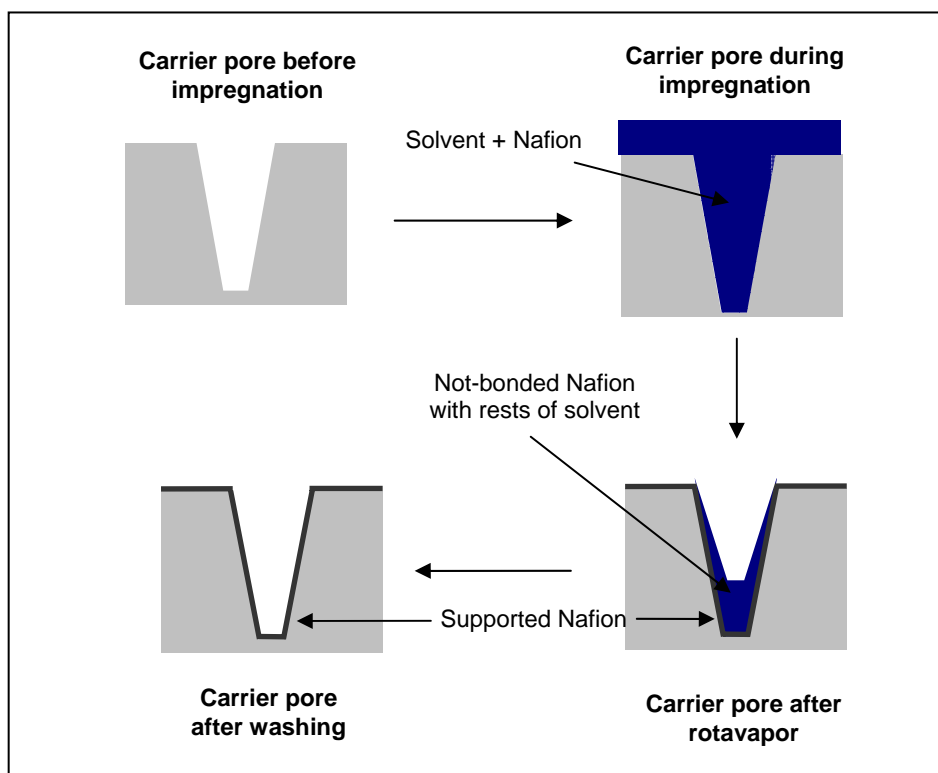


Figure 74. Steps of the impregnation process at a pore-scale

If the impregnated catalyst might not be washed, non-bonded Nafion could be released during experimentation in the autoclave reactor, acting as an homogeneous catalyst and masking the activity of the supported catalyst. The same could happen during titration.

Catalyst *Si-A_2_13* (I-7) was used to test whether washing was necessary. Different samples of this catalyst were washed with 50 mL of methanol once, twice and four times, respectively. Then their activity on the dehydration of 1-pentanol was checked and compared to

a sample which was not washed. In *Figure 75* 1-pentanol conversion for each case is presented.

As expected, washed catalysts were less active than if washing was not performed. So with this procedure some Nafion was dragged. As the same results were obtained whether washing was performed once, twice or four times, Nafion which was eliminated from the catalyst was non-bonded, since, else, the loss of activity should have increased with the number of washings.

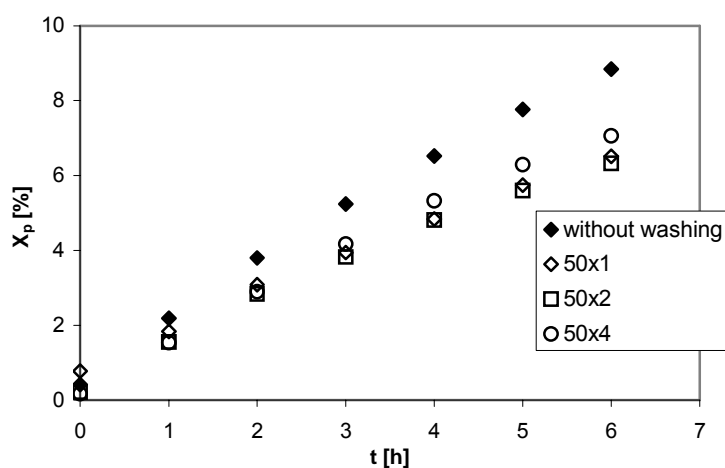


Figure 75. Effect of washing on 1-pentanol conversion

As a conclusion, it was proved the necessity of including a washing process after the evaporation of the solvent to drag all non-bonded Nafion. It was decided that two washings with 50mL of methanol each was enough to eliminate it.

I-8, **I-9** and **I-10** were prepared following M-3 using the three silicas as carriers (Si-A, Si-B and Si-C). The initial amount of Nafion was 13% wt. Results were compared to Nafion NR50, considered as an hypothetical carrier with 100% of Nafion impregnated, and to SAC-13, a nanocomposite with a 13% of Nafion. In *Table 75* the results of all of them are compared.

As expected the highest conversion (and initial reaction rate) was achieved with NR50, then with the nanocomposite and, finally, with the three silicas derived catalysts. As seen in *section 4.3.1*, the higher the acid capacity, the higher 1-pentanol conversion was. In this case, as the acid capacity was given by Nafion content, the higher the Nafion content, the higher the conversion was.

	Carrier	S _g ^a [m ² /g]	X _p [%]	S _{DNPE} [%]	Acid capacity [meq H ⁺ /g]	r ^o [mol/(kg h)]	r ^o _{eq} [mol/(eqH ⁺ h)]
I-8	Si-A	221.4	6.3	97.3	0.078	4.8	61
I-9	Si-B	306.4	8.2	98.0	0.086	6.0	70
I-10	Si-C	486.7	9.6	98.3	0.088	5.7	65
NR50	-	0.35	49.4	97.8	0.89	43.6	49.0
SAC-13	-	176.6	19.1	97.1	0.15	14.5	96.7

^a BET surface area

Table 75. I-8, I-9 and I-10 results compared to NR50 and SAC-13

Selectivity to DNPE was the same for all catalysts within the limits of experimental error. On the other hand, initial reaction rate per equivalent of H⁺, or turnover number, was clearly lower for NR50 than for the other catalysts. This fact could be caused by better accessibility and distribution of the active centers within the silica matrix. In a non-polar reacting medium, these catalysts would present a better behavior than NR50 since the accessibility to the active centers for the latter would be very difficult.

As for the three silica derived catalysts, it seems that there was a direct relationship between the BET area and the acidity (and conversion). Since all impregnated catalysts were prepared following the same method, the amount of Nafion that was supported on the carrier was higher when the BET area increased. In order to quantify the amount of Nafion that was supported on the carrier, the following parameters were defined:

$$\%Nafion_{ac,i} = \frac{acidity_i}{acidity_{NR50}} \cdot 100 \quad \text{Equation 69}$$

$$\%Nafion_{r,i} = \frac{r_i^0}{r_{NR50}^0} \cdot 100 \quad \text{Equation 70}$$

$$\%Nafion_{m,i} = \frac{r_{eq,i}^0}{r_{eq,NR50}^0} \cdot 100 \quad \text{Equation 71}$$

where sub indexes *ac*, *r*, *tn* and *i* refer to acidity, initial reaction rate, turnover number and carrier, respectively.

In *Table 76* values of these parameters for I-8, I-9, I-10 and SAC-13 are shown.

	Carrier	%Nafion _{ac}	%Nafion _r	%Nafion _{tn}
I-8	Si-A	9	11	125
I-9	Si-B	10	14	142
I-10	Si-C	10	13	133
NR50	-	100	100	100
SAC-13	-	17	33	197

Table 76. %Nafion supported for I-8, I-9 and I-10

%Nafion supported with respect to acidity, %Nafion_{ac}, was always lower than the theoretical one (13%). An efficiency of the impregnation j could be defined as follows:

$$Efficiency_j = \frac{\%Nafion_{ac,j}}{\%Nafion} \quad \text{Equation 72}$$

where %Nafion is the initial amount of Nafion on the impregnation process. An efficiency value of 0 would mean that the synthesized catalyst had not any active Nafion supported. On the other hand, a value of 1 would indicate that all Nafion introduced was supported on the carrier and was active.

Values of efficiency for I-8, I-9 and I-10 were 0.67, 0.74 and 0.76, respectively, which means that part of the Nafion was not bonded to the carrier and/or some was neutralized during the process. On the other hand, %Nafion_r calculated with respect to initial reaction rate was higher than %Nafion_{ac}, which confirms the better behavior of the active centers of supported catalysts than those of NR50. SAC-13, which is supposed to have a 13% wt. of Nafion in its silica matrix showed higher conversions and acidity than expected. Here, the distribution of active centers is still better than in supported catalysts, since both the silica and the active part grow together during the synthesis process by sol-gel reaction.

As the efficiency of the impregnation increased with BET area, and the amount of initial Nafion was crucial on the activity of the impregnated catalysts, a study of the effect of both factors was carried out with carriers Si-A (lowest BET area) and Si-C (highest BET area).

4.7.4 EFFECT OF THE INITIAL %NAFION AND BET AREA

4.7.4.1 SI-A

In *Table 77* acid capacity, 1-pentanol conversion, initial reaction rate and turnover number of impregnations of Si-A with different amounts of Nafion are shown. Furthermore, results for NR50 are also presented.

%Nafion	Acid capacity [meqH ⁺ /g]	X _p [%]	r ^o [mol/(kg h)]	r ^o _{eq} [mol/(eqH ⁺ h)]
6.5	0.029	1.7	1	34
13	0.078	6.3	4.8	62
26	0.189	18.1	12.7	67
39	0.328	27.9	23.3	71
100*	0.890	49.4	43.6	49

*NR50

Table 77. Effect of %Nafion on the impregnation of Si-A

As expected, the amount of Nafion supported on synthesized catalysts increased on increasing the initial amount of Nafion. So, acid capacity, 1-pentanol conversion and reaction rate also increased. The turnover number also augmented, but very softly from 13% of initial Nafion. In *Table 78* the efficiency and the amount of Nafion supported computed with respect to different factors are presented.

%Nafion	Efficiency	%Nafion _{ac}	%Nafion _r	%Nafion _{tn}
6.5	0.50	3	2	70
13	0.67	9	11	126
26	0.82	21	29	137
39	0.94	37	53	145

Table 78. %Nafion supported for Si-A derived catalysts

The efficiency of the impregnation increased on increasing the initial amount of Nafion. This could be explained by the fact that the first molecule of Nafion would be bonded to the silica surface by the sulfonic groups, i.e. there would be a neutralization of the active sites with the OH⁻ groups of the Si (see *Figure 76*). The second molecule could be bonded again to the carrier via neutralization reaction, or to the first molecule by means of a polymerization reaction between the chains of Nafion molecules, maintaining the active sites intact. So, when the

amount of initial Nafion increases the loss of acidity due to the first neutralization reaction would be less important compared with the total amount of Nafion impregnated.

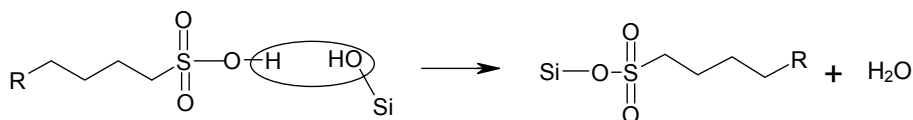


Figure 76. Neutralization of sulfonic groups during impregnation

On the other hand, values of %Nafion_{tn} shown in *Table 78* prove the better behavior of active sites on impregnated catalysts compared to NR50.

4.7.4.2 SI-C

In *Table 79* acidity, 1-pentanol conversion, initial reaction rate and turnover number of impregnations of Si-A with different amounts of Nafion is shown. Furthermore, results for NR50 are also presented.

%Nafion	Acidity [meqH ⁺ /g]	X _p [%]	r ^o [mol/(kg h)]	r ^o _{eq} [mol/(eqH ⁺ h)]
13	0.088	9.6	5.7	65
26	0.211	20.0	16.7	79
39	0.325	29.2	24.4	75
65	0.555	35.5	29.8	54
100*	0.890	49.4	43.6	49

*NR50

Table 79. Effect of %Nafion on the impregnation of Si-C

Again acidity, 1-pentanol conversion and initial reaction rate increased on increasing the initial amount of Nafion. However, a maximum was observed for the turnover number. So it seems that there was a %Nafion that made that the distribution of active centers throughout the carrier was optimum. From this point, active centers were not so efficient, though higher 1-pentanol conversion was achieved when more Nafion was added. In *Table 80* the efficiency and the amount of Nafion supported computed with respect to different factors are presented.

As happened to Si-A derived catalysts, the efficiency increased with the initial amount of Nafion, and %Nafion_r was higher than expected. %Nafion_{tn} showed again the existence of an optimum of amount of Nafion.

%Nafion	Efficiency	%Nafion _{ac}	%Nafion _r	%Nafion _{tn}
13	0.76	10	13	132
26	0.91	24	38	162
39	0.94	37	56	153
65	0.96	62	68	110

Table 80. %Nafion supported for Si-C derived catalysts

4.7.4.3 COMPARISON OF SI-A AND SI-C DERIVED CATALYSTS

In *Figure 77* 1-pentanol conversion achieved after 6 hours of experiment with impregnated catalysts versus the initial amount of Nafion is shown. Conversion values were always lower than the achieved with NR50, but they increased on increasing %Nafion. Furthermore, conversion was higher than expected in most impregnated catalysts. Si-C derived catalysts showed always more activity than Si-A, so the higher the surface area, the better the impregnation. Thus, at a %Nafion of 13, where the three silicas can be compared, the highest conversion was achieved by the Si-C derived catalyst, followed by Si-B and Si-A.

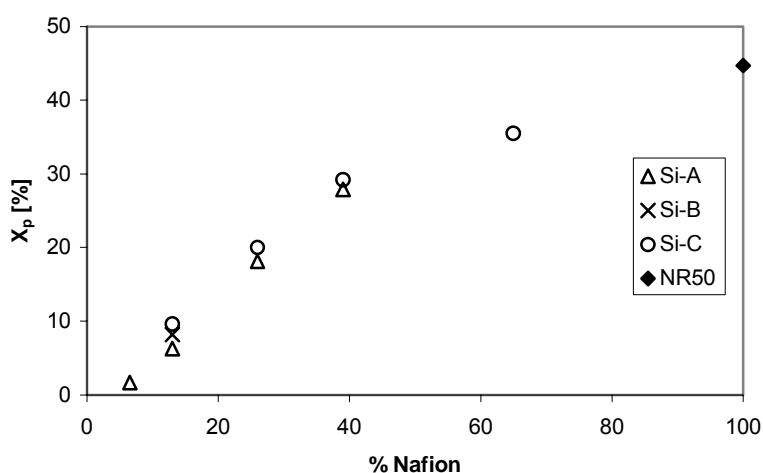


Figure 77. 1-pentanol conversion vs. %Nafion; t=6h, 180°C, 1g cat.

In *Figure 78* the efficiency of the impregnation process for Si-A and Si-C derived catalysts is shown. Again, better results were obtained with the silica with more surface area. However, from 39% of Nafion, efficiency values are very close to 1 for both carriers.

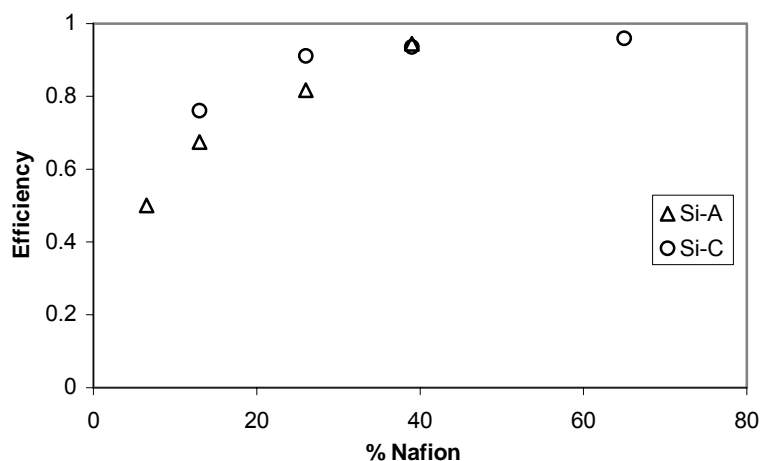


Figure 78. Impregnation efficiency vs. %Nafion

In Figure 79, the turnover number of Si-A and Si-C impregnations are compared. Higher values were obtained with the silica of more BET surface.

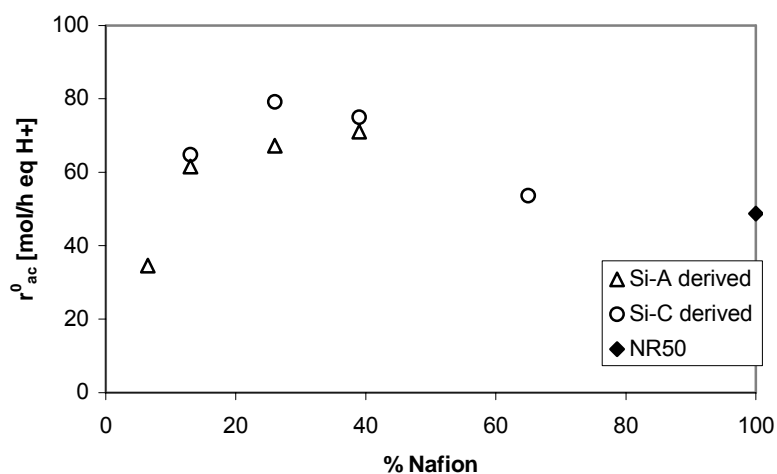


Figure 79. Turnover number vs. %Nafion

It should be noted the curious shape of Si-C derived catalysts. First there was an increase of the turnover number until a maximum was reached. Then it decreased on increasing the %Nafion until it reached turnover levels of NR50. So it seems that as %Nafion increased impregnated catalysts became more similar to pure NR50. Figure 80 tries to make an ideal approximation to this phenomenon.

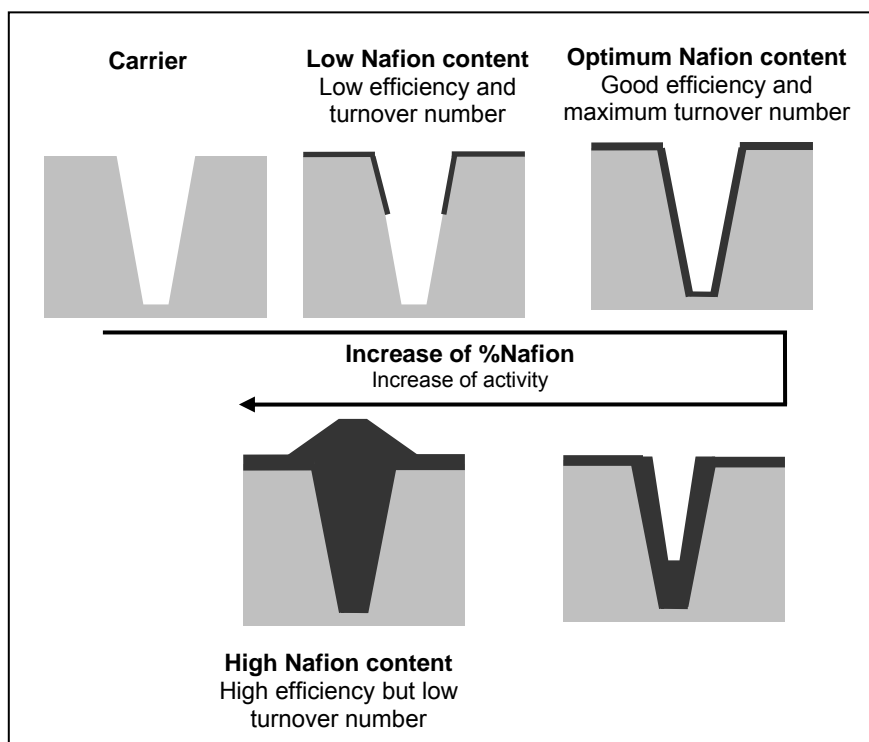


Figure 80. Effect of %Nafion increase at a pore-scale

1. As %Nafion increases, the amount of Nafion supported on the carrier increases and so the activity on 1-pentanol dehydration. Firstly the deposition would be mainly bonded to the carrier, with neutralization of some sulfonic groups, and leading to low impregnation efficiencies (as defined in *equation 66*).
2. When more Nafion is added, it would cover all accessible surfaces reaching an optimum on the turnover number, i.e. the active sites would be perfectly distributed and accessible.
3. On increasing %Nafion, it would be mainly bonded to other Nafion chains, the efficiency increases, but it could block some pores or make them smaller. So the accessibility to the inner active centers would be more difficult, resulting in a decrease of the turnover number.
4. Finally, at higher %Nafion, impregnated catalysts would behave as NR50, with very high impregnation efficiencies and activities but low accessibility to inner active centers in non-polar medium.

The same behavior should be expected to Si-A derived catalysts but with the maximum displaced to higher %Nafion. Si-A had lower BET surface than Si-C, so higher average pore diameter. As %Nafion increased, pores would be also covered, but more Nafion would be

necessary since pores are larger.

4.7.5 IMPREGNATED CATALYSTS CHARACTERIZATION

In *Table 81* results of BET analysis of impregnated catalysts are shown. These are compared to BET results of the carriers and NR50. Only results for desorption isotherm are shown.

On increasing the amount of Nafion all magnitudes shown in *Table 81* decreased, as expected. In the following figures these values are plotted versus %Nafion.

With the impregnation process pore diameter diminished with respect to the one of carriers, but did not change much on increasing %Nafion. In fact, for Si-C derived catalysts the pore diameter was practically constant over the range of %Nafion explored.

Catalyst	Pore volume [cm ³ /g]	Pore Area [m ² /g]	d _{pore} [nm]	BET area [m ² /g]
Si-A	1.440	290	19.8	221.4
Si-A_3_26	0.837	189	17.7	162.6
Si-A_3_39	0.605	141	17.1	115.8
Si-C	1.803	615	11.7	486.7
Si-C_3_13	1.030	522	7.9	400.2
Si-C_3_26	0.965	399	9.7	325.9
Si-C_3_39	0.763	320	9.5	234.7
Si-C_3_65	0.372	157	9.5	124.8
NR50	0.0002	0.263	3.0	0.35

Table 81. Results of BET analysis of impregnated catalysts

Pore volume and area decreased considerably on increasing the initial amount of Nafion, with a clear tendency to reach values of magnitudes shown in *Table 81* of NR50 level, i.e. very low pore volume and area.

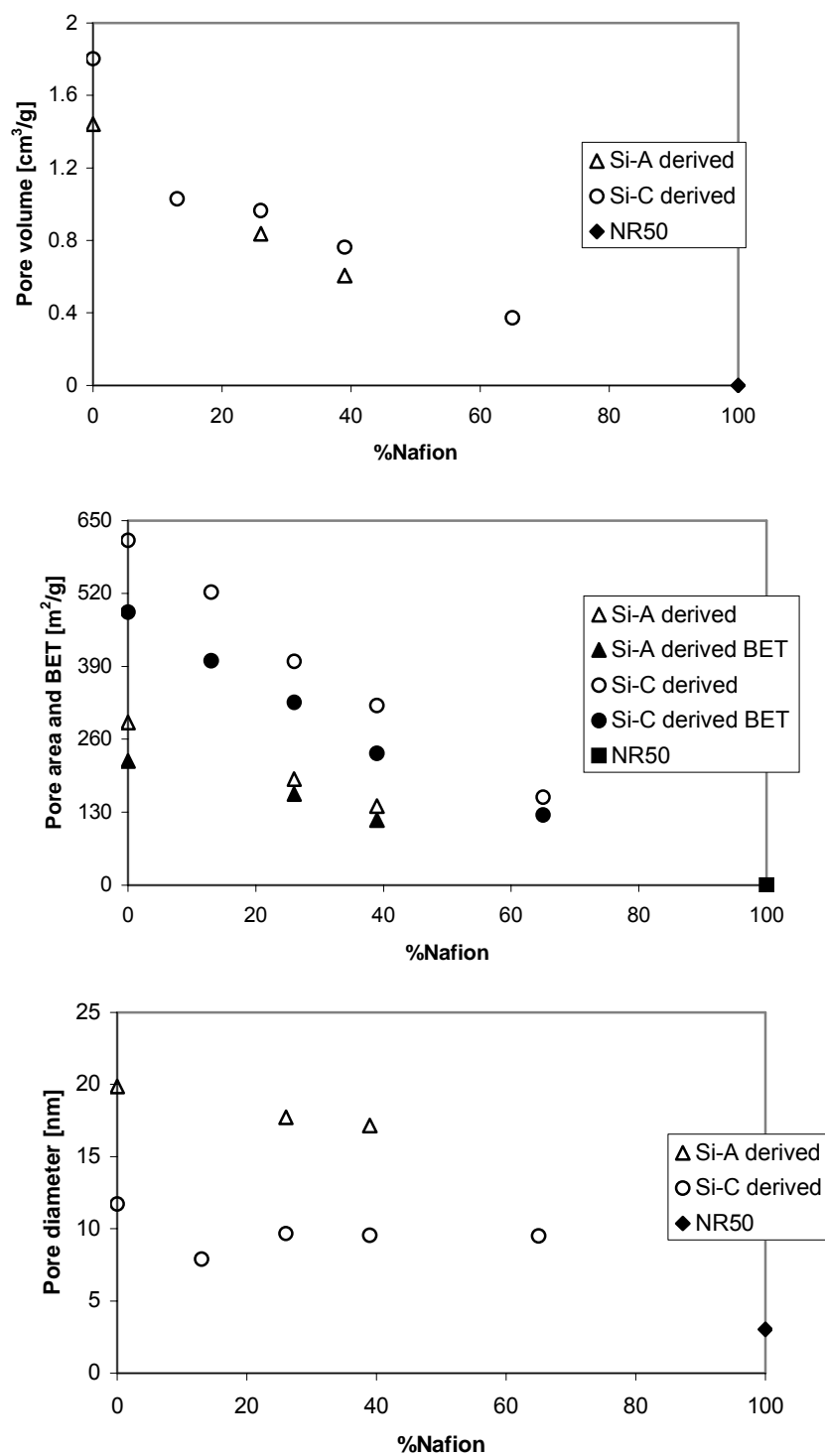


Figure 81. Plots of BET analysis results for synthesized catalysts

In Figure 82 the pore volume distribution of Si-A derived catalysts is shown.

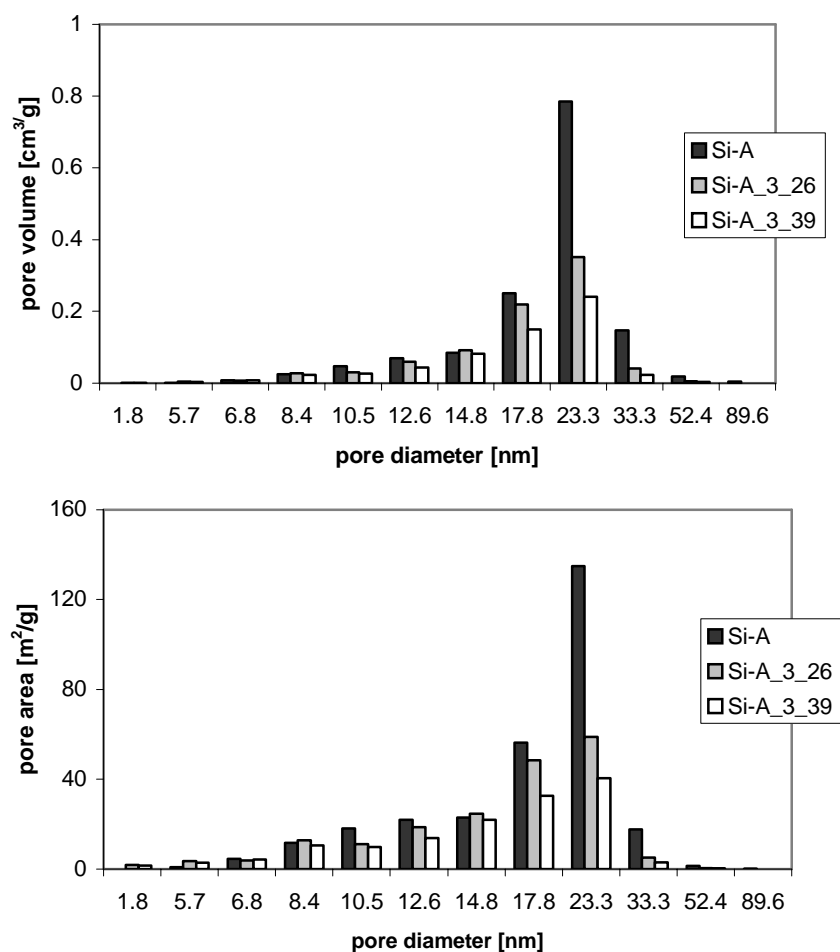


Figure 82. Desorption pore distribution of Si-A derived catalysts

As it can be seen in the figure, the impregnation of Si-A was uniform: the shape of the pore distribution of impregnated catalysts was very similar to the one of the carrier, but with a lower pore volume and area.

In *Figure 83* the pore volume distribution of Si-C derived catalysts is shown.

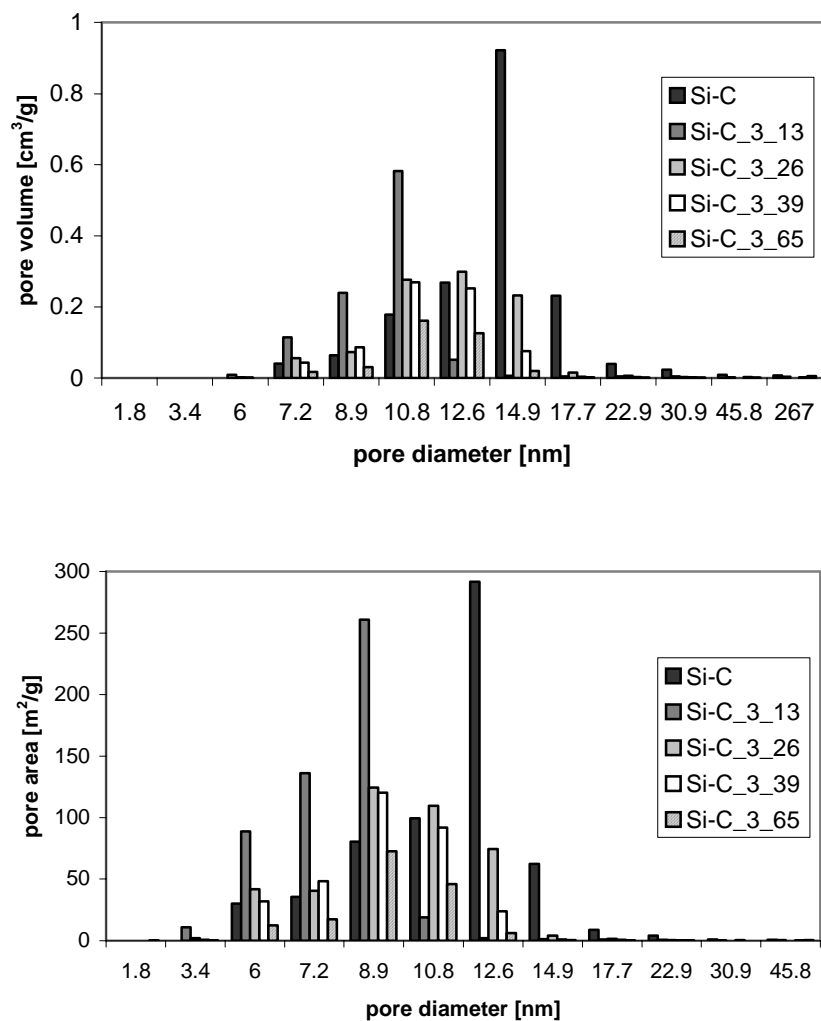


Figure 83. Desorption pore distribution of Si-C derived catalysts

The impregnation of Si-C was also uniform, since the shape of the pore distribution did not change. The difference here was that the curve was shifted to lower pore diameters. So with the impregnation process the pores were narrowed. This was more evident in Si-C derived catalysts because the initial average pore diameter was lower for Si-C than Si-A.

4.7.6 IMPREGNATION METHOD REPRODUCIBILITY AND DEACTIVATION TEST

In order to check the reproducibility of the impregnation method a new test was performed, I-17, which was a repetition of I-13 (Si-C with 26% of Nafion).

Catalyst	Acid capacity [meqH ⁺ /g]	X _p [%]	r ^o [mol/(kg h)]	r ^o _{eq} [mol/(eqH ⁺ h)]
Si-C_3_26	0.211	20.0	16.7 ± 1.5	79
Si-C_3_26b	0.203	18.3	15.9 ± 0.7	78

Table 82. Reproducibility of the method of impregnation

In Table 82 and Table 83 results of both impregnations are shown.

Catalyst	Efficiency	%Nafion _{ac}	%Nafion _r	%Nafion _{tn}
Si-C_3_26	0.91	24	38	162
Si-C_3_26b	0.88	23	36	159

Table 83. %Nafion supported for replicated catalysts

As it can be stated in the tables, the reproducibility of the impregnation method was very good, since reaction rates and turnover numbers were the same for both catalysts. In Table 84 and Figure 84 the results of BET analysis are shown.

There were some discrepancies on BET area values but the other magnitudes very quite similar. Pore distribution of Si-C_3_26b was slightly different, but the resulting average pore diameter was practically the same as the one of Si-C_3_26. So it can be concluded that the method of impregnation used (M-3) gives reproducible impregnations, which confirms the suitability of the method.

Catalyst	Pore volume [cm ³ /g]	Pore Area [m ² /g]	d _{pore} [nm]	BET area [m ² /g]
Si-C_3_26	0.965	399	9.7	325.9
Si-C_3_26b	0.840	387	8.7	292.0

Table 84. Results of BET analysis of replicated catalysts

On the other hand, some catalysts were reused in order to check whether impregnated Nafion was still bonded to the matrix after a six-hour-experiment.

Two samples of Si-C_3_26 (I-13) and Si-C_3_39 (I-14) that had been already tested in the autoclave reactor were dried and the same experiment was performed.

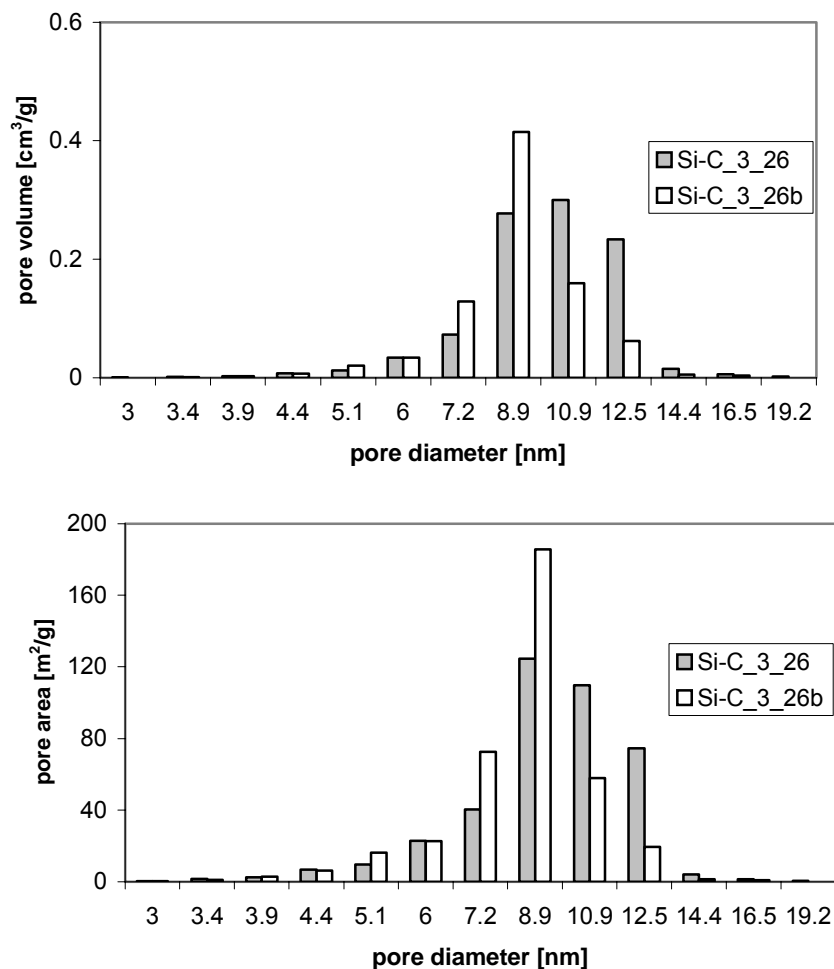


Figure 84. Desorption pore distribution of replicated catalysts

In Figure 85 reaction rates of catalysts reused are compared to results obtained with fresh catalyst. As it can be stated, there was an important loss of activity, probably due to leaching, but reused catalysts had still an important amount of active Nafion impregnated, so there was not deactivation of the active centers. I-13 lost a 47% of its activity and I-14 a 37%.

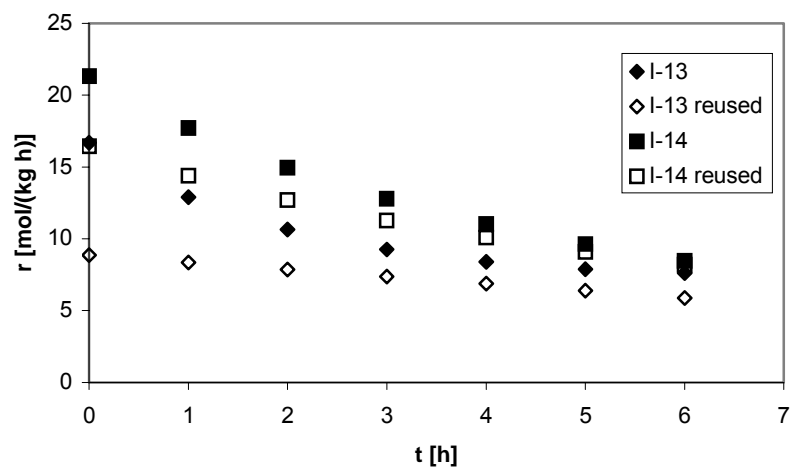


Figure 85. Reaction rates of reused catalysts



Chapter 5. Conclusions

Conclusions

The liquid-phase dehydration of 1-pentanol to DNPE and water over acidic catalysts was studied and the following conclusions could be drawn:

Influence of the variables of operation

- ✓ 1-Pentanol conversion increased on increasing the catalyst mass, while selectivity to DNPE decreased. Nevertheless, for catalyst mass > 2g the initial reaction rate decreased probably due to some saturation effect of the reaction system.
- ✓ For $N > 300$ rpm the influence of the external mass transfer was negligible.
- ✓ The influence of the internal mass transfer was not significant for all catalyst checked.

Catalysts tests

- ✓ 1-Pentanol conversion increased on increasing the temperature and the time of reaction. The highest conversion at 6 hours of experiment (68%) was achieved with Amberlyst 70 at 190°C. In general, at a constant temperature, the higher the acidity, the higher the conversion was.
- ✓ In general, selectivity to DNPE decreased with temperature, since side reactions had higher activation energies than the main one. Microporous resins yielded to higher selectivity to DNPE than macroporous ones, being Nafion NR50 the most selective catalyst.
- ✓ The reaction rate increased with temperature. In general, at a constant temperature, the higher the acidity, the higher the reaction rate was.
- ✓ At lower temperatures, up to 150°C, S/DVB resins were the most active and selective catalysts, but their low maximum working temperature was an important drawback. Among thermally stable resins, Amberlyst 70 appeared as the best choice due to its wide temperature range, high activity and acceptable selectivity.

Thermodynamic equilibrium

- ✓ The catalyst mass used had no effect on the measured equilibrium constants, and values of K_γ proved the non-ideality of the mixture.
- ✓ The equilibrium constant of the dehydration of 1-pentanol to DNPE and water decreased with temperature, so it is an exothermic reaction. K^{DNPE} values were high enough to state that the main reaction was clearly shifted to the products at equilibrium, what assures good conversion levels of 1-pentanol to ether in industrial etherification processes. $\Delta_r H_{(l)}^0$ for DNPE production was $-(6.5 \pm 0.6)$ kJ/mol if considered constant over the temperature range, $-(3.8 \pm 0.6)$ kJ/mol if considered variable with temperature.

- ✓ A value of $\Delta_f H^0_{(l)}$ of $-(423.9 \pm 1.2)$ kJ/mol is proposed for DNPE if $\Delta_f H^0_{(l)}$ is considered to be constant or $-(421.1 \pm 1.2)$ kJ/mol if variable with temperature. As for the entropy, a value of $S^0_{(l)}$ of 465.95 J/(K·mol) (473.71 if $\Delta_f H^0_{(l)}$ is considered variable with temperature) for DNPE is computed.
- ✓ The equilibrium constant of the decomposition reaction of DNPE to 1-pentene and 1-pentanol increased with temperature, so it is an endothermic reaction. $\Delta_r H^0_{(l)}$ for DNPE decomposition was (70.4 ± 0.9) kJ/mol if considered constant over the temperature range, (63.4 ± 0.9) kJ/mol if considered variable with temperature.
- ✓ The equilibrium constant of the isomerization of 1-pentene to 2-pentene decreased with temperature, so it is an exothermic reaction. $\Delta_r H^0_{(l)}$ for 1-pentene isomerization was $-(13.0 \pm 4.2)$ kJ/mol if considered constant over the temperature range, $-(14.7 \pm 4.1)$ kJ/mol if considered variable with temperature.

Kinetic analysis

- ✓ The best prediction of the reaction rate was achieved by a kinetic model derived from a Rideal-Eley mechanism, which assumes that an adsorbed 1-pentanol molecule reacts with another 1-pentanol molecule on the fluid phase. The ether formed is released to the bulk phase. The surface reaction was assumed to be the rate-limiting step. Furthermore, the number of unoccupied active centers is negligible and water does not appear in the adsorption term.
- ✓ The kinetic equation predicts well the experimental data except when the amount of water is significant. The inhibiting effect of water can be explained by the fact that water adsorbs preferably on the catalyst, hindering 1-pentanol adsorption and, therefore, the reaction. To model this effect, some correction factors were introduced on the kinetic models. These factors could be seen as the fraction of active centers free of water. The best prediction was achieved by a Freundlich isotherm-like expression. For Amberlyst 70, the modified kinetic equation was:

$$r = \frac{\hat{k}_0 \left(a_p^2 - \frac{a_w a_D}{K_{eq}} \right)}{a_p} \cdot \left(1 - K_F a_w^{1/\alpha} \right)$$

- ✓ The activation energy for the dehydration of 1-pentanol to DNPE and water over Amberlyst 70 was 114.0 ± 0.1 kJ/mol. The modified kinetic model fitted experimental data of all catalysts well, yielding to a range of activation energies of 95-120 kJ/mol. The activation energies of 1-pentanol dehydration to 1-pentene and water, and 1-pentene

isomerization to 2-pentene were 125 kJ/mol and 100 kJ/mol, respectively.

Catalyst synthesis

- ✓ A method of impregnation was successfully developed, since reproducible catalysts were synthesized.
- ✓ As the catalyst activity was very influenced by its acidic capacity, experiments performed with impregnated catalysts always led to lower conversions and reaction rates than the obtained with Nafion NR50. This fact is explained by the lower acidic capacity of impregnated catalysts and, on the other hand, by the complete accessibility of NR50 in 1-pentanol media. However, the turnover number was always better for impregnated catalysts than for Nafion NR50, which could give us the idea that these catalysts would work better in other reacting media.
- ✓ The impregnation efficiency, defined by *Equation 72*, increased on increasing the initial amount of Nafion. On the other hand, a maximum on the turnover number appeared for Si-C derived catalysts at about 26% of initial amount of Nafion.

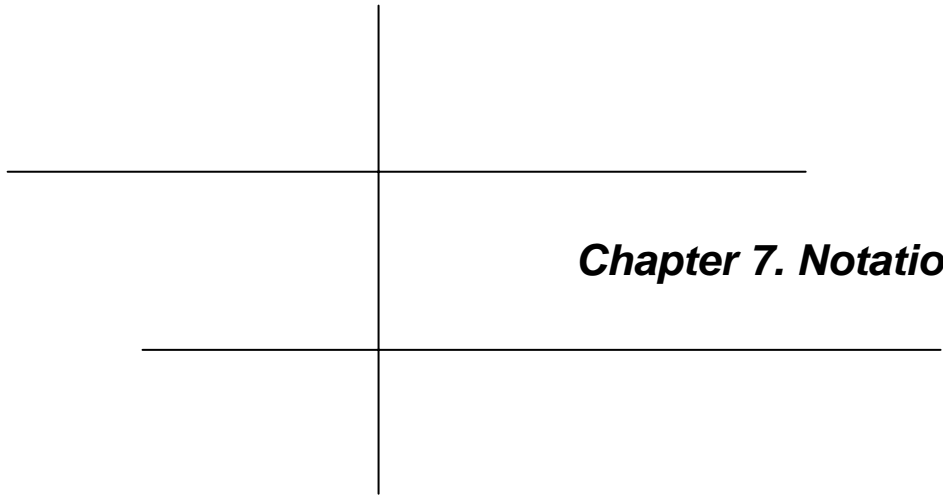


Chapter 6. Recommendations

Recommendations

Some proposals for further work derived from the present study can be listed:

1. To study the dehydration of 1-pentanol to DNPE and water in a continuous reactor in order to evaluate the kinetics results obtained in this work. Experiments with and without initial amounts of water and DNPE could be performed.
2. To study the dehydration of 1-pentanol to DNPE and water with simultaneous water removal in order to swift the reaction to the production of ether.
3. To test new commercial catalysts and compare their behavior with Amberlyst 70.
4. To synthesize new catalysts, by changing the carriers, the active solutions or the method of synthesis.



Chapter 7. Notation

Notation

A, B	constants agrupation for fitting purposes
a_j	activity of compound j
a_i, b_i, c_i, d_i	polynomial form coefficients of heat capacities expressions of compound i
a, b, c, d	temperature dependence coefficients
$b_1, b_2 \dots$	fitted parameters
$C_{p(l)i}$	molar heat capacity of compound i in the liquid-phase ($\text{J mol}^{-1}\text{K}^{-1}$)
d_p	particle diameter (μm)
d_{pore}	pore diameter (nm)
E_a	activation energy (kJ/mol)
$\Delta_r G_{(l)}^0$	standard free energy change of reaction in liquid-phase (kJ mol^{-1})
$\Delta_f H_{(l)}^0$	liquid-phase standard molar enthalpy change of formation (kJ mol^{-1})
$\Delta_r H_{(l)}^0$	standard molar enthalpy change of reaction in liquid-phase (kJ mol^{-1})
$\Delta H_j, \Delta H_{\text{ads},j}$	adsorption enthalpy of compound j (kJ/mol)
$-H_0$	Hammet activity function
I_H	van't Hoff integration constant
I_K	Kirchoff equation integration constant
\hat{k}	intrinsic rate constant ($\text{mol h}^{-1}\text{g}^{-1}$)
\hat{k}^0	true rate constant without inhibiting effect of water ($\text{mol h}^{-1}\text{g}^{-1}$)
K_j	adsorption equilibrium constant of j
K_a^j	thermodynamic equilibrium constant of reaction j
K_γ^j	activity coefficients ratio of reaction j
K_Γ	Poynting correction factor
K_x^j	thermodynamic equilibrium constant of reaction j based on molar fractions
K_F	Freundlich constant
K_w	water correction factor
n	number of active sites
n_i	number of moles of compound i
N	stirring speed (rpm)
P	pressure
r_{DNPE}	reaction rate of DNPE synthesis ($\text{mol h}^{-1}\text{kg}^{-1}$)
r_{DNPE}^0	initial reaction rate of DNPE synthesis ($\text{mol h}^{-1}\text{kg}^{-1}$)
$r_{\text{DNPE,eq}}^0$	initial reaction rate of DNPE synthesis per sulfonic group ($\text{mol h}^{-1}\text{kg}^{-1}$)

7. Notation

R	gas constant (J mol ⁻¹ K ⁻¹)
S ⁰	liquid-phase molar entropy (J mol ⁻¹ K ⁻¹)
$\Delta_r S_{(l)}^0$	standard molar entropy change of reaction in liquid-phase (J mol ⁻¹ K ⁻¹)
ΔS_j	adsorption entropy of compound j (J mol ⁻¹ K ⁻¹)
S _{DNPE}	selectivity to DNPE (%)
S _{alkenes}	selectivity to alkenes (%)
S _{ethers}	selectivity to branched ethers (%)
S _{ext}	external surface area of zeolite H-Beta (m ² g ⁻¹)
S _g	surface area (m ² g ⁻¹)
S _{meso}	surface area of meso and macropores in H-Beta (m ² g ⁻¹)
SSQ	sum of squares of the lack of fit
t	time (h)
T	temperature (K)
T _{max}	maximum operating temperature of catalysts (K)
V _i	molar volume of compound <i>i</i>
V _g	pore volume (cm ³ g ⁻¹)
V _{meso}	pore volume relative to meso and macropores in H-Beta (cm ³ g ⁻¹)
V _{sp}	specific volume of the swollen polymer phase (cm ³ g ⁻¹)
V _μ	pore volume relative to micropores of zeolite H-Beta (cm ³ g ⁻¹)
W	weight of dry catalyst (g)
x _i	molar fraction of compound <i>i</i>
X _p	conversion of 1-pentanol (%)
Y _{DNPE}	DNPE yield

Greek letters

α	Freundlich factor
δ _M	solubility parameter of the medium
δ _P	solubility parameter of the resin
Φ _i	volume fraction for the pure component <i>i</i>
φ _P	volume fraction of the resin
γ _i	activity coefficient
v _i	stoichiometric coefficient of compound <i>i</i> .
ρ _s	skeletal density (g/cm ³)
θ	porosity

σ	active center
Ψ	solubility parameter correction factor

Subscripts

D	DNPE, di-n-pentyl ether
P	1-pentanol
1-pentene	refers to DNPE decomposition reaction to 1-pentanol and 1-pentene
2-pentene	refers to 1-pentene isomerization reaction to 2-pentene
W	water

Acronyms

BET	Brunauer, Emmet and Teller
CFPP	Cold filter plugging point
CP	Cloud point
DNHE	di-n-hexil ether
DNPE, D	di-n-pentil ether
DNPM	di-n-pentoxi methane
MOE	methyl octyl ether
CN	cetane number
P	1-pentanol
PP	Pour point
W	water



Chapter 8. Index of equations, tables and figures

Equations

Equation 1	Cetane Index	11
Equation 2	Calculated cetane index	11
Equation 3	Hammett acidity function	34
Equation 4	Adsorption rate	39
Equation 5	Desorption rate	39
Equation 6	Langmuir isotherm	39
Equation 7	Logarithmic function of the heat of adsorption	39
Equation 8	Freundlich isotherm	39
Equation 9	Temkin isotherm	40
Equation 10	Hildebrandt solubility parameter of the media	41
Equation 11	Reaction medium-resin affinity	42
Equation 12	Yang's inhibition factor	42
Equation 13	Limbeck's proposed model	42
Equation 14	Limbeck's inhibition factor	42
Equation 15	Du Toit proposed model	43
Equation 16	Particle's porosity in dry state	59
Equation 17	Particle's porosity swollen in water	59
Equation 18	Mass of a compound in the reactor	82
Equation 19	Moles of a compound in the reactor	82
Equation 20	Mole fraction of a compound in the reactor	82
Equation 21	Activity of a compound in the reactor	82
Equation 22	1-pentanol conversion	83
Equation 23	Selectivity to DNPE	83
Equation 24	Yield to DNPE	83
Equation 25	Corrected 1-pentanol conversion	83
Equation 26	Corrected selectivity to DNPE	83
Equation 27	Corrected selectivity to alkenes	83
Equation 28	Corrected selectivity to branched ethers	83
Equation 29	Computed reaction rate	84
Equation 30	Initial turnover number	84
Equation 31	Mass balance	84
Equation 32	General expression of the thermodynamic equilibrium constant	108
Equation 33	DNPE thermodynamic equilibrium constant on activity coefficient basis	108
Equation 34	1-pentene thermodynamic equilibrium constant on activity coefficient basis	108
Equation 35	2-pentene thermodynamic equilibrium constant on activity coefficient basis	108
Equation 36	DNPE thermodynamic equilibrium constant on molar fraction basis	109
Equation 37	1-pentene thermodynamic equilibrium constant on molar fraction basis	109
Equation 38	2-pentene thermodynamic equilibrium constant on molar fraction basis	109

Equation 39	Poynting's correction factor of pressure	113
Equation 40	Thermodynamic equilibrium related to thermodynamic properties I	114
Equation 41	Standard Gibb's energy change of reaction	114
Equation 42	Thermodynamic equilibrium related to thermodynamic properties II	114
Equation 43	T dependence of DNPE reaction equilibrium constant when ΔH constant	115
Equation 44	T dependence of 1-pentene reaction equilibrium constant when ΔH constant	115
Equation 45	T dependence of 2-pentene reaction equilibrium constant when ΔH constant	115
Equation 46	Kirchoff equation	116
Equation 47	Heat capacity polynomial function	117
Equation 48	Standard enthalpy change of reaction as function of T	117
Equation 49	Van't Hoff equation	117
Equation 50	Thermodynamic equilibrium constant as function of T	117
Equation 51	Standard entropy change of reaction as function of T	118
Equation 52	Standard Gibb's energy change of reaction as function of T	118
Equation 53	Experimental thermodynamic equilibrium constant	127
Equation 54	T dependence of fitted parameters	127
Equation 55	Best LHHW Kinetic model	131
Equation 56	Arrhenius-type T dependence of rate constant	133
Equation 57	True rate constant	141
Equation 58	Modified kinetic model with the solubility parameter	141
Equation 59	Modified kinetic model with the inhibition factor	145
Equation 60	Inhibition factor	145
Equation 61	Modified kinetic model with the Freundlich-type factor I	147
Equation 62	Freundlich-type factor	147
Equation 63	Modified kinetic model with the Freundlich-type factor II	148
Equation 64	Modified kinetic model with the Langmuir-type factor	150
Equation 65	Water adsorption constant	150
Equation 66	Calculated 1-pentene reaction rate expression	157
Equation 67	1-pentene kinetic expression	157
Equation 68	1-pentene modified kinetic expression	157
Equation 69	Impregnated Nafion percentage with respect to acidity	174
Equation 70	Impregnated Nafion percentage with respect to initial reaction rate	174
Equation 71	Impregnated Nafion percentage with respect to initial turnover number	174
Equation 72	Impregnation efficiency	175

Tables

Table 1. Examples of stocks used in formulating diesel fuels	10
Table 2. Low temperature operability additive benefits	14
Table 3. Evolution of standards fixed by the European Union over the last years	18
Table 4. Main exhaust gases and their effects	18
Table 5. Properties of some linear ethers	19
Table 6. DNPE improvement in Diesel properties	21
Table 7. Properties and structural parameters of perfluoroalkanesulfonic resins	52
Table 8. Composition of Nafion 5 wt.% solution	54
Table 9. Properties of S/DVB resins	55
Table 10. Mean d_p in different media and volume increase with respect to air	59
Table 11. Structural parameters of resins in dry state and swollen in water	60
Table 12. Physical and structural properties of the zeolite H-Beta	62
Table 13. Physical and structural properties of carriers	63
Table 14. X-ray fluorescence	63
Table 15. Organics and water content of carriers	64
Table 16. Retention time [min] of all species	67
Table 17. Scheme of the method of impregnation	73
Table 18. Operation conditions of the rotavapor	74
Table 19. Vapor pressures at 180°C	80
Table 20. Calibrating curves PeOH system	81
Table 21. Calibrating curves 1,4-dioxan system	82
Table 22. Working conditions: catalyst loading	85
Table 23. Results of catalyst loading experiments	85
Table 24. Working conditions: stirring speed	87
Table 25. Initial reaction rates [mol/(kg·h)] vs. N for all catalyst T=150°C	88
Table 26. Working conditions: catalyst particle size	90
Table 27. Working conditions: catalyst selection	94
Table 28. 1-pentanol conversion [%] vs. T at t = 6 h for all catalysts tested	95
Table 29. Selectivity to DNPE [%] vs. T at t = 6 h for all catalysts tested	96
Table 30. DNPE yield [%] vs. T at t = 6h for all catalysts tested	100
Table 31. Initial reaction rate [mol/(kg·h)] vs. temperature	101
Table 32. Hammet acidity function	102
Table 33. Turnover numbers [mol/(eq H ⁺ ·h)] vs. temperature	102
Table 34. Working conditions: 2-methyl-1-butanol influence	105
Table 35. Working conditions: equilibrium experiments	110
Table 36. Experimental conditions and obtained equilibrium constants of the dehydration of 1-Pentanol to DNPE and Water	111
Table 37. Experimental conditions and obtained equilibrium constants of DNPE decomposition reaction to 1-Pentanol and 1-Pentene	112

Table 38. Experimental conditions and obtained equilibrium constants of the isomerization of 1-Pentene to 2-Pentene.....	113
Table 39. Molar volumes of 1-pentanol, DNPE, water, 1-pentene and 2-pentene, and correction factors for the three reactions.....	114
Table 40. Standard enthalpy, entropy and free energy changes, when considered constant over the T range	115
Table 41. Thermochemical data of 1-pentanol, DNPE, water, 1-pentene and 2-pentene.....	117
Table 42. Temperature dependence relationship parameters of $K_{\Delta} \Delta H_{(l)}^0$, $\Delta S_{(l)}^0$, $\Delta G_{(l)}^0$ for the three reactions	118
Table 43. Standard enthalpy, entropy and free energy changes, when not considered constant over the T range	120
Table 44. Energy, entropy and enthalpy changes for DNPE synthesis.....	120
Table 45. $\Delta_r H_{(l)}^0$ and $\Delta_r S_{(l)}^0$ for some alkyl ethers computed from molar formation enthalpies and entropies	121
Table 46. Energy, entropy and enthalpy changes for 1-pentene reaction.....	122
Table 47. Energy, entropy and enthalpy changes for 1-pentanol monomolecular dehydration reaction.....	123
Table 48. Energy, entropy and enthalpy changes for 2-pentene reaction.....	123
Table 49. Kinetic models.....	128
Table 50. Kinetic models that fit experimental data satisfactorily.....	130
Table 51. Constant associations of.....	133
Table 52. Apparent activation energies [kJ/mol] for models 125, 126 and 127	134
Table 53. Activation energy found in literature for catalyst CT224	134
Table 54. $\Delta H_D - \Delta H_P$ and $\Delta S_D - \Delta S_P$ for models 125, 126 and 127	135
Table 55. Initial % wt. of water and DNPE tested.....	136
Table 56. r^0 vs. %water at 180°C	139
Table 57. Individual solubility parameters	142
Table 58. Fitted parameters of Model 125 with the solubility parameter	143
Table 59. Fitted parameters of model 125 with η	145
Table 60. Fitted parameters of Model 125 + Freundlich	147
Table 61. Fitted parameters of Model 113 + Freundlich	148
Table 62. Fitted parameters of Model 125 + Langmuir	151
Table 63. Fitting results comparison of all modified kinetic models.....	152
Table 64. Rate constants for model 125 and modified kinetic models	153
Table 65. Correlation matrix of fitted parameters for catalyst A-70	155
Table 66. Fitting results of Freundlich-type expression for all catalysts tested	156
Table 67. Fitted parameters, E_a and SSQ for 1-pentene and 2-pentene synthesis.....	158
Table 68. Measured densities of carriers tested	160
Table 69. Results of BET analysis	161
Table 70. Measured particle diameters.....	165
Table 71. Organic and water content	165

Table 72. Measured acidity.....	166
Table 73. List of impregnations.....	167
Table 74. Carrier properties and 1-pentanol conversion after 6 h at 180°C of derived catalysts via M-2170	
Table 75. I-8, I-9 and I-10 results compared to NR50 and SAC-13.....	174
Table 76. %Nafion supported for I-8, I-9 and I-10.....	175
Table 77. Effect of %Nafion on the impregnation of Si-A.....	176
Table 78. %Nafion supported for Si-A derived catalysts.....	176
Table 79. Effect of %Nafion on the impregnation of Si-C.....	177
Table 80. %Nafion supported for Si-C derived catalysts.....	178
Table 81. Results of BET analysis of impregnated catalysts.....	181
Table 82. Reproducibility of the method of impregnation.....	185
Table 83. %Nafion supported for replicated catalysts.....	185
Table 84. Results of BET analysis of replicated catalysts.....	185

Figures

Figure 1. Principal petroleum products, their boiling range temperatures and their number of carbon atoms	7
Figure 2. Cetane number improver: 2-ethylhexyl nitrate	12
Figure 3. Chemical structure of a detergent additive of the poly(isobutenyl succinimide) type (PIBSI type)	13
Figure 4. U.S. and European fuel consumption trends	17
Figure 5. Spanish fuel consumption trends	17
Figure 6. DNPE synthesis route	22
Figure 7. Structure of Faujasita Y	26
Figure 8. Styrene-divinylbenzene matrix	28
Figure 9. Schematic representation of the structure of a macroporous resin	29
Figure 10. General structure of Nafion	30
Figure 11. Stylized morphology of Nafion	30
Figure 12. Degradation of a S-DVB resin	33
Figure 13. Steps of the catalytic process	35
Figure 14. Equivalence of diverse adsorption equilibria	40
Figure 15. Swelling of Nafion NR50	52
Figure 16. SEM image of Nafion NR50	53
Figure 17. SEM image of SAC 13	54
Figure 18. Swelling of Amberlyst 70 in polar solvents	55
Figure 19. Swelling of Amberlyst 36wet in polar solvents	56
Figure 20. Swelling of Amberlyst DL-H/03 in polar solvents	56
Figure 21. Swelling of Amberlyst DL-I/03 in polar solvents	57
Figure 22. Swelling of CT224 in polar solvents	58
Figure 23. Swelling of Dowex 50WX4 in polar solvents	58
Figure 24. ISEC pattern displayed by resins in water	61
Figure 25. Scheme of the DNPE synthesis experimental setup	64
Figure 26. Picture of the experimental setup	65
Figure 27. Control parameters of the oven and the column of HP 6890 GC	66
Figure 28. Chromatographic report example	68
Figure 29. Impregnation setup	69
Figure 30. Distillation column	69
Figure 31. Evaporated water vs time. 100°C atmospheric oven, 3.945 g wet A70	70
Figure 32. General scheme of the experimental procedure	79
Figure 33. Effect of catalyst mass on reaction rate	86
Figure 34. Effect of catalyst mass on X_p at $t=6h$	86
Figure 35. Initial reaction rate vs. N ; $T=150^\circ C$, 1 g catalyst	88
Figure 36. Concentration and temperature profile in the external layer. Exothermic reaction	89
Figure 37. Dowex: r^0 vs. $1/d_p$ and T ; $N=500rpm$, 1 g catalyst	91

Figure 38. A70: r^0 vs. $1/dp$; $T=190^\circ\text{C}$; $N=500\text{rpm}$, 1 g catalyst	92
Figure 39. Nafion NR50 vs. N117. $T=180^\circ\text{C}$, $N=500\text{rpm}$, 1 g catalyst	93
Figure 40. X_p vs. time. A-36 as catalyst, 150°C	94
Figure 41. S_{alkenes} and S_{ethers} vs. T at $t = 6\text{h}$ for all catalysts tested	97
Figure 42. S_{DNPE} vs. V_{sp} , $T = 150^\circ\text{C}$, $t = 6\text{h}$	98
Figure 43. S_{DNPE} vs. θ , $T = 150^\circ\text{C}$ $t = 6\text{h}$	98
Figure 44. Initial reaction rate and turnover number at 150°C	103
Figure 45. Amount of ethers formed at $t=6\text{h}$ and 170°C with different initial 2-methyl-1-butanol concentrations	105
Figure 46. Amount of olefins formed at $t=6\text{h}$ and 170°C with different initial 2-methyl-1-butanol concentrations	106
Figure 47. Equilibrium activities of DNPE at different T	108
Figure 48. Evolution of activities during an experiment at 180°C over time	109
Figure 49. Evolution of the calculated equilibrium constant of an experiment at 180°C over time	110
Figure 50. $\ln K$ vs. $1/T$. Comparison between values obtained experimentally (■) and those predicted from Eq. 43, 44, 45 (-).....	116
Figure 51. $\ln K + f(T)$ vs. $1/T$. Comparison between values obtained experimentally (■) and those predicted from Eq. 50 (-).....	119
Figure 52. Kinetic analysis methodology.....	129
Figure 53. Corrected sum of squares of Class I – type 4 models.....	132
Figure 54. Model 125 estimated vs. experimental reaction rates	132
Figure 55. Model 125 estimated vs. experimental reaction rates at all temperatures for A70	136
Figure 56. Water and DNPE activities of experiments with catalyst A70	137
Figure 57. Initial reaction rate vs. water and DNPE activities at 160°C	138
Figure 58. Initial reaction rate vs. initial %wt. of water and DNPE at 160°C	138
Figure 59. Inhibitor effect of water at different temperatures.....	139
Figure 60. Model 125 estimated vs. experimental reaction rates of experiments	140
Figure 61. Reaction rate prediction of Model 125 modified with the solubility parameter vs. experimental reaction rates.....	143
Figure 62. Computed Ψ vs. a_w at different temperatures	144
Figure 63. Reaction rate prediction of model 125 modified with the Inhibition factor vs. experimental reaction rates.....	146
Figure 64. Computed η vs. a_w at different temperatures	146
Figure 65. Reaction rate prediction of model 125 modified with the Freundlich factor vs. experimental reaction rates.....	149
Figure 66. Computed Freundlich factor vs. a_w at different temperatures	150
Figure 67. Reaction rate prediction of Model 125 modified with the Langmuir factor vs. experimental reaction rates.....	151
Figure 68. Computed Langmuir factor vs. a_w at different temperatures.....	152
Figure 69. Residuals distribution for Amberlyst 70 fitting	155

Figure 70. Reaction rate prediction of the modified model vs. experimental reaction rates for 1-pentene and 2-pentene synthesis	158
Figure 71. Desorption pore distribution of carriers	164
Figure 72. Activity of impregnated catalysts via M-2 at 180°C	170
Figure 73. Improvement of method of impregnation 2 (M2)	171
Figure 74. Steps of the impregnation process at a pore-scale	172
Figure 75. Effect of washing on 1-pentanol conversion	173
Figure 76. Neutralization of sulfonic groups during impregnation	177
Figure 77. 1-pentanol conversion vs. %Nafion; t=6h, 180°C, 1g cat.	178
Figure 78. Impregnation efficiency vs. %Nafion	179
Figure 79. Turnover number vs. %Nafion	179
Figure 80. Effect of %Nafion increase at a pore-scale	180
Figure 81. Plots of BET analysis results for synthesized catalysts.....	182
Figure 82. Desorption pore distribution of Si-A derived catalysts.....	183
Figure 83. Desorption pore distribution of Si-C derived catalysts.....	184
Figure 84. Desorption pore distribution of replicated catalysts.....	186
Figure 85. Reaction rates of reused catalysts	187



Chapter 9. References

References

- [1] J.-P. Wauquier, **Crude oil, Petroleum Products, Process Flowsheets**, Editions Technip, Paris, (1995)
- [2] Y. Chevalier, B. Fixari, S. Brunel, E. Marie, P. De Guio; **Review: the adsorption of functional polymers from their organic solutions, applications to fuel additives**, *Polymer International* 53 (2004) 475-483
- [3] **Diesel Fuels Technical review**. Chevron Products company (1998)
- [4] <http://www.oxfordprinceton.com/newsletter/newsletter0105.html> 28/02/2006
- [5] <http://www.cores.es> **Boletín estadístico de hidrocarburos** 07/03/2006
- [6] S. Rossini, **The impact of catalytic material son fuel reformulation**, *Catalysis Today* 77 (2003) 467-484
- [7] C.L. Maccarthy, W.J. Slodowske, E.J. Sienichi, R.E. Jass, **Modifying diesel fuel emissions: lower aromatics content or higher cetane number?**, *Fuel Reformulation*, vol. 3 no 2 (march/april 1993), 34-39
- [8] R. Aga Van Zeebroeck, **Los combustibles de automoción a partir del año 2005**, *Ingeniería Química* (enero 2001)
- [9] A. Douaud, **Tomorrows Engines and fuels**, *Hydrocarbon Processing* 74 (2), (1995), 55
- [10] M. Marchionna, R. Patrini, D. Sanfilippo, A. Paggini, F. Giavazzi, L. Pellegrini, **From natural gas to oxygenates for cleaner diesel fuels**, *Studies in Surface Science and Catalysis*, 136 (*Natural Gas Conversion VI*), (2001) 489-494
- [11] I. Ahmed, **Oxygenated diesel: emissions and performance characteristics of etanol-diesel blends in compression ignition engines**, *Special Publication of the Society of Automotive Engineers SP-1635*, (2001), 29-34
- [12] G.C. Pecci, M.G. Clerici, M.G. Giavazzi, F. Ancillotti, M. Marchionna, R. Patrini, **Oxygenated diesel fuels. Part 1- Structure and properties correlation**, *IX International Symposium on Alcohol Fuels*, vol. 1, (1991), 321-326
- [13] F. Cunill, C. Fité, M. Iborra, J.F. Izquierdo, J. Tejero, **El DNPE como componente para el gasoil**, *Ingeniería Química* 33 (385), (diciembre 2001), 88-93
- [14] F. Giavazzi, D. Terna, D. Patrini, F. Ancillotti, G.C. Pecci, R. Trerè, M. Benelli, **Oxygenated diesel fuels. Part 2- Practical aspects of their use**, *IX International Symposium on Alcohol Fuels*, vol. 1, (1991), 327-335
- [15] M. Marchionna, R. Patrini, F. Giavazzi, G.C. Pecci, **Linear ethers as high quality components for reformulated diesel fuels**, *Symposium on removal of aromatics, sulfur and olefins from gasoline and diesel*, 212th National Meeting, American Chemical Society, Orlando, FL, (1996), 585-589
- [16] J. Van Heerder, J.J. Botha, P.N.J. Roets, **Improvement of diesel performance with the addition of linear ethers to diesel fuels**, *12th Int. Sym. Alcohol fuels*, 1, (1998) 188-199
- [17] B. Martin, P. Aakko, D. Beckman, N. Del Giacomo, F. Giavazzi, **Influence of fuel formulations on diesel engine emissions – A joint European study**. SAE paper 972966
- [18] J. Tejero, F. Cunill, M. Iborra, J.F. Izquierdo, C. Fité, **Dehydration of 1-pentanol to di-n-pentyl ether**

- over ion-exchange resin catalysts**, *Journal of molecular catalysis A: Chemical* 182-183 (2002) 541-554
- [19] D.C. Sherrington, P. Hodge, **Syntheses and separations using functional polymers**, J. Wiley & Sons, 1988
- [20] M.A. Harmer, Q. Sun, **Solid acid catalysis using ion-exchange resins**, *Applied catalysis A: General* 221 (2001) 45-52
- [21] J. Hagen, **Industrial Catalysis: a practical approach**, Wiley-VCH (1999) 155
- [22] J. Meurig Thomas, **Solid acid catalysts**, *Scientific American* (1992) 82-89
- [23] M. Guisnet, J-P. Wilson, **Zeolites for cleaner technologies**, **Catalytic Science Series – vol. 3**, Imperial Collage Press. (2002)
- [24] R. Kunin, R.J. Myers, **Ion-exchange resins**, New York (N.Y.), Wiley London, Chapman & Hall, cop. (1950)
- [25] F.G. Helfferich, **Ion exchange**, McGraw-Hill, New York (1962)
- [26] N.G. Polyanskii, V.K. Sapozhnikoz, **New advances in Catalysis by ion-exchange resins**, *Russian Chemical Reviews* (1977)
- [27] K. Jerabek, **Inverse steric exclusion chromatography as a tool for morphology characterization**, *ACS Symp. Ser. 635* (1996) 211-224
- [28] F.J. Waller, **Catalysis with a Perfluorinated Ion-Exchange Polymer**, *Polymeric Reagents and Catalysts, Chap. 3, ACS Symposium Series 308* (1986) 42-67
- [29] <http://www.psrc.usm.edu/mauritz/nafion.html> (March 20th 2006)
- [30] M.A. Harmer, W.E. Farneth, Q. Sun, **High surface Area Nafion Resin/Silica Nanocomposites: a new class of solid acid catalyst**, *Journal of the Americal Chemical Society* 118 (33), (1996)
- [31] B. Török, I. Kiricsi, A. Molnár, G.A. Olah, **Acidity and catalytic activity of a Nafion-H/silica nanocomposite catalyst compared with a silica-supported nafion sample**, *Journal of Catalysis* 193 (2000) 132-138
- [32] A. Heidekum, M.A. Harmer, W.F. Hoelderich, **Addition of carboxylic acids to cyclic olefins catalyzed by strong acidic ion-exchange resins**, *Journal of catalysis* 181, (1999) 217-222
- [33] J.R. Anderson, M. Boudart, **Catalysis. Science and Technology. Volume 2**. Springer-Verlag, (1981)
- [34] Ch. N. Satterfield, **Mass Transfer in Heterogeneous Catalysis**, M.I.T. PRESS, Massachusetts, (1970)
- [35] J.M. Smith, **Chemical Engineering Kinetics**, 3th Edition, McGraw-Hill International Edition Singapore (1981)
- [36] Ch. N. Satterfield, **Heterogeneous Catalysis in Industrial Practice**, 2n Edition reprinted, Krieger Publishing Company, Florida, (1996)
- [37] J. J. Carberry, **Chemical and Catalytic Reaction Engineering**, McGraw-Hill Chemical Engineering series, (1976)
- [38] G.D. Halsey, H.S. Taylor, **The adsorption of Hydrogen on Tungsten Powders**, *Journal of Chemical Physics* 15 (9) (1947) 624
- [39] S. Brunauer, K.S. Love, R.G. Keenan, **Adsorption of Nitrogen and the Mechanism of Ammonia Decomposition Over Iron Catalysts**, *Journal of American Chemical Society* 64 (1942) 751

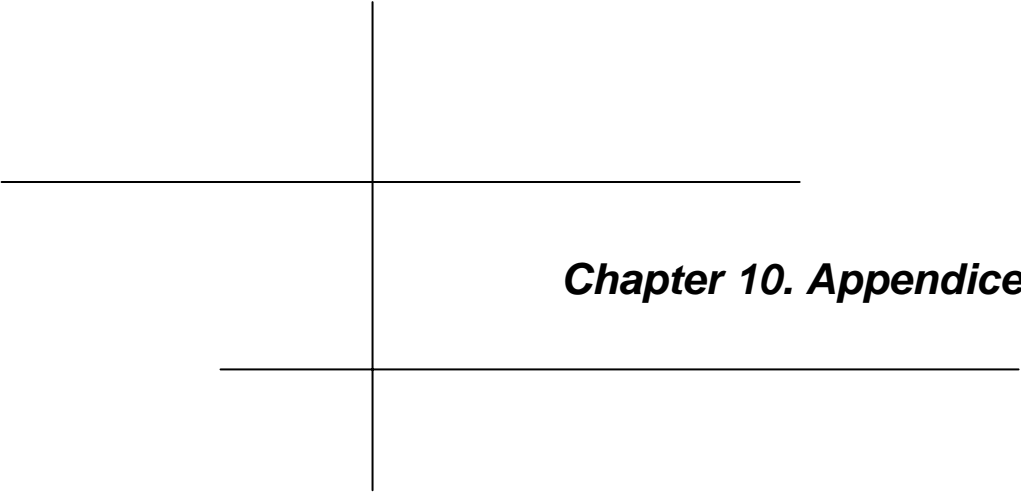
- [40] M. Boudart, **Kinetics on Ideal and Real Surfaces**, *AIChE Journal* 2 (1) (1956) 62-64
- [41] I. Hoek, T.A. Nijhuis, A.I. Stankiewicz, J.A. Moulijn, **Kinetics of solid acid catalysed etherification of symmetrical primary alcohols: zeolite BEA catalysed etherification of 1-octanol**, *Applied Catalysis A: General* 266 (2004) 109-116
- [42] F. Aiouache, S. Goto, **Kinetic study of 2-methyl-1-butanol dehydration catalysed by ion-exchange resin**, *Journal of Chemical Engineering of Japan* 35 (2002) 436-442
- [43] B. Sow, S. Hamoudi, M. H. Zahedi-Niaki, S. Kaliaguine, **1-butanol etherification over sulfonated mesostructured silica and organo-silica**, *Microporous and Mesoporous Materials* 79 (2005) 129-136
- [44] C. Fité, J. Tejero, M. Iborra, F. Cunill, J.F. Izquierdo, D. Parra, **The effect of the reaction medium on the kinetics of the liquid-phase addition of methanol to isobutene**, *Applied Catalysis A: General* 169 (1998) 165-177
- [45] L. K. Rihko-Struckmann, P. V. Latostenmaa, A. Outi, I. Krause, **Interaction between the reaction medium and an ion-exchange resin catalyst in the etherification of isoamylenes**, *Journal of Molecular Catalysis A: Chemical* 177 (2001) 41-47
- [46] V.J Cruz, R. Bingué, F. Cunill, J.F. Izquierdo, J. Tejero, M. Iborra, C. Fité, **Conversion, selectivity and kinetics of the liquid-phase dimerisation of isoamylenes in the presence of C1 to C5 alcohols catalysed by a macroporous ion-exchange resin**, *Journal of Catalysis* 238 (2006) 330-341
- [47] C. Fité, J. Tejero, M. Iborra, F. Cunill, J.F. Izquierdo, **Enhancing MTBE Rate Equation by Considering Reaction Medium Influence**, *AIChE JOURNAL* 44 (10) (1998) 2273-2279
- [48] C. Reichardt, **Solvents and Solvent Effects in Organic Chemistry**, VCH Weinheim (1988)
- [49] B.C. Gates, **Catalytic Chemistry**, Wiley New York (1992)
- [50] B-L Yang, M. Maeda, S. Goto, **Kinetics of Liquid Phase Synthesis of tert-Amyl Methyl Ether from tert-Amyl Alcohol and Methanol Catalyzed by Ion Exchange Resin**, *International Journal of Chemical Kinetics* 30 (2) (1998) 137-143
- [51] U. Limbeck, C. Altwicker, U. Kunz, U. Hoffmann, **Rate Expression for THF synthesis on acidic ion exchange resin**, *Chemical Engineering Science* 56 (2001) 2171-2178
- [52] E. du Toit, W. Nicol, **The rate inhibiting effect of water as a product on reactions catalysed by cation exchange resins: formation of mesityl oxide from acetone as case study**, *Applied Catalysis A: General* 277 (2004) 219-225
- [53] M.A. Harmer, W.E. Farneth, Q. Sun, **High Surface Area Nafion Resin/Silica Nanocomposite: A New Class of Solid Acid Catalyst**, *Journal American Chemical Society* 118 (33) (1996) 7708-7714
- [54] P. Botella, A. Corma, J.M. López-Nieto, **The influence of textural and compositional characteristics of Nafion/Silica composites on isobutane/2-butane alkylation**, *Journal of Catalysis* 185 (1999) 371-377
- [55] A.G. Ogston, **The Spaces in a Uniform Random Suspension of Fibres**, *Transactions of the Faraday Society* 54 (11) (1958) 1754
- [56] F. Collignon, M. Mariani, S. Moreno, M. Remy, G. Poncelet, **Gas phase synthesis of MTBE from methanol and isobutene over dealuminated zeolites**, *Journal of Catalysis* 166 (1997) 53
- [57] F. Collignon, G. Poncelet, **Comparative vapor phase synthesis of ETBE from ethanol and**

- isobutene over different acid zeolites**, *Journal of Catalysis* 202 (2001) 68
- [58] F. Collignon, R. Loenders, J.A. Martens, P.A. Jacobs, G. Poncelet, **Liquid phase synthesis of MTBE from methanol and isobutene over acid zeolites and amberlyst-15**, *Journal of Catalysis* 182 (1999) 302
- [59] M. Iborra, J. Tejero, C. Fité, F. Cunill, J.F. Izquierdo, **Zeolite-catalysed liquid-phase synthesis of isopropyl tert-butyl ether by the addition of 2-propanol to isobutene**, *Journal of Catalysis* 231 (2005) 77
- [60] A.A. Nikolopoulos, A. Kogelbauer, J.G. Goodwin Jr., G. Marcellin, **Effect of Dealumination on the Catalytic Activity of Acid Zeolites for the Gas-Phase Synthesis Of MTBE** *Applied Catalysis* 119 (1994) 69
- [61] M.A. Ali, B.J. Brisdon, W.J. Thomas, **Intrinsic kinetics of MTBE synthesis from methanol and isobutene using a synthesised MFI type zeolite**, *Applied Catalysis* 197 (2000) 303
- [62] M.J. Remy, G.A. Poncelet, **A New Approach to the Determination of the External Surface and Micropore Volume of Zeolites from the Nitrogen Adsorption-Isotherm at 77-K**, *Journal of Physical Chemistry* 99 (1995) 773
- [63] E.P. Barrett, L-G- Joyner, P.P. Halenda, **The Determination of Pore Volume and Area Distributions in Porous Substances. I. Computations from Nitrogen Isotherms**, *Journal of the American Chemical Society* 73 (1951) 373
- [64] R. Szostack, **Handbook of Molecular Sieves**, Van Nostrand Reinhold New York (1992)
- [65] S. Fisher, R. Kunin, **Routine exchange capacity determinations of ion-exchange resins**, *Analytical Chemistry* 27 (1955) 1191-1194
- [66] R. Wittig, J. Lohmann, **Vapor-Liquid Equilibria by UNIFAC Group Contribution. 6. Revision and Extension**, *Industrial and Engineering Chemistry Research* 42 (2003) 183-188
- [67] A. Rehfinger, U. Hofmann, **Kinetics Of Methyl Tertiary Butyl Ether Liquid-Phase Synthesis Catalyzed By Ion-Exchange Resin .1. Intrinsic Rate Expression In Liquid-Phase Activities**, *Chemical Engineering Science* 45 (6) (1990) 1605
- [68] B.C. Gates, W. Rodriguez, **General and specific acid catalysis in sulfonic acid resin**, *Journal of Catalysis* 31 (1973) 27
- [69] G.A. Olah, T. Shamma, G.K.S. Prakashm, **Catalysis by solid superacids .31. Dehydration of alcohols to ethers over Nafion-H, a solid perfluoroalkanesulfonic acid resin catalyst**, *Catalysis Letters* 46 (1997) 1
- [70] R. Banavali, **personal communication**
- [71] E.G. Lundquist, K. Beshah. *Presented at the 213th ACS National Meeting* San Francisco (2003)
- [72] A. Guyot, in: D.C. Sherrington, P. Hodge (Eds.), **Syntheses and Separations Using Polymers Supports**, Wiley Chichester (1988)
- [73] K. D. Topp, **personal communication**
- [74] D. Farcasiu, A. Ghenciu, G. Marino, K.D. Rose, **Strength of Solid Acids and Acids in Solution. Enhancement of Acidity of Centers on Solid Surfaces by Anion Stabilizing Solvents and Its Consequence for Catalysis**, *Journal of the American Chemical Society* 119 (1997) 11826

- [75] J.W. Beck, J.F. Haw, **Multinuclear NMR-Studies Reveal a Complex Acid Function for Zeolite-Beta**, *Journal of Physical Chemistry* 99 (1995) 1076
- [76] J.M. Smith, H.C. Van Ness, **Introduction to Chemical Engineering Thermodynamics**, 4th ed.; McGraw-Hill: Singapore (1987)
- [77] R.C. Reid, J.M. Prausnitz, B.E. Poling, **The Properties of Gases and Liquids**, 4th ed; McGraw-Hill (1987)
- [78] M.W. Chase Jr., **NIST-JANAF Thermochemical Tables**, Fourth Edition, *Journal of Physical and Chemical Reference Data Monograph* 9 (1998) 1-1951
- [79] C. Mosselman, H. Dekker, **Enthalpies of formation of n-alkan-1-ols**, *Journal of the Chemical Society, Faraday Transactions 1* (1975) 417-424
- [80] J.W. Murrin, S. Goldhagen, **Determination of the C-O bond energy from the heats of combustion of four aliphatic ethers**, *NAVORD Report No. 5491, U.S. Naval Powder Factory Research & Development Department* (1957) 1-14
- [81] K.B. Wiberg, D.J. Wasserman, E. Martin, **Enthalpies of hydration of alkenes. 2. The n-heptenes and n-pentenes**, *Journal of Physical Chemistry* 88 (1984) 3684-3688
- [82] J.F. Counsell, E.B. Lees, J.F. Martin, **Thermodynamic Properties of Organic Oxygen Compounds. Part XIX Low- Temperature Heat Capacity and Entropy of Propan-1-ol, 2-Methyl-propan- 1-ol, and Pentan-1-ol**, *Journal of the Chemical Society A* (1968) 1819.
- [83] S.P. Verevkin, **Improved Benson Increments for the Estimation of Standard Enthalpies of Formation and Enthalpies of Vaporization of Alkyl Ethers, Acetals, Ketals, and Ortho Esters**, *Journal of Chemical Engineering Data* 47 (2002) 1071-1097
- [84] J.F. Messerly, S.S. Todd, H.L. Finke, S.H. Lee-Bechtold, G.B. Guthrie, W.V. Steele, R.D. Chirico, **Heat capacities of pent-1-ene (10K to 320K), cis-hex-2-ene (10K to 330K), non-1-ene (10K to 400K), and hexadec-1-ene (10K to 400K)**, *Journal of Chemical Thermodynamics* 22 (1990) 1107-1128.
- [85] J. Chao, K.R. Hall, J.M. Yao, **Thermodynamic properties of simple alkenes**, *Thermochemica Acta* 64 (3) (1983) 285-303
- [86] G. Pilcher, A.S. Pell, D.J. Coleman, **Measurements of heats of combustion by flame calorimetry. Part 2-Dimethyl ether, methyl ethyl ether, methyl n-propyl ether, methyl isopropyl ether**, *Transactions of the Faraday Society* 60 (1964) 499-505
- [87] V. Majer, V. Svoboda, **Enthalpies of Vaporization of Organic Compounds: A Critical Review and Data Compilation**, *Blackwell Scientific Publications Oxford* (1985) 300
- [88] J. Chao, F.D. Rossini, **Heats of combustion, formation, and isomerization of nineteen alkanols**, *Journal of Chemical Engineering Data* 10 (1965) 374-379
- [89] H.G. Carlson, E.F. Westrum Jr., **Methanol: heat capacity, enthalpies of transition and melting, and thermodynamic properties from 5-300K**, *Journal of Chemical Physics* 54 (1971) 1464-1471
- [90] R.M. Kennedy, M. Sagenkahn, J.G. Aston, **The heat capacity and entropy, heats of fusion and vaporization, and the vapor pressure of dimethyl ether. The density of gaseous dimethyl ether**, *Journal of the American Chemical Society* 63 (1941) 2267-2272
- [91] J.B. Pedley, R.D. Naylor, S.P. Kirby, **Thermochemical Data of Organic Compounds**, *Chapman and*

Hall, New York (1986) 1-792

- [92] O. Haida, H. Suga, S. Seki, **Calorimetric study of the glassy state. XII. Plural glass-transition phenomena of ethanol**, *Journal of Chemical Thermodynamics* 9 (1977) 1133-1148
- [93] J.F. Counsell, D.A. Lee, J.F. Martin, **Thermodynamic properties of organic oxygen compounds. Part XXVI. Diethyl ether**, *Journal of the Chemical Society A* (1971) 313-316
- [94] M. Colomina, A.S. Pell, H.A. Skinner, D.J. Coleman, **Heats of combustion of four dialkylethers**, *Transactions of the Faraday Society* 61 (1965) 2641
- [95] R.J.L. Andon, J.F. Counsell, D.A. Lee, J.F. Martin, **Thermodynamic properties of organic oxygen compounds. 39. Heat capacity of n-propyl ether**, *Journal of Chemical Thermodynamics* 7 (1975) 587-592
- [96] H.A. Gundry, D. Harrop, A.J. Head, G.B. Lewis, **Thermodynamic properties of organic oxygen compounds. 21. Enthalpies of combustion of benzoic acid, pentan-1-ol, octan-1-ol, and hexadecan-1-ol**, *Journal of Chemical Thermodynamics* 1 (1969) 321-332
- [97] C.N. Hinshelwood, **The kinetics of chemical change**, Clarendon, Oxford (1940)
- [98] O.A. Hougen, K.M. Watson, **Chemical Process Principles, part 3. Kinetics and catalysis**, J. Wiley and Sons, New York (1947)
- [99] F. Cunill, J. Tejero, C. Fité, M. Iborra, J.F. Izquierdo, **Conversion, selectivity, and kinetics of the dehydration of 1-pentanol to Di-n-pentyl ether catalyzed by a microporous ion-exchange resin** *Industrial and Engineering Chemical Research* 44 (2005) 318
- [100] J. Tejero, C. Fité, M. Iborra, J.F. Izquierdo, R. Bringué, F. Cunill, **Dehydration of 1-pentanol to Di-n-pentyl ether catalyzed by a microporous ion-exchange resin with simultaneous water removal**, *Applied Catalysis A: General* 308 (2006) 223-230
- [101] A.W. Adamson, **Physical Chemistry of Surface**, Fifth Edition Wiley, N.Y. (1990) 421-26.
- [102] M. Iborra, J. Tejero, F. Cunill, J.F. Izquierdo, C. Fité, **Drying of acidic macroporous styrene-divinylbenzene resins with 12-20% cross-linking degree**, *Industrial and Engineering Chemical Research* 39 (2000) 1416
- [103] S. Wang, J.A. Guin, **Si-MCM41 supported sulfated zirconia and Nafion for ether production**, *Energy and Fuels* 15 (2001) 666-670
- [104] F. Frusteri, L. Spadaro, C. Espro, A. Parmaliana, F. Arena, **Liquid-phase selective oxidation of propane on silica-supported nafion catalysts**, *Journal of Natural Gas Chemistry* 11 (2002) 180-185
- [105] B. Rác, G. Mulas, A. Csongrádi, K. Lóki, A. Molnár, **SiO₂-supported dodecatungstophosphoric acid and Nafion-H prepared by ball-milling for catalytic application**, *Applied Catalysis A: General* 282 (2005) 255-265
- [106] J.F. Counsell, J.L. Hales, J.F. Martin, **Thermodynamic properties of organic oxygen compounds. Part 16. Butyl alcohol**, *Transactions of the Faraday Society* 61 (1965) 1869-1875.



Chapter 10. Appendices

Appendix I. Specifications of diesel fuel (class A)

Characteristics	Units	Limits (1)		Test methods		
		Minimum	Maximum	EN 590 (2)	ASTM (5)	UNE (5)
Cetane Number		51,0	-	EN ISO 5165	D-613	UNE EN ISO 5165
Cetane Index		46,0	-	EN ISO 4264	D 4737	UNE EN ISO 4264
Density at 15°C	kg/m ³	820	845	EN ISO 3675 EN ISO 12185	D 4052	UNE EN ISO 3675 UNE EN ISO 12185
Polycyclic Aromatic hydrocarbons (3)	%m/m	-	11	EN ISO 12916		UNE EN 12916
Sulphur content (4)	mg/kg	-	50	EN ISO 20846 EN ISO 20847 EN ISO 20884		UNE EN ISO 20846 UNE EN ISO 20847 UNE EN ISO 20884
Distillation:	°C			EN ISO 3405	D 86	UNE EN ISO 3405
65% recovered		250				
85% recovered			350			
95% recovered			360			
Kinematic viscosity at 40 °C	mm ² /s	2,00	4,50	EN ISO 3104	D 445	UNE EN ISO 3104
Flash point	°C	above 55		EN ISO 2719	D 93	UNE EN ISO 2719
Cold filter plugging point:	°C			EN 116		UNE EN 116
Winter (1 st Oct.-31 st March)		-	-10			
Summer (1 st April-		-	0		-	

Appendix I. Specifications of diesel fuel (Class A)

30 th Sept.)						
Carbon residue (on 10% v/v distillation residue)	%m/m	-	0,30	EN ISO 10370	D 4530	UNE EN ISO 10370
Lubricity, (corrected WSD 1.4) at 60°C	µm	-	460	EN ISO 12156-1		UNE EN ISO 12156-1
Water content	mg/kg	-	200	EN ISO 12937		UNE EN ISO 12937
Total contamination (solid particles)	mg/kg	-	24	EN ISO 12662		UNE EN 12662
Ash content	%m/m	-	0,01	EN ISO 6245	D 482	UNE EN ISO 6245
Copper strip corrosion (3 h. at 50 °C)	scale	-	class 1	EN ISO 2160	D 130	UNE EN ISO 2160
Oxidation stability	g/m ³	-	25	EN ISO 12205	D 2274	UNE EN ISO 12205
Colour			2		D 1500	
Transparency and gloss		Complies			D 4176	
Additives	Regulated by the Orden del Ministerio de la Presidencia PRE/1724/2002, July 5 th , modified by the Orden del Ministerio de la Presidencia PRE/3493/2004, October 22 nd .					

Notes:

- (1) Values shown in the specifications are real values. In order to determine the limits, the document EN ISO 4259 *Petroleum products - Determination and application of precision data in relation to methods of test* has been followed.
- (2) Other technically equivalent test methods are admissible subject to CLH approval. If there is any dispute the criteria on methods referred to in the EN 590 standard are to be followed, as well as the criteria for interpreting results for cases of discrepancies laid down in the aforesaid standard.
- (3) The difference between total aromatic hydrocarbons and monoaromatic hydrocarbons, both determined using the IP 391 method, is defined as polycyclic aromatic hydrocarbons.
- (4) Method EN ISO 20847 will not be used. To determine until 10 ppm of sulphur content, methods EN ISO 20846 y EN ISO 20884 will be used, it doesn't matter which.
- (5) Test methods will be the latest published

Appendix II. Modified UNIFAC-Dortmund method

Thermodynamic properties of pure fluids and of mixtures can be predicted with the help of group contribution methods. The group contribution concept has a great advantage, in that, although there are thousands of chemical compounds of industrial interest, the number of required functional groups to describe the thermodynamic behavior of these compounds (mixtures) is much smaller.

The group contribution method Modified UNIFAC (Dortmund) is a g^E model, which allows the prediction of liquid phase activity coefficients γ_i in nonelectrolyte systems, as a function of temperature and composition. The activity coefficient is calculated as the sum of a combinatorial part ($\ln \gamma_i^C$) and a residual part ($\ln \gamma_i^R$):

$$\ln \gamma_i = \ln \gamma_i^C + \ln \gamma_i^R$$

The combinatorial part represents the contribution of the excess entropy, which results from the different sizes and shapes of the molecules considered. The residual part represents the contribution of the excess enthalpy, which is caused by energetic interaction between the molecules. The temperature-independent combinatorial part is calculated with the help of the van der Waals volume (R_k) and surface area (Q_k) values of the functional groups.

$$\ln \gamma_i^C = 1 - V_i + \ln(V_i^*) - 5q_i \left[1 - \frac{V_i}{F_i} + \ln\left(\frac{V_i}{F_i}\right) \right]$$

with

$$V_i^* = \frac{r_i^{3/4}}{\sum_j x_j f_j^{3/4}} \quad V_i = \frac{r_i}{\sum_j x_j f_j} \quad F_i = \frac{q_i}{\sum_j x_j q_j}$$

The relative van der Waals volume (r_i) and surface area (q_i) values of molecule i can be calculated from the known van der Waals properties R_k and Q_k of the structural groups k .

$$r_i = \sum_k v_k^{(i)} R_k \quad q_i = \sum_k v_k^{(i)} Q_k$$

The residual part can be obtained using group activity coefficients of the groups k in the mixture (Γ_k) and for the pure compounds ($\Gamma_k^{(i)}$) (solution of the groups concept):

$$\ln \gamma_i^R = \sum_k v_k^{(i)} (\ln \Gamma_k - \ln \Gamma_k^{(i)})$$

The concentration dependence of the group activity coefficient Γ_k is defined as follows:

$$\ln \Gamma_k = Q_k \left(1 - \ln \left(\sum_m \Theta_m \Psi_{mk} \right) - \sum_m \frac{\Theta_m \Psi_{km}}{\sum_n \Theta_n \Psi_{nm}} \right)$$

with the surface fraction Θ_m , and the molar fraction X_m of group m :

$$\Theta_m = \frac{Q_m X_m}{\sum_n Q_n X_n} \quad X_m = \frac{\sum_j v_m^{(j)} x_j}{\sum_j \sum_n v_n^{(j)} x_j}$$

The temperature dependence of the group interaction parameter Ψ_{nm} is described by,

$$\Psi_{nm} = \exp \left(- \frac{a_{nm} + b_{nm} T + c_{nm} T^2}{T} \right)$$

The values of the parameters used in this work are shown in the following tables:

Group	Main group	Subgroup	R_k	Q_k
CH ₃	1	1	0.6325	1.0608
CH ₂	1	2	0.6325	0.7081
CH	1	3	0.6325	0.3554
CH ₂ =CH	2	5	1.2832	1.6016
CH=CH	2	6	1.2832	1.2489
OH _p	5	14	1.2302	0.8927
OH _s	5	81	1.063	0.8663
H ₂ O	7	16	1.7334	2.4561
CH=O	10	20	0.7173	0.771
CH ₂ -O-	13	25	1.1434	1.2495
CH-O-	13	26	1.1434	0.8968
c-CH ₂ OCH ₂	43	27	1.7023	1.8784

Table A-II 1. Relative van der Waals volume, R_k , and surface area, Q_k , of subgroup k

Main group	a_{mn}	b_{mn}	c_{mn}	
1--1	0	0	0	1
1--2	189.66	-0.2723	0	0.863953
1--5	2777	-4.674	0.001551	0.115666
1--7	1391.3	-3.6156	0.001144	1.027276
1--10	875.85	0	0	0.144742
1--13	233.1	-0.3155	0	0.819633
1--43	79.507	0.7089	-0.0021	1.068606
2--1	-95.418	0.06171	0	1.160506
2--2	0	0	0	1
2--5	2649	-6.508	0.004822	0.218093
2--7	778.3	0.1482	0	0.154783
2--10	476.25	0	0	0.349596
2--13	733.3	-2.509	0	2.43701
2--43	-322.1	-0.2037	0.004517	0.322267
5--1	1606	-4.746	0.000918	2.194343
5--2	1566	-5.809	0.005197	0.998172
5--5	0	0	0	1
5--7	-801.9	3.824	-0.00751	3.85967
5--10	-281.4	2.379	-0.00667	3.538103
5--13	816.7	-5.092	0.00607	1.714474
5--43	401.89	-0.4363	-0.002	1.580169
7--1	-17.253	0.8389	0.000902	0.298313
7--2	-1301	4.072	0	0.300897
7--5	1460	-8.673	0.01641	0.137369
7--7	0	0	0	1
7--10	-1545	6.512	0	0.044935
7--13	-197.5	0.1766	0	1.295942
7--43	54.962	-2.585	0.008218	0.283576
10--1	256.21	0	0	0.568134
10--2	202.49	0	0	0.63964
10--5	1590	-24.57	0.06212	0.000835
10--7	512.6	-2.145	0	2.756074
10--10	0	0	0	1
10--13	209	-0.6241	0	1.1769
10--43	-62.857	0.2898	0	0.859771
13--1	-9.654	-0.03242	0	1.055194
13--2	-844.3	2.945	0	0.338978
13--5	650.9	-0.7132	0.00082	0.334616

Appendix II. Modified UNIFAC-Dortmund method

13--7	140.7	0.05679	0	0.692613
13--10	235.7	0.1314	0	0.521244
13--13	0	0	0	1
13--43	-124.33	-0.294	0	1.765384
43--1	186.71	-1.3546	0.002402	0.86425
43--2	1182.6	-5	0.003745	2.000148
43--5	-238.36	5	-0.00819	0.465563
43--7	843.09	-2.635	0.000704	1.576919
43--10	80.038	-0.1012	0	0.927348
43--13	561.14	-0.7058	0	0.58713
43--43	0	0	0	1

Table A-II 2. Calculation of the group interaction parameter

Appendix III. Methods used for estimating physical properties

In Table A-III 1 the physical properties of the chemicals used in this work are shown. Some of them are experimental values found in the open literature, but others have been estimated by means of the methods explained below.

	PeOH	DNPE	Water	1-pentene	cis-2-pentene	trans-2-pentene
T_c [K]	588.2	626.19	647.3	464.8	476	475
P_c [atm]	39.1	20.8	221.2	35.3	36.5	36.6
V_c [cm ³ /mol]	326	613.5	57.1	300		
T_b [K]	411.1	460.15	373.2	303.1	310.1	309.5
ω	0.579	0.594	0.344	0.233	0.251	0.259
Dipm [debye]	1.7		1.8	0.4		
ϵ_r (298K)	13.9	3.1 ^{288K}	78.30	2.1 ^{293K}		
ρ (293K) [kg/m ³]	815	787	998	640	656	649
M [g/mol]	88.150	158.32	18.015	70.135	70.135	70.135
ΔH_v (25°C) [kJ/mol]	57.04	55.49	43.99	29.82	25.35	25.14

Table A-III 1. Physical properties of chemicals used

1. CRITICAL PROPERTIES

Critical properties for 1-pentanol, DNPE, water, 1-pentene and 2-pentene were found in the literature [79], while the Joback's method was used to estimate the ones of DNPE.

Joback's method

This group contribution method was used to estimate the critical properties of DNPE which were not found in the open literature.

$$T_b = 198 + \Delta_{T_b}$$

$$T_c = T_b \left[0.584 + 0.965 \cdot \sum \Delta_{T_c} - \left(\sum \Delta_{T_c} \right)^2 \right]^{-1}$$

$$P_c = \left(0.113 + 0.0032 \cdot n_A - \sum \Delta_P \right)$$

$$V_c = 17.5 + \sum \Delta_V$$

where $n_A = 33$ (for DNPE) is the molecule number of atoms.

	number	Δ_{T_b}	Δ_{T_c}	Δ_P	Δ_V
CH ₃ -	2	23.58	-0.0012	65	65
-CH ₂ -	8	22.88	0	56	56
-O-	1	22.42	0.0015	18	18

Table A-III 2. Parameters of Joback's group contribution method for DNPE

2. VAPOR PRESSURE

For DNPE and 1-pentanol the Antoine equation, which is a fit of experimental data, was used:

$$\log P_v = A - \frac{B}{T + C}$$

where P_v is the vapor pressure [bar], and T is the temperature [K].

	A	B	C	T range [K]
DNPE	3.87144	1396.465	-98.829	378.61-459.90
PeOH	4.32418	1297.689	-110.669	347.91-429.13
PeOH	3.97383	1106.11	-134.578	437.79-513.79

Table A-III 3. Antoine equation parameters

For water, 1-pentene and cis/trans-2-pentene the Wagner equation [79], which is also a fit of experimental data, was used:

$$\ln \left(\frac{P_v}{P_c} \right) = \frac{A \cdot x + B \cdot x^{1.5} + C \cdot x^3 + D \cdot x^6}{1 - x}$$

$$\text{where } x = 1 - \frac{T}{T_c}$$

P_c and T_c are the critical pressure and temperature.

	A	B	C	D	T range [K]
Water	-7.76451	1.45838	-2.77580	-1.23303	275 - T _c
1-pentene	-7.04875	1.17813	-2.45105	-2.21727	190 - T _c
cis-2-pentene	-6.80160	0.54458	-1.55279	-5.68029	275 - T _c
trans-2-pentene	-6.99461	1.00724	-2.42146	-2.51692	274 - T _c

Table A-III 4. Wagner equation parameters

3. ACENTRIC FACTOR

The acentric factor is computed as follows:

$$\omega = -\log P_{v_p} \text{ (at } T_r = 0.7) - 1$$

4. MOLAR VOLUME

To compute the molar volume at different temperatures, the extension of the HBT (Hankinson-Brost-Thomson) technique proposed by Thomson et al. [AIChE J., 28:671 (1982)] was used.

$$V = V_s \left(1 - c \cdot \ln \frac{\beta + P}{\beta + P_{vp}} \right)$$

$$\beta / P_c = -1 + a(1 - T_r)^{1/3} + b(1 - T_r)^{2/3} + d(1 - T_r) + e(1 - T_r)^{4/3}$$

where

a = -9.070217	f = 4.79594	j = 0.0861488
b = 62.45326	g = 0.250047	k = 0.0344483
d = -135.1102	h = 1.14188	

$$c = j + k \cdot \omega_{SRK}$$

$$e = \exp(f + g \cdot \omega_{SRK} + h \cdot \omega_{SRK}^2)$$

where

	PeOH	DNPE	Water	1-pentene	cis-2-pentene	trans-2-pentene
ω_{SRK}	0.5975	0.594	0.3852	0.2824	0.2039	0.2399

When ω_{SRK} is not available (DNPE),

$$\bar{\omega}_{SRK} \approx \omega$$

To estimate saturated volumes the Rackett technique and later modified by Spencer and Danner was used:

$$V_s = \frac{RT_c}{P_c} Z_{RA}^{[1+(1-T_r)^{2/7}]}$$

where

	PeOH	DNPE	Water	1-pentene	cis-2-pentene	trans-2-pentene
Z_{RA}	0.2596	0.2367	0.2338	0.2899	0.2671	0.2704

When Z_{RA} is not available (DNPE),

$$Z_{RA} = 0.29056 - 0.08775 \cdot \omega$$

The temperature dependence of the enthalpy of vaporization was computed by the Watson relation:

$$\Delta H_{v,T_2} = \Delta H_{v,T_1} \left(\frac{1-T_{r_2}}{1-T_{r_1}} \right)^{0.375}$$

Appendix IV. Thermochemical data

In Table A-IV 1 the experimental thermochemical data with their references are shown.

	$\Delta_f H_m^0$ (kJ/mol)	Ref.	S_m^0 (J mol ⁻¹ K ⁻¹)	Ref.
Methanol	-239.5 ± 0.2	90	127.19	91
Ethanol	-277 ± 0.3	93	159.86	94
Propanol	-302.6 ± 0.25	81	192.8	84
Butanol	-327 ± 0.28	81	225.73	106
Pentanol	-351.62 ± 0.5	81	258.9	84
DME ^a	-203.4 ± 0.5	88, 89	146.57	92
DEE	-271.2 ± 1.9	82	253.5	95
DNPrE	-328.8 ± 0.88	96	323.9	97
DNBE	-378 ± 1	96	N/A	-
DNPE	-435.2 ± 3	82	N/A	-
Water	-285.83 ± 0.04	80	69.95	80
1-pentene	-46.94 ± 0.42	83	262.6	86
2-pentene	-58.24 ± 0.42	83	256.8	87

^a Computed from gas phase data; N/A not available

Table A-IV 1. Experimental thermochemical data

S_m^0 for DNPE was estimated by means of the Benson group contribution method [79]:

Group	Number	Δ_s
C-(C)(H ₃)	2	127.32
C-(C) ₂ (H ₂)	6	39.44
C-(O)(H ₂)(C)	2	41.03
O-(C) ₂	1	36.34
$\sigma_{int} = 3 \times 3 = 9; \sigma_{ext} = 2; \sigma = 9 \times 2 = 18$		609.68

Table A-IV 2. Benson parameters for DNPE

$$S_g^0(298K) = 609.68 - (8.314) \ln 18 = 585.65 \text{ J/(mol K)}$$

By means of an improved Benson contribution group method, the enthalpy of vaporization can be computed in 55.49 kJ/mol [85], so the molar entropy of DNPE in the liquid phase is:

$$S_m^0(298.15K) = 585.65 - \frac{55.49 \times 1000}{298.15} = 399.44 \frac{J}{molK}$$

Shomate equation (water)

The Shomate equation is used to fit experimental data concerning thermochemical data of water [80] in the temperature range 298-500K:

$$c_{p,l}^0 = A + B \frac{T}{1000} + C \left(\frac{T}{1000} \right)^2 + D \left(\frac{T}{1000} \right)^3 + E \left(\frac{T}{1000} \right)^4 \quad J/molK$$

$$H^0 - H_{298.15}^0 = A \frac{T}{1000} + \frac{B}{2} \left(\frac{T}{1000} \right)^2 + \frac{C}{3} \left(\frac{T}{1000} \right)^3 + \frac{D}{4} \left(\frac{T}{1000} \right)^4 + F - H - E \frac{1000}{T} \quad kJ/mol$$

$$S^0 = A \ln \left(\frac{T}{1000} \right) + B \frac{T}{1000} + \frac{C}{2} \left(\frac{T}{1000} \right)^2 + \frac{D}{3} \left(\frac{T}{1000} \right)^3 - \frac{E}{2} \left(\frac{1000}{T} \right)^2 + G \quad J/molK$$

where T is in Kelvin.

A	-203.6060	E	3.855326
B	1523.290	F	-256.5478
C	-3196.413	G	-488.7163
D	2474.455	H	-285.8304
Table A-IV 3. Shomate equation parameters for water			

Estimation methods of the heat capacity

Rowlinson-Bondi method (1-pentanol) [79]

$$\frac{c_{p,L} - c_{p,g}^0}{R} = 1.45 + 0.45(1-T_r)^{-1} + 0.25\omega \left[17.11 + 25.2 \frac{(1-T_r)^{1/3}}{T_r} + 1.742(1-T_r)^{-1} \right] \left(\frac{J}{molK} \right)_v$$

valid for $T_r < 0.99$

where $c_{p,g}^0$ is the ideal gas heat capacity, $T_r = T/T_c$, T_c is the critical temperature and ω is the acentric factor.

Lyman-Dannen method (1-pentene and 2-pentene) [79]

$$c_{sat,L} - c_{p,g}^0 = A_1 + (A_2 + A_3 \bar{R})T_r + (A_4 + A_5 \bar{R})T_r^5 + A_6 \frac{\bar{R}^2}{T_r^2} + A_7 \frac{\bar{R}}{T_r^3} + \frac{A_8}{T_r^5} \\ + \kappa (B_1 + B_2 T_r^2 + B_3 T_r^5) + \kappa^2 (B_4 + B_5 T_r^2) \\ - \ln P_c - C_n (1 - T_{br}^{-1}) + D_n \ln T_{br} - 0.4218 \left(\frac{1}{P_c T_{br}^2} - 1 \right) \\ \kappa = \frac{- \ln P_c - C_n (1 - T_{br}^{-1}) + D_n \ln T_{br} - 0.4218 \left(\frac{1}{P_c T_{br}^2} - 1 \right)}{1 - T_{br}^{-1} - \ln T_{br}} \\ C_n = 4.6773 + 1.8324 \bar{R} - 0.03501 \bar{R}^2 \\ D_n = 0.7751 C_n - 2.6354$$

where $c_{sat,L}$ is the saturation heat capacity and $T_{br} = T_b/T_c$. Its relation with the constant pressure heat capacity, $c_{p,L}$, and the heat capacity, $c_{\sigma,L}$, is:

$$\frac{c_{\sigma,L} - c_{sat}}{R} = \exp(8.655T_r - 8.385) \quad \text{for } 0.8 < T_r < 0.99$$

$$\frac{c_{p,L} - c_{\sigma,L}}{R} = \exp(20.1T_r - 17.9) \quad \text{for } T_r < 0.8 \quad c_{\sigma,L} \approx c_{sat} \approx c_{p,L}$$

A₁	10.1273	A₂	-15.3546
A₃	3.2008	A₄	19.7302
A₅	-0.8949	A₆	-0.01489
A₇	0.2241	A₈	-0.04342
B₁	0.31446	B₂	2.5346
B₃	-2.0242	B₄	-0.07055
B₅	0.07264		

Table A-IV 4. Lyman-Dannen equation parameters

For every chemical, the radius of gyration of fluid, \bar{R} and the association factor should be available.

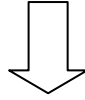
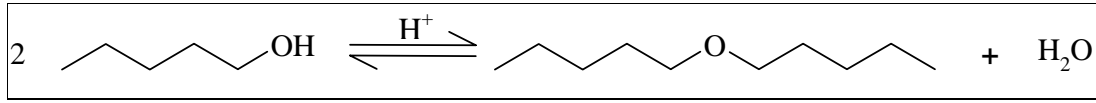
	\bar{R}	κ
1-pentene	3.1956	1.1055
2-pentene*	3.2826	-0.3495

***trans-2-pentene values**

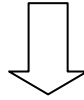
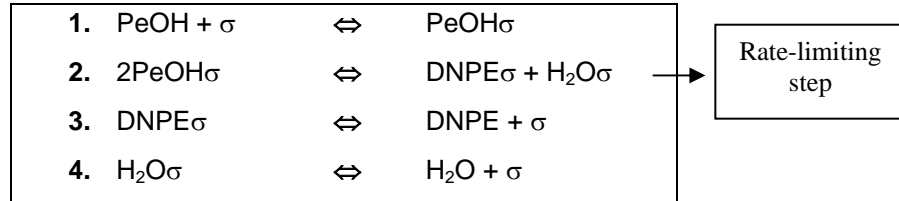
Table A-IV 5. Radius of gyration of fluid and association factor for 1-pentene and 2-pentene

Appendix V. General kinetic equation

Main Reaction



Reaction mechanism



Rate equations of the elemental steps

$$\begin{aligned} r_1 &= k_{a,P} \left(a_P \cdot \hat{c}_\sigma - \frac{\hat{a}_P}{K_{a,P}} \right) \\ r_2 &= \hat{k} \cdot \hat{a}_P^2 - \hat{k}' \cdot \hat{a}_D \cdot \hat{a}_A \\ r_3 &= k_{a,D} \left(\frac{\hat{a}_D}{K_{a,D}} - a_D \cdot \hat{c}_\sigma \right) \\ r_4 &= k_{a,A} \left(\frac{\hat{a}_A}{K_{a,A}} - a_A \cdot \hat{c}_\sigma \right) \end{aligned}$$

By definition, all the steps but the rate-limiting one reach a pseudo-equilibrium state, so their rates are equal to zero:

$$\begin{aligned} r_1 = k_{a,P} \left(a_P \cdot \hat{c}_\sigma - \frac{\hat{a}_P}{K_{a,P}} \right) &\Rightarrow \left(a_P \cdot \hat{c}_\sigma - \frac{\hat{a}_P}{K_{a,P}} \right) \rightarrow 0 \Rightarrow \hat{a}_P = K_{a,P} \cdot a_P \cdot \hat{c}_\sigma \\ r_3 = k_{a,D} \left(\frac{\hat{a}_D}{K_{a,D}} - a_D \cdot \hat{c}_\sigma \right) &\Rightarrow \left(\frac{\hat{a}_D}{K_{a,D}} - a_D \cdot \hat{c}_\sigma \right) \rightarrow 0 \Rightarrow \hat{a}_D = K_{a,D} \cdot a_D \cdot \hat{c}_\sigma \\ r_4 = k_{a,A} \left(\frac{\hat{a}_A}{K_{a,A}} - a_A \cdot \hat{c}_\sigma \right) &\Rightarrow \left(\frac{\hat{a}_A}{K_{a,A}} - a_A \cdot \hat{c}_\sigma \right) \rightarrow 0 \Rightarrow \hat{a}_A = K_{a,A} \cdot a_A \cdot \hat{c}_\sigma \end{aligned}$$

The total active site concentration is the sum of the ones occupied by the species plus the vacant ones. So,

$$\hat{C}_T = \hat{C}_\sigma + \hat{C}_P + \hat{C}_D + \hat{C}_A \Rightarrow \hat{C}_\sigma = \frac{\hat{C}_T}{1 + K_{a,P} \cdot a_P + K_{a,D} \cdot a_D + K_{a,A} \cdot a_A}$$

The thermodynamic equilibrium constant is defined as follows:

$$K = \frac{a_{D,eq} a_{A,eq}}{a_{P,eq}^2} = \frac{\left(\frac{a_D}{\hat{C}_\sigma K_{a,D}}\right)_{eq} \cdot \left(\frac{a_A}{\hat{C}_\sigma K_{a,A}}\right)_{eq}}{\left(\frac{a_P^2}{\hat{C}_\sigma^2 K_{a,P}^2}\right)_{eq}} = \left[\frac{a_D a_A}{a_P^2}\right]_{eq} \cdot \frac{K_{a,P}^2}{K_{a,D} \cdot K_{a,A}} = K \cdot \frac{K_{a,P}^2}{K_{a,D} \cdot K_{a,A}}$$

Finally, from the rate-limiting step the global rate can be deduced,

$$r = r_2 = k \cdot \left(a_P^2 - \frac{a_D a_A}{K} \right) = k K_{a,P}^2 \hat{C}_\sigma^2 \left(a_P^2 - \frac{a_D a_A}{K} \right)$$

$$r = \frac{k K_{a,P}^2 \left(a_P^2 - \frac{a_D a_A}{K} \right)}{\left(1 + K_{a,P} a_P + K_{a,D} a_D + K_{a,A} a_A \right)^2}$$

where the exponent of the denominator shows the number of active centers involved in the reaction (here 2).

Appendix VI. Kinetic models fitting

Amberlyst 36

	Model	k1	k2	k3	k4	k5	k6	k7	k8	SQ	Ea
I-1	n=1 113	2.62	10867.9							113.72	90.3
	n=2 114	2.45	9911.14							170.15	82.4
	n=3 115	2.27	8863.11							233.45	73.7
I-2	n=1 117	-1.60	21378.1							788.65	177.7
	n=2 118	-6.55	33472.5							1005.75	278.2
	n=3 119	-11.38	44787							1032.85	372.2
I-3	n=1 121	0.00	12452.1							344.49	103.5
	n=2 122	-3.47	11605.4							781.44	96.4
	n=3 123	-6.88	12376.2							926.71	102.8
I-4	n=1 125	3.11	13251.5	1.79	1100.9					3.98	110.1
	n=2 126	3.09	13175.6	1.17	574.0					3.17	109.5
	n=3 127	3.07	13146.4	0.89	550.8					2.89	109.2
I-5	n=1 129	3.25	13380.5	1.68	1567.3					7.13	111.2
	n=2 130	3.24	13336.9	1.01	1198.9					7.07	110.8
	n=3 131	3.24	13380.9	0.72	1274.7					7.72	111.2
I-6	n=1 133	21.00	-45186.1	20.99	-57638.2					344.49	-375.5
	n=2 134	30.42	-31990.3	16.95	-21797.8					781.44	-265.8
	n=3 135	68.81	168750	25.23	52124.5					926.71	1402.3
I-7	n=1 137	3.11	13251.5	1.79	1100.7	-16.2	-2071.7			3.98	110.1
	n=2 138	3.09	13175.6	1.17	574.0	-16.2	3222.3			3.17	109.5
	n=3 139	3.07	13146.4	0.89	550.9	-17.6	5781.0			2.89	109.2
II-1	n=1 141	2.78	11687.7	-46.89	-237245					66.92	97.1
	n=2 142	2.78	11712.6	-19.59	8433.6					66.93	97.3
	n=3 143	2.78	11712.6	-19.67	7642.2					66.93	97.3
II-2	n=1 145	3.12	13249.9	1.60	1001.0					4.09	110.1
	n=2 146	3.11	13180	0.76	132.7					3.36	109.5
	n=3 147	3.11	13155	0.31	-150.5					3.15	109.3
II-3	n=1 149	3.23	13316.6	1.48	1347.3					6.63	110.7
	n=2 150	3.21	13203.9	0.59	581.1					5.75	109.7
	n=3 151	3.20	13170.2	0.12	347.2					5.46	109.4
II-4	n=1 153	3.12	13249.9	-10.52	19.9	1.6	1000.7			4.09	110.1
	n=2 154	3.16	13184.3	-3.85	133.2	0.8	146.2			3.36	109.6
	n=3 155	4.47	13095.3	-0.55	-54.7	1.0	169.7			3.04	108.8
II-5	n=1 157	3.12	15924.7	-65.88	273671.9	1.2	1.54E+06			28.59	132.3
	n=2 158	3.21	13203.9	-15.43	1172.7	0.6	581.0			5.75	109.7
	n=3 159	3.20	13170.2	-14.46	12.4	0.1	347.4			5.46	109.4
II-6	n=1 161	3.12	13249.9	1.60	1000.7	-15.1	3321.6			4.09	110.1
	n=2 162	3.11	13180	0.76	132.7	-35.8	137644.9			3.36	109.5
	n=3 163	3.11	13155	0.31	-150.6	-15.0	3798.4			3.15	109.3
II-7	n=1 165	3.12	13249.9	-44.05	64168.8	1.6	1000.6	-69.3	-126468	4.09	110.1
	n=2 166	3.25	13202.7	-2.67	190.8	0.9	186.0	-21.7	-36103.8	3.35	109.7
	n=3 167	3.68	13239.4	-1.54	172.2	0.6	73.3	-6.8	-252.0	3.09	110.0

Amberlyst 70

	Model	k1	k2	k3	k4	k5	k6	k7	k8	SQ	Ea
I-1	n=1 113	2.14	10798.51							5432.07	89.7
	n=2 114	2.15	7373.496							12586.14	61.3
	n=3 115	2.11	3188.68							19162.00	26.5
I-2	n=1 117	-3.34	24093.09							9629.58	200.2
	n=2 118	-10.21	41387.16							12752.70	343.9
	n=3 119	-17.12	59076.43							13447.80	490.9
I-3	n=1 121	-1.79	20157.6							7717.28	167.5
	n=2 122	-8.31	39796.14							12482.61	330.7
	n=3 123	-14.38	57155.84							13589.17	475.0
I-4	n=1 125	2.14	13788.32	-0.27	7449.9					417.49	114.6
	n=2 126	2.13	13803.76	-0.27	5541.3					462.53	114.7
	n=3 127	2.11	13875.38	-0.27	4882.8					521.17	115.3
I-5	n=1 129	2.20	13869.07	0.20	3986.2					340.37	115.3
	n=2 130	2.24	13765.99	0.15	2216.4					340.12	114.4
	n=3 131	2.26	13786.24	0.11	1679.7					353.46	114.6
I-6	n=1 133	56.72	805994.2	58.51	785836.3					7717.28	6697.8
	n=2 134	109.37	1348574	58.84	654388.6					12482.61	11206.6
	n=3 135	13.69	207077.1	9.36	49973.8					13589.17	1720.8
I-7	n=1 137	2.24	13671.74	0.94	-14623.4	-0.3	6424.1			329.78	113.6
	n=2 138	2.33	13184.56	-87.14	422876.1	0.6	-792.8			325.59	109.6
	n=3 139	2.34	13291.29	-77.46	373034.1	0.4	-281.8			339.85	110.5
II-1	n=1 141	2.25	12335.84	-2.14	-22504.5					1058.07	102.5
	n=2 142	2.24	12362.79	-2.98	-22236.5					1058.51	102.7
	n=3 143	2.24	12370.8	-3.44	-22154.9					1058.65	102.8
II-2	n=1 145	2.16	13748.98	-2.01	13323.6					370.25	114.3
	n=2 146	2.17	13680.73	-2.55	11956.4					358.46	113.7
	n=3 147	2.17	13660.82	-2.91	11536.1					354.05	113.5
II-3	n=1 149	2.16	13979.8	-1.43	9512.4					332.76	116.2
	n=2 150	2.18	13838.14	-1.96	7901.8					321.94	115.0
	n=3 151	2.18	13797.79	-2.32	7428.3					317.79	114.7
II-4	n=1 153	57.89	-251421	55.88	-266713.2	55.9	-260267			323.27	-2089.3
	n=2 154	2.94	10583.74	-0.53	-9421.6	-0.6	2911.9			342.14	88.0
	n=3 155	2.78	11180.2	-1.28	-9334.0	-1.3	3932.5			338.83	92.9
II-5	n=1 157	58.55	-253085	56.44	-268019	56.8	-264540			290.43	-2103.1
	n=2 158	3.80	8430.986	0.28	-7198.0	0.6	-2332.7			300.46	70.1
	n=3 159	2.18	13797.75	-6139.36	1.4E+07	-2.3	7427.8			317.79	114.7
II-6	n=1 161	2.16	13979.78	-40.12	6107.5	-1.4	9512.1			332.76	116.2
	n=2 162	2.24	13478.1	0.07	-14694.2	-2.9	11934.0			310.60	112.0
	n=3 163	2.24	13445.93	-0.35	-14856.8	-3.2	11404.0			306.39	111.7
II-7	n=1 165	2.16	13979.81	-5.7E+08	3.3E+12	-50.0	-15000.0	-1.4	9512.5	332.76	116.2
	n=2 166	3.80	8429.677	0.28	-7197.7	-19.3	-32249.8	0.6	-2333.5	300.46	70.1
	n=3 167	2.09	14889.39	-76.52	360924.8	-23.1	-11113.0	-1.8	5284.2	260.82	123.7

Amberlyst DL-H/03

	Model	k1	k2	k3	k4	k5	k6	k7	k8	SQ	Ea
I-1	n=1 113	2.22	11601.96							297.82	96.4
	n=2 114	2.11	9874.436							732.53	82.1
	n=3 115	1.98	7824.603							1294.44	65.0
I-2	n=1 117	-3.12	25863.8							3628.42	214.9
	n=2 118	-9.29	42911.65							4369.91	356.6
	n=3 119	-15.37	59947.61							4463.20	498.2
I-3	n=1 121	-1.02	15282.5							2631.13	127.0
	n=2 122	-5.21	21605.39							4050.98	179.5
	n=3 123	-9.27	27868.91							4322.46	231.6
I-4	n=1 125	2.38	13299.82	0.70	857.2					6.36	110.5
	n=2 126	2.36	13370.57	0.33	1600.5					6.69	111.1
	n=3 127	2.35	13426.63	0.19	1919.4					7.28	111.6
I-5	n=1 129	2.44	13107.43	0.77	-1000.6					8.37	108.9
	n=2 130	2.44	13169.71	0.39	-119.6					10.77	109.4
	n=3 131	2.45	13206.78	0.24	256.4					14.10	109.7
I-6	n=1 133	19.02	48281.21	20.04	32998.7					2631.13	401.2
	n=2 134	43.71	7476.25	24.46	-7064.5					4050.98	62.1
	n=3 135	37.12	87979.87	15.46	20037.0					4322.46	731.1
I-7	n=1 137	2.43	12893.65	0.19	3954.1	0.1	-11795.9			5.45	107.1
	n=2 138	2.42	12885.61	-0.10	4156.2	-0.4	-10450.4			5.42	107.1
	n=3 139	2.41	12877.98	-0.21	4222.1	-0.6	-9518.2			5.62	107.0
II-1	n=1 141	2.32	12856.12	-8.77	-46464.7					52.84	106.8
	n=2 142	2.32	12856.18	-9.48	-46503.2					52.84	106.8
	n=3 143	2.32	12856.17	-9.88	-46452.0					52.84	106.8
II-2	n=1 145	2.40	13190.55	0.22	-1848.8					6.01	109.6
	n=2 146	2.40	13201.57	-0.53	-1803.7					5.87	109.7
	n=3 147	2.40	13205.29	-0.96	-1787.8					5.82	109.7
II-3	n=1 149	2.45	12918.15	0.36	-4520.0					6.56	107.3
	n=2 150	2.45	12926.2	-0.39	-4513.9					6.34	107.4
	n=3 151	2.45	12928.77	-0.82	-4513.5					6.27	107.4
II-4	n=1 153	2.40	13353.21	-143.74	1311127.2	0.3	-1820.2			5.89	111.0
	n=2 154	2.49	12666.02	-3.21	-7913.4	-0.3	-3089.2			5.72	105.3
	n=3 155	2.49	12670.27	-3.62	-7825.9	-0.8	-3018.0			5.68	105.3
II-5	n=1 157	2.47	12770.17	-4.32	-15599.0	0.4	-4747.4			6.48	106.1
	n=2 158	2.47	12757.43	-4.81	-14046.4	-0.4	-4725.5			6.26	106.0
	n=3 159	2.47	12754.48	-5.17	-13664.6	-0.8	-4714.5			6.19	106.0
II-6	n=1 161	2.44	12901.27	-0.73	4408.2	-0.1	-12595.6			5.37	107.2
	n=2 162	2.42	13063.69	-0.24	-7957.3	-59.6	539223.9			5.18	108.6
	n=3 163	2.42	13064.35	-0.66	-7984.5	-39.7	349039.5			5.12	108.6
II-7	n=1 165	2.44	12901.34	-8.21	174.7	-0.7	4403.5	-0.1	-12598.8	5.37	107.2
	n=2 166	2.47	12906.53	-4.23	202.5	-1.5	5097.5	-0.8	-12061.1	5.18	107.3
	n=3 167	2.46	12905.57	-5.01	246.5	-2.0	5374.8	-1.2	-11903.2	5.11	107.2

Amberlyst DL-I/03

	Model	k1	k2	k3	k4	k5	k6	k7	k8	SQ	Ea
I-1	n=1 113	2.55	8679.504							2267.51	72.1
	n=2 114	2.33	6471.913							3357.80	53.8
	n=3 115	2.08	4088.489							4360.09	34.0
I-2	n=1 117	-1.40	21853.54							2006.34	181.6
	n=2 118	-6.18	34381.4							3309.40	285.7
	n=3 119	-10.83	46088.47							3590.61	383.0
I-3	n=1 121	0.24	12719.73							1342.41	105.7
	n=2 122	-2.92	16387.15							3008.90	136.2
	n=3 123	-6.10	20582.66							3549.60	171.0
I-4	n=1 125	3.07	13628.07	1.78	6299.8					233.97	113.2
	n=2 126	3.04	13335.05	1.17	4494.3					199.72	110.8
	n=3 127	3.02	13370.25	0.91	4062.3					185.06	111.1
I-5	n=1 129	3.21	12865.32	1.56	3657.8					301.27	106.9
	n=2 130	3.21	12268.23	0.91	1817.1					295.35	101.9
	n=3 131	3.21	12094.77	0.64	1445.8					306.19	100.5
I-6	n=1 133	31.72	-265686	31.48	-279190.6					1338.27	-2207.8
	n=2 134	49.65	-442772	26.30	-230516.1					3001.36	-3679.4
	n=3 135	75.76	-711558	27.33	-245844.4					3512.46	-5913.0
I-7	n=1 137	3.07	13628.08	1.78	6299.8	-15.3	-13703.7			233.97	113.2
	n=2 138	3.04	13331.47	1.17	4494.0	-7.3	-23559.6			199.72	110.8
	n=3 139	3.02	13348.85	0.91	4063.0	-5.8	-22779.4			185.05	110.9
II-1	n=1 141	2.73	10463.83	-9.41	-40447.6					1262.45	87.0
	n=2 142	2.73	10463.91	-10.09	-40240.2					1262.45	87.0
	n=3 143	2.73	10463.94	-10.49	-40148.6					1262.45	87.0
II-2	n=1 145	3.09	13493.95	1.59	6740.9					235.89	112.1
	n=2 146	3.08	13061.95	0.75	4861.3					205.74	108.5
	n=3 147	3.07	12951.68	0.29	4338.9					194.99	107.6
II-3	n=1 149	3.20	12884.66	1.35	4093.8					292.95	107.1
	n=2 150	3.18	12355.92	0.47	2114.1					268.81	102.7
	n=3 151	3.17	12237.2	0.01	1622.7					259.73	101.7
II-4	n=1 153	6.51	13027.37	3.41	-621.7	5.2	5715.2			234.03	108.3
	n=2 154	18.71	15573.24	7.83	1119.5	9.0	5613.8			199.72	129.4
	n=3 155	15.00	16722.29	3.98	1140.1	4.9	5192.7			185.22	139.0
II-5	n=1 157	3.21	13238.81	-30.33	258169.0	1.4	4248.7			292.00	110.0
	n=2 158	3.22	11962.95	-4.17	-13131.8	0.5	1688.6			268.44	99.4
	n=3 159	3.22	11847.18	-4.61	-13459.6	0.0	1257.0			259.29	98.5
II-6	n=1 161	3.09	13493.94	1.59	6740.8	-15.7	-13332.1			235.89	112.1
	n=2 162	3.08	13055.58	0.75	4858.1	-7.0	-25935.0			205.74	108.5
	n=3 163	3.08	12924.8	0.30	4328.4	-6.0	-26232.3			194.97	107.4
II-7	n=1 165	3.85	13726.26	0.16	294.4	2.5	6668.8	-5.3	-12785.3	234.84	114.1
	n=2 166	8.48	15161.08	2.65	986.5	3.9	5451.9	-4.8	-21558.5	200.09	126.0
	n=3 167	5.06	14765.28	-0.05	1097.1	1.3	4849.3	-5.2	-19834.0	189.76	122.7

Purolite CT-224

	Model	k1	k2	k3	k4	k5	k6	k7	k8	SQ	Ea
I-1	n=1 113	2.73	14612.1							2.59	121.4
	n=2 114	2.61	13849.88							14.26	115.1
	n=3 115	2.47	12993.55							36.71	108.0
I-2	n=1 117	-2.38	24249.81							1147.13	201.5
	n=2 118	-7.87	36033.56							1272.23	299.4
	n=3 119	-13.21	48257.68							1281.52	401.0
I-3	n=1 121	-0.33	14136.65							655.60	117.5
	n=2 122	-4.16	10987.8							1092.57	91.3
	n=3 123	-7.83	11860.18							1217.44	98.6
I-4	n=1 125	2.78	14332.13	-0.95	-16946.1					0.89	119.1
	n=2 126	2.77	14691.67	-0.41	-3751.3					1.02	122.1
	n=3 127	2.75	14772.39	-0.29	-1323.8					1.08	122.8
I-5	n=1 129	2.79	13877.52	-0.92	-15163.6					0.62	115.3
	n=2 130	2.79	13517.82	-0.49	-9212.6					0.60	112.3
	n=3 131	2.80	13643.79	-0.36	-5638.0					0.67	113.4
I-6	n=1 133	21.24	-15061.9	21.57	-29198.8					655.60	-125.2
	n=2 134	37.86	69076.39	21.01	29044.4					1092.57	574.0
	n=3 135	56.19	9678.708	21.34	-727.3					1217.44	80.4
I-7	n=1 137	2.78	14486.34	-1.44	-21426.2	1.7	370222.0			0.79	120.4
	n=2 138	2.78	14607.89	-1.04	-14797.3	1.2	368657.1			0.73	121.4
	n=3 139	2.79	13530.97	-1.76	26820.8	-0.6	-8261.8			0.56	112.4
II-1	n=1 141	3.52	9941.728	0.08	-8264.9					0.91	82.6
	n=2 142	3.39	11580.82	-1.04	-5488.6					0.95	96.2
	n=3 143	3.40	18470.1	-1.47	9413.4					0.66	153.5
II-2	n=1 145	2.84	15214.28	-6.80	-44238.3					2.41	126.4
	n=2 146	2.84	15215.57	-7.53	-44206.8					2.41	126.4
	n=3 147	2.84	15216.02	-7.94	-44203.7					2.41	126.4
II-3	n=1 149	2.84	15188.47	-6.48	-35916.1					2.40	126.2
	n=2 150	2.84	15190.16	-7.20	-35904.4					2.40	126.2
	n=3 151	2.84	15190.77	-7.62	-35893.7					2.40	126.2
II-4	n=1 153	3.52	9941.744	0.08	-8264.9	-92.9	265126.4			0.91	82.6
	n=2 154	3.39	11580.75	-1.04	-5488.7	-356.3	26114.0			0.95	96.2
	n=3 155	3.36	11893.78	-1.56	-4956.0	-1281.0	-433801.5			0.96	98.8
II-5	n=1 157	3.52	9941.858	0.08	-8264.8	-46.5	1421238.9			0.91	82.6
	n=2 158	3.43	18572.72	-0.96	9571.2	-251.9	-268694.2			0.67	154.3
	n=3 159	3.36	11893.8	-1.56	-4955.9	-902.5	-1410185.6			0.96	98.8
II-6	n=1 161	2.84	15188.53	-19.28	-22969.4	-6.5	-35919.0			2.40	126.2
	n=2 162	2.84	15190.16	-95.04	-110866.0	-7.2	-35899.9			2.40	126.2
	n=3 163	2.84	15269.68	-52.65	4787.8	-66.9	-55342.9			2.42	126.9
II-7	n=1 165	3.52	9941.859	0.08	-8264.8	-42.7	143698.8	-71.9	70840.7	0.91	82.6
	n=2 166	3.43	18572.71	-0.96	9571.1	-34.6	391372.3	-180.7	1.57E+07	0.67	154.3
	n=3 167	7.00	-8468.63	1.14	-9220.6	0.7	-15578.7	-9.4	132672.5	0.42	-70.4

Dowex 50Wx4-50

	Model	k1	k2	k3	k4	k5	k6	k7	k8	SQ	Ea
I-1	n=1 113	2.50	11835							17.28	98.3
	n=2 114	2.38	11071.23							34.66	92.0
	n=3 115	2.24	10228.53							58.19	85.0
I-2	n=1 117	-2.90	15336.01							829.44	127.4
	n=2 118	-8.80	22855.82							932.96	189.9
	n=3 119	-14.57	29858.5							944.88	248.1
I-3	n=1 121	-0.30	17896.26							391.55	148.7
	n=2 122	-3.83	28566.3							757.70	237.4
	n=3 123	-7.29	40131.34							864.02	333.5
I-4	n=1 125	2.68	13802.51	0.74	32837.0					1.87	114.7
	n=2 126	2.67	13862.88	0.40	17669.6					1.71	115.2
	n=3 127	2.65	13884.98	0.26	12709.1					1.62	115.4
	n=1 129	2.74	14256.09	0.65	23008.6					2.65	118.5
I-5	n=2 130	2.75	14469.54	0.31	13889.3					2.85	120.2
	n=3 131	2.76	14630.5	0.17	10261.3					3.14	121.6
	n=1 133	35.80	108377.7	36.10	90481.2					391.55	900.6
I-6	n=2 134	52.65	208449.7	28.24	89941.6					757.70	1732.2
	n=3 135	47.68	25054.66	18.32	-5025.7					864.02	208.2
	n=1 137	2.68	13802.51	0.74	32837.0	-19.0	3593.3			1.87	114.7
I-7	n=2 138	2.67	13862.88	0.40	17669.7	-18.1	8848.6			1.71	115.2
	n=3 139	2.65	13884.98	0.26	12709.1	-32.7	46787.0			1.62	115.4
	n=1 141	2.61	11853.06	-5.21	-22528.2					6.36	98.5
II-1	n=2 142	2.61	11878.51	-5.94	-22200.3					6.36	98.7
	n=3 143	2.61	11886.64	-6.35	-22107.4					6.36	98.8
	n=1 145	2.71	13579.73	0.22	778702.3					2.16	112.8
II-2	n=2 146	2.71	13584.8	-0.51	488506.1					2.09	112.9
	n=3 147	2.71	13586.43	-0.92	577810.0					2.06	112.9
	n=1 149	2.73	13896.63	0.08	580908.0					2.54	115.5
II-3	n=2 150	2.73	13892.87	-0.66	818436.8					2.48	115.4
	n=3 151	2.73	13891.61	-1.08	512419.9					2.46	115.4
	n=1 153	3.86	13743.38	0.80	-85.3	1.8	584642.9			1.92	114.2
II-4	n=2 154	3.57	13758.9	-0.59	-77.6	0.3	190826.5			1.85	114.3
	n=3 155	5.47	13921.19	0.43	36.1	0.9	19232.7			1.70	115.7
	n=1 157	2.87	13851.71	-1.92	-871.1	0.3	1736671.7			2.53	115.1
II-5	n=2 158	2.85	13846.57	-2.77	-918.0	-0.5	158910.6			2.47	115.1
	n=3 159	2.86	13861.49	-3.14	-780.6	-0.9	162028.4			2.45	115.2
	n=1 161	2.71	13579.73	0.22	400715.8	-17.5	126891.9			2.16	112.8
II-6	n=2 162	2.71	13584.8	-0.51	348959.0	-18.3	69948.4			2.09	112.9
	n=3 163	2.71	13586.43	-0.92	399234.9	-19.2	114359.9			2.06	112.9
	n=1 165	3.63	13389.97	0.44	-646.0	1.5	822235.7	-22.9	119971.5	1.92	111.3
II-7	n=2 166	3.78	13506.33	-0.32	-339.0	0.5	38819.5	-14.2	42334.1	1.82	112.2
	n=3 167	4.72	13502.35	-0.02	-230.5	0.5	22549.1	-12.2	8837.1	1.73	112.2

Dowex 50Wx4-100

	Model	k1	k2	k3	k4	k5	k6	k7	k8	SQ	Ea
I-1	n=1 113	2.51	11806.11							11.39	98.1
	n=2 114	2.39	11072.83							26.12	92.0
	n=3 115	2.26	10255.38							47.56	85.2
I-2	n=1 117	-2.20	16868.83							785.39	140.2
	n=2 118	-7.47	23755.03							936.72	197.4
	n=3 119	-12.57	30582.79							958.98	254.1
I-3	n=1 121	-0.89	15435.11							551.04	128.3
	n=2 122	-5.05	19273.3							857.58	160.2
	n=3 123	-9.05	24727.82							927.17	205.5
I-4	n=1	125	2.65	12830.01	0.34	4518.3				2.98	106.6
	n=2	126	2.64	12838.15	0.14	3336.3				2.90	106.7
	n=3	127	2.63	12833.9	0.07	2765.2				2.85	106.6
I-5	n=1	129	2.67	12844.88	0.26	3396.8				3.55	106.7
	n=2	130	2.67	12910.83	0.07	2864.5				3.89	107.3
	n=3	131	2.68	12971.81	0.01	2629.0				4.28	107.8
I-6	n=1 133	23.68	-35461.8	24.57	-50896.9					551.04	-294.7
	n=2 134	59.57	-1001764	32.31	-510518.8					857.58	-8324.7
	n=3 135	48.13	-2527039	19.06	-850588.9					927.17	-20999.7
I-7	n=1 137	2.65	12830.06	0.34	4519.6	-17.1	5238.6			2.98	106.6
	n=2 138	2.64	12838.13	0.14	3336.1	-17.6	331.5			2.90	106.7
	n=3 139	2.63	12511.67	0.06	1601.8	-52.7	-294821.5			2.63	104.0
II-1	n=1 141	2.62	12206.76	-95.69	-521989.5					3.61	101.4
	n=2 142	2.62	12206.75	-64.33	-343980.4					3.61	101.4
	n=3 143	2.62	12206.75	-57.85	-305734.2					3.61	101.4
II-2	n=1	145	2.66	12792.89	-0.68	7822.3				3.05	106.3
	n=2	146	2.66	12797.31	-1.38	7715.8				3.03	106.3
	n=3	147	2.66	12798.75	-1.78	7674.6				3.03	106.4
II-3	n=1	149	2.67	12758.5	-0.86	4827.3				3.25	106.0
	n=2	150	2.67	12761.37	-1.56	4730.3				3.24	106.0
	n=3	151	2.67	12762.4	-1.96	4702.0				3.23	106.1
II-4	n=1 153	2.66	12481.5	-6.24	-23434.0	-0.7	5212.4			2.97	103.7
	n=2	154	6.89	12346.83	1.99	-285.4	2.2	3252.5		2.92	102.6
	n=3	155	5.91	13068.23	0.68	116.5	0.8	3433.7		2.90	108.6
II-5	n=1 157	2.66	12401.8	-10.11	-46819.5	-0.9	-648.7			3.04	103.1
	n=2 158	2.66	12431.48	-13.06	-59190.1	-1.6	-172.9			3.00	103.3
	n=3 159	2.66	12395.91	-9.66	-37750.7	-2.0	-4.4			3.05	103.0
II-6	n=1 161	2.66	12793.35	-0.68	7894.6	-6.4	1933.2			3.05	106.3
	n=2 162	2.66	12797.31	-1.38	7716.5	-13.7	1775.3			3.03	106.3
	n=3 163	2.66	12795.94	-1.80	7410.9	-6.1	1873.5			3.03	106.3
II-7	n=1 165	2.66	12443.96	-25.75	-133825.3	-19.6	278814.3	-0.9	-12.7	2.98	103.4
	n=2 166	5.18	12785.13	0.94	-36.3	1.2	3819.7	-10.6	-2862.5	2.93	106.2
	n=3 167	7.65	13306.14	1.46	193.5	1.6	3221.0	-12.3	-4441.5	2.87	110.6

Dowex 50Wx4-200

	Model	k1	k2	k3	k4	k5	k6	k7	k8	SQ	Ea
I-1	n=1 113	2.50	11803.03							17.90	98.1
	n=2 114	2.38	11073.76							34.60	92.0
	n=3 115	2.25	10272.48							56.89	85.4
I-2	n=1 117	-2.68	16982.93							829.11	141.1
	n=2 118	-8.35	25787.55							932.47	214.3
	n=3 119	-13.89	33863.66							943.76	281.4
I-3	n=1 121	0.13	19044.6							355.68	158.3
	n=2 122	-2.95	31055.29							734.74	258.1
	n=3 123	-5.99	43678.4							854.13	363.0
I-4	n=1 125	2.69	13816.89	0.60	30909.8					2.03	114.8
	n=2 126	2.67	13881.43	0.24	17146.7					1.89	115.4
	n=3 127	2.65	13909.94	0.09	12354.1					1.82	115.6
I-5	n=1 129	2.75	14355.74	0.41	20669.5					3.09	119.3
	n=2 130	2.77	14595.01	0.05	12779.5					3.44	121.3
	n=3 131	2.79	14786.81	-0.10	9455.3					3.90	122.9
I-6	n=1 133	26.06	78207.37	25.93	59162.6					355.68	649.9
	n=2 134	60.36	-296807	31.65	-163931.9					734.74	-2466.5
	n=3 135	52.24	9797.247	19.41	-11293.9					854.13	81.4
I-7	n=1 137	2.69	13816.89	0.60	30909.9	-26.6	-15912.6			2.03	114.8
	n=2 138	2.67	13881.43	0.24	17146.7	-19.3	7027.3			1.89	115.4
	n=3 139	2.79	14786.81	-28.52	257515.0	-0.1	9455.3			3.90	122.9
II-1	n=1 141	2.63	12671.76	-3.76	762956.3					7.37	105.3
	n=2 142	2.61	11804.92	-5.94	-22362.6					7.03	98.1
	n=3 143	2.61	11813.25	-6.35	-22256.5					7.03	98.2
II-2	n=1 145	2.71	13609.69	0.12	694556.4					2.24	113.1
	n=2 146	2.71	13615.23	-0.61	583235.3					2.16	113.1
	n=3 147	2.71	13616.99	-1.03	537007.2					2.13	113.2
II-3	n=1 149	2.74	13997.38	-0.14	562343.3					2.82	116.3
	n=2 150	2.74	13992.52	-0.88	485865.3					2.75	116.3
	n=3 151	2.60	11915.16	-48.36	-402563.0					17.07	99.0
II-4	n=1 153	3.55	13699.6	0.30	-162.8	1.3	481800.9			2.07	113.8
	n=2 154	3.90	13813.7	-0.18	6.3	0.5	33653.4			1.96	114.8
	n=3 155	5.06	13524.16	0.19	-209.0	0.5	19875.6			1.88	112.4
II-5	n=1 157	2.74	13996.18	-6.23	-1134.6	-0.1	228000.3			2.82	116.3
	n=2 158	2.74	13992.93	-7.03	-449.2	-0.9	191500.5			2.75	116.3
	n=3 159	2.75	13995.26	-5.23	-399.3	-1.3	171689.3			2.73	116.3
II-6	n=1 161	2.71	13609.69	0.12	406997.5	-18.5	112855.4			2.24	113.1
	n=2 162	2.71	13615.22	-0.61	373413.6	-17.7	102905.0			2.16	113.1
	n=3 163	2.74	13990.88	-222.03	10286429.7	-1.3	631170.9			2.73	116.3
II-7	n=1 165	3.48	13651.69	0.18	-241.1	1.2	848702.5	-27.3	125128.6	2.08	113.4
	n=2 166	5.87	13227.42	1.37	-400.9	1.7	20209.3	-9.1	9372.8	1.91	109.9
	n=3 167	4.33	13508.12	-0.31	-265.6	0.1	24634.4	-18.0	37414.9	1.90	112.3

Dowex 50Wx4-400

	Model	k1	k2	k3	k4	k5	k6	k7	k8	SQ	Ea	
I-1	n=1	113	2.50	12105.12						2.01	100.6	
	n=2	114	2.39	11466.69						8.43	95.3	
	n=3	115	2.27	10738.1						21.46	89.2	
I-2	n=1	117	-2.59	22627.49						830.19	188.0	
	n=2	118	-8.07	39163.44						934.48	325.4	
	n=3	119	-13.39	54461.77						942.63	452.6	
I-3	n=1	121	-0.80	12290.23						503.01	102.1	
	n=2	122	-4.87	10964.92						814.03	91.1	
	n=3	123	-8.77	12459.03						896.68	103.5	
I-4	n=1	125	2.54	11768.13	-1.13	-17342.4				1.11	97.8	
	n=2	126	2.52	11927.46	-0.49	-5819.6				1.17	99.1	
	n=3	127	2.51	12007.42	-0.34	-2540.3				1.19	99.8	
I-5	n=1	129	2.54	11403.03	-1.13	-17028.8				1.01	94.8	
	n=2	130	2.54	11071.96	-0.60	-10358.5				1.08	92.0	
	n=3	131	2.55	11422.37	-0.42	-5364.1				1.24	94.9	
I-6	n=1	133	32.75	-1592485	33.55	-1604774.8				503.01	-13233.5	
	n=2	134	57.90	103431.9	31.38	46233.4				814.03	859.5	
	n=3	135	60.58	-91906.2	23.12	-34788.6				896.68	-763.7	
	n=1	137	2.54	11406.59	-4.87	-14651.9	-1.2	-17093.0			1.01	94.8
I-7	n=2	138	2.53	11282	-0.96	-599.0	-1.6	-15442.5		0.98	93.8	
	n=3	139	2.52	11928.53	-0.71	-9055.8	1.6	352752.9		1.02	99.1	
	n=1	141	3.45	7045.195	0.40	-7795.5				1.24	58.5	
II-1	n=2	142	3.25	9171.587	-0.86	-4641.4				1.28	76.2	
	n=3	143	3.26	15863.45	-1.30	7822.0				1.01	131.8	
	n=1	145	2.60	12615.53	-6.90	-39254.9				2.40	104.8	
II-2	n=2	146	2.60	12616.12	-7.62	-39242.1				2.40	104.8	
	n=3	147	2.60	12616.35	-8.02	-39210.5				2.40	104.8	
	n=1	149	2.60	12581.81	-6.30	-34573.2				2.40	104.6	
II-3	n=2	150	2.60	12583.41	-7.03	-34566.0				2.40	104.6	
	n=3	151	2.60	12583.82	-7.44	-34551.3				2.40	104.6	
	n=1	153	3.43	16434.75	0.36	8845.7	-43.8	82458.2		1.07	136.6	
II-4	n=2	154	3.25	9171.604	-0.86	-4641.4	-59.0	113613.9		1.28	76.2	
	n=3	155	3.21	9518.352	-1.39	-4118.3	-1365.1	-130439.3		1.29	79.1	
	n=1	157	3.45	7045.156	0.40	-7795.5	-28.0	120971.9		1.24	58.5	
II-5	n=2	158	3.25	9171.626	-0.86	-4641.4	-31.5	598205.0		1.28	76.2	
	n=3	159	3.19	7814.206	-1.43	-6421.0	-1181.9	-7900408.7		11.33	64.9	
	n=1	161	2.60	12648.06	-40.63	25666.1	-34.5	38537.3		2.41	105.1	
II-6	n=2	162	2.60	12616.13	-7.62	-39256.6	-34.6	-144865.6		2.40	104.8	
	n=3	163	2.60	12616.35	-8.04	-39288.3	-32.4	-134489.5		2.40	104.8	
	n=1	165	3.43	16434.77	0.36	8845.7	-32.7	58311.9	-33.8	10680.7	1.07	136.6
II-7	n=2	166	3.25	9171.581	-0.86	-4641.4	-325.5	77987.6	-257.5	-9186.3	1.28	76.2
	n=3	167	3.21	9518.408	-1.39	-4118.2	-342.2	90601.2	-33.6	73042.9	1.29	79.1

Nafion NR50

	Model	k1	k2	k3	k4	k5	k6	k7	k8	SQ	Ea
I-1	n=1 113	1.92	10156.93							1599.51	84.4
	n=2 114	1.97	7597.552							3961.46	63.1
	n=3 115	1.99	4529.527							6876.95	37.6
I-2	n=1 117	-3.39	21642.44							9440.03	179.8
	n=2 118	-9.70	35025.93							12353.08	291.1
	n=3 119	-15.89	48187.99							13042.67	400.4
I-3	n=1 121	-2.11	18001.75							7449.79	149.6
	n=2 122	-7.49	29614.23							11291.29	246.1
	n=3 123	-12.77	41183.16							12206.11	342.2
I-4	n=1 125	1.69	13144.76	-3.88	22215.3					433.74	109.2
	n=2 126	1.64	13411.99	-2.14	12809.5					459.94	111.5
	n=3 127	1.60	13553.67	-1.58	9729.8					489.07	112.6
I-5	n=1 129	1.68	13391.01	-2.86	16851.6					413.71	111.3
	n=2 130	1.64	13665.4	-1.17	7632.8					424.80	113.6
	n=3 131	1.65	13728.68	-0.59	4440.0					441.05	114.1
I-6	n=1 133	61.58	436231.8	63.69	418229.8					7449.79	3625.1
	n=2 134	24.50	74822.26	16.00	22603.7					11291.29	621.8
	n=3 135	-8.86	40370.92	0.98	395.7					12121.76	335.5
I-7	n=1 137	1.71	13190.83	-0.16	-17997.0	-3.0	17505.7			412.81	109.6
	n=2 138	1.71	13287.17	-0.11	-12960.0	-1.6	9589.6			419.72	110.4
	n=3 139	1.71	13335.91	-0.22	-10435.0	-1.2	6970.7			431.33	110.8
II-1	n=1 141	1.71	13335.91	-0.22	-10435.0					431.33	110.8
	n=2 142	2.19	10473.51	-1.35	-14784.6					506.89	87.0
	n=3 143	2.18	10537.51	-1.85	-14474.3					507.60	87.6
II-2	n=1 145	1.84	12555.69	-75.00	365893.6					443.84	104.3
	n=2 146	1.99	11411.18	0.41	-31463.0					521.21	94.8
	n=3 147	1.99	11422.63	-0.05	-31128.6					521.45	94.9
II-3	n=1 149	1.82	12695.73	-144.82	707740.1					434.31	105.5
	n=2 150	2.05	11115.62	0.89	-25567.4					514.19	92.4
	n=3 151	2.05	11128.04	0.43	-25149.8					514.45	92.5
II-4	n=1 153	2.48	10945.67	0.12	-5052.5	-12.7	63884.1			422.42	91.0
	n=2 154	2.38	11219.44	-0.93	-4399.5	-14.9	70355.0			420.19	93.2
	n=3 155	2.36	11295.26	-1.44	-4234.9	-16.0	73264.3			419.39	93.9
II-5	n=1 157	2.79	12173.29	0.67	-1620.9	-4.4	26947.4			411.23	101.2
	n=2 158	2.56	12315.02	-0.63	-1420.8	-5.7	27553.8			408.28	102.3
	n=3 159	2.51	12353.53	-1.18	-1369.7	-6.3	27728.2			407.21	102.7
II-6	n=1 161	1.84	12582.7	-0.33	-36722.6	-28.5	137719.5			433.31	104.6
	n=2 162	2.05	11115.69	-29.94	-36333.4	0.9	-25568.4			514.19	92.4
	n=3 163	1.84	12622.58	-1.60	-36748.1	-33.8	158240.3			428.19	104.9
II-7	n=1 165	2.83	12243.41	0.71	-1397.4	-0.1	-25602.0	-4.2	26298.2	411.16	101.7
	n=2 166	2.56	12315.4	-0.63	-1420.2	-14.9	8420.8	-5.7	27554.0	408.28	102.3
	n=3 167	2.51	12353.23	-1.18	-1369.9	-168.4	-1010996.6	-6.3	27718.4	407.21	102.7

Appendix VII. Error analysis

For error analysis the following parameters were calculated:

Arithmetic mean:

$$\bar{y} = \frac{\sum_{i=1}^n y_i}{n}$$

Variance:

$$s_y^2 = \frac{\sum_{i=1}^n (y_i - \bar{y})^2}{(n-1)n}$$

Standard deviation:

$$s_y = \sqrt{s_y^2}$$

For estimating the error limits in parametric curve fitting the **Jackknife method** was used:

1. Delete the first data point from the original data set.
2. Fit the "jackknifed" set to compute fitting the parameters
3. Repeat steps 1 and 2 n times (where n is the number of data points) deleting now point 2, 3... n , to obtain a set of n parameter sets.
4. Compute the standard deviation of the parameter sets

Outliers can be easily detected by examining the sum of the squares of the residuals (SSQ) of the jackknifed sets: if deleting a data point decreases significantly the SSQ of the resulting reduced set, that point is probably in error.

Appendix VIII. Modified kinetic models

In this section all the results of the modified kinetic models are presented. First the prediction of models 125, 126 and 127 are shown, and afterwards the modifications proposed by different researchers, and the one proposed in this work are detailed. Discussion of results is presented in section 4.6.5. To discriminate among the modified kinetic models, only data of catalyst A70 was used, including all the experiments with initial amounts of water and DNPE.

Class I-type 4 models (models 125, 126 and 127) were the following:

$$r = \frac{A \left(a_p^2 - \frac{a_D a_W}{K_{eq}} \right)}{(a_p + B a_D)^n}$$

where $n = 1, 2$ and 3 . A, which included the kinetic constant, and B, which dealt with the equilibrium adsorption constants $B = K_{aD}/K_{aP}$, had the following dependence with the temperature:

$$A = \exp(b_1) \exp \left[-b_2 \left(\frac{1}{T} - \frac{1}{\bar{T}} \right) \right]$$

$$B = \exp(b_3) \exp \left[-b_4 \left(\frac{1}{T} - \frac{1}{\bar{T}} \right) \right]$$

where \bar{T} was 423.15K. b's were the fitted parameters. Values of b's for the three models are shown in the following Table, as well as the activation energy and the sum of squares.

	Model		
	125	126	127
b_1	1.827 ± 0.002	1.67	1.47
b_2	15601 ± 19	16387	17439
b_3	-1.14 ± 0.02	-0.973	-0.942
b_4	12941 ± 108	9996.2	9098.0
E_a [kJ/mol]	129.7 ± 0.2	136.2	144.9
SQ	2598	3477	4649

Table A-VI 1. Fitted parameters of models 125, 126 and 127

SOLUBILITY PARAMETER

The modified kinetic equation with the solubility parameter was:

$$r = \frac{A \cdot \Psi \left(a_p^2 - \frac{a_D a_W}{K_{eq}} \right)}{(a_p + B a_D)^n}$$

with $n = 1, 2$ and 3 and Ψ defined as follows:

$$\Psi = \exp \left[\frac{\bar{V}_M \phi_p^2}{RT} (\delta_M - \delta_p)^2 \right]$$

where \bar{V}_M is the molar volume of the reaction medium and ϕ_p is the volume fraction of the resin (0.426). δ_p is the solubility parameter of the resin. δ_M is the solubility parameter of the reacting medium, which was computed from:

$$\delta_M = \sum_i \Phi_i \delta_i = \sum_i \Phi_i \frac{\sqrt{\Delta H_{v,i} - RT}}{V_i^L}$$

where $\Delta H_{v,i}$ is the molar enthalpy of vaporization, V_i^L the liquid molar volume and Φ_i is the volume fraction for the pure component i . Liquid molar volumes were estimated by means of the modified HBT technique and $\Delta H_{v,i}$ at all the temperatures were estimated by the Watson relationship (Appendix X).

T [K]	δ_i (J/m ³) ^{1/2}				
	PeOH	DNPE	Water	1-pentene	2-pentene
373.15	20290	15681	45683	11877	11361
393.15	19589	15201	44446	11066	10896
403.15	19225	14953	43802	10515	10466
413.15	18849	14699	43142	9873	9920
423.15	18461	14439	42465	9136	9267
433.15	18061	14173	41770	8285	8508
443.15	17646	13899	41053	7266	7630
453.15	17214	13617	40313	5901	6586
463.15	16763	13326	39546	2524	5204

Table A-VI 2. Individual solubility parameters of 1-pentanol, DNPE, water, 1-pentene and 2-pentene

The following Table shows the fitted parameters (b 's and δ_p), the activation energy, the sum of squares and the increase [%] of SQ of fittings of models with the solubility parameter with respect to models without it.

	Model		
	125 + δ	126 + δ	127 + δ
δ_p	28923 \pm 11	30021	31199
b_1	1.68 \pm 0.002	1.51	1.31
b_2	14419 \pm 22	14711	14961
b_3	-1.763 \pm 0.021	-1.422	-1.260
b_4	13269 \pm 140	9904	8410
E_a [kJ/mol]	119.9 \pm 0.2	122.3	124.3
SQ	3477	4115	4857
% variation	34	18	4

Table A-VI 3. Fitted parameters of models 125, 126 and 127 with the solubility parameter

Inhibition factor

The modified kinetic equation with the inhibition factor was:

$$r = \eta(a_w) \frac{A \left(a_p^2 - \frac{a_w a_D}{K} \right)}{\left(a_p + B \cdot a_D \right)^n}$$

$$\eta(a_w) = \frac{1}{1 + K_w \sqrt{a_w}}$$

$$K_w = \exp(K_{w1}) \exp \left[-K_{w2} \left(\frac{1}{T} - \frac{1}{\bar{T}} \right) \right]$$

where $\eta(a_w)$ is the inhibition factor, and the proportionality factor K_w is comparable to a sorption constant of water. Again, $n = 1, 2$ and 3 . With respect to LHHW models, two more parameters were included (K_{w1} and K_{w2}).

	Model		
	125 + η	126 + η	127 + η
K_{w1}	1.46 ± 0.01	2.01	2.44
K_{w2}	-6615 ± 77	-7871	-8239
b_1	2.81 ± 0.01	3.04	3.25
b_2	11595 ± 38	10761	10238
b_3	-1.82 ± 0.02	-1.330	-1.172
b_4	12906 ± 99	9404	8199
E_a [kJ/mol]	96.4 ± 0.3	89.4	85.1
SQ	1748	2131	2638
% variation	-33	-39	-43

Table A-VI 4. Fitted parameters of models 125, 126 and 127 with the inhibition factor

Freundlich-type factor

The modified kinetic equation with a Freundlich Adsorption isotherm-like expression factor was:

$$r = \frac{A \left(a_p^2 - \frac{a_w a_D}{K} \right)}{\left(a_p + B \cdot a_D \right)^n} \cdot \left(1 - K_F a_w^{1/\alpha} \right)$$

where

$$\alpha = \frac{K_\alpha}{T}$$

$$K_F = \exp(K_{F_1}) \exp \left[-K_{F_2} \left(\frac{1}{T} - \frac{1}{\bar{T}} \right) \right]$$

	Model		
	125 + Freundlich	126 + Freundlich	127 + Freundlich
K_{α}	358 ± 1	484	611
K_{F1}	495 ± 4	0.13	0.12
K_{F2}	2971 ± 49	1888	1491
b_1	2.122 ± 0.003	2.15	2.20
b_2	13716 ± 2	13817	13854
b_3	-17.4 ± 5	-1.65	-1.18
b_4	-33649 ± 37871	2785	2487
E_a [kJ/mol]	114.0 ± 0.1.	114.8	115.1
SQ	690	687	710
% variation	-73	-80	-85

Table A-VI 5. Fitted parameters of models 125, 126 and 127 with the Freundlich factor

Langmuir-type factor

$$r = \frac{A \left(a_p^2 - \frac{a_w a_D}{K} \right)}{\left(a_p + B \cdot a_D \right)^n} \cdot \frac{1}{1 + K_w a_w}$$

$$K_w = \exp \left[K_{w1} - K_{w2} \left(\frac{1}{T} - \frac{1}{\bar{T}} \right) \right]$$

	Model		
	125 + Freundlich	126 + Freundlich	127 + Freundlich
b_1	2.410 ± 0.003	2.27	2.28
b_2	12700 ± 24	13596	13625
b_3	-2.27 ± 0.02	-1.32	-1.15
b_4	14023 ± 100	8560	7506
K_{w1}	1.461 ± 0.008	1.11	1.47
K_{w2}	-5317 ± 70	-1946	-2745
E_a [kJ/mol]	105.6 ± 0.2	113.0	113.2
SSQ	1465	2107	2748
% variation	-44	-39	-41

Table A-VI 6. Fitted parameters of models 125, 126 and 127 with the Langmuir factor

Appendix IX. Material Safety Data Sheets

MATERIAL SAFETY DATA SHEETS

PartNumber/TradeName: PRIMARY AMYL ALCOHOL (1-PENTANOL)

This MSDS is valid for all grades and catalog numbers

General Information

Company's Name: PHARMCO PRODUCTS, INC.

Company's Street: 58 VALE RD.

Company's City: BROOKFIELD

Company's State: CT

Company's Zip Code: 06804

Company's Emerg Ph #: (203) 740-3471

Company's Info Ph #: (203) 740-3471

Date MSDS Revised: 12/00

Safety Data Review Date: 12/00

Preparer's Company: PHARMCO PRODUCTS, INC.

Preparer's St Or P. O. Box: 58 VALE RD.

Preparer's City: BROOKFIELD

Preparer's State: CT

Preparer's Zip Code: 06804

Ingredients/Identity Information

Ingredient: 1-Pentanol (1-AMYL ALCOHOL)

Formula: C₅H₁₁OH

May contain up to 38% 2-methyl butanol and/or other isomers.

Ingredient CAS: Pentanol 71-41-0

Ingredient CAS: 2-Methyl Butanol 137-32-6

Physical/Chemical Characteristics

Appearance And Odor: TRANSPARENT COLORLESS, MILD ODOR

Physical State: LIQUID

pH: NOT CURRENTLY AVAILABLE

Boiling Point (760 mmHg): 133.2°C, 271.8°F

Melting Point: -79°C

Vapor Pressure @ 20°C: 0.29 kPa 2.2 MMHg

Vapor Density (Air=1): 3

Specific Gravity (H₂O = 1): 0.815 20°C/68°F

Evaporation Rate (Butyl Acetate = 1): 0.3
Solubility In Water (Wt %): 20°C, 2.7%
Percent Volatiles : 100 Wt%
Molecular Weight: 88.15 g/mol

=====
=====
Hazard Identification
=====

=====
DANGER! CAUSES EYE AND SKIN IRRITATION. HARMFUL AND IRRITATING IF SWALLOWED. HARMFUL IF INHALED. COMBUSTIBLE. ASPIRATION MAY CAUSE LUNG DAMAGE. MAY CAUSE DIZZINESS AND DROWSINESS.

=====
=
Fire and Explosion Hazard Data
=====

=====
Flash Point-Closed Cup: TAG CLOSED CUP
ASTM D56 33C
Flash Point-Open Cup: TAG OPEN CUP
ASTM D1310 51°C 123°F
Autoignition Temperature: 300 C

Flammable Limits In Air: LOWER 1.2% (V)
UPPER 10.0%
Extinguishing Media: APPLY ALCOHOL-TYPE OR ALL-PURPOSE-TYPE FOAM BY MANUFACTURER'S RECOMMENDED SMALL FIRES
Extinguishing Media To Avoid: NO
INFORMATION CURRENTLY AVAILABLE

Special Fire Fighting Procedures: NO
INFORMATION CURRENTLY AVAILABLE
Unusual Fire And Expl Hazards: SEE
SECTION 8.3 –ENGINEERING CONTROLS.
THIS MATERIAL MAY PRODUCE A
FLOATING FIRE HAZARD IN EXTREME
FIRE CONDITIONS.
Special Protective Equipment For Firefighters:
USE SELF-CONTAINED BREATHING
APPARATUS AND PROTECTIVE
CLOTHING.

Hazardous Combustion Products: BURNING CAN PRODUCE THE FOLLOWING PRODUCTS:
CARBON MONOXIDE AND/OR CARBON DIOXIDE. CARBON MONOXIDE IS HIGHLY TOXIC IF
INHALED; CARBON DIOXIDE IN SUFFICIENT CONCENTRATIONS CAN ACT AS AN
ASPHYXIANT.

=====
=====
Reactivity Data
=====

=====
Stability: STABLE
Materials To Avoid: STRONG OXIDIZING AGENTS. STRONG INORGANIC ACIDS.
Hazardous Polymerization: WILL NOT OCCUR
Inhibitors/Stabilizers: NOT APPLICABLE

=====
=====
Health Hazard Data
=====

=====
SINGLE ACCUTE OVEREXPOSURE:

Route Of Entry - Inhalation: INHALATION MAY CAUSE IRRITATION OF THE RESPIRATORY TRACT, EXPERIENCED AS NASAL DISCOMFORT AND DISCHARGE, WITH CHEST PAIN, COUGHING, HEADACHE, NAUSEA, VOMITING, DIZZINESS, AND DROWSINESS. PROLONGED OVEREXPOSURE TO HIGH CONCENTRATIONS OF VAPOR MAY RESULT IN THE INHALATION OF HARMFUL AMOUNTS OF MATERIAL.

Route Of Entry – Eyes: LIQUID CAUSES SEVERE IRRITATION, EXPERIENCED AS DISCOMFORT OR PAIN, EXCESS BLINKING AND TEAR PRODUCTION, MARKED EXCESS REDNESS AND SWELLING OF THE CONJUNCTIVA, AND CHEMICAL BURNS OF THE CORNEA. VAPOR OR MIST MAY BE IRRITATING ALSO, EXPERIENCED AS DISCOMFORT OR PAIN, EXCESS BLINKING AND TEAR PRODUCTION, WITH MARKED EXCESS REDNESS OF THE CONJUNCTIVA.

Route Of Entry - Skin: **BRIEF CONTACT** MAY CAUSE SLIGHT IRRITATION WITH ITCHING AND LOCAL REDNESS. PROLONGED CONTACT MAY CAUSE MORE SEVERE IRRITATION, WITH DISCOMFORT OR PAIN, LOCAL REDNESS AND SWELLING, AND POSSIBLE TISSUE DESTRUCTION. **SKIN ABSORPTION** – PROLONGED OR WIDESPREAD CONTACT MAY RESULT IN THE ABSORPTION OF POTENTIALLY HARMFUL AMOUNTS OF MATERIAL. EFFECTS MAY INCLUDE THOSE DESCRIBED FOR SWALLOWING.

Route Of Entry - Ingestion: (SWALLOWING) MODERATELY TOXIC. MAY CAUSE ABDOMINAL DISCOMFORT, NAUSEA, VOMITING, AND DIARRHEA. HEADACHE MAY OCCUR. DIZZINESS AND DROWSINESS MAY OCCUR. LOSS OF CONSCIOUSNESS MAY OCCUR. ASPIRATION INTO THE LUNGS MAY OCCUR DURING INGESTION OR VOMITING, RESULTING IN LUNG INJURY.

CHRONIC, PROLONGED OR REPEATED OVEREXPOSURE:

Signs/Symptoms Of Overexposure: REPEATED INHALATION OF AEROSOLS MAY RESULT IN PULMONARY EDEMA AND KIDNEY INJURY. OTHER EFFECTS OF OVEREXPOSURE – NONE CURRENTLY KNOWN.

Medical Conditions Aggravated By Exposure: SKIN CONTACT MAY AGGRAVATE AN EXISTING DERMATITIS. INHALATION OF MATERIAL MAY AGGRAVATE ASTHMA AND INFLAMMATORY OR FIBROTIC PULMONARY DISEASE.

Emergency/First Aid Procedures:

Inhalation: REMOVE TO FRESH AIR. GIVE ARTIFICIAL RESPIRATION IF NOT BREATHING. IF BREATHING IS DIFFICULT, OXYGEN MAY BE GIVEN BY QUALIFIED PERSONNEL. OBTAIN MEDICAL ATTENTION.

Eye Contact: IMMEDIATELY FLUSH EYES WITH WATER AND CONTINUE WASHING FOR AT LEAST 15 MINUTES. **DO NOT** REMOVE CONTACT LENSES, IF WORN. OBTAIN MEDICAL ATTENTION WITHOUT DELAY, PREFERABLY FROM AN OPHTHALMOLOGIST.

Skin Contact: IMMEDIATELY REMOVE CONTAMINATED CLOTHING AND SHOES. WASH SKIN THOROUGHLY WITH SOAP AND WATER FOR AT LEAST 15 MINUTES. OBTAIN MEDICAL ATTENTION WITHOUT DELAY, WASH CLOTHING BEFORE REUSE. DISCARD CONTAMINATED LEATHER ARTICLES SUCH AS SHOES AND BELT.

Swallowing: IF PATIENT IS FULLY CONSCIOUS, GIVE TWO GLASSES OF WATER. DO NOT INDUCE VOMITING. OBTAIN MEDICAL ATTENTION.

Notes To Physician: THERE IS NO SPECIFIC ANTIDOTE. TREATMENT OF OVEREXPOSURE SHOULD BE DIRECTED AT THE CONTROL OF SYMPTOMS AND THE CLINICAL CONDITION OF THE PATIENT.

DUE TO THE IRRITATING NATURE OF THE MATERIAL, ANY ASPIRATION DURING VOMITING COULD RESULT IN SEVERE LUNG INJURY, THEREFORE, EMESIS SHOULD NOT BE INDUCED MECHANICALLY OR PHARMACOLOGICALLY. HOWEVER, THE ACUTE PERORAL SYSTEMIC TOXICITY OF THE MATERIAL INDICATES THAT EVACUATION OF THE STOMACH CONTENTS SHOULD BE UNDERTAKEN AT THE EARLIEST POSSIBLE TIME BY MEANS CARRYING THE LEAST LIKELIHOOD OF ASPIRATION (e.g., THE USE OF GASTRIC LAVAGE WITH ENDOTRACHEAL INTUBATION).

=====
===

Precautions for Safe Handling and Use

=====
===
Steps If Material Released/Spill: SMALL SPILLS CAN BE FLUSHED WITH LARGE AMOUNTS OF WATER; LARGER SPILLS SHOULD BE COLLECTED FOR DISPOSAL.

Precautions-Handling/Storing: DO NOT GET IN EYES, ON SKIN, ON CLOTHING. DO NOT SWALLOW. AVOID BREATHING VAPOR AND AEROSOL. KEEP AWAY FROM HEAT AND FLAME. KEEP CONTAINER CLOSED. USE WITH ADEQUATE VENTILATION. WASH THOROUGHLY AFTER HANDLING. FOR INDUSTRY USE ONLY.

Personal Precautions: AVOID CONTACT WITH EYES. WEAR SUITABLE PROTECTIVE EQUIPMENT.

Control Measures

=====
===
Respiratory Protection: USE SELF-CONTAINED BREATHING APPARATUS IN HIGH VAPOR CONCENTRATIONS

Ventilation: GENERAL (MECHANICAL) ROOM VENTILATION IS EXPECTED TO BE SATISFACTORY WHERE THIS PRODUCT IS STORED AND HANDLED IN CLOSED EQUIPMENT. SPECIAL, LOCAL VENTILATION IS NEEDED AT POINTS WHERE VAPORS CAN BE EXPECTED TO ESCAPE TO THE WORKPLACE AIR.

Protective Gloves: NEOPRENE, NITRILE (NBR)

Eye Protection: MONOGOGGLES

Other Protective Equipment: CHEMICAL APRON, EYE BATH, SAFETY SHOWER.

Engineering Controls-Process Hazard: SUDDEN RELEASE OF HOT ORGANIC CHEMICAL VAPORS OR MISTS FROM PROCESS EQUIPMENT OPERATING AT ELEVATED TEMPERATURE AND PRESSURE, OR IGNITIONS WITHOUT THE PRESENCE OF OBVIOUS IGNITION SOURCES. PUBLISHED "AUTOIGNITION" OR "IGNITION" TEMPERATURE VALUES CANNOT BE TREATED AS SAFE OPERATING TEMPERATURES IN CHEMICAL PROCESSES WITHOUT ANALYSIS OF THE ACTUAL PROCESS CONDITIONS. ANY USE OF THIS PRODUCT IN ELEVATED-TEMPERATURE PROCESSES SHOULD BE THOROUGHLY EVALUATED TO ESTABLISH AND MAINTAIN SAFE OPERATING CONDITIONS. FURTHER INFORMATION IS AVAILABLE IN A TECHNICAL BULLETIN ENTITLED "IGNITION HAZARDS OF ORGANIC CHEMICAL VAPORS."

Toxicological Information

Acute Toxicity

Peroral: RAT LD50 3880 (3340-4510) MG/KG 10% DILUTION IN CORN OIL

Major Signs: PROSTRATION, TREMORS

Gross Pathology: LUNGS, LIVER, GASTROINTESTINAL TRACT DISCOLORED, SURFACE BURNS OF KIDNEY AND ADRENAL WHERE IN CONTACT WITH GASTROINTESTINAL TRACT

Percutaneous: RABBIT LD50 24 HR OCCLUDED CONTACT 4.49 (2.46-8.21) ml/kg

Major Signs: ERYTHEMA AND NECROSIS AT APPLICATION SITE

Gross Pathology: LUNGS, LIVER, KIDNEYS DISCOLORED

Inhalation: DYNAMIC GENERATION OF VAPOR. EXPOSURE TIME 8 HR

Rat: Room Temperature Kill Rate: 0/6

Major Signs: LIGHT ANESTHESIA

Irritation-Skin: RABBIT 4 HR COVERED NECROSIS IN _

Skin: RABBIT 24HR UNCOVERED NO IRRITATION

Eye: RABBIT 0.005 ml SEVERE CORNEAL INJURY

Eye: RABBIT 0.5ml 15% DILUTION IN PROPYLENE GLYCOL NO INJURY

Additional Studies: REPEATED INHALATION OF AEROSOLS MAY RESULT IN PULMONARY EDEMA AND KIDNEY INJURY.

=====
==
Transportation Data
=====

====
DOT Proper Shipping Name: AMYL ALCOHOLS
DOT Class: 3
DOT ID Number: UN1105
DOT Pack Group: PG III

THIS INFORMATION IS NOT INTENDED TO CONVEY ALL SPECIFIC REGULATORY OR OPERATIONAL REQUIREMENTS/INFORMATION RELATING TO THIS PRODUCT. ADDITIONAL TRANSPORTATION SYSTEM INFORMATION CAN BE OBTAINED THROUGH YOUR SALES OR CUSTOMER SERVICE REPRESENTATIVE. IT IS THE RESPONSIBILITY OF THE TRANSPORTING ORGANIZATION TO FOLLOW ALL APPLICABLE LAWS, REGULATIONS AND RULES RELATING TO THE TRANSPORTATION OF THE MATERIAL.

=====
====
Disposal Data
=====

====
INCINERATE IN A FURNACE WHERE PERMITTED UNDER FEDERAL, STATE, AND LOCAL REGULATIONS. DISPOSE IN ACCORDANCE WITH ALL APPLICABLE FEDERAL, STATE, PROVINCIAL, AND LOXAL ENVIRONMENTAL REGULATIONS. EMPTY CONTAINERS SHOULD BE RECYCLED OR DISPOSED OF THROUGH AN APPROVED WASTE MANAGEMENT FACILITY.

AT VERY LOW CONCETRATIONS IN WATER, THIS PRODUCT IS BIODEGRADABLE IN A BIOLOGICAL WASTEWATER TREATMENT PLANT. DISPOSAL METHODS IDENTIFIED ARE FOR THE PRODUCT AS SOLD. FOR PROPER DISPOSAL OF USED MATERIAL, AN ASSESSMENT MUST BE COMPLETED TO DETERMINE THE PROPER AND PERMISSIBLE WASTE MANAGEMENT OPTIONS PERMISSIBLE UNDER APPLICABLE RULES, REGULATIONS AND/OR LAWS GOVERNING YOUR LOCATION.

=====
====
Ecological Information
=====

====
BOD: (% Oxygen Consumption)
Day: 5 57%
Day: 10 73%
Day: 20 74%
Day: 30

Ecotoxicity To Fish: FATHEAD MINNOW LC50 96 HR 500 mg/l

Further Information-THOD: (CALCULATED) 2.73 mg/mg
Environmental Precautions: THIS PRODUCT MAY BE TOXIC TO FISH; AVOID DISCHARGE TO NATURAL WATERS.

=====
=====
Label Data
=====

=====
Common Name: PRIMARY AMYL ALCOHOL

Signal Word: DANGER

Hazards Of The Product: CAUSES EYE AND SKIN IRRITATION. HARMFUL AND IRRITATING IF SWALLOWED. HARMFUL IF INHALED. COMBUSTIBLE. ASPIRATION MAY CAUSE LUNG DAMAGE. MAY CAUSE DIZZINESS AND DROWSINESS.

Protect Eye: YES

Protect Skin: YES

Protect Respiratory: YES

The information contained herein is based on data considered to be accurate. However, no warranty is expressed regarding the accuracy of these data or the results to be obtained from the use thereof. It is the user's obligation to determine the conditions of safe use of the product.

Pentyl Ether, 99% (GC)/HMIS_Msds/WEB/wcd0004c/wcd04ce2.htm (16 hits)

Pentyl Ether, 99% (GC) ACROS64655

**** SECTION 1 - CHEMICAL PRODUCT AND COMPANY IDENTIFICATION ****

MSDS Name: Pentyl Ether, 99% (GC)

Catalog Numbers: AC417030000, AC417030250, AC417031000

Synonyms: Amyl Ether; N-Amyl Ether; Diamyl Ether; Di-N-Amyl Ether; Dipentyl Ether; Ether, Di-N-Pentyl-; 1,1'-Oxybis-pentane; Pentane,1,1'-Oxybis-

Company Identification (Europe): Acros Organics N.V. Janssen Pharmaceuticaaan 3a
2440 Geel, Belgium

Company Identification (USA): Acros Organics One Reagent Lane
Fairlawn, NJ 07410

For information in North America, call: 800-ACROS-01

For information in Europe, call: 0032(0) 14575211

For emergencies in the US, call CHEMTREC: 800-424-9300

For emergencies in Europe, call: 0032(0) 14575299

****** SECTION 2 - COMPOSITION, INFORMATION ON INGREDIENTS ******

CAS#	Chemical Name	%	EINECS#
693-65-2	Amyl Ether	99%	211-756-8

****** SECTION 3 - HAZARDS IDENTIFICATION ******

EMERGENCY OVERVIEW

Appearance: colorless liquid. Flash Point: 57 deg C.

Caution! Combustible liquid. The toxicological properties of this material have not been fully investigated. May cause eye and skin irritation. May cause respiratory and digestive tract irritation.

Target Organs: None known.

Potential Health Effects

Eye:

May cause eye irritation. Causes redness and pain. The toxicological properties of this material have not been fully investigated.

Skin:

May cause skin irritation. The toxicological properties of this material have not been fully investigated.

Ingestion:

May cause irritation of the digestive tract. The toxicological properties of this substance have not been fully investigated.

Inhalation:

May cause respiratory tract irritation. The toxicological properties of this substance have not been fully investigated.

Chronic:

No information found.

**** SECTION 4 - FIRST AID MEASURES ****

Eyes:

Flush eyes with plenty of water for at least 15 minutes, occasionally lifting the upper and lower eyelids. Get medical aid.

Skin:

Get medical aid. Flush skin with plenty of soap and water for at least 15 minutes while removing contaminated clothing and shoes. Wash clothing before reuse.

Ingestion:

Never give anything by mouth to an unconscious person. Get medical aid. Do NOT induce vomiting. If conscious and alert, rinse mouth and drink 2-4 cupfuls of milk or water. Wash mouth out with water.

Inhalation:

Remove from exposure to fresh air immediately. If not breathing, give artificial respiration. If breathing is difficult, give oxygen. Get medical aid.

Notes to Physician:

Treat symptomatically and supportively.

**** SECTION 5 - FIRE FIGHTING MEASURES ****

General Information:

As in any fire, wear a self-contained breathing apparatus in pressure-demand, MSHA/NIOSH (approved or equivalent), and full protective gear. During a fire, irritating and highly toxic gases may be generated by thermal decomposition or combustion. Will burn if involved in a fire. Use water spray to keep fire-exposed containers cool. Combustible Liquid. Vapors may be heavier than air. They can spread along the ground and collect in low or confined areas. Containers may explode when heated.

Extinguishing Media:

Use water spray to cool fire-exposed containers. Use agent most appropriate to extinguish fire. In case of fire use water spray, dry chemical, carbon dioxide, or appropriate foam.

**** SECTION 6 - ACCIDENTAL RELEASE MEASURES ****

General Information: Use proper personal protective equipment as indicated in Section 8.

Spills/Leaks:

Absorb spill with inert material, (e.g., dry sand or earth), then place into a chemical waste container. Avoid runoff into storm sewers and ditches which lead to waterways. Clean up spills immediately, observing precautions in the Protective Equipment section. Remove all sources of ignition. Use a spark-proof tool. Provide ventilation.

**** SECTION 7 - HANDLING and STORAGE ****

Handling:

Use with adequate ventilation. Use spark-proof tools and explosion proof equipment. Avoid breathing dust, vapor, mist, or gas. Avoid contact with eyes, skin, and

clothing. Empty containers retain product residue, (liquid and/or vapor), and can be dangerous. Keep container tightly closed. Avoid contact with heat, sparks and flame.

Avoid ingestion and inhalation. Do not pressurize, cut, weld, braze, solder, drill, grind, or expose empty containers to heat, sparks or open flames.

Storage:

Keep away from heat, sparks, and flame. Keep away from sources of ignition. Store in a tightly closed container. Store in a cool, dry, well-ventilated area away from incompatible substances.

**** SECTION 8 - EXPOSURE CONTROLS, PERSONAL PROTECTION ****

Engineering Controls:

Facilities storing or utilizing this material should be equipped with an eyewash facility and a safety shower. Use adequate ventilation to keep airborne concentrations low.

Exposure Limits

Chemical Name	ACGIH	NIOSH	OSHA - Final PELs
Amyl Ether	none listed	none listed	none listed

OSHA Vacated PELs:

Amyl Ether:

No OSHA Vacated PELs are listed for this chemical.

Personal Protective Equipment

Eyes:

Wear appropriate protective eyeglasses or chemical safety goggles as described by OSHA's eye and face protection regulations in 29 CFR 1910.133 or European Standard EN166.

Skin:

Wear appropriate protective gloves to prevent skin exposure.

Clothing:

Wear appropriate protective clothing to prevent skin exposure.

Respirators:

Follow the OSHA respirator regulations found in 29CFR 1910.134 or European Standard EN 149. Always use a NIOSH or European Standard EN 149 approved respirator when necessary.

**** SECTION 9 - PHYSICAL AND CHEMICAL PROPERTIES ****

Physical State: Liquid
Appearance: colorless liquid
Odor: Not available.
pH: Not available.
Vapor Pressure: .7 hPa @20 deg C
Vapor Density: 5.46

Evaporation Rate: Not available.
Viscosity: Not available.
Boiling Point: 183.0 - 185.0 deg C @ 760.00m
Freezing/Melting Point: 0 deg C
Autoignition Temperature: 170 deg C (338.00 deg F)
Flash Point: 57 deg C (134.60 deg F)
NFPA Rating: (est.) Health: 1; Flammability: 2; Reactivity: 0
Explosion Limits, Lower: 2.00 vol %
Upper: 8.00 vol %
Decomposition Temperature:
Solubility: immiscible with water
Specific Gravity/Density: .7800g/cm3
Molecular Formula: C10H22O
Molecular Weight: 158.28

**** SECTION 10 - STABILITY AND REACTIVITY ****

Chemical Stability:

On long term storage, substances with similar functional groups form explosive peroxides.

Conditions to Avoid:

Incompatible materials, light, ignition sources, exposure to air, excess heat.

Incompatibilities with Other Materials:

Oxidizing agents.

Hazardous Decomposition Products:

Carbon monoxide, irritating and toxic fumes and gases, carbon dioxide.

Hazardous Polymerization: Will not occur.

**** SECTION 11 - TOXICOLOGICAL INFORMATION ****

RTECS#:

CAS# 693-65-2: SC2900000

LD50/LC50:

Not available.

Carcinogenicity:

Amyl Ether -

Not listed by ACGIH, IARC, NIOSH, NTP, or OSHA.

Epidemiology:

No information available.

Teratogenicity:

No information available.

Reproductive Effects:

No information available.

Neurotoxicity:

No information available.

Mutagenicity:

No information available.

Other Studies:

See actual entry in RTECS for complete information.

**** SECTION 12 - ECOLOGICAL INFORMATION ****

**** SECTION 13 - DISPOSAL CONSIDERATIONS ****

Chemical waste generators must determine whether a discarded chemical is classified as a hazardous waste.

US EPA guidelines for the classification determination are listed in 40 CFR Part 261. Additionally, waste generators must consult state and local hazardous waste regulations to ensure complete and accurate classification.

RCRA P-Series: None listed.

RCRA U-Series: None listed.

**** SECTION 14 - TRANSPORT INFORMATION ****

US DOT

Shipping Name: FLAMMABLE LIQUID, N.O.S.
(PENTYL ETHER)

Hazard Class: 3

UN Number: UN1993

Packing Group: III

Canadian TDG

No information available.

**** SECTION 15 - REGULATORY INFORMATION ****

US FEDERAL

TSCA

CAS# 693-65-2 is listed on the TSCA inventory.

Health & Safety Reporting List

None of the chemicals are on the Health & Safety Reporting List.

Chemical Test Rules

None of the chemicals in this product are under a Chemical Test Rule.

Section 12b

None of the chemicals are listed under TSCA Section 12b.

TSCA Significant New Use Rule

None of the chemicals in this material have a SNUR under TSCA.

SARA

Section 302 (RQ)

None of the chemicals in this material have an RQ.

Section 302 (TPQ)

None of the chemicals in this product have a TPQ.

Section 313

No chemicals are reportable under Section 313.

Clean Air Act:

This material does not contain any hazardous air pollutants.

This material does not contain any Class 1 Ozone depleters.

This material does not contain any Class 2 Ozone depleters.

Clean Water Act:

None of the chemicals in this product are listed as Hazardous Substances under the CWA.

None of the chemicals in this product are listed as Priority Pollutants under the CWA.

None of the chemicals in this product are listed as Toxic Pollutants under the CWA.

OSHA:

None of the chemicals in this product are considered highly hazardous by OSHA.

STATE

Amyl Ether is not present on state lists from CA, PA, MN, MA, FL, or NJ.

California No Significant Risk Level:

None of the chemicals in this product are listed.

European/International Regulations

European Labeling in Accordance with EC Directives

Hazard Symbols: Not available.

Risk Phrases:

Safety Phrases:

S 16 Keep away from sources of ignition - No smoking.

S 28A After contact with skin, wash immediately with plenty of water.

S 37 Wear suitable gloves.

S 45 In case of accident or if you feel unwell, seek medical advice immediately (show the label where possible).

WGK (Water Danger/Protection)

CAS# 693-65-2: No information available.

United Kingdom Occupational Exposure Limits

Canada

CAS# 693-65-2 is listed on Canada's DSL/NDSL List.

This product has a WHMIS classification of B3.

CAS# 693-65-2 is not listed on Canada's Ingredient Disclosure List.

Exposure Limits

**** SECTION 16 - ADDITIONAL INFORMATION ****

MSDS Creation Date: 2/24/1999 Revision #1 Date: 8/02/2000

The information above is believed to be accurate and represents the best information currently available to us. However, we make no warranty of merchantability or any other warranty, express or implied, with respect to such information, and we assume no liability resulting from its use. Users should make their own investigations to determine the suitability of the information for their particular purposes. In no way shall the company be liable for any claims, losses, or damages of any third party or for lost profits or any special, indirect, incidental, consequential or exemplary damages, howsoever arising, even if the company has been advised of the possibility of such damages.



Product Information (203) 740-3471 / Emergency Assistance CHEMTREC 1-800-424-9300 or 202-483-7616

MATERIAL SAFETY DATA SHEETS

Part Number/Trade Name: DIOXANE
This MSDS is valid for all grades and catalog numbers

General Information

Company's Name: PHARMCO PRODUCTS, INC.	Date MSDS Revised: Nishant-8/23/99
Company's Street: 58 VALE RD.	Safety Data Review Date: 8/23/99
Company's City: BROOKFIELD	Preparer's Company: PHARMCO PRODUCTS, INC.
Company's State: CT	Preparer's St Or P. O. Box: 58 VALE RD.
Company's Zip Code: 06804	Preparer's City: BROOKFIELD
Company's Emerg Ph #: (203) 740-3471	Preparer's State: CT
Company's Info Ph #: (203) 740-3471	Preparer's Zip Code: 06804

Ingredients/Identity Information

Ingredient: 1,4-DIOXANE (DIETHYLENE DIOXIDE) (SARA III)	CAS Number: 123-91-1
Ingredient Sequence Number: 01	OSHA PEL: S, 100 PPM
NIOSH (RTECS) Number: JG8225000	ACGIH TLV: S, 25 PPM; 9293
	Other Recommended Limit: NONE SPECIFIED

Physical/Chemical Characteristics

Appearance And Odor: COLORLESS LIQUID - ETHEREAL ODOR	Decomposition Temperature: UNKNOWN
Boiling Point: 214F,101C	Evaporation Rate And Ref: 2.7 (N-BUTYL ACETATE=1)
Melting Point: 53.2F,11.8C	Solubility In Water: MISCIBLE
Vapor Pressure (MM Hg/70 F): 29	Percent Volatiles By Volume: 100
Vapor Density (Air=1): 3.03	Viscosity: UNKNOWN
Specific Gravity: 1.035	Corrosion Rate (IPY): UNKNOWN

Fire and Explosion Hazard Data

Flash Point: 54.0F,12.2C
Flash Point Method: CC
Lower Explosive Limit: 2.0
Upper Explosive Limit: 22.0

Extinguishing Media: USE WATER FOG, CARBON DIOXIDE, ALCOHOL FOAM, OR DRY CHEMICAL.

Special Fire Fighting Proc: WEAR FIRE FIGHTING PROTECTIVE EQUIPMENT AND A FULL FACED SELF CONTAINED BREATHING APPARATUS. COOL FIRE EXPOSED CONTAINERS WITH WATER SPRAY.

Unusual Fire And Expl Hazrds: VAPORS FORM EXPLOSIVE MIXTURES IN AIR; VAPORS ARE HEAVIER THAN AIR AND CAN TRAVEL CONSIDERABLE DISTANCE TO A SOURCE OF IGNITION AND FLASH BACK.

=====
=====
Reactivity Data
=====

=====
Stability: YES

Cond To Avoid (Stability): HIGH HEAT, SPARKS, OPEN FLAMES AND OTHER SOURCES OF IGNITION. PROLONGED STORAGE CAN FACILITATE FORMATION OF PEROXIDE.

Materials To Avoid: NICKEL, OXIDIZERS, OXYGEN, HALOGENS, HCL, SO3, SILVER PERCHLORATE, HYDROGEN PEROXIDE

Hazardous Decomp Products: COX, PEROXIDES

Hazardous Poly Occur: NO

Conditions To Avoid (Poly): NOT APPLICABLE
=====

=====
Health Hazard Data
=====

=====
LD50-LC50 Mixture: LD50 (ORAL RAT) IS UNKNOWN

Route Of Entry - Inhalation: YES

Route Of Entry - Skin: YES

Route Of Entry - Ingestion: NO

Health Haz Acute And Chronic: ACUTE-TOXIC AMOUNTS CAN BE ABSORBED THROUGH SKIN; REPEATED INHALATION OF LOW CONCENTRATIONS CAN BE FATAL. MAY CAUSE INJURY TO LIVER AND KIDNEYS, POSSIBLY LEADING TO DEATH. CAUSES IRRITATION OF EYES, SKIN AND RESPIRATORY PASSAGES. CHRONIC-MAY CAUSE LIVER AND KIDNEYS INJURY.

Carcinogenicity - NTP: YES

Carcinogenicity - IARC: YES

Carcinogenicity - OSHA: NO

Explanation Carcinogenicity: SUSPECTED CARCINOGEN PER 1979 NIOSH REGISTRY OF TOXIC EFFECTS OF CHEMICAL SUBSTANCES (MSDS).

Signs/Symptoms Of Overexp: HEADACHE, NAUSEA AND EYE IRRITATION

Med Cond Aggravated By Exp: PERSONS WITH PRE-EXISTING SKIN DISORDERS OR EYE PROBLEMS OR IMPAIRED LIVER, KIDNEY OR RESPIRATORY FUNCTION MAY BE MORE

SUSCEPTIBLE TO THE EFFECTS OF THE SUBSTANCE.

Emergency/First Aid Proc: GET IMMEDIATE MEDICAL ASSISTANCE FOR ALL CASES OF OVEREXPOSURE. INHALATION: REMOVE TO FRESH AIR. EYES: IMMEDIATELY FLUSH WITH

WATER FOR 15 MINUTES HOLDING EYELIDS OPEN. SKIN: REMOVE CONTAMINATED CLOTHING. WASH SKIN WITH SOAP AND WATER. INGESTION: GET IMMEDIATE HELP.
=====

=====
Precautions for Safe Handling and Use
=====

=====
Steps If Matl Released/Spill: ELIMINATE ALL SOURCES OF IGNITION. ABSORB

MATERIAL IN VERMICULITE/OTHER SUITABLE ABSORBENT & PLACE IN IMPERVIOUS CONTAINER.

Neutralizing Agent: NOT APPLICABLE.

Waste Disposal Method: DISCHARGE, TREATMENT OR DISPOSAL MAY BE SUBJECT TO LOCAL, STATE AND FEDERAL REGULATIONS.

Precautions-Handling/Storing: STORAGE-STORE IN A COOL, DRY, WELL VENTILATED AREA AWAY FROM OXIDIZERS, HEAT, FLAME, COMBUSTIBLE.

Other Precautions: PEROXIDE CONTENT SHOULD BE CHECKED BEFORE USE OF MATERIAL WHICH HAS BEEN STORED FOR A LONG TIME. WASH THOROUGHLY AFTER HANDLING. AVOID CONTACT WITH EYES AND SKIN. DO NOT BREATHE VAPORS.

=====
===

Control Measures

=====
===

Respiratory Protection: USE NIOSH/MSHA APPROVED ORGANIC VAPOR RESPIRATOR AS REQUIRED IF ABOVE PEL/TLV OR SELF CONTAINED BREATHING APPARATUS IN AN ENCLOSED AREA.

Ventilation: LOCAL/MECHANICAL (NON-SPARKING) EXHAUST TO MAINTAIN PEL/TLV.

Protective Gloves: NEOPRENE, NITRILE, OR NATURAL RUBBER

Eye Protection: SAFETY GOGGLES WITH OPTIONAL FACE SHIELD

Other Protective Equipment: EYE WASH STATION AND SAFETY SHOWER, WORK CLOTHING AND APRON AS REQUIRED.

Work Hygienic Practices: OBSERVE GOOD PERSONAL HYGIENE PRACTICES AND RECOMMENDED PROCEDURES. DO NOT WEAR CONTAMINATED CLOTHING OR FOOTWEAR.

=====
===

Transportation Data

=====
===

DOT PSN Code: FNF

DOT Proper Shipping Name: DIOXANE

DOT Class: 3

DOT ID Number: UN1165

DOT Pack Group: II

DOT Label: FLAMMABLE LIQUID

IMO PSN Code: GED

IMO Proper Shipping Name: DIOXANE

IMO Regulations Page Number: 3217

IMO UN Number: 1165

IMO UN Class: 3.2

IMO Subsidiary Risk Label: -

IATA PSN Code: KEZ

IATA UN ID Number: 1165

IATA Proper Shipping Name: DIOXANE

IATA UN Class: 3

IATA Label: FLAMMABLE LIQUID

AFI PSN Code: KEZ

AFI Prop. Shipping Name: DIOXANE

AFI Class: 3

AFI ID Number: UN1165

AFI Pack Group: II

AFI Label: FLAMMABLE LIQUID

AFI Basic Pac Ref: 7-7

Additional Trans Data: NONE

=====
===

Disposal Data

=====
===

Refer to applicable regional, state and federal codes.

=====
===

Label Data

=====
===

Common Name: DIOXANE, ACS

Special Hazard Precautions: ACUTE-TOXIC AMOUNTS CAN BE ABSORBED THROUGH

SKIN; REPEATED INHALATION OF LOW CONCENTRATIONS CAN BE FATAL. MAY CAUSE INJURY TO LIVER AND KIDNEYS, POSSIBLY LEADING TO DEATH. CAUSES IRRITATION OF EYES, SKIN AND RESPIRATORY PASSAGES. CHRONIC-MAY CAUSE LIVER AND KIDNEYS INJURY. HEADACHE, NAUSEA AND EYE IRRITATION

The information contained herein is based on data considered to be accurate. However, no warranty is expressed regarding the accuracy of these data or the results to be obtained from the use thereof. It is the user's obligation to determine the conditions of safe use of the product.



Product Information (203) 740-3471 / Emergency Assistance CHEMTREC 1-800-424-9300 or 202-483-7616

MATERIAL SAFETY DATA SHEETS

Part Number/Trade Name: PENTANE
This MSDS is valid for all grades and catalog numbers

General Information

Company's Name: PHARMCO PRODUCTS, INC.	Date MSDS Revised: Nishant-8/23/99
Company's Street: 58 VALE RD.	Safety Data Review Date: 8/23/99
Company's City: BROOKFIELD	Preparer's Company: PHARMCO PRODUCTS, INC.
Company's State: CT	Preparer's St Or P. O. Box: 58 VALE RD.
Company's Zip Code: 06804	Preparer's City: BROOKFIELD
Company's Emerg Ph #: (203) 740-3471	Preparer's State: CT
Company's Info Ph #: (203) 740-3471	Preparer's Zip Code: 06804

Ingredients/Identity Information

Ingredient: PENTANE	CAS Number: 109-66-0
Ingredient Sequence Number: 01	OSHA PEL: 1000 PPM/750 STEL
NIOSH (RTECS) Number: RZ9450000	ACGIH TLV: 600 PPM/750STEL;9293

Physical/Chemical Characteristics

Appearance And Odor: CLEAR, COLORLESS LIQUID WITH A MILD HYDROCARBON ODOR.	Vapor Density (Air=1): 2.5
Boiling Point: 96.9F,36.1C	Specific Gravity: SUPP DATA
Vapor Pressure (MM Hg/70 F): 420 @ 20C	Evaporation Rate And Ref: CA 29 (BUAC=1)
	Solubility In Water: 0.04% @ 20C
	Percent Volatiles By Volume: CA 100

Fire and Explosion Hazard Data

Flash Point: -40F,-40C
Flash Point Method: TCC
Lower Explosive Limit: 1.5%
Upper Explosive Limit: 7.8%
Extinguishing Media: CARBON DIOXIDE, DRY CHEMICAL OR FOAM.
Special Fire Fighting Proc: WEAR NIOSH/MSHA APPRVD SCBA & FULL PROT EQUIP

(FP N).WATER WILL NOT BE EFTIVE IN EXTING FIRE & MAY SPREAD IT,BUT WATER SPRAY CAN BE USED TO COOL EXPOSED CNTNRS.
Unusual Fire And Expl Hazrds: HEAT WILL BUILD PRESSURE AND MAY RUPTURE CLOSED STORAGE CONTAINERS.

=====
=====
Reactivity Data
=====

=====
Stability: YES
Cond To Avoid (Stability): HEAT, SPARKS, OPEN FLAME, OPEN CONTAINERS, AND POOR VENTILATION.
Materials To Avoid: STRONG OXIDIZING AGENTS.
Hazardous Decomp Products: INCOMPLETE COMBUSTION CAN GENERATE CARBON MONOXIDE AND OTHER TOXIC VAPORS.
Hazardous Poly Occur: NO
Conditions To Avoid (Poly): NOT RELEVANT
=====

=====
Health Hazard Data
=====

=====
LD50-LC50 Mixture: NONE SPECIFIED BY MANUFACTURER.
Route Of Entry - Inhalation: YES
Route Of Entry - Skin: YES
Route Of Entry - Ingestion: YES
Health Haz Acute And Chronic: PENTANE IS A MILD EYE AND MUCOUS MEMBRANE IRRITANT, PRIMARY SKIN IRRITANT, AND CENTRAL NERVOUS SYSTEM DEPRESSANT. ACUTE: EXPOSURE IRRITATES THE EYES AND RESPIRATORY TRACT. EXTREME EXPOSURE CAN CAUSE DERMATITIS.
Carcinogenicity - NTP: NO
Carcinogenicity - IARC: NO
Carcinogenicity - OSHA: NO
Explanation Carcinogenicity: NOT RELEVANT
Signs/Symptoms Of Overexp: INHAL: EXPOSURE CAN CAUSE DIZZINESS, HEADACHE, NAUSEA, AND NARCOSIS. EYE: LIQUID AND HIGH VAPOR CONCENTRATION CAN BE IRRITATING. SKIN: PROLONGED OR REPEATED SKIN CONTACT CAN CAUSE IRRITATION AND DERMATITIS THROUGH DEFATTING OF SKIN. INGEST: CAN CAUSE GASTROINTESTINAL TRACT DISCOMFORT.
Med Cond Aggravated By Exp: PRECLUDE FROM EXPOSURE THOSE INDIVIDUALS SUSCEPTIBLE TO DERMATITIS.
Emergency/First Aid Proc: INHAL:IMMED REMOVE TO FRESH AIR. IF NOT BRTHG, ADMIN MOUTH-TO-MOUTH RESCUE BRTHG. IF THERE IS NO PULSE ADMIN CPR. CONT MD IMMED. EYE: RINSE W/COPIOUS AMTS OF WATER FOR @ LST 15 MINS. GET EMER MED ASSISTANCE. SKIN:FLUSH THORO FOR @ LST 15 MINS. WASH AFFECTED AFFECTED SKIN W/SOAP & WATER. REMOVE CONTAMD CLTHG & SHOES. WASH CLTHG BEFORE RE-USE, &
DISCARD CONTAMD SHOES. GET EMER MED (SUPP DATA)
=====

=====
Precautions for Safe Handling and Use
=====

=====
Steps If Matl Released/Spill: PROT FROM IGNIT.WEAR PROT CLTHG & USE NIOSH/MSHA APPRVD RESP EQUIP.ABSORB SPILLED MATL IN ABSORB RECD FOR SOLV SPILLS &
REMOVE TO SAFE LOCATION FOR DISP BY APPRVD METHS.IF RELEASED TO ENVIRON, COMPLY W/ALL REGULATORY NOTIFICATION REQMTS. (SUPP DATA)

Neutralizing Agent: NONE SPECIFIED BY MANUFACTURER.
Waste Disposal Method: DIPOSE OF PENTANE AS AN EPA HAZ WASTE. CONTACT STATE ENVIRON AGENCY FOR LISTING OF LICENSED HAZARDOUS WASTE DISPOSAL FACILITIES AND APPLICABLE REGULATIONS. HAZARDOUS WASTE NUMBER: D001 (IGNITABLE). DISPOSE OF I/A/W FED, STATE AND LOCAL REGS (FP N).
Precautions-Handling/Storing: PENTANE SHLD BE PROTECTED FROM TEMP EXTREMES & DIRECT SUNLIGHT. PROPER STOR OF PENTANE MUST BE DETERM BASED ON OTHER MATLS STORED & THEIR (ING 5)
Other Precautions: GROUND AND BOND METAL CONTAINERS TO MINIMIZE STATIC SPARKS. STOR OF PENTANE UNDER HOT CNDTNS (>36C) WILL CAUSE BOILING OF LIQ. IF CNTNR IS OPENED BEFORE ALLOWING LIQ TO COOL TO ROOM TEMP (22C), THE LIQ COULD BOIL OVER OUT OF THE CONTAINER.

=====
===

Control Measures

=====
===

Respiratory Protection: USE NIOSH/MSHA APPROVED RESPIRATOR EQUIPMENT. FOLLOW NIOSH AND EQUIPMENT MFR'S RECOMMENDATIONS TO DETERMINE APPROPRIATE EQUIPMENT (AIR-PURIFYING, AIR-SUPPLIED, OR SCBA).
Ventilation: ADEQ VENT IS REQD TO PROT PERS FROM EXPOS TO CHEM VAPS EXCEEDING PEL & TO MINIMIZE FIRE HAZ. THE CHOICE OF (SUPP DATA)
Protective Gloves: NEOPRENE OR NITRILE RUBBER GLOVES.
Eye Protection: CHEM WORK GOG/FULL LGTH FSHLD (FP N).
Other Protective Equipment: EMER EYEWASH FOUNTAINS & SAFETY SHOWERS SHLD BE AVAILABLE IN VICINITY OF ANY POTENTIAL EXPOS. PROTECTIVE (ING 2)
Work Hygienic Practices: NONE SPECIFIED BY MANUFACTURER.
Suppl. Safety & Health Data: SPEC GRAV:0.626 @ 20C (H*2O=1).FIRST AID PROC:ASSISTANCE. INGEST:CALL LOC POISON CONTROL CENTER FOR ASSISTANCE. CONT
MD IMMED. ASPIR HAZ - DO NOT INDUCE VOMIT. SPILL PROC: CERCLA REPORTABLE QUANTITY - 5,000 LBS. VENT: VENT EQUIP, EITHER LOC/GEN, WILL DEPEND ON CNDTNS OF USE, QTY OF MATL & OTHER OPERATING PARAMETERS.

=====
===

Transportation Data

=====
===

Trans Data Review Date: 93096	IATA PSN Code: TAU
DOT PSN Code: LHZ	IATA UN ID Number: 1265
DOT Proper Shipping Name: PENTANES *	IATA Proper Shipping Name: PENTANES, *
DOT Class: 3	IATA UN Class: 3
DOT ID Number: UN1265	IATA Label: FLAMMABLE LIQUID
DOT Pack Group: I	AFI PSN Code: TAU
DOT Label: FLAMMABLE LIQUID	AFI Prop. Shipping Name: N- PENTANE OR ISOPENTANE *
IMO PSN Code: LGJ	AFI Class: 3
IMO Proper Shipping Name: PENTANES	AFI ID Number: UN1265
IMO Regulations Page Number: 3140	AFI Pack Group: I
IMO UN Number: 1265	AFI Label: FLAMMABLE LIQUID
IMO UN Class: 3.1	AFI Basic Pac Ref: 7-6
IMO Subsidiary Risk Label: -	

=====
===

Disposal Data

=====
===

Refer to applicable regional, state and federal codes.

=====
=====
Label Data
=====

=====
Label Required: YES
Common Name: PENTANE
Chronic Hazard: NO
Signal Word: DANGER!
Acute Health Hazard-Moderate: X
Contact Hazard-Moderate: X
Fire Hazard-Severe: X
Reactivity Hazard-None: X
Special Hazard Precautions: FLAMMABLE.
KEEP AWAY FROM HEAT, SPARKS AND
FLAME. ACUTE: INHALATION CAN
CAUSE DIZZINESS, HEADACHE, NAUSEA
AND
NARCOSIS. SWALLOWING CAN CAUSE
GASTROINTESTINAL TRACT
DISCOMFORT. CAN CAUSE
EYE AND SKIN IRRITATION. CAN CAUSE
DERMATITIS. CHRONIC: NONE LISTED BY
MANUFACTURER.
Protect Eye: Y
Protect Skin: Y
Protect Respiratory: Y

The information contained herein is based on data considered to be accurate. However, no warranty is expressed regarding the accuracy of these data or the results to be obtained from the use thereof. It is the user's obligation to determine the conditions of safe use of the product.



MATERIAL SAFETY DATA SHEETS

Product Information (203) 740-3471 / Emergency Assistance CHEMTREC 1-800-424-9300

SECTION I

PRODUCT AND COMPANY IDENTIFICATION

PRODUCT: n-Hexane, 85% min
This MSDS is valid for all grades of 85% min
(Cat# 35900HPLC, 359000DIS)

Synonyms: n-hexane, hexyl hydride, dipropyl, normal hexane

Formula: CH₃(CH₂)₄CH₃; note that this product is a mixture of n-hexane and other hexane isomers

Manufacturer: Pharmco Products Inc.
58 Vale Road
Brookfield, Connecticut 06804, USA
Phone (203) 740-3471
Fax (203) 740-3481

Emergency Contact:
CHEMTREC 1-800-424-9300

SECTION II

COMPOSITION /INFORMATION ON INGREDIENTS

%wt	Material	CAS	Exposure Limits
100%	Hexanes (n-Hexane)	110-54-3	50ppm OSHA/PEL; ACGIH/ TLV

SECTION III

HAZARDS IDENTIFICATION

Routes of Exposure:

Swallowing: This material can enter lungs during swallowing or vomiting and cause lung damage. May cause irritation of the digestive tract, nausea, nervous system depression and giddiness.

Skin Absorption: No harmful effects reported.

Inhalation: May cause irritation of the throat and nose.

Skin Contact: Prolonged or repeated contact may cause irritation and drying of the skin.

Eye Contact: May cause irritation including stinging, tearing, and redness.

Effects of Repeated Overexposure: Irritation of nose, throat or digestive system. Depression of nervous system.

Medical Conditions Aggravated by Overexposure:

Repeated exposure may aggravate skin disorders respiratory disorder, male reproductive disorders and peripheral nerve disorders Exposure to high concentrations may cause irregular heartbeats. Persons with pre-existing heart disorders may be more susceptible to this effect.

SECTION IV FIRST AID

Obtain medical attention for all cases of over-exposure.

Swallowing: Aspiration hazard - DO NOT induce vomiting. Obtain medical attention immediately.

Skin: Wash skin with soap and water for at least 15 minutes

Inhalation: Remove to fresh air; Give artificial respiration if not breathing; If breathing is difficult oxygen may be given by qualified personnel; Obtain medical assistance is discomfort persists.

Eye Contact: Flush eyes with water for at least 15 minutes. Obtain medical assistance.

SECTION V FIRE FIGHTING MEASURES

Fire/Explosive Properties

Flash Point: -22C Tag Closed Cup

Flammable Limits in Air:

1.0 - 8.0%

Flammability Classification: 3 (NFPA)

1993 Emergency Response Guidebook: Guide 27

1996 North American Emergency Response Guidebook:

Guide 128

Extinguishing Media:

Small Fires: Use dry chemical, carbon dioxide, water spray or regular foam.

Large Fires: Water spray, fog or foam.

Special Fire Fighting Procedures: Use water spray to cool fire-exposed containers and structures; Use water spray to disperse vapors - re-ignition is possible; Use self-contained breathing apparatus and protective clothing.

Unusual Fire and Explosion Hazards:

Vapors may travel to source of ignition and flash back.

Vapors may settle in low or confined spaces.

May produce a floating fire hazard.

Static ignition hazard can result from handling and use.

SECTION VI

SPILL/ACCIDENTAL RELEASE MEASURES

All spills: Eliminate all ignition sources; ground all equipment; do not walk through spill; stop spill if possible; prevent entry into sewers, confined spaces, etc.; use a vapor suppressing foam to reduce vapors; absorb spill with non-combustible matter and transfer to containers; use non-sparking tools to collect absorbed material.

SECTION VII HANDLING AND STORAGE

Flammable material - keep away from heat, sparks, and flame; sudden releases of hot organic vapors or mists from process equipment operating at elevated temperature may result in ignitions without the presence of obvious ignition sources.

Avoid contact with eyes.

Keep container closed.

Use with adequate ventilation.

Ground container when transferring product.

Vapors may collect in containers; treat empty containers as hazardous.

Wash thoroughly after handling

Vapors may settle in low or confined areas

SECTION VIII EXPOSURE CONTROLS / PERSONAL PROTECTION

Ventilation: Special, local ventilation is needed where vapors escape to the workplace air

Respiratory Protection: Use self-contained breathing apparatus in high vapor concentration

Personal Protective Equipment: gloves, lab coat or uniform, safety glasses, eye wash, safety shower

SECTION IX

PHYSICAL AND CHEMICAL PROPERTIES

Appearance: clear, colorless liquid

Odor: characteristic, gasoline-like

Vapor pressure: 150 mm Hg @24.8C

Vapor density: 3.0 (air =1)

Boiling point @ 760mm Hg: Approximately 69C

Melting Point: -95C

Solubility in Water: Insoluble

Specific Gravity : 0.66

Evaporation Rate: not available

Percent Volatiles: 100%

SECTION X

STABILITY/REACTIVITY INFORMATION

Stability: Stable

Conditions to avoid: Heat, flame, etc.

Incompatibility/Materials to avoid: strong oxidizing/reducing agents

Hazardous Combustion/Decomposition Products:

Carbon monoxide and/or carbon dioxide

Hazardous Polymerization: Will not occur

SECTION XI DISPOSAL CONSIDERATIONS

Vapors may collect in empty containers. Treat empty containers as hazardous.

Dispose of spill-clean up and other wastes in accordance with Federal, State, and local regulations.

SECTION XII TRANSPORTATION INFORMATION

Proper Shipping Name: Hexanes

Hazard Class: 3

UN Number: 1208

Packing Group II

IMO Information: Hexanes

Label of Class: 3

Packing Group II

Low flashpoint group

SECTION XIII REGULATORY INFORMATION

Federal EPA

Comprehensive Environmental Response Compensation, and Liability Act of 1980 (CERCLA) requires notification of the National Response Center of release quantities of Hazardous Substances equal to or greater than the reportable quantities (RQs) in CFR. Components present in this product at a level which could require reporting under this statute are:

Chemical	CAS Number	Upper Bound Conc. %
Hexanes	110-54-3	100%

Superfund Amendments and Reauthorization Act of 1986 (SARA) Title III requires emergency planning based on threshold planning quantities and release reporting based on reportable quantities in 40 CFR 355 (used for SARA 302, 304, 311, and 312). Components present in this product at a level which could require reporting under this statute are: Hexane

Superfund Amendments and Reauthorization Act of 1986 (SARA) Title III requires submission of annual reports of release of toxic chemicals that appear in 40 CFR 372 (for SARA 313). This information must be included in all MSDS's that are copied and distributed for this material. Components present in this product at a level which could require reporting under the statute are:

Hexane (CAS 110-54-3) upper bound conc. 100%

Toxic Substances Control Act (TSCA) Status:

The ingredients of this product are on the TSCA inventory.

State Right to Know

California Proposition 65: This product may contain trace levels of benzene known to the State of California to cause cancer. This product may contain trace levels of toluene known to the State of California to be a developmental toxicant.

This product contains hexane which may be identified as a hazardous substance by individual States.

California SCAQMD Rule 443.1 (VOC's)

A Volatile Organic Compound (VOC) is any volatile compound of carbon excluding methane, carbon monoxide, carbonic acid, metallic carbides, or carbonates, ammonium carbonate, 1,1,1 tri-chloroethane, methylene chloride, (FC-23), (CFC-113), (CFC-12), (CFC-11), (CFC-22), (CFC-114) and (CFC-115).

674 g/l

The information contained herein is based on data considered to be accurate. However, no warranty is expressed regarding the accuracy of these data or the results to be obtained from the use thereof. It is the user's obligation to determine the conditions of safe use of the product.



Abstract in Spanish

1. INTRODUCCIÓN

Los gasóleos o combustibles diesel son mezclas de hidrocarburos de 12 a 22 átomos de carbono, de intervalo de punto de ebullición 200 – 375 °C a 1 atm. El combustible diesel que se comercializa es habitualmente una mezcla de corrientes de diversos procesos de refino, cuyo resultado es una mezcla líquida compleja de hidrocarburos saturados y aromáticos. Su composición está regulada, dentro de unos límites, por ejemplo en España sus propiedades están definidas por el RD 61/2006 (de 31 de enero).

La normativa no sólo especifica las propiedades del diesel sino también los límites de emisión de algunas sustancias. Estos límites se han reducido progresivamente, a medida que la preocupación sobre el efecto medioambiental de los gases de emisión de los motores diesel ha aumentado (al mismo tiempo que lo ha hecho el parque de vehículos diesel). Para cumplir con los límites de emisión dictados, los futuros combustibles diesel se caracterizarán, respecto a los actuales, por un mayor número de cetano, menor densidad, y menor contenido de aromáticos, poliaromáticos y de azufre.

Desde mediados de los noventa se ha apuntado la utilización de compuestos oxigenados de forma similar al empleo de oxigenados en las gasolinas de automoción. En este sentido, las características deseables en un compuesto oxigenado para ser introducido en el diesel son: elevado número de cetano, punto de ebullición elevado para satisfacer las especificaciones del “flash point”, buen comportamiento de flujo a baja temperatura (CP y CFPP bajos), miscible con varios tipos de gasóleo, densidad apropiada y materias primas adecuadas.

Los oxigenados convencionales (MTBE, TAME, MEK, etc.) no son adecuados para su uso en los gasóleos. El etanol, aunque compatible, no se mezcla de forma efectiva con el diesel, ya que la mezcla etanol-diesel separa fases cuando se exponen a pequeñas cantidades de agua y/o bajas temperaturas, de forma que deben añadirse diversos aditivos para asegurar una buena mezcla. Otros alcoholes tienen un número de cetano reducido. En un estudio sobre propiedades de mezcla de compuestos oxigenados en combustibles diesel se probaron 84 compuestos, incluyendo éteres, poli-éteres y ésteres. Se observó que los éteres lineales, simétricos o asimétricos con ≥ 9 átomos de carbono mostraban el mejor balance entre el NC de mezcla y las propiedades de flujo en frío. En la *Tabla 1* se muestran algunas propiedades de diversos éteres lineales como componentes del diesel

	Diesel	DNPE	DNHE	MOE	DNPM
Densidad a 15-20°C (kg/m ³)	850	787	793	790	840
Punto de ebullición (°C)	170-380	187	229		218
Viscosidad (cSt)	3-4	1.6		0.9	
Número de cetano	48-51	109	118	89	97
CP (°C)*	-2 a +5	-20	-5	-17	0
CFPP (°C)*	-4 a +3	-22	-7		-7
Punto de inflamación (°C)*	67	57	78		

*propiedades de mezcla; DNPE (di-n-pentil éter), DNHE (di-n-hexil éter), MOE (metil n-octil éter), DNPM (di-n-pentoxi metano)

Tabla I. Propiedades de algunos éteres lineales

De otros trabajos se puede concluir que, desde un punto de vista técnico, el DNPE es un oxigenado apropiado para mezclar con el diesel, pues mejora las propiedades del diesel base, y la disponibilidad de materias primas potenciales es atractiva. Además, el DNPE se ha mostrado muy eficaz en reducir emisiones del diesel como CO, NO_x, hidrocarburos sin quemar, humos y partículas.

Es necesaria la presencia de un catalizador ácido para que la reacción de deshidratación intermolecular de 1-pentanol a DNPE y agua tenga lugar. Desgraciadamente, algunas reacciones secundarias son inevitables, como la deshidratación del 1-pentanol a 1-penteno, la isomerización del 1-penteno a 2-penteno (cis y trans), además de la formación de éteres ramificados.

2. OBJETIVOS

Con este trabajo se pretende estudiar la reacción de deshidratación del 1-pentanol para obtener DNPE y agua en fase líquida y usando catalizadores ácidos. Los objetivos de este trabajo se resumen en los siguientes puntos:

1. Hacer una puesta en marcha de la instalación experimental así como estudiar la influencia de las variables de operación (carga de catalizador, velocidad de agitación y tamaño de partícula).
2. Probar distintos catalizadores comerciales con el objetivo de seleccionar uno con el que realizar el análisis cinético y los experimentos de equilibrio.
3. Estudiar el equilibrio termodinámico de la reacción.
4. Realizar un estudio cinético empleando los modelos cinéticos clásicos (Langmuir-Hinshelwood-Hougen-Watson), así como teniendo en cuenta la influencia de los productos de reacción, en especial el agua, sobre la ecuación cinética, y

proponiendo ecuaciones cinéticas corregidas.

5. Preparar catalizadores de Nafion NR50 soportados en SiO₂ y Al₂O₃ con el fin de aumentar el área superficial del mismo.

3. DISPOSITIVOS EXPERIMENTAL

Los ensayos de catalizadores y el estudio de la reacción de síntesis de DNPE se han llevado a cabo en un reactor tanque agitado discontinuo Autoclave Engineers de 100 mL de volumen nominal.

El análisis de las muestras se ha realizado en un cromatógrafo HP 6890 equipado con TCD. Las muestras del reactor se introducen directamente mediante válvulas de líquidos de 0,2 µL de capacidad. Se ha empleado una columna capilar HP 190915-001, HP-Pona Methyl Siloxane, de 50 m de longitud, 20 µm de diámetro y 0,5 µm de grosor de fase estacionaria. El portador es He, con un caudal total de 30 mL·min⁻¹. El análisis se ha realizado a flujo de He constante, aumentando por ello la presión en cabeza de columna a lo largo de un análisis. La temperatura de la columna se mantuvo inicialmente a 45°C durante 6 min, siguió una rampa de 30 °C min⁻¹ hasta 180°C que se mantuvo durante 5 min.

Se analizaron las sustancias siguientes 1-pentanol, DNPE y agua; olefinas C₅ (1-penteno, cis y trans-2-penteno); éteres ramificados (2,2-oxibis pentano, 2-metil-1-butil 2-pentil éter, 2-metil-1-butil 1-pentil éter, 1,2-oxibis pentano y 2-metil-1-butil éter); e impurezas del 1-pentanol (2-metil-1-butanol y pentanal).

El volumen inicial de líquido se fijó en 70 mL, suficiente para sumergir el termopar y el filtro, y dejar una cámara para la expansión del líquido al calentarse. Para mantener la mezcla en fase líquida se fijó una presión de trabajo de 16 bares para impedir la vaporización de las sustancias más ligeras durante el experimento. A excepción de los experimentos de equilibrio, su duración se fijó en 6 horas, suficiente para obtener datos con buena precisión.

4. RESULTADOS Y DISCUSIÓN

Experimentos preliminares han demostrado que la influencia de la transferencia de materia es negligible si se usa 1 gramo de catalizador, una velocidad de agitación de 500rpm y cualquier tamaño de partícula, debido a que la mayoría de los catalizadores se hinchan en el medio polar.

4.1 ENSAYO DE CATALIZADORES

Se ensayaron 8 catalizadores para hallar el más apropiado para uso industrial. Idealmente, debe ser lo bastante activo y selectivo, y resistente térmica y mecánicamente en el rango de temperatura explorado. Finalmente ha de ser atractivo económicamente. Los catalizadores ensayados fueron: la resina perfluoroalcanosulfónica **NR50**, la zeolita **H-BEA-25**, cuatro resinas macroporosas de S/DVB, **Amberlyst 36 y 70, DL-H/03 y DL-I/03**, y dos microporosas, **CT-224** y **Dowex 50Wx4** (como los 4 lotes de diferente d_p , dan resultados similares, se exponen sólo los obtenidos con **Dow 50**).

Catalizador	Estado	Nafion (%peso)	Forma	Tamaño	Cap. ácida (eq H ⁺ /kg)
NR-50	Sólido	100	Esferas	$d_p = 2350 \mu\text{m}$	0.89
N-117	Sólido	100	Membrana	Área: 8 x 10 in Anchura: 0,007in	0.91
SAC-13	Sólido	13	Extrudados	Long = 1 - 4.5mm	0.15
Nafion (5% peso)	Líquido	5	--	--	--

Catalizador	T _{max} (°C)	ρ_s (g/cm ³)	Contenido de agua (%)	S _g (m ² /g)	V _g (cm ³ /g)	d _{poro} (nm)
NR-50	220	2.04	2-3	0.35 ± 0.01	---	---
N-117	200	2	4-5	0.005	---	---
SAC-13	200	2.09	2-3	177 ± 1	0.6	13.6

Tabla II. Propiedades y parámetros estructurales de las resinas perfluoroalcanosulfónicas

En las *Tabla III* se muestran las principales características de las resinas de estireno/divinilbenceno (S/DVB) ensayadas.

	Abreviado	Estructura	%DVB	d_p [μm]	% agua	Cap. ácida [eq H ⁺ /kg]	T _{max} [°C]
Amberlyst 36	A36	Macroporosa	15	634	46-48	4.87	150
Amberlyst DL-I/03	DL-I/03	Macroporosa	Medio	644	51-55	5.46	170
Amberlyst DL-H/03	DL-H/03	Macroporosa	Bajo	698	50-52	3.39	170
Amberlyst 70	A70	Macroporosa	Bajo	551	53-55	3.01	200
CT-224	CT224	Geliforme	4	466	55-60	5.14	150
Dowex 50Wx4-50	Dow50	Geliforme	4	499	63-64	4.95	150
Dowex 50Wx4-100	Dow100	Geliforme	4	211	61-62	4.95	150
Dowex 50Wx4-200	Dow200	Geliforme	4	105	63-64	4.83	150
Dowex 50Wx4-400	Dow400	Geliforme	4	52	64-66	4.87	150

Tabla III. Propiedades de las resinas de S/DVB

Los experimentos se llevaron a cabo en discontinuo y se prolongaron durante 6 h. Se siguió la evolución con el tiempo de X_p , S_{DNPE} , Y_{DNPE} y r_{DNPE} . En la *Tabla III*, se indican las condiciones

de trabajo de estos experimentos.

Catalizador	T [°C]	N [rpm]	W _{cat} [g]
A36	120 a 150	500	1
A70	140 a 190	500	1
DLH/03	130 a 170	500	1
DLI/03	130 a 170	500	1
CT224	120 a 150	500	1
Dow 50	120 a 150	500	1
NR50	140 a 190	500	1
BEA25	140 a 190	500	1

Tabla III. Condiciones de ensayo de catalizadores

4.1.1 CONVERSIÓN DE 1-PENTANOL

Como es de esperar, la conversión de 1-pentanol aumenta con el tiempo y con la temperatura, cuando se está lejos del equilibrio. En la *Tabla IV* se muestra X_p a las 6 h. de reacción para los catalizadores ensayados. La máxima conversión alcanzada es 67,7% a 190°C con la resina termoestable Amberlyst 70. A continuación vienen NR50 y la zeolita, también térmicamente estables. La gran sensibilidad de X_p con la temperatura hace de la $T_{m\acute{a}x}$ de operación un parámetro importante al escoger un catalizador para la reacción.

T(°C)	A36	A70	DLH/03	DLI/03	CT224	Dow50	NR50	BEA25
120	3.6				1.9	2.1		
130	8.0		4.1	8.1	4.7	5.1		
140	13.9	7.0	8.1	13.5	11.5	10.6	4.4	2.2
150	23.8 ±0.02	13.7	15.6	25.9	20.9±0.7	19.4±0.7	9.7	4.3
160		25.1	27.5	33.8			17.5	8.9
170		41.8	43.5±0.4	44.7±0.5			33.5	16.8
180		54.1					49.4	32.0±0.6
190		67.7±0.3					59.4±0.9	50.3

Tabla IV. Conversión de 1-pentanol [%] a t = 6 h para los catalizadores ensayados

A una misma temperatura, por ejemplo 150°C, al comparar los catalizadores se observa que, a mayor capacidad ácida mayor es X_p . A 150°C la mayor conversión se alcanzó sobre DL-I/03 seguido por A-36, siendo los menos activos A-70, NR50 y BEA-25 (los de capacidad ácida más baja). A todas las temperaturas se observa el mismo comportamiento. X_p disminuye en el orden: resinas S/DVB, NR50 y H-BEA-25. La mayor fuerza ácida de NR50 puede ser la

explicación de la mayor actividad de NR50 respecto a H-BEA-25.

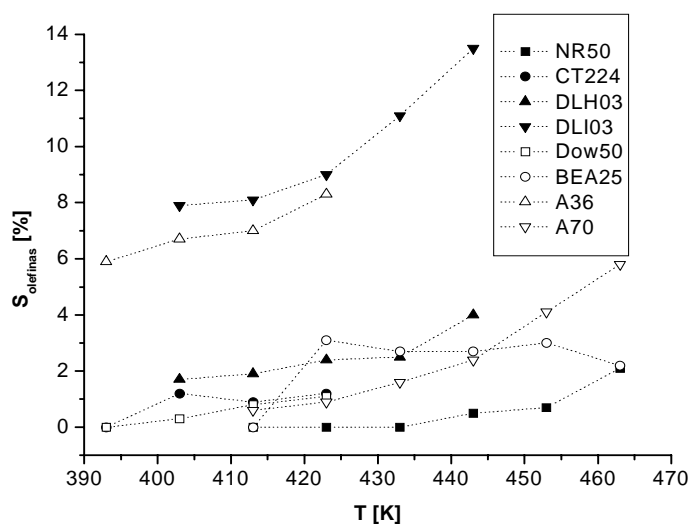
4.1.2 SELECTIVIDAD

La *Tabla V* muestra la selectividad a DNPE a $t = 6$ h de los catalizadores probados. En general, la selectividad a DNPE disminuye al aumentar la temperatura debido a la formación de alquenos y, en consecuencia, éteres ramificados. Es posible que la energía de activación de la formación de 1 y 2 penteno sea mayor que la de formación del éter, de forma que la formación de olefinas sea más competitiva al aumentar la temperatura (*Figura 1*).

T°C	A36	A70	DLH/03	DLI/03	CT224	Dow50	NR50	BEA25
120	91.2				96.4	100.0		
130	89.7		95.7	87.9	96.8	99.5		
140	88.4	98.1	96.2	86.6	97.6	98.8	99.0	89.0
150	85.2	97.8	95.5	83.6	97.3	97.3	99.0	89.6
160		96.8	94.9	79.9			98.9	91.8
170		95.5	92.5	75.6			98.3	92.2
180		93.0					97.8	92.2
190		90.8					96.2	94.8

Tabla V. Selectividad a DNPE [%] a $t = 6$ h para los catalizadores

Dow50 a bajas temperaturas (120-140°C) y NR50 a temperaturas elevadas (150-190°C) son los catalizadores más selectivos a DNPE.



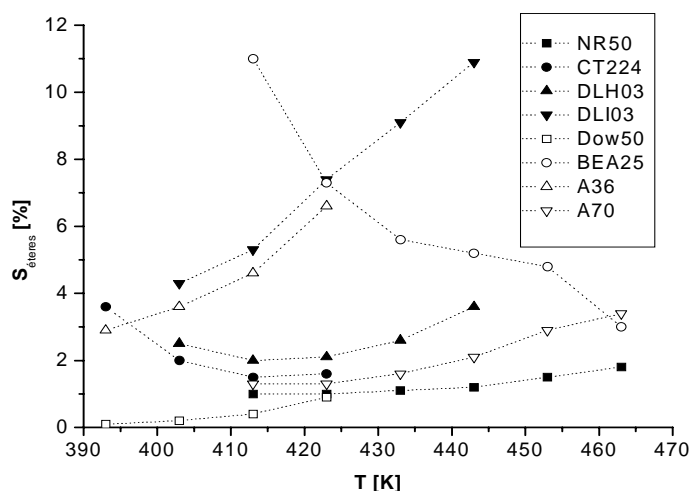


Figura I. S_{alquenos} y S_{eteres} frente a la temperatura a $t = 6\text{h}$

La zeolita H-BEA-25 mostró distinto comportamiento: S_{DNPE} aumenta con la temperatura. Además, la selectividad a éteres ramificados desciende, y se observa un ligero incremento de la selectividad a alquenos. Todo ello sugiere que a temperaturas más elevadas este catalizador puede ser una buena opción para catalizar la deshidratación de 1-pentanol a DNPE.

T [°C]	A36	A70	DLH/03	DLI/03	CT224	Dow50	NR50	H-Beta
120	3.3				1.8	2.1		
130	7.2		3.9	7.1	4.6	5.1		
140	12.3	6.9	7.7	11.7	11.2	10.5	4.4	2.0
150	20.2	13.4	14.9	21.7	20.3	18.8	9.6	3.8
160		24.3	26.1	27.0			17.3	8.1
170		39.9	40.2	33.8			32.9	15.5
180		50.3					48.3	29.5
190		61.4					57.1	47.7

Tabla VI. Y_{DNPE} [%] a $t = 6\text{h}$ para los catalizadores ensayados

4.1.3 RENDIMIENTO EN DNPE

El rendimiento considera conjuntamente X_P y S_{DNPE} , y es un buen indicador de la bondad de un catalizador para una reacción. Como se observa en la *Tabla VI* el rendimiento en DNPE a $t = 6\text{h}$ aumenta con la temperatura. Las resinas termoestables permiten el mayor rendimiento a temperaturas elevadas. En concreto, para A-70 seguido de NR50 a 190°C. El Y_{DNPE} con DL-I/03 es menor del que podría esperarse dada su elevada actividad pues su selectividad a DNPE es baja a todas las temperaturas. Sin embargo, las resinas convencionales de S/DVB

son mejores a bajas temperaturas. Finalmente, señalar que la zeolita H-Beta muestra resultados prometedores a 190°C y podría ser útil a temperaturas aún más elevadas.

4.1.4 VELOCIDAD DE REACCIÓN Y “TURNOVER NUMBER” INICIAL

La *Tabla VII* muestra las velocidades iniciales de reacción. Como podía esperarse, r_{DNPE}^0 aumenta fuertemente con la temperatura y, de nuevo, el mayor valor se alcanza a 190°C con A-70, seguido de NR50. Si se comparan a 150°C, se ve que a mayor capacidad ácida mayor velocidad de reacción. Las resinas macroporosas Amberlyst 36 y DL-I/03, y la microporosa CT224, con la mayor capacidad ácida, presentan los valores de r_{DNPE}^0 más altos a 150 °C. Los valores de r_{DNPE}^0 obtenidos con NR50, mucho mayores de lo esperado a partir de su capacidad ácida, se explican por la fuerza ácida de los grupos $-\text{SO}_3\text{H}$ en las resinas Nafion.

T(°C)	A36	A70	DLH/03	DLI/03	CT224	Dow50	NR50	BEA25
120	1.8				1.0	1.2		
130	4.5		2.2	5.2	2.5	2.9		
140	9.1	3.9	5.6	9.3	7.3	5.8	2.5	0.8
150	18.9	8.1	11.0	18.4	15.7	13.2	5.8	1.8
160		15.6	21.4	36.1			10.9	4.3
170		33.6	41.9	60.2			24.8	8.8
180		48.7					43.6	18.2
190		111.9					67.3	32.7

Tabla VII. Velocidad inicial de reacción [mol/(kg·h)]

La influencia de la fuerza ácida sobre la actividad es clara cuando la velocidad de reacción se expresa por equivalente de sitios ácidos o “turnover number”, r_{eq}^0 , (*Tabla VIII*).

T(°C)	A36	A70	DLH/03	DLI/03	CT224	Dow50	NR50	BEA25
120	0.4				0.2	0.2		
130	0.9		0.6	1.0	0.5	0.6		
140	1.9	1.3	1.7	1.7	1.4	1.2	2.8	0.7
150	3.9	2.7	3.2	3.4	3.1	2.7	6.5	1.5
160		5.2	6.3	6.6			12.2	3.6
170		11.2	12.4	11.0			27.8	7.3
180		16.2					49.0	15.2
190		37.3					75.6	27.3

Tabla VIII. “Turnover numbers” [mol/(eq H⁺·h)]

4.1.5 SELECCIÓN DEL CATALIZADOR

A temperaturas bajas, hasta 150°C, las resinas de S/DVB son los catalizadores más activos y selectivos. Su temperatura máxima de trabajo es un inconveniente notable para la producción de DNPE.

Entre las resinas termoestables, A70 es la mejor opción para la deshidratación de 1-pentanol a DNPE, ya que es la más selectiva a éter. Respecto a las otras resinas de S/DVB, su estabilidad térmica permite conversión y rendimiento elevados, con razonable selectividad, aún a 190°C.

NR50 es el catalizador más selectivo, y a las temperaturas más elevadas es bastante activo debido a su elevada fuerza ácida. Pero a las temperaturas más bajas es poco activo debido a la baja concentración de grupos sulfónicos en la matriz polimérica. Además, podría resultar demasiado caro para uso industrial.

La zeolita H-Beta es la menos activa de los catalizadores probados, aunque a 190°C se alcanza una conversión elevada, lo que indica que es un catalizador prometedor a temperaturas todavía más elevadas.

Para uso industrial se necesita un catalizador activo, barato y, en especial, selectivo. Del estudio realizado se desprende que si desea producir DNPE eliminando simultáneamente el agua producida (destilación reactiva, 135-155°C, o con membranas catalíticas), una resina de DVB, tal vez **Dowex 50Wx4**, podría ser útil por su elevada selectividad a DNPE y actividad a 150°C. Si se desea trabajar en un reactor sin eliminación de agua, será preciso trabajar a 170-190°C. Entonces, la mejor opción es la resina termoestable **Amberlyst 70**, por su amplio intervalo de temperatura de operación, actividad elevada y aceptable selectividad.

4.2 **EQUILIBRIO TERMODINÁMICO**

No se encontró información en la literatura sobre la entalpía, la entropía, o la energía libre de reacción de la deshidratación de 1-pentanol a DNPE en fase líquida y, en consecuencia de la constante de equilibrio. Por ello, se realizó una serie de experimentos para obtener la constante de equilibrio por medida directa de la composición de la mezcla en equilibrio a varias temperaturas.

4.2.1 DETERMINACIÓN DE LA CONSTANTE DE EQUILIBRIO

Partiendo de pentanol puro, alcanzar el equilibrio era bastante lento, y dada la complejidad

de la mezcla en equilibrio o quasi-equilibrio, que incluye agua y tiene el peligro de separación de fases, se cargó inicialmente en el reactor una mezcla cerca del equilibrio para acortar los experimentos. En la *Tabla IX* se muestran las condiciones de trabajo en estos experimentos.

Catalizador	Disolvente	T [°C]	N [rpm]	W _{cat} [g]
A70	1,4-dioxano	150 a 190	350	1 a 5

Tabla IX. Condiciones de trabajo: experimentos de equilibrio

Para asegurar una sola fase durante el experimento se usó 1,4-dioxano como disolvente, ya que mantiene una sola fase a 20°C y en experimentos en blanco no mostraba reacción. Como catalizador se usó A-70 por ser estable térmicamente hasta 190°C. La velocidad de agitación se fijó en 350rpm (> 300rpm, libre pues de la influencia de la transferencia externa de materia) para prevenir la atrición del catalizador. El tiempo necesario para llegar al equilibrio depende de la temperatura y de la masa de catalizador. Típicamente, se tardaban 48-72 horas.

Como alcanzar una composición constante a elevadas temperaturas es difícil, la constancia de la constante de equilibrio se tomó como indicador de que la reacción estaba en equilibrio dentro de los límites del error experimental. Los datos obtenidos ponen de manifiesto que se tienen 3 reacciones casi en equilibrio: 1) deshidratación de 1-pentanol a DNPE y agua; 2) descomposición de DNPE a 1-pentanol y 1-penteno; y 3) isomerización de 1-penteno a 2-penteno. La *Tabla X* muestra las condiciones experimentales y las constantes de equilibrio de la deshidratación de 1-pentanol a DNPE y agua.

T [°C]	W _{cat} [g]	K _x	K _γ	K _a	K _a (DNPE)
150	4.265	22.7	2.440	55.5	55.5 ± 0.5
160	3.226	23.3	2.371	55.2	54.6 ± 0.9
160	3.63	23.0	2.342	53.9	
170	1.666	23.7	2.200	52.0	52.1 ± 0.1
170	4.215	24.8	2.104	52.2	
180	1.014	23.7	2.150	50.8	49.5 ± 1.9
180	1.700	23.1	2.088	48.2	
190	2.100	24.4	1.954	47.7	47.7 ± 1.2

Tabla X. Condiciones experimentales y constantes de equilibrio de la deshidratación de 1-pentanol a DNPE y agua

A algunas temperaturas se realizaron réplicas y la reproducibilidad se juzgó buena. K_{DNPE} es el valor medio de K_a cuando se dispone de experimentos. Se observa que la masa de catalizador no afecta la medida de la constante de equilibrio, y los valores de K_y prueban que la mezcla es no ideal. K_a disminuye con la temperatura: la reacción es exotérmica. Sin embargo, su variación con la temperatura es pequeña, lo que implica que la entalpía de reacción es pequeña.

4.2.2 FACTOR CORRECTOR DE LA PRESIÓN

La desviación en los valores de K_a debido a la diferencia entre la presión de trabajo y la del estado estándar de referencia se evaluó mediante el factor de Pointing. Los valores calculados indican que ignorar la corrección de la presión introduce un error en el cálculo de K_a menor que el experimental. Por tanto, puede aceptarse que las constantes de equilibrio sólo dependen de la temperatura.

4.2.3 DEPENDENCIA DE K_a CON LA TEMPERATURA

Si la entalpía de reacción se considera constante en el intervalo de temperatura explorado, la entalpía molar de la reacción, $\Delta_r H_{(l)}^0$, se obtiene de la pendiente de la recta $\ln K_a$ vs $1/T$ y la entropía molar, $\Delta_r S_{(l)}^0$, de la ordenada en el origen. La variación de K_a con la temperatura para la reacción es:

$$\ln K_a = \frac{(783 \pm 75)}{T} + (2,18 \pm 0,17)$$

Por consiguiente: $\Delta_r H_{(l)}^0 = - 6.5 \pm 0.6$ kJ/mol (supuesta constante en el intervalo de temperaturas), $\Delta_r S_{(l)}^0 = 18.1 \pm 1.4$ J/(mol K) y $\Delta_r G_{(l)}^0 = - 11.9 \pm 1.1$ kJ/mol.

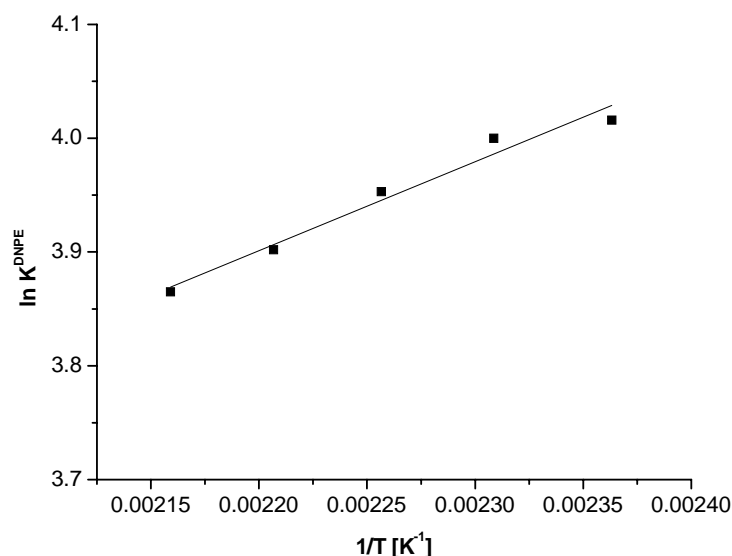


Figura III. Variación de K_a con la temperatura

Por otro lado, la variación de la entalpía de reacción y la constante de equilibrio con la temperatura pueden determinarse con las conocidas ecuaciones de Kirchoff y Van't Hoff, a partir de los datos termoquímicos mostrados en la *Tabla XI*.

	unidades	1-pentanol	DNPE	agua
$C_p=a+bT+cT^2+dT^3$	J/(mol·K)			
a	J·(mol·K) ⁻¹	177.73	-126.85	106.61
b	J·(mol·K) ⁻²	0.1872	2.3799	-0.2062
c	J·(mol·K) ⁻³	$-3.456 \cdot 10^{-4}$	$-3.240 \cdot 10^{-3}$	$3.777 \cdot 10^{-4}$
d	J·(mol·K) ⁻⁴	$7.892 \cdot 10^{-7}$	$1.550 \cdot 10^{-6}$	$-1.226 \cdot 10^{-7}$
$\Delta_f H_m^0$ (298.15 K)	kJ/mol	-351.62	-435.2	-285.830
S_m^0 (298.15 K)	J/(mol K)	258.9	394.44	69.95

Tabla XI. Datos termoquímicos de 1-pentanol, DNPE, agua

En la *Figura IV* se representa el ajuste del $\ln K_a$ vs $1/T$ teniendo en cuenta que la entalpía de la reacción no es constante en el intervalo de T. La entalpía, entropía y energía libre de la reacción 25°C, considerando que éstas varían en el intervalo de temperatura explorado son: $\Delta_r H_{(l)}^0 = -3.8 \pm 0.6$ kJ/mol, $\Delta_r S_{(l)}^0 = 25.9 \pm 3.1$ J/(mol K), y $\Delta_r G_{(l)}^0 = -11.5 \pm 0.3$ kJ/mol.

La entalpía, entropía y energía libre de la reacción de deshidratación de 1-pentanol a DNPE a 25°C, estimada suponiendo $\Delta_r H_{(l)}^0$ constante y, también, función de T se dan en la *Tabla 37*,

junto con los valores estimados a partir de $\Delta_f H_m^0$, y S_m^0 (Tabla XII).

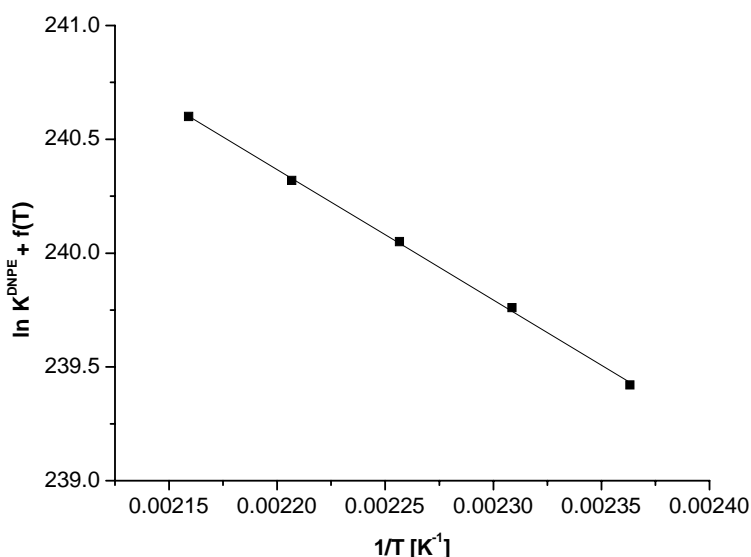


Figura IV. $\ln K_a + f(T)$ vs. $1/T$.

$\Delta_r H_{(l)}^0$ para la producción de éter es pequeña. Los valores obtenidos, tanto si se considera constante como variable con la temperatura son menores que el calculado de las entalpías molares de formación de 1-pentanol, DNPE y agua. No obstante, concuerdan bien con los de obtención de otros éteres, estimados de las entropías y entalpías de formación encontrados en los bancos de datos.

DNPE	$\Delta_r H_{(l)}^0$ (KJ·mol ⁻¹)	$\Delta_r S_{(l)}^0$ (J·mol ⁻¹ K ⁻¹)	$\Delta_r G_{(l)}^0$ (kJ·mol ⁻¹)
$\Delta_r H_{(l)}^0$ constante	-6.5 ± 0.6	18.1 ± 1.4	-11.9 ± 1.1
$\Delta_r H_{(l)}^0$ en f(T)	-3.8 ± 0.6	25.7 ± 3.1	-11.5 ± 0.3
Estimado	-17.8	-48.4	-3.4

Tabla XII. Energía libre, entropía y entalpía de la reacción de la síntesis de DNPE

Para el DNPE, de $\Delta_r H_{(l)}^0$ y $\Delta_f H_{(l)}^0$ de agua y 1-pentanol, se obtiene $\Delta_f H_{(l)}^0 = -(423.9 \pm 1.2)$ kJ/mol si $\Delta_r H_{(l)}^0$ se considera constante, o $-(421.1 \pm 1.2)$ kJ/mol variable con la temperatura. Estos valores son menores en un 3% de los de Murrin et al., estimado de calores de combustión, y en un 1.5% del estimado mediante el método de Benson mejorado -430.1 kJ/mol.

Comparando el $\Delta_r S_{(l)}^0$ de las reacciones de obtención de algunos alquil éteres, parece que la

entropía de reacción aumenta con el número de átomos de C de la molécula. El valor hallado para el DNPE sigue esta tendencia, pero el hallado de las entropías de formación no. La entropía molar del DNPE no está en los bancos de datos, y el método de Benson modificado parece subestimarla. Una $S^0_{(l)}$ de **465.95** J/(K·mol) (**473.71** si $\Delta_f H^0_{(l)}$ es variable con T) se ha estimado a partir de $\Delta_r S^0_{(l)}$, que es casi un 20% mayor que la estimada por el método de Benson.

El mismo tratamiento matemático se hizo para las constantes de equilibrio de las reacciones de descomposición del DNPE para dar 1-pentanol y 1-penteno e isomeración del 1-penteno a 2-penteno. En la *Tabla XIII* se muestra la energía libre, entropía y entalpía de la reacción descomposición de DNPE.

1-penteno	$\Delta_r H^0_{(l)}$ (KJ·mol ⁻¹)	$\Delta_r S^0_{(l)}$ (J·mol ⁻¹ K ⁻¹)	$\Delta_r G^0_{(l)}$ (kJ·mol ⁻¹)
$\Delta_r H^0_{(l)}$ constante	70.4 ± 0.9	101.9 ± 2.0	40.0 ± 2.0
$\Delta_r H^0_{(l)}$ en f(T)	63.4 ± 0.9	83.1 ± 4.8	38.6 ± 0.5
Estimado	36.7	122.1	0.3

Tabla XIII. Energía libre, entropía y entalpía de la reacción descomposición de DNPE

La descomposición del DNPE es endotérmica. Los valores experimentales de la energía libre, entropía y entalpía de la reacción difieren de los estimados debido a que la cantidad de 1-penteno presente en el medio era muy pequeña ya que rápidamente reaccionaba para dar 2-penteno. En la *Tabla XIV* se muestra la energía libre, entropía y entalpía de la reacción de isomerización del 1-penteno.

2-penteno	$\Delta_r H^0_{(l)}$ (KJ·mol ⁻¹)	$\Delta_r S^0_{(l)}$ (J·mol ⁻¹ K ⁻¹)	$\Delta_r G^0_{(l)}$ (kJ·mol ⁻¹)
$\Delta_r H^0_{(l)}$ constante	-21.2 ± 2.1	-25.6 ± 4.7	-13.6 ± 3.5
$\Delta_r H^0_{(l)}$ en f(T)	-19.7 ± 2.1	-21.6 ± 11.0	-13.3 ± 1.2
Esimado	-11.3	-6.0	-9.5

Tabla XIV. Energía libre, entropía y entalpía de la reacción descomposición de DNPE

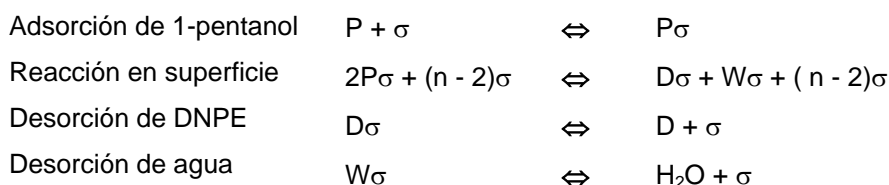
Los valores experimentales difieren de los estimados. De todas formas, si sólo se tiene en cuenta el intervalo de temperaturas de 170-190°C, la $\Delta_r H^0_{(l)}$ si es considerada constante es de – (14.7 ± 4.1) kJ/mol (–(13.0 ± 4.2) kJ/mol si se considera variable). Este valor se acerca más al teórico.

4.3 ANÁLISIS CINÉTICO

El principal objetivo del estudio cinético consiste en obtener una ecuación cinética con base físico-química, que describa apropiadamente las velocidades de reacción determinadas experimentalmente.

4.3.1 MODELOS CINÉTICOS LHHW

El mecanismo LHHW propuesto es el siguiente:



Donde $n (\geq 2)$ es el número de centros activos involucrados en el proceso. Asimismo, se planteó un mecanismo de Eley-Rideal (ER) donde una molécula de alcohol adsorbida reacciona con otra no adsorbida. En este caso, la reacción en superficie sería (suponiendo que el DNPE permanece adsorbido):



Se considera la posibilidad de que en ambos mecanismos, uno o más centros adicionales, participen en la reacción en superficie. Dado que el sistema es no ideal, las ecuaciones de velocidad se expresaron en función de las actividades de 1-pentanol, DNPE y agua. Los coeficientes de actividad se estimaron mediante el método UNIFAC-DORTMUND. Suponiendo que la reacción en superficie es la etapa limitante de la velocidad de reacción (hipótesis bien aceptada en este tipo de reacciones), los formalismos de LHHW y ER conducen respectivamente a las siguientes ecuaciones cinéticas básicas:

$$r = \frac{\hat{k} \cdot K_P^2 \cdot \left(a_P^2 - \frac{a_D \cdot a_W}{K_{eq}} \right)}{\left(1 + K_P \cdot a_P + K_D \cdot a_D + K_W \cdot a_W \right)^n}$$

$$r = \frac{\hat{k} \cdot K_P \cdot \left(a_P^2 - \frac{a_D \cdot a_W}{K_{eq}} \right)}{\left(1 + K_P \cdot a_P + K_D \cdot a_D \right)^n}$$

donde: \hat{k} = constante de velocidad directa de la reacción en superficie

a_i = actividad del compuesto i en el fluido (P=1-PeOH, D=DNPE y W=agua)

K_i = constante de equilibrio de adsorción del compuesto i

K_{eq} = constante termodinámica de equilibrio

n = número de centros activos que participan en la etapa de reacción en superficie

TIPO	CLASE I	N	Modelo	CLASE II	n	Modelo
1	$r = A \frac{\left(a_p^2 - \frac{a_D a_W}{K_{eq}}\right)}{a_p^n}$	1	113	$r = \frac{k_1 \left(a_p^2 - \frac{a_D a_W}{K_{eq}}\right)}{\left(1 + K_p a_p\right)^n}$	1	141
		2	114		2	142
		3	115		3	143
2	$r = A \frac{\left(a_p^2 - \frac{a_D a_W}{K_{eq}}\right)}{a_D^n}$	1	117	$r = \frac{k_1 \left(a_p^2 - \frac{a_D a_W}{K_{eq}}\right)}{\left(1 + K_D a_D\right)^n}$	1	145
		2	118		2	146
		3	119		3	147
3	$r = A \frac{\left(a_p^2 - \frac{a_D a_W}{K_{eq}}\right)}{a_W^n}$	1	121	$r = \frac{k_1 \left(a_p^2 - \frac{a_D a_W}{K_{eq}}\right)}{\left(1 + K_W a_W\right)^n}$	1	149
		2	122		2	150
		3	123		3	151
4	$r = \frac{A \left(a_p^2 - \frac{a_D a_W}{K_{eq}}\right)}{\left(a_p + B a_D\right)^n}$	1	125	$r = \frac{k_1 \left(a_p^2 - \frac{a_D a_W}{K_{eq}}\right)}{\left(1 + K_p a_p + K_D a_D\right)^n}$	1	153
		2	126		2	154
		3	127		3	155
5	$r = \frac{A \left(a_p^2 - \frac{a_D a_W}{K_{eq}}\right)}{\left(a_p + B a_W\right)^n}$	1	129	$r = \frac{k_1 \left(a_p^2 - \frac{a_D a_W}{K_{eq}}\right)}{\left(1 + K_p a_p + K_W a_W\right)^n}$	1	157
		2	130		2	158
		3	131		3	159
6	$r = \frac{A \left(a_p^2 - \frac{a_D a_W}{K_{eq}}\right)}{\left(a_D + B a_W\right)^n}$	1	133	$r = \frac{k_1 \left(a_p^2 - \frac{a_D a_W}{K_{eq}}\right)}{\left(1 + K_D a_D + K_W a_W\right)^n}$	1	161
		2	134		2	162
		3	135		3	163
7	$r = \frac{A \left(a_p^2 - \frac{a_D a_W}{K_{eq}}\right)}{\left(a_p + B a_D + C a_W\right)^n}$	1	137	$r = \frac{k_1 \left(a_p^2 - \frac{a_D a_W}{K_{eq}}\right)}{\left(1 + K_p a_p + K_D a_D + K_W a_W\right)^n}$	1	165
		2	138		2	166
		3	139		3	167

Tabla XV. Modelos cinéticos ajustados

Para encontrar el mejor modelo cinético para cada catalizador, se ajustaron las ecuaciones con $n = 1, 2$ y 3 , y los modelos simplificados suponiendo la adsorción de éter, alcohol y/o agua despreciable. Los 42 modelos ajustados (Tabla XV) se dividieron en dos grupos: Clase I, donde la cantidad de sitios activos libres se supone despreciable, de forma que el 1 del término de adsorción puede ignorarse; Clase II, donde el 1 del término de adsorción no se ignora.

La constante termodinámica de equilibrio experimental es

$$K_{eq} = \exp\left(\frac{783}{T} + 2.1776\right)$$

Las constantes cinética y de equilibrio se agrupan para facilitar el ajuste. La variación con la temperatura de A, B, C, k_1 , K_P , K_W y K_D se define como (por ejemplo para A):

$$A = \exp(b_i) \exp\left[-b_{i+1}\left(\frac{1}{T} - \frac{1}{\bar{T}}\right)\right]$$

Los parámetros a ajustar son los b's. La resta de la temperatura media experimental se incluye para minimizar la correlación matemática entre los parámetros. Como función objetivo se define la minimización de la suma de cuadrados del desajuste (SSQ). El método de Marquardt-Levenberg se utilizó para minimizar SSQ.

4.3.2 SELECCIÓN DEL MODELO CINÉTICO

Ajustados los modelos, se selecciona el modelo que tenga el mejor ajuste desde el punto de vista estadístico (suma de cuadrados mínima, residuos aleatorios y baja correlación de parámetros) y a la vez consistencia fisicoquímica (energía de activación positiva, entalpías y entropías de de adsorción negativas). Los mejores modelos resultaron ser, para todos los catalizadores, los agrupados como Clase I – tipo 4:

$$r = \frac{A\left(a_p^2 - \frac{a_D a_W}{K_{eq}}\right)}{(a_p + B a_D)^n} \quad n = 1, 2 \text{ y } 3$$

Es difícil discernir el valor de n, ya que la SSQ es muy parecida para $n = 1, 2$ y 3 . En cuanto a SSQ (corregidas para poder comparar las de todos los catalizadores) se distinguen dos grupos de catalizadores. El principal está integrado por DL-H/03, CT224, A36, BEA25 y Dow que tienen sumas de cuadrados pequeñas. El gráfico de velocidad de reacción calculada por el modelo 125 frente a la experimental para DL-H/03 muestra que el ajuste es satisfactorio (Figura V). Los residuos son aleatorios y los parámetros A y B se obtienen con baja correlación. Gráficos similares se obtienen para los otros catalizadores del grupo (y $n = 2$ y 3).

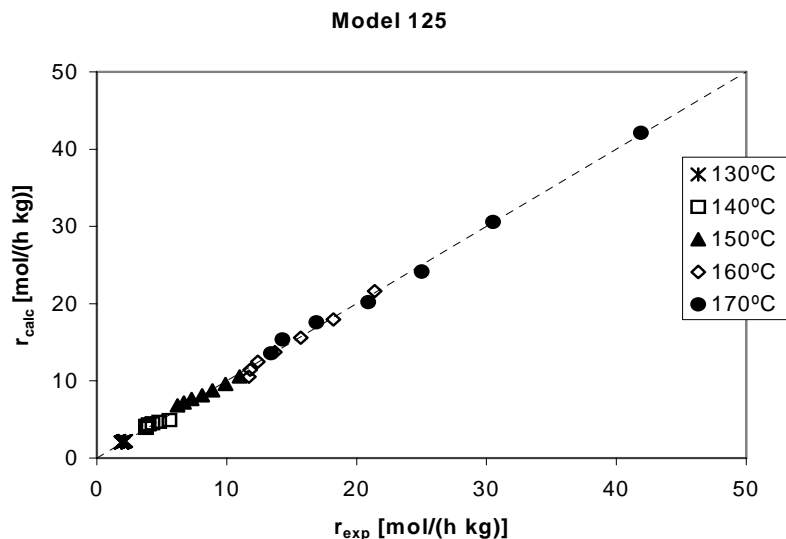


Figura V. r_{calc} (modelo 125) frente a r_{exp} para DL-H/03

Los catalizadores NR50, A70 y DL-I/03 tienen SSQ mucho mayores que el primer grupo de catalizadores. El comportamiento de DL-I/03 podría explicarse por el hecho de que tiene poca resistencia osmótica, y al producirse finos durante los experimentos las velocidades no corresponden a estados del catalizador comparables. En el caso de NR50 y A70 que no sufren cambios aparentes (aparte del hinchamiento), la diferencia principal respecto el primer grupo es que la temperatura de trabajo aumentó a 190°C.

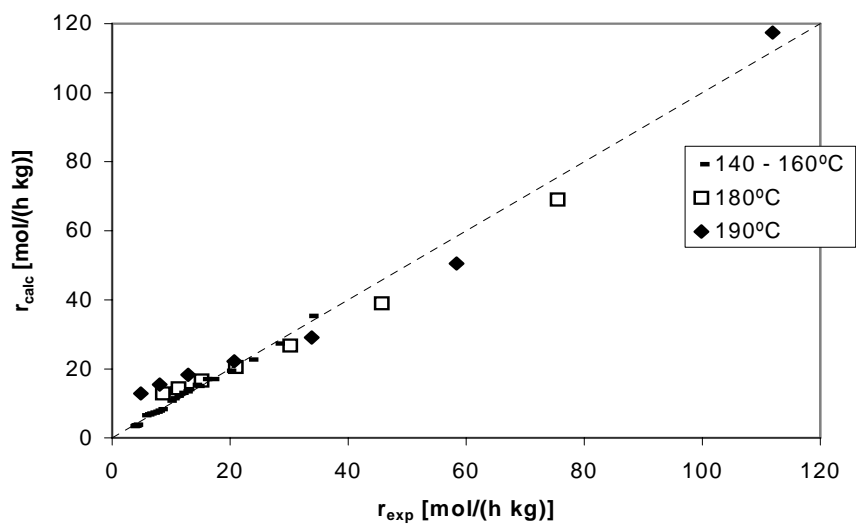


Figura VI. r_{calc} (modelo 125) frente a r_{exp} para A70

La Figura VI muestra que el desajuste mayor aparece a las temperaturas más elevadas

(180 y 190°C). A mayor temperatura se forma más agua y DNPE en los experimentos. El agua tiene un efecto inhibitor de los centros activos por adsorción casi irreversible que los modelos Clase I – tipo 4 no tienen en cuenta. Hay, pues, que mejorar el modelo cinético.

En cuanto a la coherencia termodinámica, de la variación de A (que incorpora la constante cinética) con la temperatura puede extraerse la energía de activación aparente. En la *Tabla XVI*, se muestra la energía de activación aparente correspondiente a la ecuación 25 para $n = 1$. Para $n = 1, 2$ y 3 , la energía de activación aparente es similar para cada catalizador, de 110 a 120 kJ/mol. El error se estimó con el método Jackknife con un intervalo de confianza del 99%.

Catalizador	E_a	A_0
DL-H/03	110.5 ± 0.2	4.8E+14
DL-I/03	113.2 ± 0.8	2.1E+15
CT224	119.1 ± 0.5	8.2E+15
NR50	109.2 ± 0.6	1.7E+14
Dow50	114.7 ± 0.4	2.1E+15
A70	114.6 ± 1.1	1.2E+15
A36	110.1 ± 0.4	8.9E+14
BEA25	121.2 ± 0.4	1.8E+15

Tabla XVI. Energía de activación aparente [kJ/mol] del modelo 125 (n=1)

De los modelos agrupados en Clase I-tipo 4, se optó por el modelo 125, atendiendo a las consideraciones siguientes: en la mayor parte de catalizadores proporciona la SSQ menor, es termodinámicamente coherente, y además proviene de un mecanismo de reacción sencillo (ER) y con base fisicoquímica. El mecanismo supone la reacción en superficie entre 1-PeOH adsorbido y una molécula de pentanol desde la fase fluida, el número de centros activos libres sería muy pequeño.

4.3.3 EFECTO DEL AGUA Y DNPE SOBRE LA VELOCIDAD DE REACCIÓN

La ecuación propuesta no explica el papel cinético del agua. No figura en el término de adsorción, aunque las medidas de tamaño de partícula muestran que se hincha en medio acuoso. Por tanto, la resina debe retener parte del agua producida en la reacción.

Para determinar el efecto del agua y del DNPE sobre la cinética de la deshidratación de 1-pentanol a DNPE, se realizaron experimentos adicionales partiendo de mezclas 1-pentanol

/agua y 1-pentanol/DNPE con A70 ($W_{\text{cat}} = 1\text{g}$; $N = 500\text{ rpm}$ y a $T = 160^\circ\text{C}$ y 180°C). En la *Figura VII* se ve que a 160°C la velocidad inicial de reacción apenas cambia al aumentar la cantidad inicial de DNPE de 0 a 32 % en peso. El mismo comportamiento se observa a 180°C .

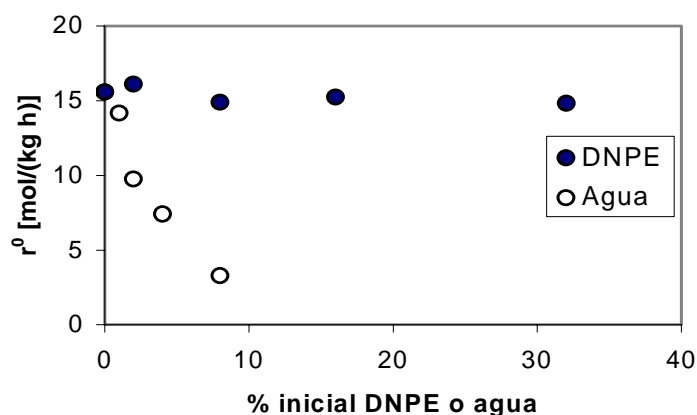


Figura VII. r^0 frente a % peso inicial de agua y DNPE a 160°C

Por otro lado, la velocidad inicial de reacción (y la conversión de 1-pentanol a las 6 h) disminuye mucho al aumentar la cantidad de agua en el reactor. Con sólo un 8% inicial de agua, r^0 es un 79% menor, y el DNPE obtenido tras 6 h de experimentos un 60% menos del que se obtenía con 1-pentanol puro. Si este efecto se debiera sólo a dilución, sería mucho mayor en el caso del DNPE. En consecuencia, la presencia de agua inhibe los centros activos.

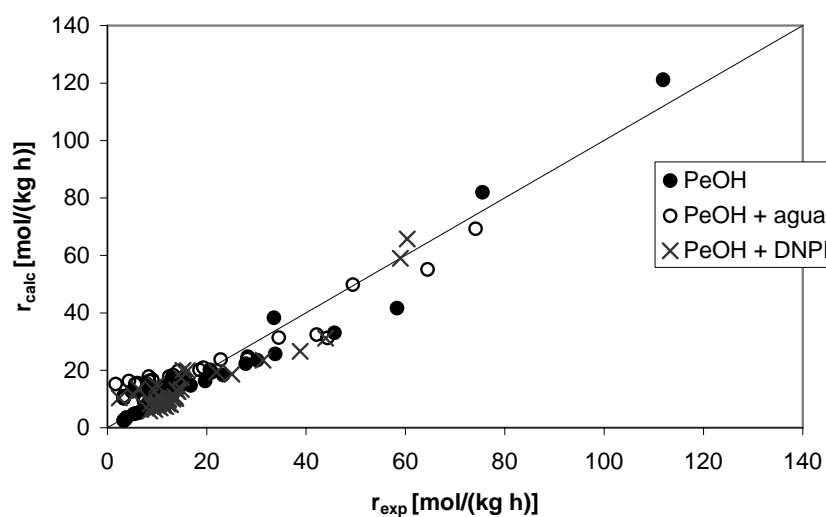


Figura VIII. r_{calc} (modelo 125) frente a r_{exp} . Distintas mezclas iniciales

La *Figura VIII* representa velocidades predichas por el modelo 125 frente a experimentales,

incluyendo los experimentos con agua y DNPE iniciales. El ajuste es bueno con pequeñas cantidades de agua (temperaturas y conversiones bajas) pero se detectan desviaciones cuando hay agua en cantidades relativamente grandes.

4.3.4 MODELOS CINÉTICOS MODIFICADOS

4.3.4.1 Parametro Ψ

En un primer intento de explicar el efecto del agua se corrigió la ecuación cinética (modelo 125) introduciendo el parámetro Ψ propuesto para modelizar el efecto sobre la estructura de la resina de la variación progresiva de la polaridad del medio de reacción. Dicho factor se incluyó en el modelo cinético de la forma siguiente:

$$r = \frac{\hat{k} \cdot \Psi \left(a_p^2 - \frac{a_D a_W}{K_{eq}} \right)}{(a_p + B a_D)} ; \quad \Psi = \exp \left[\frac{\bar{V}_M \phi_p^2}{RT} (\delta_M - \delta_p)^2 \right] \quad \text{y} \quad \delta_M = \sum_i \Phi_i \frac{\sqrt{\Delta H_{v,i} - RT}}{V_i}$$

Donde $\Delta H_{v,i}$ es la entalpía molar de vaporización, V_i el volumen molar del compuesto i , Φ_i la fracción en volumen del componente i , \bar{V}_M el volumen molar del medio, ϕ_p es la fracción de volumen de la resina, δ_M es el parámetro de solubilidad del medio y δ_p es el parámetro de solubilidad de la resina.

δ_p (J/m ³) ^{1/2}	28923 ± 11	δ_p , que se supuso constante en el intervalo de temperatura, es un nuevo parámetro a ajustar junto con b_1 , b_2 , b_3 y b_4). La <i>Tabla XVII</i> muestra los parámetros ajustados, la energía de activación, la suma de cuadrados del desajuste (SSQ) y su variación respecto la del modelo 125 para A70. La introducción de la función Ψ proporciona un ajuste peor. El estimado de δ_p es similar al obtenido por Cruz y col. 25.3 (MJ/m ³) ^{1/2} para Amberlyst 35.
b_1	1.68 ± 0.002	
b_2	14419 ± 22	
b_3	-1.763 ± 0.021	
b_4	13269 ± 140	
E_a [kJ/mol]	119.9 ± 0.2	
SSQ	3477	
% SSQ variación	34	

Tabla 43. Ajuste de la ecuación 29

4.3.4.2 Factor de inhibición

Como la adecuación progresiva de la resina al medio de reacción no parece una hipótesis viable, se propone alternativamente que el agua inhibe la reacción por adsorción sobre los grupos ácidos, impidiendo la adsorción de 1-PeOH y por tanto el progreso de la reacción. Para cuantificar el efecto del agua sobre la velocidad de reacción se introduce un factor de corrección, de forma que la constante de velocidad se expresa como producto de la constante

de velocidad verdadera, \hat{k}_0 , y un factor inhibidor $f(a_w, T)$, que depende de la temperatura y actividad del agua en el líquido y debe tener valores entre 0 y 1. En primera instancia puede considerarse como la fracción de centros activos libre de agua

$$\hat{k} = \hat{k}_0 \cdot f(a_w, T) = \hat{k}_0 (1 - \theta_w)$$

En esta línea, en la bibliografía se hallan algunas propuestas para incluir el efecto inhibidor del agua. Entre ellos, expresar θ_w según un modelo de adsorción de Langmuir en doble centro con disociación, o en adsorción simple o bien mediante un modelo de Freundlich modificado. Las ecuaciones de la *Tabla XVIII* se han ajustado a los datos obtenidos sobre A70 a todas las temperaturas, incluyendo experimentos con agua y DNPE inicial.

Modelo cinético	Ecuación
$r = \frac{\hat{k} \left(a_p^2 - \frac{a_w a_D}{K_{eq}} \right)}{(a_p + B \cdot a_D) \cdot 1 + K_w \sqrt{a_w}}$	$; K_w = \exp \left[K_{w,1} - K_{w,2} \left(\frac{1}{T} - \frac{1}{T'} \right) \right]$ (a)
$r = \frac{\hat{k} \left(a_p^2 - \frac{a_w a_D}{K_{eq}} \right)}{(a_p + B \cdot a_D) \cdot 1 + K_w a_w}$	$; K_w = \exp \left[K_{w,1} - K_{w,2} \left(\frac{1}{T} - \frac{1}{T'} \right) \right]$ (b)
$r = \frac{\hat{k} \left(a_p^2 - \frac{a_w a_D}{K_{eq}} \right)}{(a_p + B \cdot a_D)} \left(1 - K_F a_w^{1/\alpha} \right)$	$; \alpha = \frac{K_\alpha}{T} \quad y \quad K_F = \exp \left[K_{F,1} - K_{F,2} \left(\frac{1}{T} - \frac{1}{T'} \right) \right]$ (c)

Tabla 44. Modelos cinéticos incluyendo un factor de inhibición

La *ecuación (a)* incorpora un factor inhibidor basado en suponer la adsorción de agua en doble centro con disociación, la *ecuación (b)* en un modelo de adsorción de Langmuir en un solo centro, y la *ecuación (c)* en una expresión tipo de adsorción de Freundlich. Respecto al modelo 125 el ajuste mejora en todos los casos significativamente como muestra la *Tabla XIX*. En el caso de la *ecuación (c)*, los parámetros b_3 y b_4 tienen valores tales que B resulta ser próximo a cero, por esta razón la *ecuación (c)* se transforma en:

$$r = \frac{A \left(a_p^2 - \frac{a_w a_D}{K} \right)}{a_p} \cdot \left(1 - K_F a_w^{1/\alpha} \right)$$

La ecuación (a) mejora la predicción del modelo 125. Introduce un factor empírico pues la adsorción de agua sobre dos centros con disociación no es realista.

Con la ecuación (b) se tiene una mejor predicción con significado físico: la adsorción de una molécula de agua por centro, bloqueando las moléculas de 1-pentanol. K_w sería la constante de equilibrio de adsorción con $\Delta H_{ads,w}$ de $-(44.2 \pm 0.6)$ kJ/mol. Este modelo, aunque no es el mejor, da significado al fenómeno inhibitor del agua sobre las resinas y debería considerarse para estudios posteriores.

	Modelo 125	Ecuación a	Ecuación b	Ecuación c
b_1	1.827 ± 0.002	2.808 ± 0.006	2.410 ± 0.003	2.122 ± 0.003
b_2	15601 ± 19	11595 ± 38	12700 ± 24	13710 ± 15
b_3	-1.14 ± 0.02	-1.82 ± 0.02	-2.27 ± 0.02	
b_4	12941 ± 108	12906 ± 99	14023 ± 100	
K_{w1}		1.46 ± 0.01	1.461 ± 0.008	
K_{w2}		-6615 ± 77	-5317 ± 70	
K_{F1}				495 ± 1
K_{F2}				2971 ± 13
K_α				358 ± 1
E_a [kJ/mol]	129.7 ± 0.2	96.4 ± 0.3	105.6 ± 0.2	114.0 ± 0.1
SSQ	2602	1748	1465	690
SSQ variación	0	-33	-44	-73
$\Delta H_{ads,w}$ [kJ/mol]		-55.0 ± 0.6	-44.2 ± 0.6	

Tabla XIX. Ajustes de los ecuaciones a, b y c

La mejor predicción se tiene con la ecuación (c). La mejora en el ajuste podría justificarse por el parámetro adicional, o también a que la función potencial tipo-Freundlich para el agua es suficientemente flexible para ajustar los datos apropiadamente. La expresión final de este modelo es para A-70:

$$r = \frac{\hat{k}_0 \left(a_p^2 - \frac{a_w a_D}{K_{eq}} \right)}{a_p} \cdot \left(1 - K_F a_w^{1/\alpha} \right)$$

$$\hat{k}_0 = \exp \left[(2.122 \pm 0.003) + (13710 \pm 15) \cdot \left(\frac{1}{T} - \frac{1}{423} \right) \right]$$

$$K_{eq} = \exp\left(\frac{778.69}{T} + 2.1886\right)$$

$$K_F = \exp\left[(495 \pm 1) + (2971 \pm 13) \cdot \left(\frac{1}{T} - \frac{1}{423}\right)\right] \quad y \quad \alpha = \frac{(358 \pm 1)}{T}$$

Este modelo se basa en las hipótesis mecanísticas siguientes:

- La reacción en superficie es la etapa limitante de la velocidad de reacción.
- Una molécula de 1-pentanol de la fase fluida reacciona con una adsorbida.
- Se forma DNPE y se libera al fluido.
- El agua formada bloquea los sitios activos impidiendo la adsorción del 1-pentanol.

La expresión cinética tendría carácter empírico y puede asimilarse a un proceso de desactivación, siendo K_F la constante de velocidad de la desactivación. La desactivación tendría una energía de activación de 24.7 ± 0.1 kJ/mol. La energía de activación aparente de la reacción de deshidratación de 1-pentanol a DNPE es 114.0 ± 0.1 kJ/mol. Este valor es muy similar al obtenido cuando no se añadía agua o éter inicialmente.

La ecuación (c) fue ajustada para todos los catalizadores ensayados, obteniéndose una mejora clara especialmente con los catalizadores que peor se ajustaban al modelo 125: NR50 y DL-I/03. Éstos, y A70, eran los más activos y, como consecuencia, producían más agua.

4.4 CATALIZADORES DE NAFION IMPREGNADO

El Nafion NR50 podría ser un catalizador prometedor a 170-210°C a pesar de su reducida área superficial y capacidad ácida como indica la elevada X_P y S_{DNPE} a 190°C. Su elevada fuerza ácida es la responsable de que su actividad sea mayor que la que cabe esperar de su capacidad ácida. El inconveniente de su reducida área se supera en parte por la capacidad de hincharse en presencia de 1-pentanol y agua. Es posible que no todos los centros ácidos sean accesibles en el medio de reacción, por ello se han preparado catalizadores por impregnación de Nafion y su comportamiento se compara con NR50 y el nanocompuesto SAC-13.

4.4.1 SELECCIÓN DEL SOPORTE.

En la *Tabla XX* se muestran algunas propiedades físicas y estructurales de los soportes.

Soporte	Abrev.	ρ_s [g/cm ³]	S_g [m ² /g]	V_g [cm ³ /g]	d_{poro} [nm]	d_p [μm]	Cap. Ácida [eq H ⁺ /kg]
γ-Alúmina (pH ≈ 6)	Al-1	3.1869	176.5	0.2110	4.5	115.8	-
γ-Alúmina (pH ≈ 4,5)	Al-2	3.2202	157.2	0.2330	5.1	104.7	-
Sílica A	Si-A	2.1942	221.4	1.426	24.4	39.68	0.01
Sílica B	Si-B	2.1513	306.4	1.728	22.0	79.12	0.01
Sílica C	Si-C	2.1054	486.7	1.765	13.7	67.11	0.01
Sílica-alúmina	Si-Al	2.0538	470.6	0.6449	4.8	63.56	2.7

Tabla XX. Propiedades físicas y estructurales de los soportes

Los catalizadores preparados se identifican como soporte_método de impregnación_% teórico de Nafion; por ejemplo: Si-B_3_13 es un catalizador de soporte Si-B impregnado con el método 3 y 13% en peso de Nafion. **I-2** a **I-7** se prepararon con el objeto de pulir el método de impregnación y seleccionar los soportes. Su contenido teórico de Nafion fue del 13% y su actividad se determinó mediante un experimento patrón a 180°C ($W_{cat} = 1$ g; $N = 500$ rpm). En la *Tabla XXI* se muestran los resultados de las primeras impregnaciones.

La muy reducida actividad de los catalizadores soportados en Al-1, Al-2 y Si-Al, puede deberse a su estructura de poros. Si-A, Si-B y Si-C tienen mayor volumen y diámetro de poros por lo que la impregnación resulta efectiva. Asimismo, la acidez del soporte puede ser un problema con las alúminas y la sílica-alúmina, como sugiere el hecho de que la alúmina débilmente ácida (Al-1_2_13) sea ligeramente más activa que la ácida (Al-2_2_13).

Impregnación	Soporte	Catalizador	S_g , (m ² /g)	V_g (cm ³ /g)	d_{poro} [nm]	X_p [%]
I-2	Si-B	Si-B_2_13	306,4	1.728	24.4	8.8
I-3	Si-C	Si-C_2_13	486,7	1.765	22	8.4
I-4	Al-1	Al-1_2_13	176,5	0.211	4.5	0.5
I-5	Al-2	Al-2_2_13	157,2	0.233	5.1	0.1
I-6	Si-Al	Si-Al_2_13	470,6	1.426	4.8	1.1
I-7	Si-A	Si-A_2_13	221,4	0.645	13.7	10.5

Tabla XXI. Catalizadores preparados con un 13% teórico de Nafion

4.4.2 CATALIZADORES CON DISTINTO CONTENIDO DE NAFION

En adelante se empleó sólo Si-A, Si-B y Si-C como soporte y en el método de preparación se incluyó un lavado con metanol para eliminar el Nafion no unido al soporte. Se prepararon de esta forma los catalizadores **I-8** (Si-A_3_13), **I-9** (Si-B_3_13) e **I-10** (Si-C_3_13), siendo la cantidad de Nafion a impregnar del 13% en peso. Los resultados se comparan con NR50

(100% de Nafion) y con SAC-13 (nanocompuesto con 13% de Nafion) en la *Tabla XXII*.

	Soporte	S _g [m ² /g]	X _p [%]	S _{DNPE} [%]	Cap. Ácida [meq H ⁺ /g]	r ^o [mol/(kgh)]	r ^o _{eq} [mol/(eqH ⁺ h)]
I-8	Si-A	221.4	6.3	97.3	0.078	4.8	61
I-9	Si-B	306.4	8.2	98.0	0.086	6.0	70
I-10	Si-C	486.7	9.6	98.3	0.088	5.7	65
NR50	-	0.35	49.4	97.8	0.89	43.6	49.0
SAC-13	-	176.6	19.1	97.1	0.15	14.5	96.7

Tabla XXII. Resultados de I-8, I-9 y I-10 comparados con NR50 y SAC-13

La mayor conversión (y velocidad inicial de reacción) se tiene con NR50, luego SAC-13 y, finalmente, las tres preparaciones. A mayor capacidad ácida (contenido de Nafion) mayor X_p. La selectividad a DNPE es aproximadamente la misma para todos ellos. Sin embargo, el contenido de Nafion aumenta ligeramente con el área superficial del soporte. Para cuantificar la cantidad de Nafion depositada de forma efectiva se definieron los siguientes parámetros:

$$\% Nafion_{ca,j} = \frac{Capacidad\ ácida_j}{Capacidad\ ácida_{NR50}} \cdot 100$$

Los subíndices *ca* y *j* se refieren, respectivamente, a capacidad ácida y soporte. De la *Tabla XXII* se desprende que la cantidad de Nafion soportado de forma efectiva es menor que el 13 % objetivo. Por ello, se definió la eficacia de la impregnación respecto a la cantidad teórica de nafion a impregnar (%Nafion) como:

$$Eficacia_j = \frac{\% Nafion_{ca,j}}{\% Nafion}$$

La *Tabla XXIII* muestra los valores de % Nafion_{ac} y eficacia para I-8, I-9, I-10 y SAC-13. Las eficacias son menores de la unidad, lo que implica que parte del Nafion no se ha ligado al soporte o ha sido neutralizado durante el proceso. Por otro lado, la velocidad de reacción es mayor de la que podría esperarse de su capacidad ácida (incluyendo a SAC-13), lo que indica mayor actividad por centro activo que NR50, lo que sugiere mejor accesibilidad y distribución de los sitios activos sobre el soporte de sílice.

Catalizador	Soporte	% Nafion _{ca}	Eficacia
I-8	Si-A	9	0,67
I-9	Si-B	10	0,74
I-10	Si-C	10	0,76
NR50	-	100	-
SAC-13	-	17	-

Tabla XXIII. % Nafion_{ca} y eficacia de I-8, I-9 y I-10

A continuación se prepararon catalizadores con cantidades crecientes de Nafion sobre Si-A (menor S_g) y Si-C (mayor S_g). En la *Tabla XXIV* se muestran la capacidad ácida, X_p , velocidad inicial de reacción y “turnover number” de estos catalizadores y se comparan con NR50.

La cantidad de Nafion soportada de forma efectiva sobre los soportes (%Nafion_{ca}) aumenta con la cantidad inicial de Nafion. La capacidad ácida, X_p y la velocidad de reacción aumentan progresivamente tendiendo a los valores de NR50. Sin embargo, el “turnover number” es, en algunos catalizadores, mayor que para NR50, y cabe destacar que pasa por un valor máximo. Debe haber, pues, un %Nafion que hace óptima la distribución de sitios activos en el soporte.

Catalizador	Prep.	Cap. Ác. [meqH ⁺ /g]	%Nafion _{ac}	Eficacia	X_p [%]	r^o [mol/(kgh)]	r^o_{eq} [mol/(eqH ⁺ h)]
Si-A_3_6,5	I-12	0.029	3	0.50	1.7	1	34
Si-A_3_13	I-8	0.078	9	0.67	6.3	4.8	62
Si-A_3_26	I-11	0.189	21	0.82	18.1	12.7	67
Si-A_3_39	I-15	0.328	37	0.94	27.9	23.3	71
Si-C_3_13	I-10	0.088	10	0.76	9.6	5.7	65
Si-C_3_26	I-13	0.211	24	0.91	20.0	16.7	79
Si-C_3_39	I-14	0.325	37	0.94	29.2	24.4	75
Si-C_3_65	I-16	0.555	62	0.96	35.5	29.8	54
NR50		0.890			49.4	43.6	49

Tabla XXIV. Efecto del %Nafion sobre la impregnación de Si-A y de Si-C

La X_p a 6 h. siempre es menor que para NR50 y aumenta con el %Nafion. Los catalizadores de Si-C son siempre más activos que los de Si-A, de forma que a mayor S_g mejor la impregnación. Así, con 13% de Nafion, la conversión mayor se tiene con el catalizador soportado en Si-C, después en Si-B y en Si-A. La eficacia de la impregnación aumenta con la cantidad de Nafion a soportar y, ligeramente, con el área específica del soporte. Observese que a partir del 39% Nafion, la eficacia tiende a 1. El aumento de la eficacia de la impregnación con

la cantidad inicial de Nafion, se explica porque parte del mismo se uniría directamente a la sílice por los grupos sulfónicos (neutralizando sitios activos con los grupos OH⁻ del Si). Otra parte se uniría a las anteriores formando puentes sulfona por deshidratación de grupos sulfónicos. Al aumentar la cantidad inicial de Nafion, la pérdida de capacidad ácida debido a los grupos sulfónicos neutralizados en la fijación es cada vez menos importante respecto a la cantidad total de Nafion impregnada.

Por otra parte, al aumentar la cantidad de Nafion lo hace la actividad. Este comportamiento se observa mientras el Nafion cubre progresivamente la superficie del soporte. El "turnover number" máximo se tiene cuando una capa muy fina de Nafion recubre toda la superficie del soporte: el número de centros activos accesibles es máximo. Por ello, para la misma cantidad de Nafion el "turnover number" es mayor con S_g mayor. Cantidades adicionales de Nafion se depositan sobre la capa anterior y los centros accesibles apenas crecen pese al hinchamiento del polímero: el "turnover number" disminuye. En el límite (% de Nafion próximos a 100) el comportamiento del catalizador soportado tiende al de NR50.

Se hicieron análisis de poros de los catalizadores preparados y se compararon al de los soportes y NR50. Al aumentar el % de Nafion el volumen y el área de poros disminuyen de acuerdo con el modelo descrito con una tendencia clara a alcanzar los valores de NR50. El diámetro de poro disminuye respecto al de los soportes, pero apenas cambia al aumentar el %Nafion. De hecho, para los soportados en Si-C d_{poro} es casi constante en el intervalo de %Nafion explorado.

La impregnación de Si-A fue uniforme: la distribución de poro de los sólidos impregnados era muy similar a la del soporte, pero con menor área y volumen de poros. La impregnación en Si-C fue también uniforme, ya que la forma de la distribución no cambia. La diferencia es que la curva se desplazó a diámetros de poro más pequeños. Los poros se estrechan con la impregnación. Esto es más claro en los soportados en Si-C porque el diámetro medio de poro inicial era menor para Si-C que para Si-A.

4.4.3 REPRODUCIBILIDAD DEL METODO DE IMPREGNACION

Para comprobar la reproducibilidad del método de impregnación se preparó el I-17, que era una réplica del I-13 (Si-C con 26% de Nafion). La reproducibilidad del método es bastante buena, pues la velocidad de reacción y el "turnover number" fueron los mismos para los dos catalizadores y, aunque había algunas discrepancias en cuanto a las áreas y volúmenes de poro, el tamaño medio de poro fue prácticamente el mismo.

Finalmente, algunos catalizadores ya usados se ensayaron de nuevo para comprobar si el Nafion estaba todavía unido a la matriz después de un experimento de 6-h. Se reutilizaron dos muestras de Si-C_3_26 (I-13) y Si-C_3_39 (I-14) ya probadas en el reactor. La capacidad ácida había disminuido un 47 % en el caso de I-13 y un 37% en el caso de I-14. El "leaching" es pues considerable. No obstante los catalizadores reusados daban un "turnover number" similar a los catalizadores "frescos".

Con todo no parece que los catalizadores soportados mejoren a NR50 ni a las resinas de intercambio iónico, pues su conversión y velocidad por unidad de masa están lejos de las resinas de S/DVB.

5. CONCLUSIONES

- ✓ Las resinas de S/DVB típicas (polisulfonadas o no) son los catalizadores más activos y selectivos por debajo de 150°C. Del estudio realizado se desprende que si se desea producir DNPE eliminando simultáneamente el agua producida (destilación reactiva, 135-155°C), las resinas Dowex 50Wx4 y CT224, podrían ser útiles por su elevada selectividad a DNPE y actividad tales temperaturas.
- ✓ Entre las resinas termoestables, Amberlyst 70 es la mejor opción para la deshidratación de 1-pentanol a DNPE. Si se desea trabajar sin eliminación de agua, es preciso trabajar a 170-190°C para obtener ventaja de la mayor velocidad de reacción. Respecto a las otras resinas de S/DVB, la estabilidad térmica de Amberlyst 70 permite obtener conversión y rendimiento elevados, con buena selectividad hasta 190°C.
- ✓ NR50 es el catalizador más selectivo, y a 190°C es bastante activo por la elevada fuerza ácida de los grupos sulfónicos debida a los átomos de fluor del polímero. Pero a las temperaturas bajas es poco activa debido a la baja concentración de grupos sulfónicos en la matriz polimérica.
- ✓ Los catalizadores de Nafión soportado no mejoran ni a NR50 ni a las resinas de intercambio iónico, pues la velocidad de reacción (por unidad de masa) están lejos de las resinas de S/DVB. No obstante las velocidades por centro activo mejoran sustancialmente, mostrando una mejor distribución y accesibilidad de los grupos sulfónicos.
- ✓ La zeolita H-Beta es la menos activa entre los catalizadores probados, aunque a 190°C se tienen conversiones elevadas. Es un catalizador prometedor a temperaturas todavía más elevadas siempre que su selectividad a éter aumente todavía más.
- ✓ La mejor predicción de la velocidad de reacción se tiene con un modelo cinético derivado del mecanismo de Rideal-Eley donde una molécula de 1-pentanol reacciona

desde la fase fluida con una adsorbida en la superficie del catalizador, siendo la reacción en superficie la etapa limitante de la velocidad de reacción. El éter formado se desorbe y se libera a fluido. Como hipótesis adicionales hay que citar que la adsorción de éter es muy pequeña respecto la del alcohol, y la fracción de sitios activos libres es muy pequeña ($\rightarrow 0$).

- ✓ La ecuación cinética representa bien los datos experimentales excepto cuando la cantidad de agua presente es significativa. El efecto inhibitor del agua se explica porque el agua formada se adsorbe preferentemente en la resina impidiendo la adsorción de 1-pentanol, y por tanto la reacción. Para cuantificar este efecto, y mejorar la ecuación cinética, se ha introducido un factor de corrección de la constante cinética. Dicho factor se interpreta como la fracción de centros ácidos no ocupados por el agua. La fracción de centros ácidos ocupados por el agua se expresa por una función potencial tipo isoterma de Freundlich. La expresión del modelo cinético es para Amberlyst-70:

$$r = \frac{\hat{k}_0 \left(a_p^2 - \frac{a_w a_D}{K_{eq}} \right)}{a_p} \cdot \left(1 - K_F a_w^{1/\alpha} \right)$$

- ✓ La energía de activación aparente de la reacción, sobre Amberlyst 70, 114.0 ± 0.1 kJ/mol. El modelo cinético explica bien los datos cinéticos sobre todos los catalizadores ensayados.